



UNIVERSITY OF  
LIVERPOOL



---

# THE ROLE OF CARDIAC MICROVASCULAR ENDOTHELIAL CELLS IN DRUG INDUCED CARDIOVASCULAR TOXICITY

---

Thesis submitted in accordance with the requirements  
of the University of Liverpool for the degree of Doctor  
in Philosophy

July 2015

Emma Louise Smith



## **Declaration**

This thesis is the result of my own work. The material contained within this thesis has not been presented, nor is currently being presented wholly, or in part, for any other degree or qualification.

Emma Louise Smith

This research was undertaken at the Department of Molecular and Clinical Pharmacology and the MRC Centre for Drug Safety Science at the University of Liverpool.

## The role of cardiac microvascular endothelial cells in drug induced cardiovascular toxicity

Emma Louise Smith

Cardiovascular toxicity is defined as a severe and potentially fatal adverse reaction to certain drugs. It is one of the leading causes of attrition in drug development. Cardiovascular toxicity research has primarily focused on the role of cardiomyocytes in functional and structural cardiovascular toxicity. However, there is a growing awareness that non-myocyte cells may contribute to cardiovascular toxicity.

The heart is a highly vascularised organ. Endothelial cells from the heart were compared between rat and human, as well as between different vascular beds with the use of human cardiac microvascular endothelial cells (HCMECs) and human dermal microvascular endothelial cells (HDMECs). This data demonstrated ligand induced activation of EGFR-1 in HCMEC indicating the presence of functional EGFR1. Analysis of mRNA expression of *EGFR1-4* revealed higher expression of both *EGFR1* and *EGFR2* in HCMEC compared with HDMEC.

The role of EGFR-2 (Her2) in drug-induced cardiovascular toxicity was analysed with use of Herceptin® and doxorubicin treatment. Herceptin® and doxorubicin are known to induce cardiovascular toxicity in the clinic. The effect of these drugs on the endothelial tight junction barrier was tested, revealing that Herceptin® and doxorubicin are able to induce barrier perturbation and decreased barrier function in HCMEC. Herceptin® treatment had no effect on the tight junction barrier function in HDMECs.

Previous work in the group has identified a role for extracellular-signal-regulated kinase 5 (ERK5) in regulation of endothelial cell survival. The role of ERK5 in endothelial tight junction regulation was investigated using small molecule inhibitors, siRNA transient gene silencing and adenoviral-mediated overexpression of ERK5 to reveal that ERK5 plays an important role in tight junction regulation and endothelial barrier function. Statins are clinically used to lower plasma LDL-cholesterol levels in patients via inhibition of 3-hydroxy-3-methyl-glutaryl-CoA reductase (HMG-CoA reductase). Simvastatin activated ERK5 in endothelial cells via a pathway requiring MEKK3 and MEK5 leading to increased tight junction formation and increased barrier function, providing a possible mechanism for the pleiotropic effects of statins on endothelial cells.

Analysis of the effects of a range of anti-cancer drugs with known cardiovascular toxicity liability revealed these drugs could disrupt tight junctions and decrease barrier function. Pre-incubation with simvastatin protected the endothelial cells from drug induced perturbation of

endothelial tight junction formation and the associated decrease in barrier function.

The data shows the importance of drug-induced endothelial injury in cardiovascular toxicity and highlights potential for therapeutically targeting vasculature to protect against drug-induced vascular injury.



## Acknowledgements

I would like to thank my Academic supervisor Dr. Michael Cross (University of Liverpool), for his support and guidance during the completion of this Ph.D. and for reading this thesis. I would also like to thank my industrial supervisor Dr. James Sidaway for his support on this project. I am thankful to the MRC for providing the financial support that has enabled me to complete this project.

I would especially like to thank my fiancè (Daniel Wilkinson) for helping me through the last 4 years, without you I wouldn't have made it to the end! I would also like to thank my mum (Lynn Smith), dad (Paul Smith), grandma (Mary Ollerton) and grandad (John Ollerton) for their help through the last 4 years and making jokes about Dr. Rubicin that's really doxorubicin. I would like to thank my brother (Christopher Smith) for his help with the computer side of the thesis and putting up with my constant questions about how to use word. I would like to thank my soon to be mother (Shirley Wilkinson) and father (Neil Wilkinson) in law for their support throughout this project.

I would like to thank the members of Angio group for their support throughout the project Gopika Jones, Mohammad Aljasir, Ahmed Alrumayh, Ahmad Alghanem and Awel Williams. Also the members of the MRC (Marathon Running Club) Fiona Mutter, Nathalie DBB, Amy Schofield, Chris Pridgeon, James Heslop, Rob Hornby and Sumaya Dauleh.

Table of Contents

<b>Declaration</b> .....	<b>i</b>
<b>Abstract</b> .....	<b>ii</b>
<b>Acknowledgements</b> .....	<b>iv</b>
Table of Contents .....	<b>v</b>
<b>Abbreviations</b> .....	<b>ix</b>
<b>Chapter 1</b> .....	<b>1</b>
<b>1.1 Cardiovascular physiology</b> .....	<b>2</b>
1.1.1 <i>Overview</i> .....	2
1.1.2 <i>Cardiac embryogenesis and morphogenesis</i> .....	2
1.1.2 <i>Cardiac cell types</i> .....	5
<b>1.2 Endothelial Cell Barrier</b> .....	<b>12</b>
1.2.1 <i>Paracellular route</i> .....	13
1.2.2 <i>Transcellular route</i> .....	16
1.3 <i>Cellular regulation</i> .....	17
1.3.1 <i>Growth factor regulation</i> .....	18
VEGF .....	18
EGF .....	21
FGF .....	23
HGF .....	23
1.3.2 <i>Intracellular signalling</i> .....	24
ERK1/2 .....	26
ERK5 .....	27
<b>1.4 Cardiovascular Toxicity</b> .....	<b>33</b>
<b>1.5 Drug induced cardiovascular toxicity</b> .....	<b>40</b>
1.5.1 <i>Anti-cancer treatments</i> .....	40
1.5.2 <i>Sunitinib (Sutent®)</i> .....	43
1.5.3 <i>Sorafenib (Nexavar®)</i> .....	46
1.5.4 <i>Doxorubicin</i> .....	47
1.5.5 <i>Herceptin® (Trastuzumab)</i> .....	50
<b>1.6 Statins</b> .....	<b>51</b>
<b>1.7 Project Aims</b> .....	<b>57</b>
<b>Chapter 2</b> .....	<b>59</b>
<b>2.1 Materials</b> .....	<b>60</b>
2.1.1 <i>Reagents and materials</i> .....	60
2.1.2 <i>Cell lines, culture medium and solutions</i> .....	61
<b>2.2 Methods</b> .....	<b>69</b>
2.2.1 <i>Cell Culture</i> .....	69
2.2.1.1 <i>Cell culture techniques</i> .....	69

2.2.1.2 Coating of culture dishes .....	69
2.2.3 Western Blotting .....	80
2.2.3 Immunofluorescence .....	82
2.2.4 Gene Analysis.....	83
<b>Chapter 3 .....</b>	<b>93</b>
<b>3.1 Introduction.....</b>	<b>94</b>
<b>3.2 Results.....</b>	<b>96</b>
3.2.1 Rat heart structure.....	96
3.2.2 Characterising rat cells.....	98
3.2.3 Comparing intracellular signalling responses to growth factors in endothelial cells.....	99
3.2.4 Physiological relevance of growth factor stimulation .	102
3.2.5 Further differences between endothelial cells .....	107
3.2.6 Comparison of cellular viability across endothelial cells .....	110
<b>3.3 Discussion.....</b>	<b>112</b>
3.3.1 Rat heart structure and characterising rat cells .....	112
3.3.2 Comparing intracellular signalling responses to growth factors in endothelial cells.....	112
3.3.3 Physiological relevance of growth factor stimulation .....	113
3.3.4 Further differences between endothelial cells .....	114
3.2.5 Comparison of cellular viability across endothelial cells .....	115
<b>Chapter 4 .....</b>	<b>116</b>
<b>4.1 Introduction.....</b>	<b>117</b>
<b>4.2 Results.....</b>	<b>119</b>
4.2.1 Investigation of kinase phosphorylation following growth factor stimulation .....	119
4.2.2 Analysis of growth factor receptor expression in different endothelial cells.....	123
4.2.3 Herceptin® and doxorubicin combination therapy in endothelial cells.....	124
4.2.4 Doxorubicin cellular uptake .....	135
<b>4.3 Discussion.....</b>	<b>140</b>
4.3.1 Investigation of kinase phosphorylation following growth factor stimulation .....	140
4.3.3 Herceptin® and doxorubicin combination therapy in endothelial cells.....	141
4.3.4 Doxorubicin cellular uptake .....	142
<b>Chapter 5 .....</b>	<b>145</b>
<b>5.1 Introduction.....</b>	<b>146</b>
<b>5.2 Results.....</b>	<b>148</b>
5.2.1 ERK5 inhibition alters endothelial tight junction, adherens junction and gap junction formation.....	148
5.2.2 Inhibition of ERK5 induced barrier perturbation.....	149

5.2.3 Small interfering RNA mediated ERK5 silencing reduces endothelial cell barrier function.....	156
5.2.4 Activation of ERK5 by statins .....	165
5.2.5 Analysis of ERK5 signalling cascade .....	169
5.2.7 Simvastatin regulates tight junction formation in endothelial cells in an ERK5 dependent manner .....	172
5.2.8 Simvastatin is able to overcome XMD8-92 induced barrier perturbation but not BIX02189 induced barrier perturbation .....	174
<b>5.3 Discussion.....</b>	<b>182</b>
5.3.1 ERK5 regulates the tight junction barrier in endothelial cells..	182
5.3.2 Activation of ERK5 by statins stimulates endothelial tight junctions .....	184
5.3.3 Linking cholesterol biosynthesis to barrier protection .....	186
<b>Chapter 6 .....</b>	<b>188</b>
<b>6.1 Introduction.....</b>	<b>189</b>
<b>6.2 Results.....</b>	<b>190</b>
6.2.1 Drug screen.....	190
6.2.2 Protein expression changes in junctions following drug treatment.....	201
6.2.3 Barrier recovery following anti-cancer drug treatment .....	211
6.2.5 <i>Simvastatin protects against drug-induced barrier perturbation in endothelial cells.....</i>	<i>214</i>
6.2.5 <i>Simvastatin alters cell viability .....</i>	<i>219</i>
<b>6.3 Discussion.....</b>	<b>221</b>
6.3.1 Drug Screen .....	221
6.3.2 Protein expression changes in junctions following drug treatment .....	222
6.3.3 Barrier recovery following anti-cancer drug treatment .....	223
6.3.4 Statins alter cell viability .....	224
<b>Chapter 7 .....</b>	<b>226</b>
<b>7.1 Cardiovascular toxicity .....</b>	<b>227</b>
7.1 <i>Current approaches.....</i>	<i>227</i>
7.2.1 <i>Rat cardiac endothelial cells respond differently to human cardiac endothelial cells following growth factor stimulation.....</i>	<i>228</i>
7.2.2 <i>Herceptin only induces barrier perturbation in human cardiac endothelial cells.....</i>	<i>230</i>
7.2.3 <i>ERK5 regulates the endothelial tight junction barrier.....</i>	<i>233</i>
7.2.3.1 <i>ERK5 inhibition induces endothelial barrier perturbation.....</i>	<i>234</i>
7.2.4 <i>Pleiotropic effects of statins and regulation of ERK5 in endothelial cells.....</i>	<i>237</i>
7.2.5 <i>Barrier perturbation is not limited to one class of anti-cancer drugs .....</i>	<i>241</i>
<b>7.2 Study limitations and further directions .....</b>	<b>242</b>
<b>7.3 Overall conclusions.....</b>	<b>246</b>

**Chapter 8: References.....247**

## Abbreviations

ACTN2	Alpha actinin 2
ADCC	Antibody directed cell cytotoxicity
ADR	Adverse drug reaction
BBB	Blood brain barrier
BSA	Bovine serum albumin
CA	Constitutively active
CD31/PECAM1	Cluster of Differentiation 31 / Platelet Endothelial Cell Adhesion Molecule 1
cTnI	Cardiac Troponin I
CYP	Cytochrome P450
DDR2	Discoidin domain receptor 2
DMSO	Dimethyl sulfoxide
EGF	Epithelial Growth Factor
EGFR	Epidermal Growth Factor receptor
eNOS	Endothelial nitric oxide synthase
ERK	Extracellular signal regulated kinase
FCS	Foetal Calf Serum
FGF	Fibroblast Growth Factor
FGM	Full growth medium
GAPDH	Glyceraldehyde 3-phosphate dehydrogenase
H9c2	Rat immortalised myocytes
HBMEC	Human brain microvascular endothelial cells
HCAEC	Human coronary artery endothelial cells
HCF	Human cardiac fibroblasts
HCMEC	Human cardiac microvascular endothelial cells
HDMEC	Human dermal microvascular endothelial cells
hERG	Human Ether-a-go-go
HGF	Hepatocyte Growth Factor
HMG-CoA	3-hydrox-3-methylglutaryl-coenzyme A

HO1	Haem oxygenase 1
IGF	Insulin-like Growth Factor
IPA	Isopropanol
JNK	c-jun-N-terminal kinase
KLF	Krüppel-like factor
LVEF	Left ventricle ejection fraction
MAKK	Mitogen activated protein kinase kinase
MAPK	Mitogen activated protein kinase
MAPKKK	Mitogen activated protein kinase kinase kinase
MEF2	Myocyte enhancer factor
MEK	MAPK/ERK kinase
MEKK	MEK kinase
mRNA	Messenger RNA
NFκB	Nuclear factor kappa B
NG2	Chondroitin sulfate proteoglycan 4
NHDF	Normal human dermal fibroblasts
NLS	Nuclear localization signal
NQO1	NAD(P)H dehydrogenase quinone 1
NRF2	Nuclear factor erythroid-derived 2
NRG-1	Neuregulin 1
OCT	Optimum temperature embedding cryomatrix
PAGE	Polyacrylamide gel electrophoresis
PBS	Phosphate balanced salt solution
PDGF	Platelet Derived Growth Factor
PFA	Paraformaldehyde
PI3K	Phosphoinositide kinase 3
qRT-PCR	Quantitative real time polymerase chain reaction
r.p.m	Revolutions per minute
RCEC	Rat cardiac endothelial cells
RECA1	Rat endothelial cell antigen 1
RTK	Receptor tyrosine kinase
SDS	Sodium dodecyl sulfate

SLC(O)	Solute carrier (organic)
TBS	Tris balanced salt solution
TGF	Transforming Growth Factor
TNF	Tumor Necrosis Factor
VCAM1	Vascular cell adhesion molecule 1
VE-cadherin	Vascular endothelial cadherin
VEGF	Vascular Endothelial Growth Factor
VEGFR	Vascular Endothelial Growth Factor Receptor
WB	Western blot
WT	Wild type





# Chapter 1

## Introduction



## **1.1 Cardiovascular physiology**

### *1.1.1 Overview*

The cardiovascular system is comprised of the heart and peripheral vasculature. Through a closed circulation system the cardiovascular system functions to provide oxygen, solutes and free fatty acids to every organ within the body. As the heart is such an important organ it is the first fully functioning organ to develop during embryogenesis (Rossant and Howard, 2002). The heart is comprised of multiple cell types including myocyte, fibroblast, endothelial, pericyte and smooth muscle cells. The heart is known to possess low regenerative potential, so cell death during events such as myocardial infarction has the potential to become fatal. The human left ventricle is comprised of approximately 2 - 4 billion cardiomyocytes; of these 0.5 - 1 billion can undergo cell death within a few hours of myocardial infarction onset (Laflamme and Murry, 2011).

### *1.1.2 Cardiac embryogenesis and morphogenesis*

The heart develops early during embryogenesis as it is fundamental in life. The morphogenic process leading to the generation of the three germ layers: ectoderm, mesoderm and endoderm is termed gastrulation (Van Vliet et al., 2012). These germ layers interact to aid differentiation of the cells during embryogenesis (Van Vliet et al., 2012). Within the embryo there are three main cell precursors for the heart that have been identified, these are summarised in figure 1.1. These include: the cardiogenic mesoderm, which can give rise to the endocardial cells as well as atrial and ventricular myocytes; the cardiac neural crest, which is able to give rise to aorta smooth muscle cells and the autonomic nervous

system and finally the proepicardium, giving rise to coronary artery smooth muscle, endothelium forming the coronary arteries and fibroblasts (Laugwitz et al., 2008).

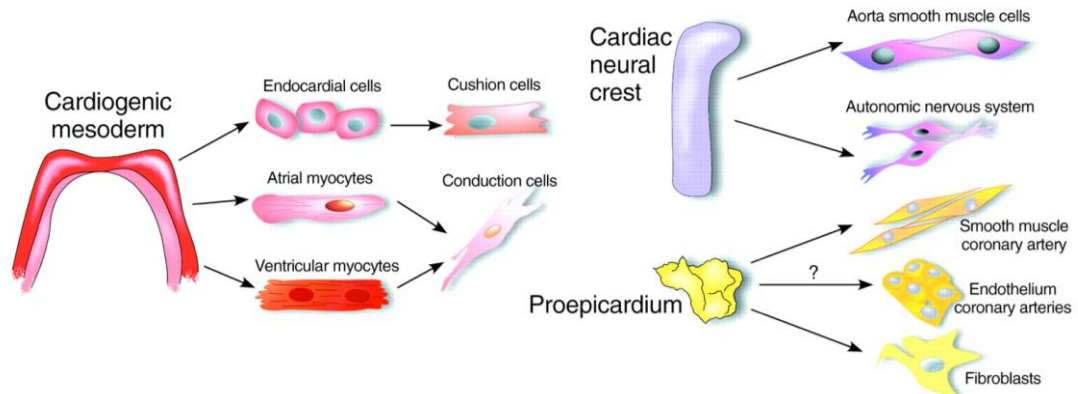


Figure 1.1. **Cardiac cell precursors.** There are three distinct pools of cardiac precursors each giving rise to a different subset of cells. The cardiogenic mesoderm gives rise to the endocardial and myocyte cells. The cardiac neural crest gives rise to aortic smooth muscle and the autonomic nervous system. The proepicardium gives rise to smooth muscle and endothelium making up the coronary arteries and the fibroblasts. Image from (Laugwitz et al., 2008).

During embryogenesis the haemangioblast begins differentiation into endothelial cells in response to activin A, bone morphogenic protein (BMP) and basic fibroblast growth factor (bFGF) (Dyer and Patterson, 2010; Laflamme and Murry, 2011). This differentiation proceeds with the expression of fetal liver kinase 1 (Flk1), vascular endothelial cadherin (VE-cadherin) and stem cell leukaemia (SCL). Cells positively expressing these precursors are able to form blood island clusters through swelling (Dyer and Patterson, 2010). Aggregation of the clusters between the ectoderm and endoderm occurs in response to vascular endothelial growth factor – A (VEGF-A). At this stage the outer cells form the endothelium through flattening whereas the inner cell population differentiates to form hematopoietic cells. The cell lineage is summarised

in figure 1.2. The endothelial cell population is now able to form a capillary plexus of interconnecting tubes. This process is tightly regulated through migratory proteins including PlexinD1 (PLD1) and Semaphorin3A, which regulate endothelial directionality allowing regulated movement of endothelial cells (Dyer and Patterson, 2010). Following heart contraction, endothelial cells undergo vast changes in response to known stimuli. Endothelial cells lining the lumen are exposed to shear stress induced by circulation. Shear stress is able to induce transcription factor changes leading to regulation of cellular permeability through regulation of various endothelial junctions; gap, adherens and tight. The endothelial cells line the endocardium which is separated from the myocardium by a highly structured extracellular matrix (Armstrong and Bischoff, 2004; Kirby, 2002). Following heart functioning there is development of the epicardium, occurring at the looping stage of heart development. The epicardium forms the outer layer of the heart, surrounding the myocardium and inner endocardium (Kirby, 2002).

The differentiation of the cardiac mesoderm is regulated by transcription factors; endothelial cells are controlled by smooth muscle and myocytes by Nkx2-5 (Laugwitz et al., 2008).

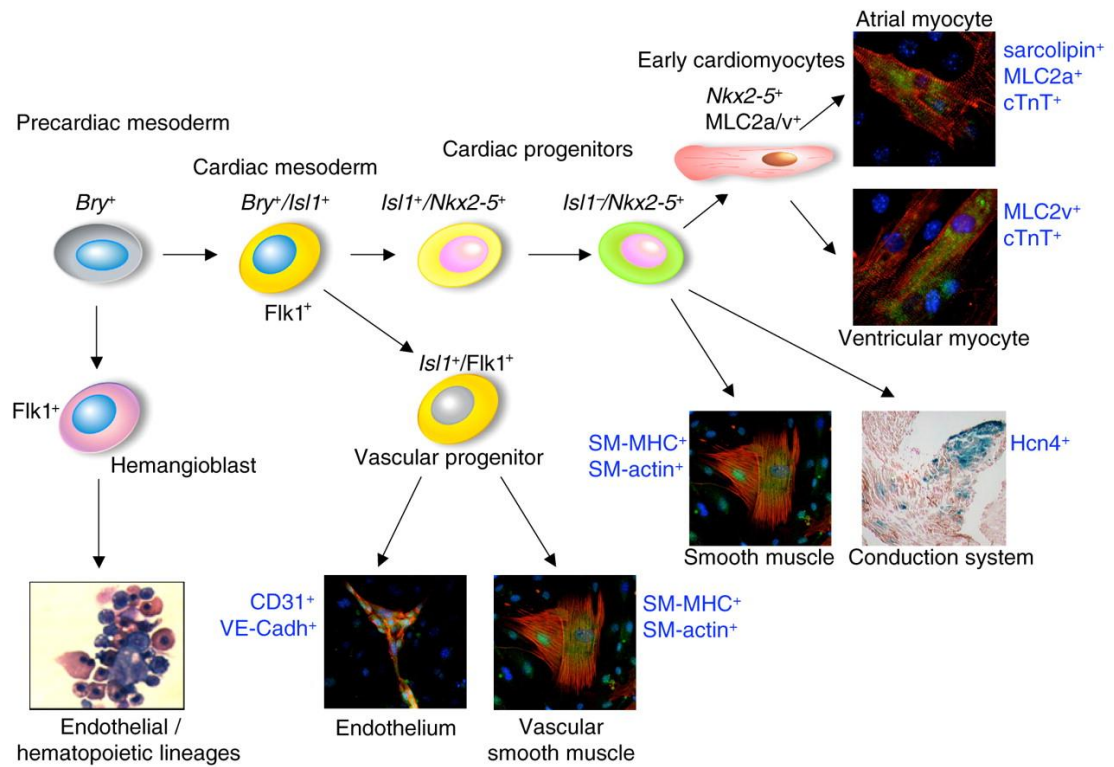


Figure 1.2. **Cardiac progenitor cells and their lineage.** Endothelial and hematopoietic lineages form from a hemangioblast which originates from precardiac mesoderm. The remaining cardiac cell types form from the cardiac mesoderm. The transcription factors *Isl1*, *Nkx2-5* and *Flk1* lead to the differentiation of the major cell types: myocytes, smooth muscle and endothelial cells. Image from (Laugwitz et al., 2008).

Cardiac morphogenesis is characterised by the same processes across species. These include fusion in the ventral midline of the myocardium and endocardium to form the heart's tubular structure, a looping of the right portion leading to development of defined chambers, mature valve formation, conduction of myocytes and flow of circulation (Kirby, 2002).

### 1.1.2 Cardiac cell types

#### Myocytes

The heart is a continually beating entity that functions to provide blood circulation throughout the body. The heart is comprised of 30% cardiac

myocytes making up 2 - 4 billion cells, which are responsible for the contractions resulting in continual regulated beating, resulting in blood circulation (Walker and Spinale, 1999; Tirziu et al., 2010). Within the heart around 1% of the myocytes are able to generate action potentials. These action potentials regulate heart contraction via nodal cells. Sinoatrial node cells, located in the right atrium, generate action potentials leading to depolarisation of the atrioventricular nodes which are located between the atrium and the ventricles. This in turn leads to depolarisation of the bundle of his which is able to generate a heart rate of around 40 - 60 beats per minute.

Contraction within cardiac myocytes is tightly regulated by calcium levels. Intracellular calcium levels increase through calcium entry utilising L-type calcium channels, which through interaction with ryanodine receptors leads to calcium-induced calcium release (CICR) from the sarcoplasmic reticulum. This vast increase in calcium allows for sufficient binding to cardiac troponin C (cTnC), which releases the cardiac troponin inhibitor (cTnI) from the myofilaments allowing for cellular contraction. Relaxation of the cardiac myocyte is regulated using the ATP transporter sarcomeric and endoplasmic reticulum calcium ATPase (SERCA) to transport calcium back into the sarcoplasmic reticulum. Additionally calcium can be removed from the cardiac myocyte by the sodium calcium exchanger (NCX) which removes one calcium ion in exchange for three sodium ions.

The heart is regulated by the parasympathetic nervous system by the cranial nerve X. This regulates cardiac homeostasis. In events such as stress, the sympathetic nervous system takes over to increase the rate and force of contraction allowing the body to exert the 'fight or flight' response.

### *Non-myocyte cells*

The additional 70% of the cardiac myocardium is comprised of fibroblast, endothelial, pericyte and smooth muscle cells. Fibroblasts account for the largest portion of the non-cardiomyocyte cells. They are located between cardiomyocytes and function to provide structure to the myocardium by regulation of the extracellular matrix (Souders et al., 2009). Fibroblasts regulate the phenotype of cardiomyocytes through extracellular matrix generation. Cardiac fibroblasts are also thought to facilitate cardiomyocyte contraction (Souders et al., 2009). Cardiac fibroblasts are able to regulate the microvasculature through secretion of proteins including: collagen 1 and fibronectin (Souders et al., 2009).

Endothelial cells form the luminal face of the vasculature. From a single layer of cells they form tubular structures possessing the ability to regulate the movement of ions, oxygen and free fatty acids from the circulation to surrounding cells in the tissue. Vasculature can be divided into two main vessel types: macrovasculature and microvasculature (Fig. 1.3). The macrovascular comprises a monolayer of endothelial cells (*tunica intima*) surrounded by basement membrane, and smooth muscle which allows for vessel contraction (*tunica media*) and supportive connective tissue (*tunica adventia*). The microvasculature comprises of *tunica intima* and a basement membrane. Approximately 95% of the vasculature within humans is comprised of microvessels. Endothelial cells are heterogenous in size and morphology in different anatomical regions.

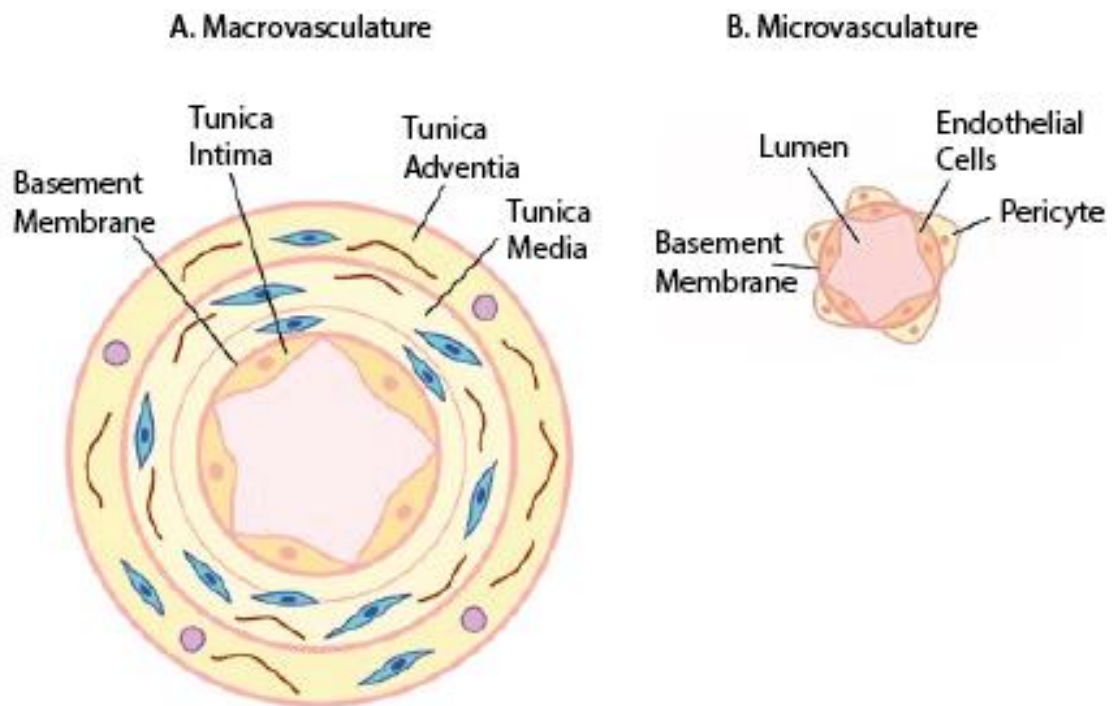


Figure 1.3. **Structure of vasculature.** A. Macrovasculature is comprised of tunica intima surrounded by basement membrane, tunica media and tunica adventia. B. Microvasculature has a more simplistic structure consisting of a single layer of endothelial cells surrounded by a basement membrane and pericytes.

Endothelial cells express a wide range of proteins including: adhesion proteins PECAM-1 (platelet endothelial cell adhesion molecule -1 also known as CD31, cluster of differentiation 31) and RECA-1 (rat endothelial cell antigen-1) (Ulger et al., 2002). CD31 is currently the most widely used endothelial cell marker for human and rat. However, there is increasing popularity for the more recently discovered RECA1, rat specific endothelial cell marker that can be utilised when staining rat cells. CD31 and RECA1 are transmembrane proteins involved in endothelial cell adhesion (Ulger et al., 2002; Duijvestijn et al., 1992). CD31 belongs to the IgG superfamily involved in inflammatory responses. CD31 is expressed on platelets, monocytes and neutrophils as well as endothelial cells (Chiba et al., 1999). Through hemophilic and heterophilic interactions, CD31 regulates physiological events including recruitment of monocytes and neutrophils to the site of inflammation through trans-



endothelial migration (Chiba et al., 1999). Additionally CD31 is key in endothelial – leukocyte interactions. Microvascular endothelial cells are surrounded by specialist smooth muscle cells, known as pericytes. Pericytes function to provide structure to the microvasculature and are thought to be embedded within the basement membrane (Armulik et al., 2011). There are many interactions between endothelial cells and pericytes controlling physiological processes such as proliferation, vessel stabilisation, pericyte coverage and differentiation (Armulik et al., 2011). It is also known that pericyte markers are notoriously difficult to define as many are also present within other cell types. The most widely used pericyte marker is NG2 (chondroitin sulphate proteoglycan 4, CSGP4).

The formation of a new blood vessel is known as vasculogenesis and the formation of a blood vessel from a preexisting vessel is known as angiogenesis, these processes are outlined in figure 1.4. Tumour blood vessels lack the pericytes and organisation that normal vasculature expresses, they are also known to be unable to reach the quiescent state exerted by normal vasculature as they remain a proliferating entity (Furuya et al., 2005). The neovascularisation of a tumour is outlined in figure 1.5.

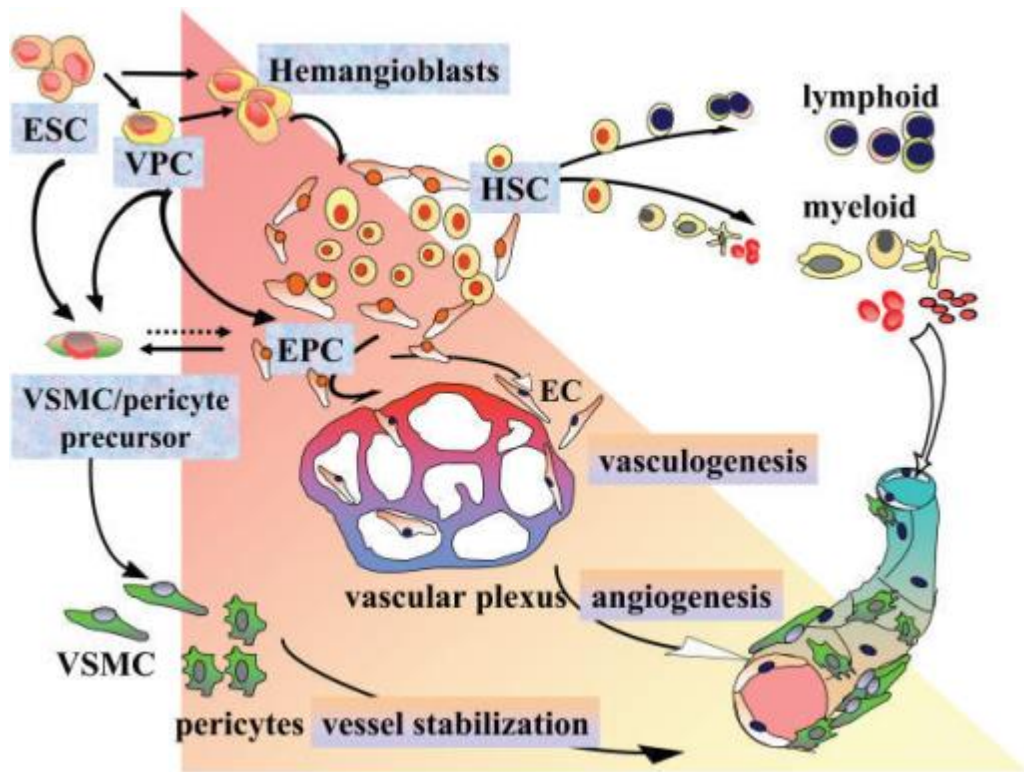


Figure 1.4. ***Vasculogenesis and angiogenesis following stem cell differentiation.*** Endothelial cells are able to form a vascular plexus following differentiation which leads to formation of new blood vessels, termed vasculogenesis. From these blood vessels new vessels can form in a process known as angiogenesis. Capillary vessels can further recruit pericytes a specialist smooth muscle cell that is able to promote vessel stabilisation. Image from (Furuya et al., 2005).

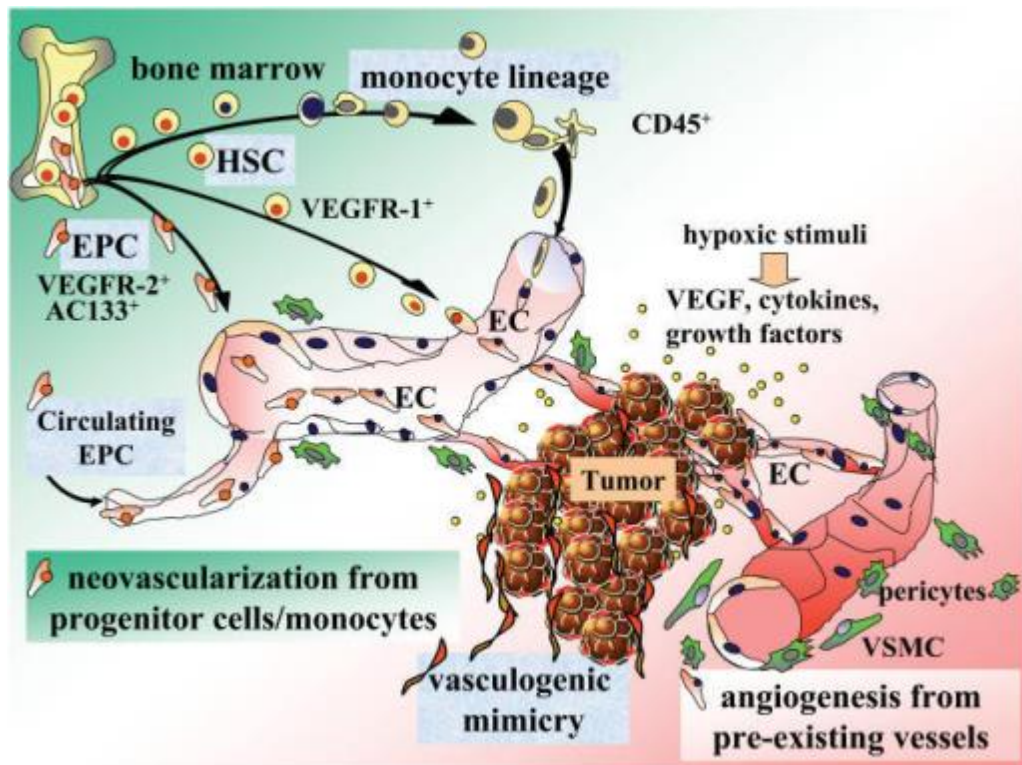


Figure 1.5. **Tumour neovascularisation.** The formation of vascular in tumours forms mainly from angiogenesis. The tumour vascular lacks the normal stabilisation from pericytes as the vasculature is unable to recruit them. This figure shows how tumour vascular is irregular where the normal vascular forms organized tubes surrounded by pericytes. This gives a clear indication of differences in vessel structure. Image from (Furuya et al., 2005).

Endothelial cells regulate transport between blood/lymph and tissues through expression of various influx and efflux transporter proteins. These transporters are able to regulate the trans-cellular movement of essential solutes, oxygen, fatty acids and ions from the circulation to surrounding cells and enable normal physiological functions such as cardiomyocyte contraction. The transporters are important to maintain an optimum concentration of solutes and electrolytes within the cells and play a role in maintaining the concentration gradients that are required for cellular processes such as removal of toxins (Cheng and Force, 2010). Drugs and their metabolites are able to utilise these transporters in order to gain entry to the cells.

Endothelial cells are quiescent until the presence of growth factors or cytokines, in which case they have the ability to migrate in order for wound healing (cellular migration) and angiogenesis (Lamallice et al., 2007). Angiogenesis is defined as the formation of a new blood vessel as an extension from preexisting vessels (Seghezzi et al., 1998). In order for these processes to occur the cells must be exposed to certain growth factors. The most important growth factors in migration and angiogenesis includes vascular endothelial cell growth factor (VEGF), fibroblast growth factor (FGF) and the angiopoietins (Lamallice et al., 2007). Other cytokines that play a smaller role in migration and angiogenesis include hepatocyte growth factor (HGF), platelet-derived growth factor (PDGF), epithelial growth factor (EGF), transforming growth factor (TGF- $\beta$ ), interleukins, tumor necrosis factor (TNF- $\alpha$ ), platelet-activating factor, ephrins, soluble adhesion molecules, endoglin and angiogenin (Lamallice et al., 2007).

## **1.2 Endothelial Cell Barrier**

The endothelial barrier has a critical role in preventing drugs and toxins permeating from the circulation to surrounding tissues (Ishiguro et al., 2004; Gonzalez-Mariscal et al., 2005). The barrier is tightly regulated with junctions and transporters that only allow ions, solutes and free fatty acids that are important for maintaining tissue physiological processes to permeate the barrier. As different tissues require different ions, solutes and free fatty acids the junctions and transporters expressed on endothelial cells from different anatomical locations are thought to vary.

The blood brain barrier (BBB) is a highly impermeable barrier, which is well documented for the inability of drugs to permeate to the brain (Garg et al., 2015). In contrast to this, the liver microvasculature is fenestrated, which allow the endothelial cells to be highly permeable to drugs. This is important for normal hepatic function as the liver provides the main site

of drug metabolism; in order for drugs to be metabolised they need to pass from the circulation to the hepatocytes.

There are many proteins involved in maintaining the endothelial barrier. These proteins form various types of junctions and transporters. The two methods of drug permeation to the underlying myocytes are outlined in figure 1.6.

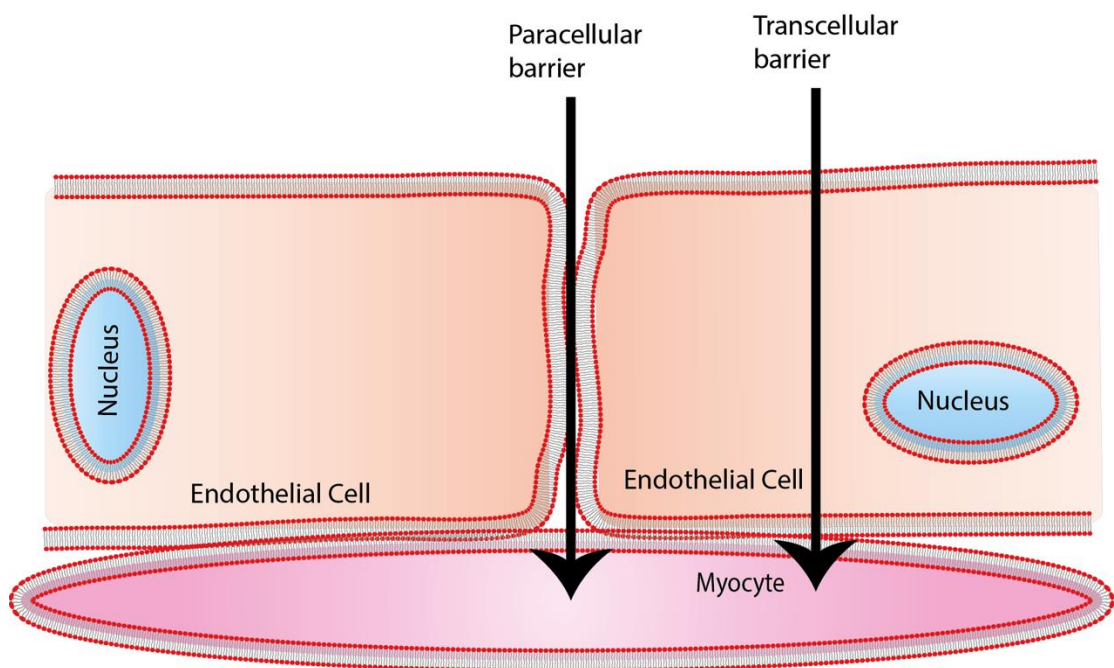


Figure 1.6. **Transport routes for solutes, ions and free fatty acids through endothelial cells.** Endothelial cells provide a barrier to underlying cells; within the heart these cells include myocytes, fibroblasts or smooth muscle cells. This barrier is comprised of two transport routes paracellular transporter (between endothelial cells) and transcellular transport (through the endothelial cells).

### 1.2.1 Paracellular route

There are a number of different junctions between endothelial cells, which are involved in cell-cell communication and permeability. An outline of the different junctions and their anatomical locations is shown in figure

1.7. Between most endothelial cells the tight junctions are located apically, these junctions function to regulate permeability (Niessen, 2007; Fazakas et al., 2011). During development cell-cell adhesion is critical (Katsuno et al., 2008). The molecules involved in cellular adhesion associate with peripheral membrane proteins through integral membrane proteins (Katsuno et al., 2008). Tight junctions play an important role in both high (brain) and low (aorta) resistant endothelial cells (Li and Poznansky, 1990). Their main role is to limit the paracellular movement of ions, water and drugs (Gonzalez-Mariscal et al., 2005; Fazakas et al., 2011). Tight junctions comprise several proteins, these include the transmembrane proteins: occludin, claudin and adhesion molecules; and cytoplasmic plaque proteins, functioning to connect the transmembrane proteins of junctions to the cytoskeleton, these include: ZO-1 – 3 and cingulin. ZO-1 is used as a classical marker for tight junctions (Fazakas et al., 2011). ZO-1 belongs to the membrane associated guanylate kinase (MAGUK) family (Katsuno et al., 2008). The MAGUK ZO-1 contains a PDZ domain and a guanylate kinase (GUK) domain, which interacts with claudins and occludins respectively (Katsuno et al., 2008). It has been reported by (Katsuno et al., 2008) that the ZO-1 knock out produced a lethal phenotype at embryonic day 9.5-10.5, indicating a crucial role for ZO-1 in tissue organisation and remodeling in embryogenesis (Katsuno et al., 2008).

The transmembrane proteins can vary in expression depending on their anatomical location. Permeability is regulated by the various subtypes of these transmembrane proteins demonstrating different selective permeability. Adherens junctions are commonly located basolaterally to tight junctions; there is evidence to show they are involved in the maintenance and development of tight junctions (Fazakas et al., 2011). Adherens junctions are also comprised of transmembrane proteins, known as cadherins and cytoplasmic proteins known as catenins (Fazakas et al., 2011). Assembly of tight and adherens junctions involves the activation of intracellular signaling cascades, these include afadin



activation (Birukova et al., 2012). Afadin is a scaffold protein that contains actin-binding and Ras-binding domains that can be activated by Rap1, a small GTPase involved in cell adhesion dynamics (Birukova et al., 2012).

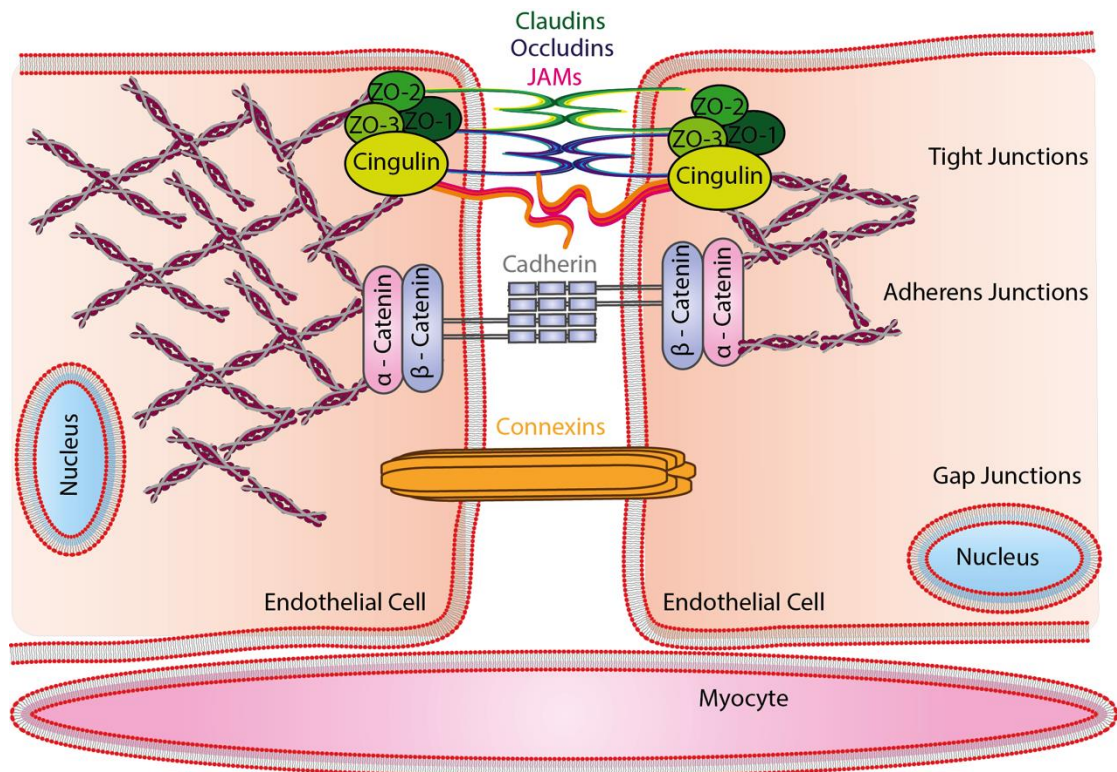


Figure 1.7. **Endothelial cell paracellular barrier.** Endothelial cells express tight, adherens and gap junctions that function to regulate paracellular permeability. Tight junctions comprise transcellular claudins, occludins and JAMs connected to intracellular ZO-1-3 and cingulin, which connects to the actin cytoskeleton. Adherens junctions utilise  $\alpha$  and  $\beta$  catenins to connect the actin cytoskeleton to transcellular cadherins. Gap junctions form a pore of connexins allowing paracrine signalling between adjacent endothelial cells. Influx and efflux transporters utilise concentration gradients to passively or actively transport ions, fatty acids or toxins into or out of cells. ZO-1 – zona occludins 1.

VE-cadherin is an important protein in adherens junctions where its role is to help form a protective barrier between adjacent endothelial cells (Kevil et al., 1998). This is achieved by  $\alpha$  and  $\beta$  catenins and plakoglobin interactions with the cytoskeleton actin filaments forming homotypic

calcium dependent bonds (Kevil et al., 1998). VE-cadherin also has a role in mediating adhesion of intracellular proteins (Kevil et al., 1998). The structure of the junctions can be observed in figure 1.7.

### *1.2.2 Transcellular route*

The plasma membrane provides a barrier to hydrophilic compounds. Drugs that have lipophilic properties are able to freely diffuse through the plasma membrane and gain entry to the cells. Other drugs have more hydrophilic properties and are able to use transporters to gain entry to the cells, outlined in figure 1.8. Transporters are able to facilitate the movement of ions across the plasma membrane with the use of concentration gradients and ATP. Endothelial cells also poses the potential for transcellular transport mediated by endocytosis. This transport method utilises vesicles, either by pinocytosis or a receptor-mediated method, where drugs bind to a receptor and the drug becomes endocytosed into a vesicle to gain entry to the cell.

Endothelial cells express many transporters on their cell membrane that function as drug efflux and influx transporters. They have an important role in allowing drugs that do not have lipophilic properties to gain access to cells. The current efflux transporters of interest for anticancer treatment, specifically doxorubicin, includes: P-glycoprotein (P-gp, MDR1 or ABCB1), multidrug resistant-associated protein (MRP, ABCC1), ABCG2, ABCC2 and ABCC4 (Sugiyama et al., 2001; Okabe et al., 2005; Calcagno et al., 2008). These transporters are known to be utilised in doxorubicin removal from cells (Sugiyama et al., 2001). Many of the efflux transporters belong to the ATP binding cassette (ABC) transporters class (Calcagno et al., 2008). These transporters utilise ATP to pump toxins such as drugs out of the cell against the concentration gradient (Calcagno et al., 2008).



Transporters that are utilised, in anti-cancer drugs influx, belong to the organic cation transporter (OCT) family. The ones currently known to be involved in anti-cancer drug influx include: SLC22A1 (OCT1), SLC22A2 (OCT2), SLC22A3 (OCT3), SLC22A4 (OCTN1) and SLC22A5 (OCTN2) (Okabe et al., 2005).

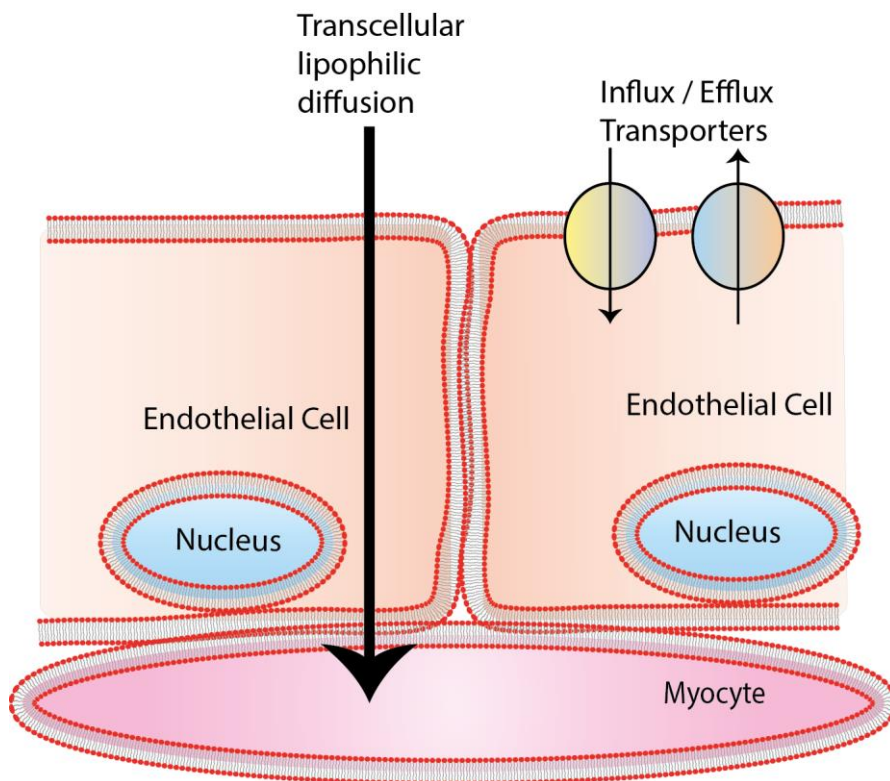


Figure 1.8. **Transcellular mediated transport through endothelial cells.** Endothelial cells allow transcellular transport of drugs primarily through two methods depending on the drugs physical-chemical properties. Drugs that possess lipophilic properties are able to freely diffuse across the membrane in transcellular lipophilic diffusion. Drugs with more hydrophobic properties are able to utilise transporters to gain entry to the cell.

### 1.3 Cellular regulation

Endothelial cell physiology is tightly regulated by a range of signalling cascades, which allow the endothelial cells to respond to the external environment. These signalling cascades are activated by extracellular stimuli such as growth factors, cytokines or oxidative stress which lead to

transmembrane receptor dimerisation and phosphorylation of downstream signalling molecules.

### 1.3.1 Growth factor regulation

#### VEGF

The VEGF family of growth factors includes: VEGF-A, VEGF-B, VEGF-C, VEGF-D and VEGF-E (Lamallice et al., 2007; Harhaj et al., 2006; Jia et al., 2004; Bruns et al., 2010; Besse et al., 2010; Sulpice et al., 2009). VEGF-A is predominantly responsible for the majority of the endothelial physiological responses by activating VEGFR-2. There are many different splice variants of VEGF-A, each differing in the number of amino acids, the most abundant in human being VEGF-A<sub>165</sub> and in rat being VEGF-A<sub>164</sub> (Lamallice et al., 2007; Chiusa et al., 2012). VEGF-A is produced by cells such as endothelial, cancer and vascular smooth muscle cells and exerts its actions on endothelial cells in either an paracrine or autocrine manner (Chiusa et al., 2012). VEGF-A is released from cells in response to hypoxia, angiotensin II and reactive oxygen species (Chen et al., 2013). The promotor region of *VEGF-A* is known to contain a hypoxia responsive element (HRE) which explains why the effects of hypoxia and oxygen levels play an important role in VEGF-A expression (Seghezzi et al., 1998). It is known that hypoxia increase the level of VEGF-A in certain cancers reviewed by (Holmes et al., 2007). Increased VEGF-A is a known response to the external hypoxia. Hypoxic conditions are important in tumour angiogenesis as many tumours without an established vasculature survive in hypoxic conditions. Tumour cells rely on glucose so under hypoxic conditions they are able to upregulate glucose transporters allowing for increase cellular uptake of glucose (Hanahan and Weinberg, 2011).

The angiogenic growth factor VEGF-A is known to activate both VEGFR-1 (also known as Flt-1) and VEGFR-2 (also known as Flk1 and KDR) (Chiusa et al., 2012). There is an additional receptor present on vascular as well as lymphatic endothelial cells, termed VEGFR-3 (also known as Flt4) (Cudmore et al., 2012). VEGF-A has a higher affinity for VEGFR-1 (Jia et al., 2004) but VEGFR-2 has a higher expression level within endothelial cells (Chiusa et al., 2012). It is thought that most, if not all of the response to VEGF-A on vascular endothelial cells, is mediated by VEGFR-2 activation (Lamallice et al., 2007). The biological function of VEGFR-1 has not currently been extensively researched but is thought to be involved in VEGF-A sequestering in endothelial cells (Jia et al., 2004; Barkefors et al., 2008). VEGFR-2 is stimulated by the VEGF-A ligand which leads to receptor dimerisation and phosphorylation of the tyrosine residues: Tyr-951 and Tyr-996; Tyr-1054 and Tyr-1059; Tyr-1175 and Tyr-1214 in the kinase domain, kinase insert domain and C-terminus (Jia et al., 2004). VEGF-A<sub>165</sub> is the most abundantly expressed isoform of VEGF-A (Barkefors et al., 2008). It also has the ability to not only interact with VEGFR-2 but also bind to heparin sulfate proteoglycans (HSPGs) present on the surface of cells and neuropilins (Barkefors et al., 2008).

VEGFR-2 is known to be critical for embryogenesis (Matthews et al., 1991; Yamaguchi et al., 1993). It has been demonstrated that the VEGFR-2<sup>-/-</sup> mice, produce an embryonic lethal phenotype at E8.5-9.5 (Shalaby et al., 1995). This phenotype was lethal due to the defects in the blood islands, endothelial cells and haematopoietic cells (Shalaby et al., 1995; Millauer et al., 1993). It has been observed that the blood islands are missing from the yolk sac at E7.5 in VEGFR-2<sup>-/-</sup> mice (Shalaby et al., 1995).

VEGFR-2 is known to be important in vasculogenesis (Shalaby et al., 1995). VEGFR-2 is known to be important in vascular homeostasis not just embryogenesis (Peters et al., 1993). VEGFR-2 phosphorylation allows for the coordinated differentiation and migration of endothelial cells

characterised as angiogenesis (Barkefors et al., 2008). It is involved in endothelial cell migration in response to VEGFR-2 activation (Cudmore et al., 2012; Bruns et al., 2010; Sulpice et al., 2009). VEGFR-2 belongs to the family of receptor tyrosine kinases (RTKs). These receptors upon activation lead to the phosphorylation of intracellular signalling kinases. The kinases signalling downstream of VEGFR-2 include ERK and AKT as they are involved in proliferation and survival respectively, the simplified pathways are shown in figure 1.9.

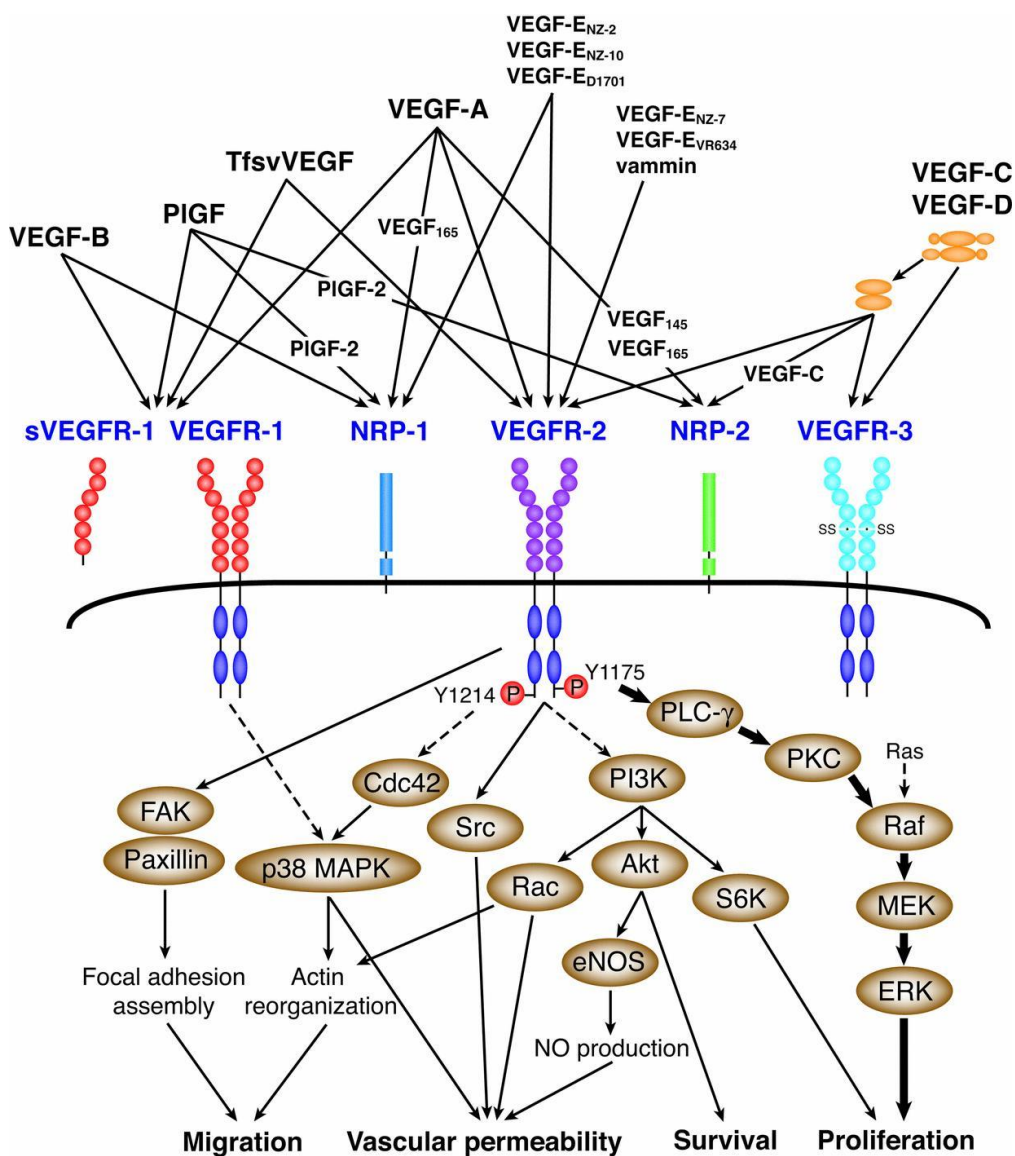


Figure 1.9. **Receptor signalling cascade following receptor dimerisation.** VEGFR-2 dimerises upon the ligand binding to the

receptor ligand binding domain. This ligand can include VEGF-A-E, depending on the cell type and specific receptor expressed. On endothelial cells this is primarily VEGFR-2. Ligand binding induces receptor phosphorylation stimulating a downstream signalling cascade involving PI3K and AKT which functions to regulate physiological processes such as vascular permeability and endothelial cell survival. An additional pathway also known to regulate proliferation includes the Ras, Raf, MAPK and ERK signalling pathway. VEGFR activation can also stimulate migration through signaling kinases FAK and p38. *VEGF – vascular endothelial growth factor, VEGFR – vascular endothelial growth factor receptor, PI3K – phosphoinositide kinase 3, MAPK – mitogen activated protein kinase, ERK – extracellular regulated kinase, FAK – focal adhesion kinase, eNOS – endothelial nitric oxide synthase.* Image from (Takahashi and Shibuya, 2005).

## EGF

The EGFRs belong to the receptor tyrosine kinase family and consists of four members EGFR1-4 (Bazley and Gullick, 2005). EGFRs are also referred to as HER1-4 and ErbB1-4. These receptors can be activated in response to growth factors such as EGF, TGF- $\alpha$  and NRG-1 (Bazley and Gullick, 2005). These growth factors interact with the ligand binding domains located on EGFR1, 3 and 4 (Bazley and Gullick, 2005), currently there is no ligand binding domain known to be expressed on EGFR2. Upon ligand binding EGFR1, 3 and 4 are able to homodimerise or heterodimerise with EGFR2 (Fig. 1.10) leading to receptor phosphorylation and intracellular signalling cascade phosphorylation which can result in cell survival, proliferation, migration and angiogenesis (Bazley and Gullick, 2005; Arkhipov et al., 2013). EGFRs are known to be over expressed in many cancers. There are several monoclonal antibodies that target EGFRs, such as Erbitux® (cetuximab) for EGFR1 and Herceptin® (trastuzumab) for EGFR2. Protein kinase inhibitor (PKI) lapatinib (Tykerb®) has been demonstrated to inhibit both EGFR1 and EGFR2 (Yewale et al., 2013). These anti-cancer therapies have success in cancer overexpressing EGFRs as they are a direct target for the receptor that is over expressed in the cancer.

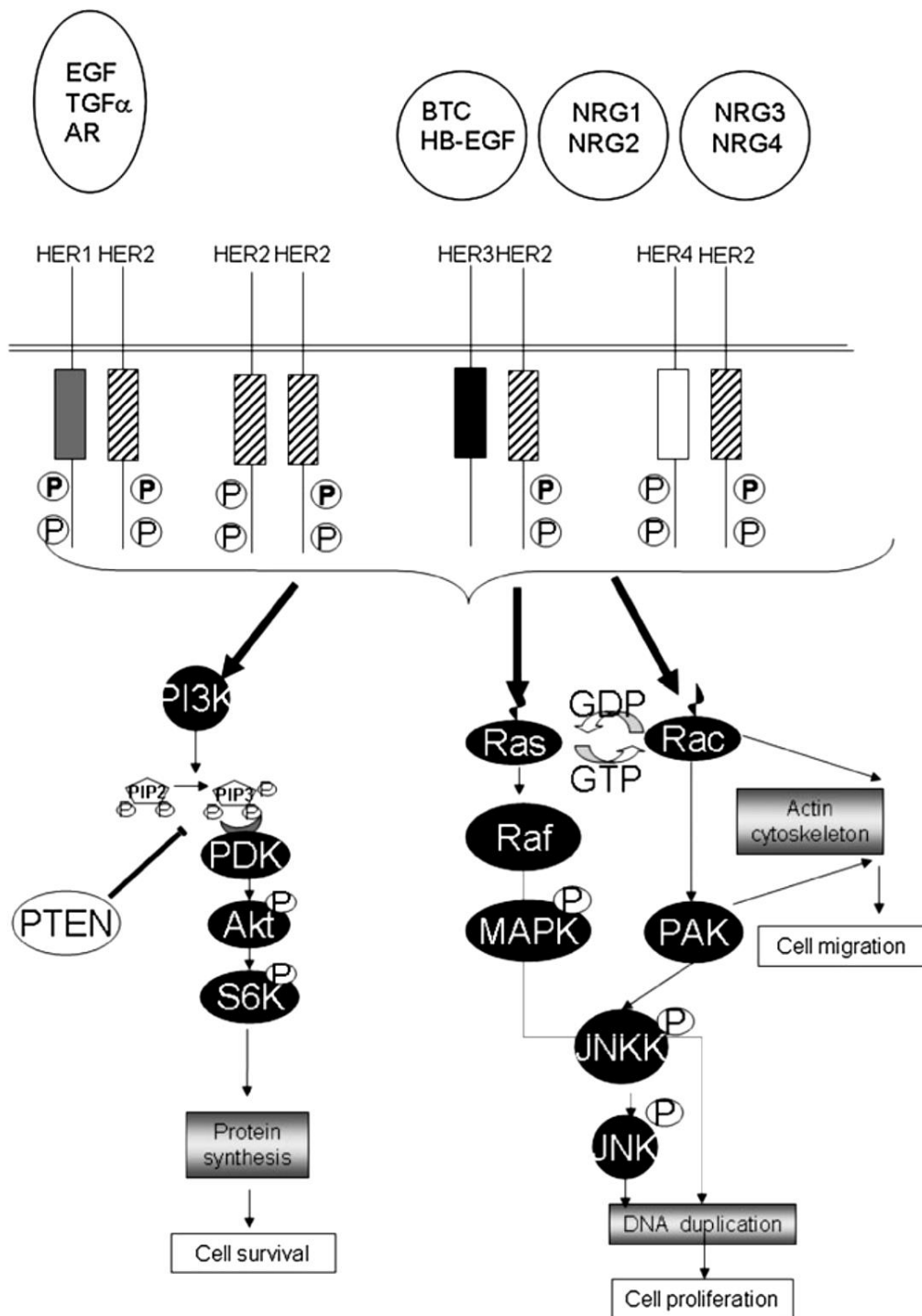


Figure 1.10. **EGFR dimerisation.** EGFR2 heterodimerises with EGFR1, 3 and 4. EGFR3 heterodimerises with EGFR2 only. Receptor activation induces cell proliferation, survival and permeability. Figure from (Valabrega et al., 2007). *HER* – human epidermal growth factor receptor.



## FGF

FGF is another angiogenic factor that also plays an important role in endothelial survival, migration and proliferation (Barkefors et al., 2008). Currently there are twenty four different known FGF isoforms, four of which belong to the FGF-2 isoform. FGF-2 (basic FGF) is thought to be the most important FGF in endothelial physiology (Seghezzi et al., 1998). The 4 main isoforms of FGF-2, are distinguished by molecular weight, these include 18, 22, 22.5, and 24 kDa (Seghezzi et al., 1998). Each isoform of FGF-2 has different physiological functions, for example the low molecular weight FGF-2 (18 kDa) is responsible for FGF receptor down regulation, migration as well as proliferation, it can be found extracellularly (Seghezzi et al., 1998). In contrast, the highest molecular weight FGF-2 (24 kDa) can only be found in the nucleus where it functions in cell proliferation (Seghezzi et al., 1998). FGFs mediate their biological effects by activating FGF receptors present on a range of cells including fibroblasts and endothelial cells.

## HGF

HGF is also thought to be involved in angiogenesis (Ding et al., 2003). HGF is also known as scatter factor (SF) (Ding et al., 2003). HGF is able to induce angiogenesis indirectly through stimulating surrounding cells to release angiogenic mitogens (Ding et al., 2003). HGF directly activates HGFR the MET proto-oncogene (c-met), which encodes a tyrosine kinase. Upon activation of HGFR leads to an intracellular signalling cascade via receptor phosphorylation that leads to angiogenesis, VEGFR-2 expression, vascular matrix degradation, migration, proliferation, tubular formation and release of anti-apoptotic factors (Ding et al., 2003).

### *1.3.2 Intracellular signalling*

Plasma membrane receptor activation precedes a downstream intracellular signalling cascades resulting in cellular responses such as cell survival, proliferation, migration or permeability. Regulation of these physiological responses is controlled by a multitude of mitogen-activated protein kinases (MAPKs). MAPKs phosphorylate serine and threonine residues following proline residues (Drew et al., 2012). MAPKs can be activated via G-protein coupled receptors as well as RTKs in response to a stimuli leading to phosphorylation of a typically three tier signalling cascade starting with activation of mitogen activated kinase kinase kinase (MAPKKK), which can further phosphorylate downstream mitogen activated kinase kinase (MAPKK) and in turn mitogen activated kinase (MAPK), illustrated in figure 1.11 (Drew et al., 2012; Roskoski, 2012). The protein kinase family represents 1.7% of the total genome and includes 518 genes; divided into 385 serine/threonine kinases, 90 tyrosine kinases, 43 tyrosine kinase like and 106 pseudogenes (Roskoski, 2012).



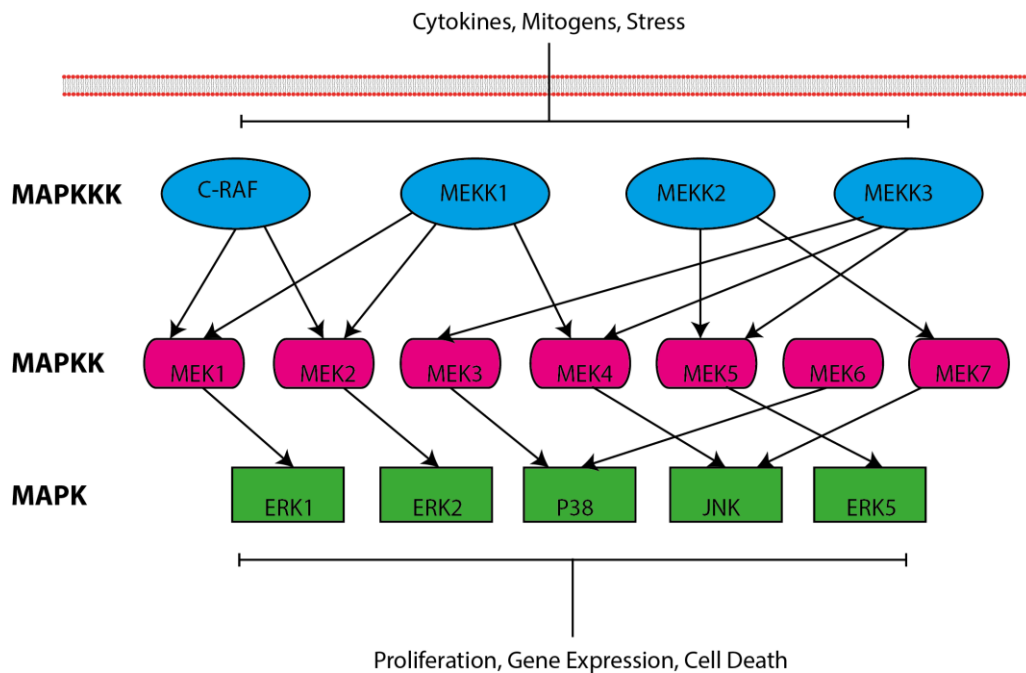


Figure 1.11. **Intracellular signalling of mitogen activated protein kinases.** Extracellular factors including cytokines, mitogens and stress lead to activation of cellular receptors, which upon activation lead to downstream signalling. Receptor activation induced phosphorylation of the MAPKKKs C-RAF, MEKK1-3 which can in turn phosphorylate downstream MAPKK: C-RAF which phosphorylates MEK1 and 2, MEKK1 which phosphorylates MEK1,2 and 4, MEKK2 which phosphorylates MEK5 and 7, MEKK3 which phosphorylates MEK3,4 and 5. These can phosphorylate the downstream MAPKs. MEK1 phosphorylates ERK1, MEK2 phosphorylates ERK2, MEK3 phosphorylates P38, MEK4 phosphorylates JNK, MEK5 phosphorylates ERK5, MEK6 phosphorylates P38 and MEK7 phosphorylates JNK. Adapted from (Drew et al., 2012). *MAPKKK/MEKK* – mitogen activated kinase kinase kinase, *MAPKK/MEK* – mitogen activated kinase kinase, *MAPK* – mitogen active kinase, *ERK* – extracellular signal regulated kinase, *JNK* – c-jun-N-terminal kinase.

The subfamily members that are involved in mammalian cellular response such as proliferation, apoptosis and gene expression including MAPKKK C-RAF, MEKK1, MEKK2 and MEKK3, the MAPKK includes MEK1-7 and the MAPK includes ERK1-8, P38 $\alpha/\beta/\gamma/\delta$  and JNK1-3 (Drew et al., 2012; Roskoski, 2012).

Some anti-cancer therapies target receptor tyrosine kinases and intracellular protein kinases and hence will have effects on the intracellular MAPKs. Sorafenib (Nexavor®) and sunitinib (Sutent®) target VEGFR-2 as well as other kinases. Doxorubicin an anthracycline antibiotic chemotherapeutic agent is known to have effects on ERK, p38 and JNK signalling (Choi et al., 2008; Spallarossa et al., 2010; Yang et al., 2013; Grethe et al., 2006).

## ERK1/2

Prototypic MAPK ERK1/2 are ubiquitously expressed and share 84% sequence homology (Mori et al., 2000; Cale and Bird, 2006). ERK1/2 contributes to the Ras-Raf-MEK-ERK signalling cascade (Mori et al., 2000; Cale and Bird, 2006). The cascade results in cellular processes including cell cycle progression, migration, survival, adhesion, transcription, proliferation and metabolism (Mori et al., 2000). ERK1/2 have been implicated in the regulation of endothelial barrier permeability (Liu et al., 2014). Human ERK1 comprises 379 amino acids while rat ERK1 comprises 380 amino acids; human ERK2 comprises 360 amino acids while rat ERK2 comprises 358 amino acids, it is thought that ERK1/2 differs more between species than between the two ERK isoforms (Cale and Bird, 2006).

ERK1 and 2 have a flexible hinge region which allows for positioning of the ATP adenosine to form a hydrophobic interaction with the conserved

valines in ERK1 V56 and ERK2 V39 that proceed the glycine rich region (Roskoski, 2012).

There is evidence to suggest that ERK2 plays a more critical role within development of mice than ERK1 as ERK2 null mice produce a lethal phenotype.

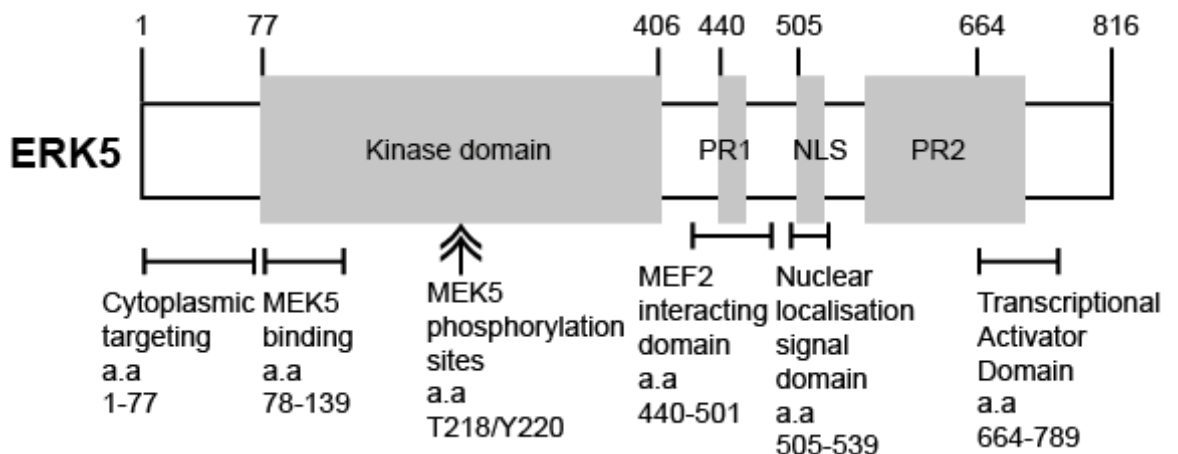


Figure 1.12. **Structure of human extracellular regulated kinase 5 (ERK5).** ERK5 is composed of 816 amino acids (a.a). ERK5 comprised a cytoplasmic targeting N-terminal domain (a.a 1-77) followed by a kinase domain (a.a 77-406) which contains a MEK5 binding domain (a.a 78-139) and MEK5 phosphorylation sites (a.a T218/Y220). The extended C terminal expresses proline rich regions 1 (a.a 434-485) and 2 (a.a 578-701), (PR1, 2) and nuclear localisation signal (a.a 505 – 539, NLS). MEF2 is able to interact with the C-terminus at a.a 440-501, and C terminal transcription activation occurs at a.a 664-789. Adapted from (Nithianandarajah-Jones et al., 2012; Roskoski, 2012). *ERK* – extracellular regulated kinase, *NLS* – nuclear localisation signal, *PR* – proline rich, *MEK* – mitogen activated protein kinase kinase, *a.a* – amino acids.

## ERK5

ERK5 was identified in 1995 by two independent research groups (English et al., 1999; Zhou et al., 1995; Lee et al., 1995). ERK5 has been demonstrated to be expressed in a range of tissues but appears most abundant in heart, placenta, kidney and skeletal muscle (Lee et al., 1995; Zhou et al., 1995). ERK5 contains a kinase domain with 66% homology

to ERK2. ERK5 differs from conventional MAPKs in its size as it has been demonstrated to be almost double the size. The extended size is primarily due to its extended C-terminal (approximately 400 amino acids) tail consisting of a nuclear localisation signal (NLS) amino acids 505-539 and proline rich region 1 and 2 (PR1 and 2) amino acids 434-465 and 578-701 (Hayashi et al., 2004; Lee et al., 1995). The structure of ERK5 is outlined in figure 1.12. The nuclear targeting of ERK5 is regulated by the NLS domain. This domain allows ERK5 to be translocated to the nucleus when expressed as an unfolded protein and expressed in the cytoplasm in a folded conformation. This occurs in response to the generation of a nuclear export signal (NES) interaction between the N and C terminals (Hayashi et al., 2004). The C-terminal of ERK5 contains a unique transcriptional activation domain, amino acids 664-789, which regulates gene transcription through autophosphorylation, a unique feature of ERK5 (Kasler et al., 2000). The proline rich regions are thought to provide MEF2 and Src-homology 3 (SH3) binding sites (Hayashi et al., 2004).

Each of the four known MAPKs have been identified within the heart and implicated in various disease states. The ERK5 pathways specifically have been implicated in angiogenesis as well as vasculogenesis and cardiac hypertrophy (Roberts et al., 2010; Hayashi et al., 2004). ERK5<sup>-/-</sup> mice demonstrate a lethal phenotype at E 9.5-11.5 summarised in table 1.1 (Hayashi et al., 2004). The vasculature from the heart in ERK5<sup>-/-</sup> appears to be irregular and rounded suggesting that cell death is occurring, it has also been noted that there are gaps between the cells potentially producing a leaky phenotype (Hayashi et al., 2004).

<b>Genotype</b>	<b>Phenotype</b>	<b>Reference</b>
MEKK3 <sup>-/-</sup>	Lethal at E 11.0 due to severe angiogenesis defects. Vasculogenesis appears unaffected	(Yang et al., 2000)
MEKK2 <sup>-/-</sup>	Mice are viable with normal development. Alterations in cytokines are observed	(Kesavan et al., 2004; Garrington et al., 2000; Guo et al., 2002)
MEK5 <sup>-/-</sup>	Lethal at E 10.5 due to defective cardiac development.	(Wang et al., 2005)
ERK5 <sup>-/-</sup>	Lethal at E 9.5 – 11.5 due to defects in cardiac development and heart folding.	(Hayashi et al., 2004; Yan et al., 2003; Regan et al., 2002; Sohn et al., 2002)
ERK5 <sup>-/-</sup> Endothelial	Lethal at E 9.5-10.5 due to cardiovascular defects and irregular endothelial formation.	(Hayashi et al., 2004)
ERK5 <sup>-/-</sup> Myocyte	Mice develop normally and are viable.	(Hayashi et al., 2004)

Table 1.1. **Summary of knock out mice phenotypes.**

Initial research provided evidence that ERK5 was activated in response to both osmotic and oxidative stresses (Abe et al., 1996). This was further expanded demonstrating that ERK5 can also be activated by growth factors present in serum (Kato et al., 1997). Specific growth factors that have been identified as activating ERK5 include: VEGF-A (Hayashi et al., 2005), EGF (Kato et al., 1997; Kamakura et al., 1999), bFGF-2 (Kesavan et al., 2004), TGF- $\beta$  (Browne et al., 2008) and PDGF (Izawa et al., 2007). ERK5 can also be activated in response to inflammatory cytokines like IL6, shear-stress (outlined in figure 1.13), hypoxia and ischemia (Carvajal-Vergara et al., 2005).

ERK5 is phosphorylated within the activation loop TEY motif on Thr<sup>218</sup>/Tyr<sup>220</sup> by MEK5, which is phosphorylated by MEKK2 and MEKK3 on Ser<sup>313</sup>/Thr<sup>317</sup> (Hayashi et al., 2004). The myocyte enhancer factor 2 (MEF2) family of transcription factors is a known downstream target for ERK5. MEF2C is phosphorylated by ERK5 on Ser<sup>387</sup> leading to increased MEF2C transcriptional activity and c-Jun gene expression increase. MEF2A and C are regulated by ERK5 and P38 whereas MEF2D is regulated specifically by ERK5. ERK5 has been implicated in AKT regulation, where it has been demonstrated to play a role in cell survival following VEGF-A stimulation (Roberts et al., 2010). ERK5 has been demonstrated to play a critical role in angiogenesis (Roberts et al., 2010). ERK5 siRNA mediated gene silencing prevents tubular morphogenesis *in vitro* indicating a role in angiogenesis (Roberts et al., 2010).

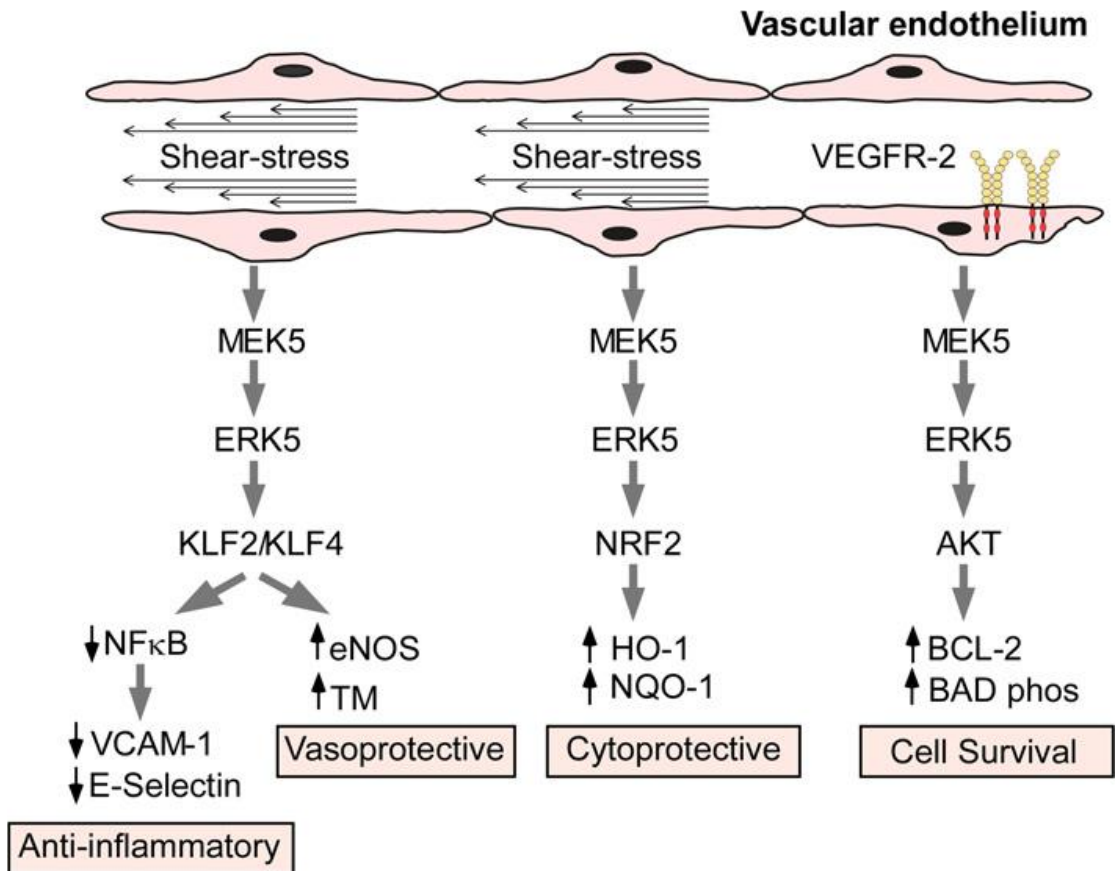


Figure 1.13. **ERK5 signalling and vascular effects.** ERK5 signalling is regulated by extracellular stimuli such as kinase receptor signaling (VEGFR-2) or shear-stress. Activation by receptor tyrosine kinase VEGFR-2 leads to cell survival through signaling with MEK5, ERK5, AKT, BCL-2 and BAD. Shear-stress leads to cytoprotective effects through MEK5, ERK5, NRF2, HO-1 and NQO-1. Shear-stress also induces vasoprotection and anti-inflammatory effects through MEK5, ERK5, KLF2/KLF4, eNOS, TM, NF $\kappa$ B, VCAM-1 and E-selectin. Image from (Nithianandarajah-Jones et al., 2014).

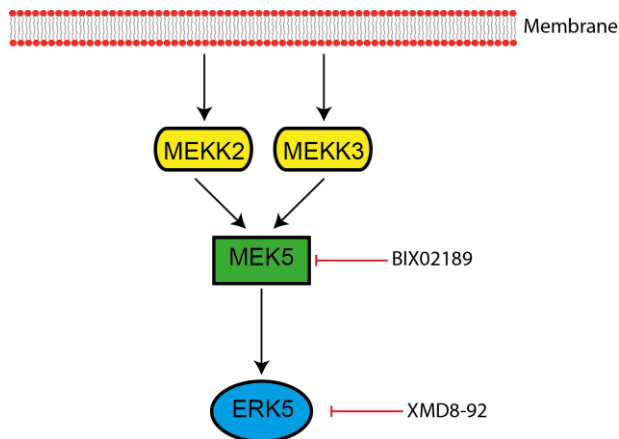


Figure 1.14. **ERK5 small molecule inhibitors.** Small molecule inhibitors known to inhibit ERK5 signalling include BIX02189 and XMD8-92. BIX02189 has been demonstrated to inhibit upstream of ERK5, at MEK5 preventing the phosphorylation of ERK5 on the T218/Y220 phosphorylation site. XMD8-92 has been demonstrated to directly inhibit ERK5.

ERK5 is inhibited by small molecule inhibitors BIX02189 and XMD8-92 (Fig. 1.14) (Tatake et al., 2008; Yang and Lee, 2011; Yang et al., 2010). It has been demonstrated that BIX02189 inhibits ERK5 phosphorylation at the T218/Y220, MEK5 phosphorylation site. This inhibition is achieved through inhibition of the upstream signalling kinase MEK5 (Tatake et al., 2008). XMD8-92 has been demonstrated to directly inhibit ERK5 preventing its activation (Yang and Lee, 2011; Yang et al., 2010). ERK5 siRNA transient mediated gene silencing shows defects in endothelial angiogenesis and overexpression of CA-MEK5 increases angiogenesis, clearly demonstrating that ERK5 has a critical role in angiogenesis regulation (Roberts et al., 2010).



## 1.4 Cardiovascular Toxicity

Drug-induced cardiovascular toxicity is defined as a severe and potentially fatal adverse reaction to certain drugs. Cardiovascular toxicity involves the heart and/or the vasculature (Mellor et al., 2011). Cardiovascular toxicity can occur in response to drugs and/or their metabolites. Cardiovascular toxicity is one of the current leading causes of drug withdrawal, in both clinical trials and post approval from the market the percentages are outlined in table 1.2 (Wu et al., 2010). Additional to adverse events for the patient this causes a great financial loss to pharmaceutical companies and additional costs to the NHS due to patient admission from adverse drug reactions (ADR) (Wu et al., 2010).

Phase	Non-clinical	Phase I	Phase I-III	Phase III/ post-approval	Post-approval	Post-approval	Post-approval
Information	Causes of attrition	Serious ADRs	Causes of attrition	ADRs on label	Serious ADRs	Withdrawal from sale	Withdrawal from sale
Source	Car (2006)	Sibille et al. (1998)	Olson et al. (2000)	BioPrint® (2006)	Budnitz et al. (2006)	Fung et al., (2001)	Stevens & Baker (2009)
Sample size	88 CDs stopped	1,015 subjects	82 CDs stopped	1,138 drugs	21,298 patients	121 drugs	47 drugs
Cardiovascular	27%	9%	21%	38%	15%	9%	45%
Hepatotoxicity	8%	7%	21%	13%	0%	20%	20%



Table 1.2. **Percentage of drug withdrawals at the different stages of drug development.** Image from (Lavery et al., 2011).

Some anti-cancer drugs are known to induce cardiovascular toxicity following long term administration. As drug efficacy is improving patients are surviving longer following cancer diagnosis, leading to the long term adverse effects of drug administration emerging and becoming an increasing problem.

There are many theories outlining possible mechanisms for drug-induced cardiovascular toxicity with many involving adverse effects on cardiomyocytes. The severity of the toxicity is dependent on the area

affected. One of the most severe forms of cardiotoxicity is decreased left ventricular ejection fraction (LVEF) which has potential to advance to heart failure or fatality (Mellor et al., 2011). There have been previous attempts to understand the mechanism of cardiotoxicity and these have led to the discovery of the involvement of the human ether-a-go-go (hERG) potassium channel (Curran et al., 1995; Babij et al., 1998). This channel plays a pivotal role in cardiomyocyte cellular repolarisation following an action potential (Walker and Spinale, 1999). During an action potential there are distinct stages of depolarisation and repolarisation that allow the cardiomyocytes to contract. Generally potassium channels, such as hERG, are involved in the repolarisation stage. Inhibition of these channels can lead to prolonged Q - T intervals, ultimately resulting in arrhythmias (Chouabe et al., 1998; Clancy and Rudy, 2001). These arrhythmias can become fatal with the onset of a condition known as Torsades de Pointes, which leads to sudden cardiac fatality (Hoppe et al., 2001). All drugs are screened for interaction with this channel. Any drugs found to have interaction with this channel have been removed to rule out cardiovascular toxicity; however, instances of cardiovascular toxicity still occur indicating the potential for an alternative mechanism of toxicity.

At present, research into cardiovascular toxicity is being conducted in four areas of current interest, summarised in figure 1.15. Within the field of cardiovascular toxicity, research focuses on two main areas; these include structural and functional toxicity. Structural toxicity specifically focuses on cellular changes following drug treatment including necrosis and apoptosis. This area investigates physiological responses including vascular remodeling and vasculopathies. In order to effectively assess structural changes individual cell types are investigated with the aim to understand which of the cardiac cell types are involved in toxicity onset. Functional toxicity focuses on the events occurring in patients following treatment. Functional toxicity includes changes in the electrophysiology of the heart which could be observed as arrhythmias or changes in rate and force of contraction. These changes can also affect the blood

pressure, possibly via the endocrine system, leading to oedema. Some of the drug-induced cardiovascular toxicity is known to be dose-dependent, as increases concentrations of drugs lead to more severe toxicity (Mellor et al., 2011).

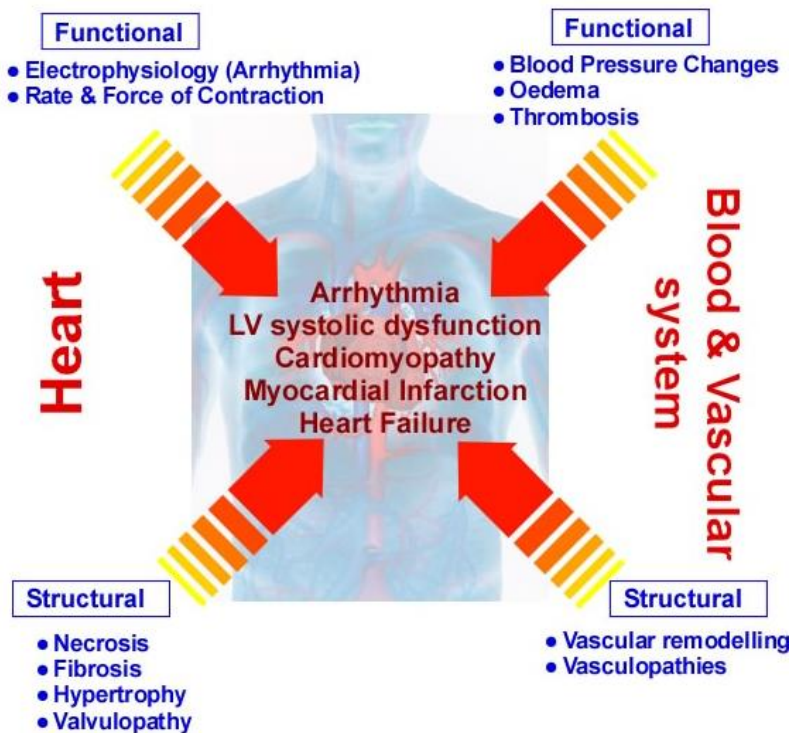


Figure 1.15. **Current areas of research in the field of cardiovascular toxicity.** Areas of current interest in the field of cardiovascular toxicity include functional and structural investigations. Functional investigations involved patient observations including determination of how drugs affect a patient's blood pressure and electrocardiogram (ECG), these are observed in the clinic. Structural effects look into how drugs affect cells *in vitro* as well as *in vivo*. These studies include investigation in cellular models as well as animal models and then the results are extrapolated to predict patient symptoms. *ECG* – *electrocardiogram*.

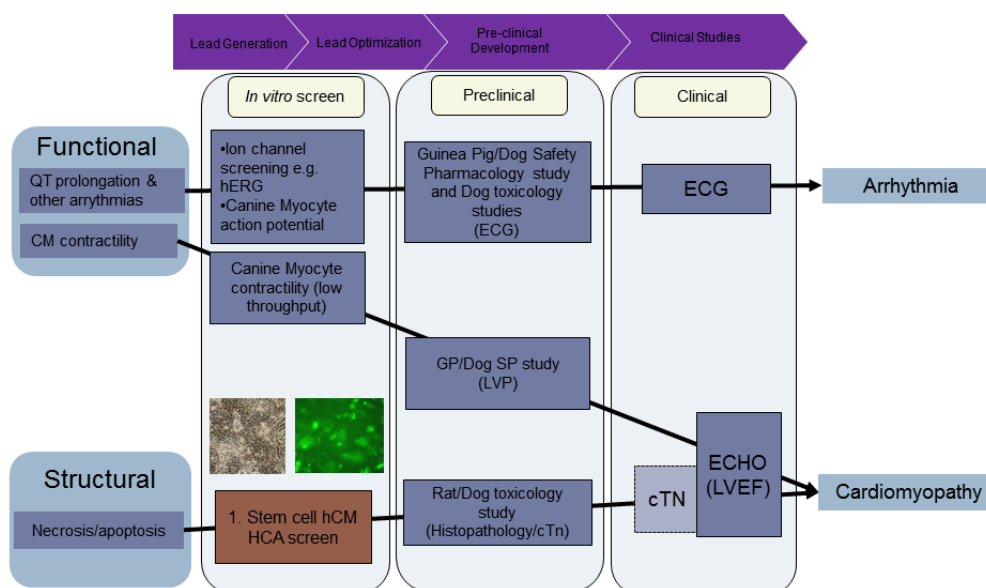


Figure 1.16. **Pharma testing cascade for toxicity.** Cardiovascular toxicity is divided into functional toxicity and structural toxicity. This diagram summarises the toxicity tests available at the different stages in the drug development process. Image courtesy of James Sidaway.

Functional studies are being conducted primarily in industry with the use of *in vivo* monitoring of heart function. Functional studies focus on factors such as heart rate, blood pressure and cardiomyocyte contractility. Functional screens are becoming more advanced in the detection of cardiovascular toxicity, but are limited as they only detect the toxicity once symptoms appear. There are studies being conducted on telemetered dogs to analyse heart function following drug treatments. Long term rodent studies are also designed to provide evidence as to the cardiac effects of drugs after repeat dosing over prolonged periods. These studies, however, are very costly to pharmaceutical companies so development of a structural model to predict the long term cardiac effects of drugs would be beneficial and reduce costs. These studies are only able to investigate functional effects such as arrhythmias and prolonged QT through measurement of action potentials and ion channel conduction.

Current screens are proficient in testing drugs for interaction with the potassium channel hERG. However, there is an additional mechanism for toxicity that cannot be predicted by interaction with this channel. This provides evidence for the requirement to determine an underlying mechanism of cardiovascular toxicity. To investigate structural toxicity *in vitro* cell models are utilised. These have advanced in recent years with the use of stem cell derived cardiomyocytes which allow investigation of drugs on beating cardiomyocytes.

In order to determine this mechanism, structural properties of cells are investigated. Structural studies focus on cellular apoptosis and necrosis as well as cell morphology. Many of these studies are conducted on cardiomyocytes as these cells have extremely low regenerative potential. Emerging research has begun to focus on non-cardiomyocyte cell types as these cells are increasingly receiving interest for their role in cardiovascular toxicity (Chiusa et al., 2012; Greineder et al., 2011; Wolf and Baynes, 2006). Structural toxicity studies investigate both on-target and off-target effects of the drugs, looking at various biochemical pathways and physiological responses to try to determine a mechanism for structural toxicity. There are several observed toxicities becoming apparent and these are outlined in figure 1.16.

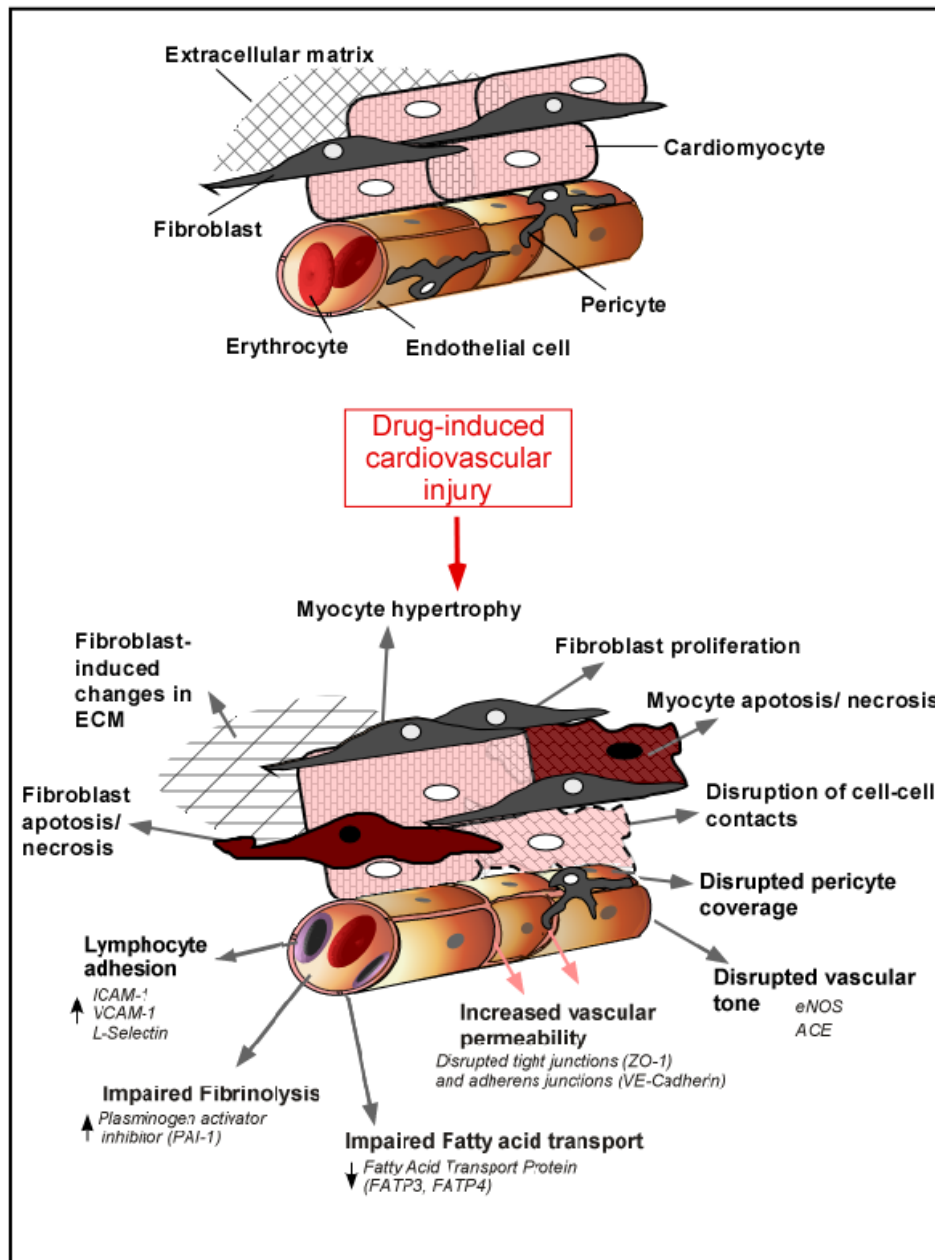


Figure 1.17. **Mechanism of drug-induced structural toxicity.** Cardiac microvasculature comprises a single layer of endothelial cells that is surrounded by specialised smooth muscle cells known as pericytes that help to support vascular structure. Proceeding drug induced cardiovascular injury there are several hypothesis explaining toxicity onset. These include: myocyte hypertrophy, fibroblast proliferation, myocyte apoptosis/ necrosis, disruption of cell-cell contacts, disrupted pericyte coverage, disrupted vascular tone, increased vascular permeability, impaired fatty acid transport, impaired fibrinolysis, lymphocyte adhesion, fibroblast apoptosis/ necrosis and fibroblast induced changes in extracellular matrix.

Drug-induced cardiovascular toxicity can result in several cellular changes. Endothelial cell specific changes include: disruption to vascular tone through changes in eNOS and ACE signaling. The renin-angiotensin system is known to be able to regulate vascular tone. The synergy observed between the renin-angiotensin system and the sympathetic nervous system is important in this regulation. Noradrenaline increase from the sympathetic nervous system stimulates the secretion of aldosterone, which functions to regulate vascular tone as well as sodium excretion and fluid volume (Brunner et al., 1993). Increased activation of the renin-angiotensin system leads to vasoconstriction through the production of endothelin. Endothelin production is stimulated through a range of stimuli one of which is an increase in angiotensin II. Angiotensin II is formed from the precursor angiotensin I with the enzymatic action of ACE. Changes in ACE signalling lead to changes in the levels of angiotensin II which is one of the ways vasoconstriction is regulated. Vasoactive mediators known to induce vasodilation can be secreted by the endothelial cells, including mediators such as prostaglandin I<sub>2</sub> and nitric oxide (NO). NO is produced by endothelial cells through activation of intracellular signalling involving Ca<sup>2+</sup> the signalling cascade is activated in response to mechanical shear stress or receptor activation including: acetylcholine, bradykinin and substance P. Increased vascular permeability, results as a consequence of disruption to tight and adherens junctions. This is thought to be a result of changes to intracellular MAPK signalling (Samak et al., 2011). Changes in intracellular signalling can be altered by changes in the membrane transporters inducing alteration in substances such as fatty acids entering and leaving the cell.

Other cellular changes include impaired fibrinolysis, this occurs by inducing changes in plasminogen activator inhibitor (PAI-1), which affects the composition of the blood circulating the body. Changes in cell



survival and onset of apoptosis are observed, which could be a result of increased lymphocyte adhesion or disrupted pericyte coverage, leading to increased vascular permeability via a decrease in the number of pericytes and reduced vascular stability. Within the body cells in close proximity are able to secrete growth factors or hormones that regulate in a paracrine manner surrounding cells. Disruption in cell-cell contacts and paracrine or autocrine signalling can induce fibroblast or myocyte apoptosis or necrosis and changes in the extracellular matrix (Fig. 1.17).

## **1.5 Drug induced cardiovascular toxicity**

### *1.5.1 Anti-cancer treatments*

This project focuses on anti-cancer drugs that belong to two classes; protein kinase inhibitors (PKI) and anthracycline antibiotics. Protein kinases function as catalytic enzymes in the transfer of phosphates from ATP to tyrosine sites (Mellor et al., 2011; Cheng and Force, 2010). This process leads to intracellular signalling cascades via continual phosphorylation of downstream signalling molecules. Receptors in this class are targets for anti-cancer drugs due to the fact that mutations in these cascades allow the cells to continually proliferate and avoid apoptosis. It is currently unclear if the toxicity is a result of on-target or off-target pharmacological activity as it is known that the drugs interact with many different kinases (Force et al., 2007). The multitarget properties are possible as kinases have similar ATP-binding domains, which is the target site for these inhibitors. Inhibition of the ATP-binding domain prevents phosphate transfer from ATP molecules resulting in the receptor remaining unphosphorylated and the downstream signalling cascade inactivated (Cheng and Force, 2010).

Anti-cancer drugs that are known to cause cardiovascular toxicity include doxorubicin (Adriamycin®) and epirubicin (Pharmorubicin®), belonging to



the anthracycline antibiotic class of anti-cancer drugs (Kik et al., 2009). Doxorubicin is widely investigated for its cardiovascular toxicity effects. Protein kinase inhibitors (PKIs) that induce cardiovascular toxicity include: sorafenib (Nexavar®), sunitinib (Sutent®), nilotinib (Tasigna®), imatinib (Gleevec®) and lapatinib (Tykerb®) (Cheng and Force, 2010). These drugs are summarised in table 1.3. Treatment with PKIs can be long-term in order to prevent reoccurrence. This leaves patients susceptible to any long term effects of repeat dosing (Force et al., 2007).

<b>Drug</b>	<b>Company</b>	<b>Class</b>	<b>Cancer treatment</b>	<b>Cardiovascular toxicity</b>
 <b>Doxorubicin (Adriamycin®)</b>	ALZA	Anthracycline antibiotic	Leukaemia, bladder, breast, stomach, lung, ovaries, thyroid, soft tissue carcinoma, multiple myeloma	Cardiomyopathy and heart failure Arrhythmia
 <b>Epirubicin (Pharmorubicin®)</b>	Pharmacia	Anthracycline antibiotic	Breast, ovarian, gastric, lung and lymphomas.	Cardiomyopathy and heart failure Arrhythmia
 <b>Sorafenib (Nexavar®)</b>	Bayer	RTK inhibitor – VEGFR-2, PDGFR and Raf Kinases	Renal, liver current approvals and in trials for kidney, thyroid, lung and brain.	Hypertension Cardiac ischaemia
 <b>Sunitinib (Sutent®)</b>	Pfizer	RTK inhibitor – VEGFR-2 and PDGFR	Renal cell carcinoma and imatinib-resistant gastrointestinal stromal tumor.	Hypertension LVEF decrease Heart failure
 <b>Nilotinib (Tasigna®)</b>	Novartis	RTK inhibitor – BCR-ABL, KIT, LCK, EPHA3, DDR1, DDR2, PDGFRB, MAPK11 and ZAK	Chronic myelogenous leukaemia	Heart failure
 <b>Imatinib (Gleevec®)</b>	Novartis	RTK inhibitor – BCR-ABL	Philadelphia chromosome-positive chronic myelogenous leukemia	Heart failure
 <b>Lapatinib (Tykerb®)</b>	GSK	RTK inhibitor – EGFR1 and EGFR2	Breast cancer	LVEF decrease

Table 1.3. **Anti-cancer drugs, their targets and cardiovascular toxic events following prolonged treatment.** Anti-cancer drugs have been reported to induce cardiovascular toxic effects following prolonged use. Details of drug classes, their use in cancer treatment as well as the cardiovascular toxic event following treatment. *RTK* – receptor tyrosine kinase, *VEGFR-2* – vascular endothelial growth factor receptor 2, *PDGFR* – platelet derived growth factor receptor, *LVEF* – left ventricle ejection fraction.

### 1.5.2 Sunitinib (Sutent®)

Sunitinib (SU11248, Sutent) is a multi-target PKI, known to inhibit VEGFR-1-3, PDGFR $\alpha/\beta$ , colony-stimulating factor 1 receptor (CSF1R) and c-kit. One primary mechanism is outlined in figure 1.18 (Mego et al., 2007). Clinically sunitinib is used in the treatment of renal cell carcinoma (RCC), and imatinib-resistant gastrointestinal stromal tumour (GIST) (Force et al., 2007). For RCC treatment there have been low efficacy rates (5-20%) with interferon alpha (IFN $\alpha$ ) and interleukin-2. Treatment with sunitinib more than doubles the progression-free survival time for patients. It is known that 20% of GIST patients do not respond to imatinib so sunitinib provides an alternative for these patients that have shown positive outcomes such as reduced tumour progression. Sunitinib has also been shown to have effects in neuroendocrine, colorectal and chronic myeloid leukaemia; however, sunitinib is not currently licensed for use in these cancers. Current known adverse cardiotoxic effects include hypertension, LVEF decrease and heart failure (Mego et al., 2007).

Sunitinib treatment typically involves a 50mg daily capsule (can be lowered to 12.5, 25 or 37.5mg) for 28 days followed by a 14 day break. This cycle can be repeated. Sunitinib is known to reach a maximum plasma concentration (C<sub>max</sub>) at 6-12 hours following administration. Sunitinib is cleared renally (16%) and in the faeces (61%) at a rate of 34-62 L/h. Sunitinib undergoes cytochrome P450 3A4 (CYP3A4) metabolism.

Inhibition of PDGFR and VEGFR-2 is considered to be highly important in the efficacy of sunitinib treatment. There is however speculation that inhibition of these pathways can lead to cardiovascular toxicity. The dimeric glycoprotein growth factor, PDGF, is important in signalling for multiple cell types including endothelial and myocytes as well as smooth

muscle and stromal cells. PDGF is thought to be important for paracrine signalling between myocytes and adjacent endothelial cells to promote angiogenesis. This disruption in heart signalling following inhibition of PDGF by sunitinib treatment could be a potential cause of cardiovascular toxicity. Additionally, sunitinib inhibits VEGFR-2 an important receptor in endothelial cell physiology (Force et al., 2007). VEGFR-2 signalling in endothelial cells regulates cell survival, proliferation, migration and permeability; disruption to physiological endothelial cell functions could be a further potential mechanism for cardiovascular toxicity (Holmes et al., 2007).

Sunitinib has been demonstrated to have detrimental effect on pericytes (Chintalgattu et al., 2013). These effects are thought to be due to inhibition of PDGFR. Pericytes provide vascular stabilisation to the microvasculature and disruption of these leads to reduce vessel stabilisation which could also be a cause for toxicity (Chintalgattu et al., 2013).

Contraindications with sunitinib treatment include: pancreatitis, severe uncontrolled high blood pressure, Torsades de Pointes, heart failure, acute haemorrhage, liver failure, seizures, underactive/overactive thyroid, decreased function of the adrenal gland, low/high amount of magnesium in the blood, high/low amount of potassium in the blood, anaemia, decreased blood platelets (Schmidinger et al., 2008). Other effects that occur less common include: fatigue, diarrhea, nausea, anorexia, hypertension, a yellow skin discoloration, nose bleeds, hypothyroidism, chest pain, depression, piles, hot flushes, sleeping difficulty, high levels of uric acid in blood, arrhythmias, brain haemorrhage, inflammation of liver and pancreas.

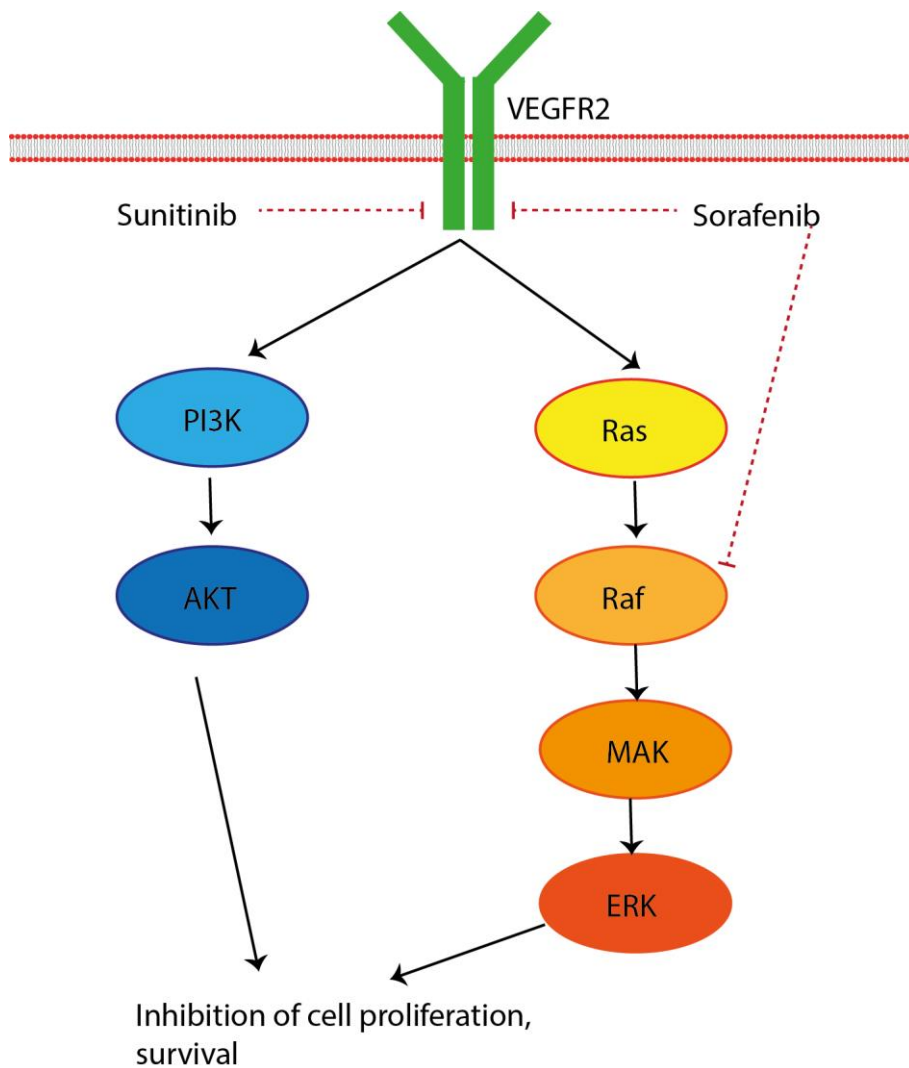


Figure 1.18. **Primary mechanism of action of sorafenib and sunitinib.** VEGFR-2 dimerises upon the ligand VEGF-A binding to the receptor ligand binding domain which induces receptor phosphorylation stimulating a downstream signalling cascade involving PI3K and AKT which function to regulate physiological processes such as vascular permeability and endothelial cell survival. An additional pathway also known to regulate the physiological processes permeability, proliferation and survival includes the Ras, Raf, MAPK and ERK signalling pathway. Additional ways these signalling pathways are activated include EGFRs, EGFR can homodimerise or heterodimerise with EGFR2 upon binding of EGF or TGF- $\alpha$ . Both sorafenib and sunitinib are able to inhibit the VEGFR-2 directly, sorafenib is also able to inhibit Raf downstream in this pathway. *VEGF* – vascular endothelial growth factor, *VEGFR* – vascular endothelial growth factor receptor, *PI3K* – phosphoinositide kinase 3, *MAPK* – mitogen activated protein kinase, *ERK* – extracellular regulated kinase, *EGF* – epithelial growth factor, *EGFR* – epithelial growth factor receptor, *TGF* – transforming growth factor.

### 1.5.3 Sorafenib (Nexavar®)

Sorafenib is a PKI that is known to inhibit VEGFR-2, PDGFR and Raf kinases (C-Raf and B-Raf) and with lower affinity VEGFR-1 and 3; the primary mechanism for sorafenib is outlined in figure 1.18. In 2005, sorafenib was clinically approved for use in the treatment of RCC (Duran et al., 2014) and advanced hepatocellular carcinoma (HCC) and it is currently in clinical trials for treatment of liver, kidney, thyroid, lung and brain tumours. Current known cardiovascular toxic effects include hypertension and cardiac ischaemia (Duran et al., 2014).

Sorafenib is typically administered as a 400 mg tablet twice daily without food. Sorafenib is known to reach C<sub>max</sub> within 3 hours. Sorafenib has low bioavailability (38-49%) due to 99.5% protein binding. Sorafenib is metabolized by CYP3A4 and UGT1A9 glucuronidation leading to 77% faeces elimination and 19% renal elimination. Sorafenib contraindications include: hand-foot syndrome (palmer-plantar erythrodysesthesia), diarrhoea, fatigue, alopecia, hypertension, nausea, haemorrhage, GI perforation, increased incidence of cardiac ischaemia/infarction and bleeding.

Sorafenib and sunitinib are able to inhibit tumour angiogenesis and proliferation by inhibition of intracellular signalling pathways; a common pathway includes the hypoxia-inducible gene pathway (Schmidinger et al., 2008). Both sorafenib and sunitinib also inhibit VEGF signalling which is an important factor in RCC treatment (Duran et al., 2014). Patients with elevated VEGF have poor prognosis due to the potential for angiogenesis and tumour metastasis (Duran et al., 2014). Sorafenib and sunitinib inhibit VEGF leading to improved prognosis. Sorafenib is able to inhibit B-Raf and Raf1 upstream signalling molecules in the VEGF signalling pathway, which provides further advantages in RCC treatment with elevated VEGF (Duran et al., 2014).

#### 1.5.4 Doxorubicin

Doxorubicin (Adriamycin) belongs to the anthracycline antibiotic class of chemotherapeutic agents (Sartiano et al., 1979). Doxorubicin as an anti-neoplastic chemotherapeutic agent has several clinical uses including: treatment of haematological and solid tumours such as leukaemia, breast and kidney cancer, hepatocellular and lung carcinomas and lymphomas (Choi et al., 2008; Yang et al., 2013; Sartiano et al., 1979; Ren et al., 2014; Kim et al., 2012). Doxorubicin is a 14-hydroxylated chemically synthesised derivative of daunorubicin. It was synthesised following fatal cardiotoxicity observations in clinical trials with daunorubicin in the 1960s. Doxorubicin proved to have therapeutic effects against a wider range of tumours than its predecessor daunorubicin, however, the cardiotoxicity remained. The dose-dependent cardiotoxicity plays a limiting role in the clinical efficacy of doxorubicin, there have been reports that cardiovascular toxic events can occur as late as 10 years after treatment is discontinued (Ren et al., 2014; Kik et al., 2009; Kim et al., 2012). Additional adverse effects with a less severe nature include bone marrow suppression, hair loss and inflammation (Lu et al., 2004; Cheng et al., 2010). Further limitations on doxorubicin clinical efficacy are as a result of cellular drug resistance, potentially a result of efflux transporters namely P-glycoprotein (P-gp, MDR, ABCB1) (Kik et al., 2009; Hor et al., 2008).

Doxorubicin is a photosensitive red compound that is administered to patients intravenously in either a hydrochloride salt (Adriamycin PFS, Adriamycin RDF or Rubex) or a liposome-encapsulated (Doxil, Myocet or Caelyx). Liposomes have only been utilised for clinical administration of drugs since the 1990s, despite development in the 1960s (Lu et al., 2004). There are four current classes of liposomal formulations including conventional and pegylated which doxorubicin is available in. The additional classes include long-circulating and modified liposomes (Lu et al., 2004).

Doxorubicin is predicted to exert cytotoxicity by generation of reactive oxygen species (ROS) such as  $H_2O_2$ , DNA intercalation and inhibition of topoisomerase II, an enzyme involved in DNA repair. This inhibition by doxorubicin leads to not only apoptosis but also  $G_1$  and  $G_2$  growth arrest (Heger et al., 2013; Ahmed and El-Maraghy, 2013). Despite many clinical uses for doxorubicin there is a limit to its use in the clinic due to the cardiovascular toxic side effects, which include: arrhythmias, congestive heart failure and cardiomyopathy (Heger et al., 2013).

The primary mechanism for doxorubicin's chemotherapeutic benefit is believed to be inhibition of topoisomerase II (Mizutani et al., 2005). Topoisomerase enzymes function to regulate the topological state of DNA, which is regulated by removal of super helical tension and knots (Deweese and Osheroff, 2009; Pommier et al., 2010). There are two major classes of topoisomerase enzymes, type I functioning on single stranded DNA and type II functioning on double stranded DNA with the use of ATP and divalent metal ions (Deweese and Osheroff, 2009). Topoisomerase II has the ability to bind both segments of double stranded DNA, create a strand break in one to allow the translocation of the other segment followed by relegation. This mechanism is outlined in figure 1.19 (Deweese and Osheroff, 2009). Inhibition of topoisomerase II can occur at two stages; the DNA binding stage, which is inhibited by high doxorubicin concentrations, and the DNA religation stage, which is inhibited by low concentrations of doxorubicin. Additional to topoisomerase II inhibition, doxorubicin is thought to be able to induce  $H_2O_2$  production which, through oxidative DNA damage and PARP activation, can lead to activation of caspase 3 inducing apoptosis within the cell (Mizutani et al., 2005). Doxorubicin is predicted to induce toxicity in cardiomyocytes by inhibition of topoisomerase II  $\beta$  (Vejpongsa and Yeh, 2014). As has been demonstrated in this paper if the topoisomerase II  $\beta$  within the heart is degraded before doxorubicin treatment the toxicity is reduced (Vejpongsa and Yeh, 2014). This shows a potential



cardiomyocyte protective mechanism that has the potential to reduce cardiovascular toxicity associated with doxorubicin.

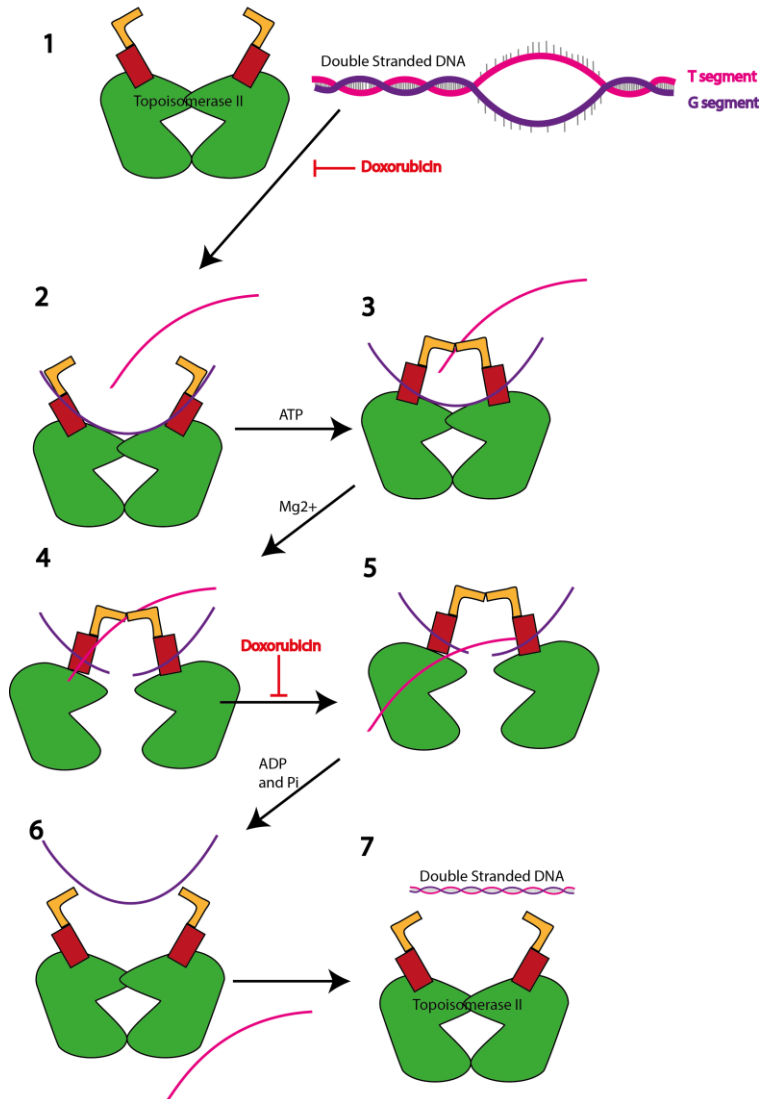


Figure 1.19. **Doxorubicin inhibition of topoisomerase II.** The topoisomerase II enzyme binds to the G (or gate) segment of DNA separating the double stranded DNA (1) to allow the passage of the T segment upon binding of ATP and clamp closure (2) this induces G segment cleavage in the presence of magnesium (4) before DNA religation (5) and release of ADP and inorganic phosphate ( $P_i$ ) leading to clamp opening (6) and G segment release (7). Doxorubicin is able to inhibit this process in two steps, high concentrations of doxorubicin leading to DNA being unable to bind to the topoisomerase II enzyme and low concentrations of doxorubicin leading to blockage of DNA religation. Both pathways of inhibition induce cell death. Adapted from (Pommier et al., 2010; Nitiss, 2009b; Nitiss, 2009a).

Doxorubicin has been implicated in endothelial barrier dysfunction (Wolf and Baynes, 2006). It has been demonstrated that doxorubicin treatment increases permeability of the endothelial cell barrier (Wolf and Baynes, 2006). This is thought to be due to the increase in H<sub>2</sub>O<sub>2</sub> production following doxorubicin treatment.

### 1.5.5 Herceptin® (*Trastuzumab*)

Herceptin® was the first monoclonal antibody drug to be FDA approved for breast cancer therapy. It was developed by Genentech and belongs to the humanised monoclonal antibody class of drugs. Herceptin® is able to provide effective treatment for adjuvant and metastatic breast cancer as well as metastatic gastric cancer (Baselga et al., 1998). Herceptin® is effective against EGFR2 (HER2) positive cancers. Patients with metastatic breast cancer are given 4 mg/kg IV for 90 minutes in the presence or absence of paclitaxel initially followed by 2 mg/kg IV for 30 minutes once a week. Herceptin® half-life is 10 days. Contraindications include: cardiotoxicity, pulmonary toxicity, infusion reactions, fever, headache, nausea, and diarrhea.

Herceptin® is known to directly inhibit EGFR2 (Jones and Buzdar, 2009). A summarised mechanism of action is outlined in figure 1.20. Herceptin® binds to EGFR2 which leads to three distinct mechanisms: sequestering of the immunosystem, this is an effect that is not normally mimicked when testing Herceptin® *in vitro* (Valabrega et al., 2007). Herceptin® also leads to EGFR2 internalisation and degradation which reduces the level of receptor present on the cell surface (Jones and Buzdar, 2009). Herceptin® is also able to inhibit tumourigenic signaling pathways and lead to cell cycle arrest (Jones and Buzdar, 2009). These three mechanisms of action lead to cell death and tumour regression (Valabrega et al., 2007; Jones and Buzdar, 2009).

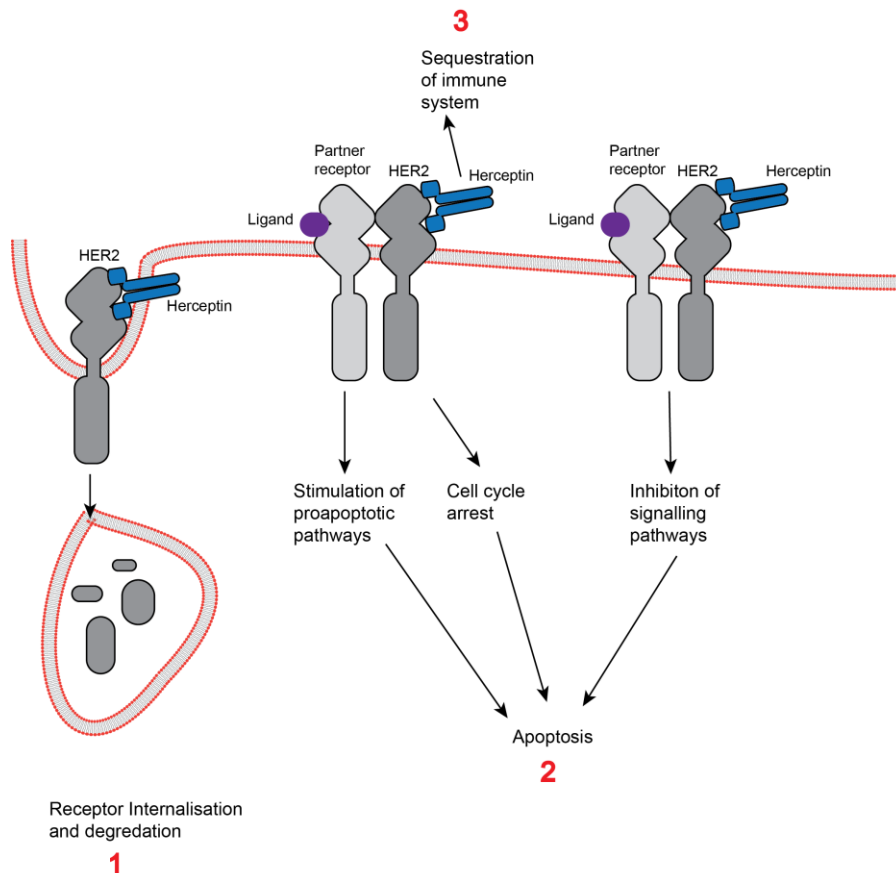


Figure 1.20. **Herceptin®'s mechanism of action.** Herceptin® binds directly to EGFR2 leading to three cellular processes. 1. EGFR2 internalisation and degradation. 2. Inhibition of signaling pathways and 3. Sequestering of the immune system. All three mechanisms lead to cell death.

## 1.6 Statins

Statins were identified in the 1980's for their cholesterol lowering ability (1986; East et al., 1986). Statins target the HMG Co-A reductase enzyme leading to reduced mevalonate and ultimately reduced levels of circulating low density lipoprotein (LDL) cholesterol (Fig. 1.21) (Sviridov et al., 1990). This is an advantageous effect as this reduced the buildup of cholesterol reducing the incidence of atherosclerosis and thrombotic events that would otherwise lead to blood vessel blockages (Sviridov et al., 1990). Cholesterol has physiological relevance as it provides a precursor for many steroid hormones such as cortisol and progesterone

(Nubel et al., 2006). When the levels of cholesterol increase this can lead to problems such as cardiovascular disease. Cholesterol levels can increase within the body through diet. The body is able to produce cholesterol through a process termed cholesterol biosynthesis (Stancu and Sima, 2001). In patients with high cholesterol levels this pathway is targeted by statins (Stancu and Sima, 2001).

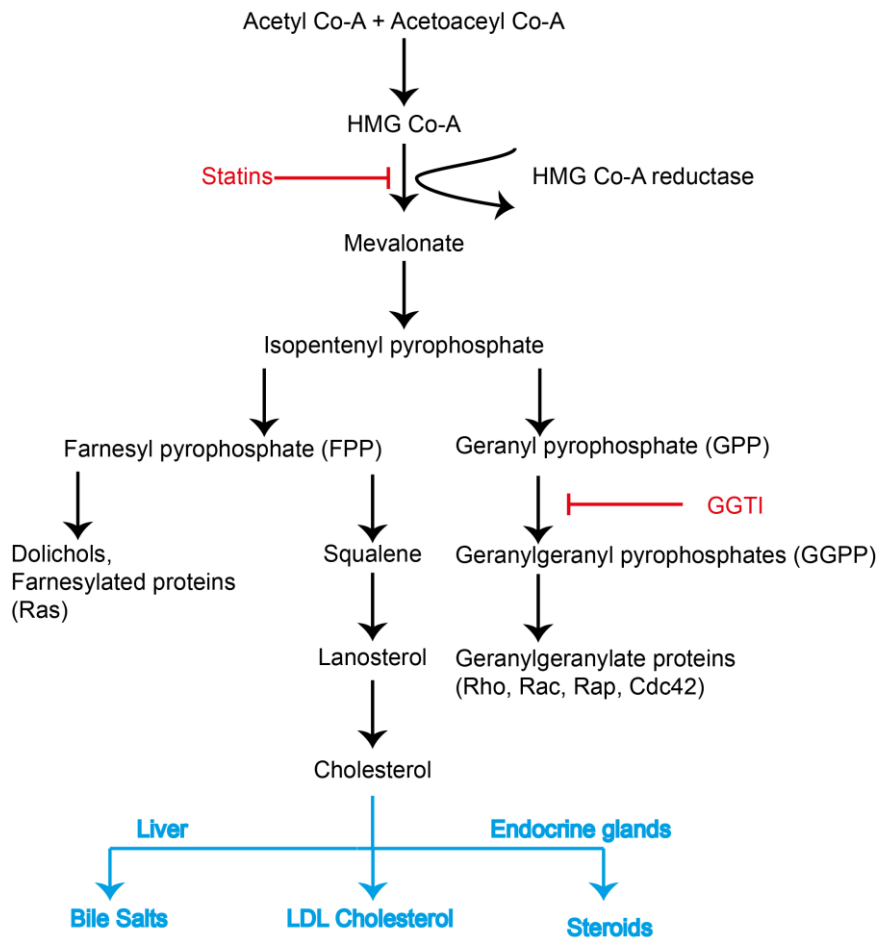


Figure 1.21. **Cholesterol biosynthesis.** Cholesterol biosynthesis involves a multi-step process utilising over 20 different enzymes. Acetyl Co-A and acetoacetyl Co-A are converted to HMG Co-A which with the HMG Co-A reductase enzymes is converted to mevalonate, leading to production of the prenylated proteins, isopentenyl pyrophosphate, which can be further converted to geranyl pyrophosphate (GPP) then geranylgeranyl pyrophosphates (GGPP) and finally geranylgeranyl proteins including Rho, Rac, Rap and Cdc42. Alternative conversion to farnesyl pyrophosphate (FPP) can be converted to dolichols, farnesylated proteins including Ras or it can be converted to squalene, lanosterol and finally cholesterol which can be utilised to make LDL cholesterol or within the liver for bile salts or within the endocrine system from production of steroids. Statins inhibit this process at an early stage where HMG Co-A reductase catalyzes the transportation of HMG Co-A to mevalonate. Adapted from (Faust and Kovacs, 2014). *HMG* – 3-hydroxy-3-methyl-glut-aryl, *Co-A* – coenzyme A, *FPP* – farnesyl pyrophosphate, *GPP* – geranyl pyrophosphate, *GGPP* – geranylgeranyl pyrophosphates.

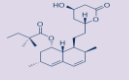
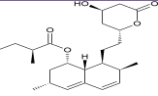
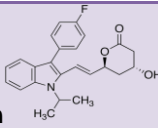
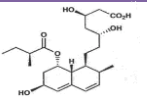
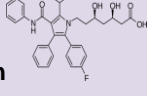
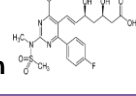
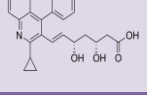
<b>Statin</b>	<b>Half life (hours)</b>	<b>Metabolism</b>	<b>Influx transporters</b>	<b>% Bioavailability</b>	<b>Physico-chemical properties</b>	<b>Specific activity</b>
<b>Simvastatin</b> 	2-5	CYP3A4, CYP3A5, CYP2C8	SLCO1B1	5	Lipophilic	Inactive lactone form
<b>Lovastatin</b> 	2-5	CYP3A4, CYP3A5, CYP2C8	SLCO1B1	5	Lipophilic	Inactive lactone form
<b>Fluvastatin</b> 	1-3	CYP2C9	SLCO1B1	24-30	Lipophilic	Active acid form
<b>Pravastatin</b> 	1-3	Minimal CYP3A4	SLCO1B1, SLCO2B1	18	Hydrophilic	Active acid form
<b>Atorvastatin</b> 	7-20	CYP3A4, CYP2C8	SLCO1B1	12	Lipophilic	Active acid form
<b>Rosuvastatin</b> 	19	Minimal CYP2C9, CYP2C19	SLCO1B1, SLCO1B3, SLCO2B1, SLCO1A2, SLC10A1	20	Hydrophilic	Active acid form
<b>Pitavastatin</b> 	10-13	Minimal CYP2C9, CYP2C8	SLCO1B1, SLCO1B3, SLCO2B1, SLCO1A2	60-80	Lipophilic	Active acid form

Table 1.4. **Properties of common statins.** Details of statin's origin, metabolism, percentages remaining in liver and circulation, physical-chemical properties, and specific activity. Adapted from (Stancu and Sima, 2001). *CYP* – cytochrome P450, *SLC(O)* – solute carrier (organic).

Cardiovascular protective pleiotropic properties are associated with statins, for this reason statins are prescribed to patients who have risk of cardiovascular problems and also have hyperlipidemia (Sundararaj et al., 2008). The cardioprotective effects of statins are emerging to have potential in reducing drug-induced cardiovascular toxicity, with specific focus on doxorubicin (Riganti et al., 2008; Sadeghi-Aliabadi et al., 2010; Werner et al., 2013; Werner et al., 2004). Statins have been demonstrated to reduce cell death *in vitro* associated with doxorubicin treatment (Damrot et al., 2006; Henninger et al., 2015; Huelsenbeck et al., 2011; Riad et al., 2009; Werner et al., 2013). It is predicted that the cardioprotective effects stem from the statins anti-proliferative and anti-inflammatory properties (Werner et al., 2013). Another property of statins that is providing interest is their ability to reduce tumours (Werner et al., 2013). Statins have been shown to decrease the risk of cancer in patients taking them for 5 years or longer (Sadeghi-Aliabadi et al., 2010). There is evidence from *in vivo* studies in rats that co-administration of statins with doxorubicin reduced the cardiovascular toxicity observed (Kim et al., 2012). Treatment of rats with rosuvastatin and doxorubicin reduced myocardial injury, oxidative stress and fibrosis as well as improved cardiac function in comparison to rats treated with doxorubicin only (Kim et al., 2012).

Statins have been implicated in ERK signalling, and it has been hypothesised that farnesyl pyrophosphate induces phosphorylation of Ras/Raf1 leading to downstream phosphorylation of ERK1/2, which induces the physiological responses proliferation and angiogenesis (Miura et al., 2004). Statins are able to deplete the isoprene precursor pool, which in turn reduces the Ras/Rho GTPases that are farnesylated or geranylgeranylated preventing the phosphorylation of MAPKs (Fritz et al., 2003). This has been demonstrated to be important in increasing the sensitivity of human cancer cells, specifically HeLa, to  $\gamma$ -rays hence increasing the efficiency of radiotherapy (Fritz et al., 2003).

More recent evidence suggests that statins can induce ERK5 phosphorylation, which has potential to inhibit reactive oxygen species and NF- $\kappa$ B which prevents inflammation and atherosclerosis (Le et al., 2014; Wu et al., 2013). Current research has shown that statins reduce endothelial damage, resulting from inflammatory responses through actions on nitric oxide (Stancu and Sima, 2001). ERK5 has been implicated in nitric oxide synthase signalling via KLF2 and 4 (Fig. 1.13) (Le et al., 2014).



## 1.7 Project Aims

The overall aim for this project was to identify a potential cellular mechanism for drug-induced cardiovascular toxicity with particular focus on endothelial cells.

To achieve this objective, the project focused on:

1. Identification of differences in expression of potential receptor tyrosine kinases (RTKs) between endothelial cells from different anatomical locations and species. This information will provide an initial understanding of suitable *in vitro* endothelial models for studying cardiovascular toxicity. Therefore, investigating endothelial cells from different anatomical locations aims to identify if signalling in endothelial cells differs, potentially making cardiac endothelial cells more susceptible to toxicity. Comparing cardiac endothelial cells between species will provide evidence if rodent models are a suitable animal model for drug-induced cardiovascular toxicity.

2. Investigation of the mechanisms by which Herceptin® and doxorubicin gain access to underlying cells. Currently theories of cardiovascular toxicity implicate cardiomyocytes as the target cell for toxicity, however, there is little research into how the drugs are able to gain access to the cardiomyocytes in order to induce toxicity.

This section of work primarily aims to identify the effects of Herceptin® and doxorubicin on the endothelial tight junction barrier to determine if the drugs are able to permeate to the underlying myocytes and induce cardiovascular toxicity implicated in many current theories.

3. Understanding the role of ERK5 in tight junction regulation. MAPKs have been shown to be involved in the regulation of endothelial and epithelial junctions. The role of ERK5 in endothelial physiology is becoming increasingly investigated, and has begun to be linked to regulation of gap junctions.

This section of work primarily aims to investigate if ERK5 is involved in the regulation of tight, adherens and gap junctions. Furthermore, I will investigate if ERK5 is involved in junction regulation in HDMEC, HCMEC and RCEC aiming to understand if this regulation is conserved across vascular beds and species.

4. Determine if statin induced ERK5 activation is able to prevent drug-induced barrier perturbation. Statins have also shown off-target cardio-protective effects as well as have the ability to activate ERK5.

This section of work aims to determine if statin induced ERK5 activation leading to tight junction stimulation could prevent drug-induced barrier perturbation.



# **Chapter 2**

## Materials and Methods



## 2.1 Materials

### 2.1.1 Reagents and materials

Growth factors VEGF-A<sub>165</sub>, bFGF-2, PDGF-BB, EGF, NRG-1, TGF- $\alpha$  and HGF were purchased from Peptidech EC (Rocky Hill, NJ, U.S.A). Doxorubicin (S1208), sorafenib (S1040), sunitinib malate (S1042), lapatinib GW-572016 (S2111), nilotinib (S1033), imatinib mesylate (S1026), XMD8-92 (S7525), BIX02189 (S1531) and staurosporine (S1421) were purchased from Selleckchem (U.S.A). Cytochalasin D (1233) was purchased from R&D systems.

Ultrapure ProtoGel® solution, was purchased from Geneflow Ltd. (National Diagnostics, Staffordshire, U.K). Tetramethylethylenediamine (TEMED), Ethylenediaminetetraacetic acid (EDTA), Sodium chloride, Tris base, Glycine, polyoxyethylenesorbitan monolaurate (Tween-20), Sodium dodecyl sulfate (SDS), were purchased from Fisher Scientific. Ammonium persulfate (APS), ammonium chloride, bicinechonic acid solution, copper (II) sulfate solution, Triton X-100, ethidium bromide, Tris-EDTA (TE) buffer solution (pH8.0), Dimethyl sulfoxide (DMSO), Aprotinin, leupeptin, pepstatin, phenylmethylsulfonyl fluoride (PMSF), sterile RNase and DNase free water, sodium orthovanadate (Na<sub>3</sub>VO<sub>4</sub>), paraformaldehyde, 2-mercaptoethanol, gelatin purchased from Sigma-Aldrich (Poole, U.K). Nu-PAGE® 4-12% Bis-Tris gels, 1.5mm cassettes, 4X lithium dodecyl sulfate (LDS) sample buffer, Lipofectamine™ RNAiMAX transfection reagent, prolong gold anti-fade reagent purchased from Life Technologies™ (Paisley, U.K). Full-range rainbow molecular weight marker (12-225kDa), Hybond™ ECL™ nitrocellulose membrane, enhanced chemiluminescence (ECL) were purchased from GE healthcare (Amersham, U.K). Agarose (electrophoresis grade), 3-N-Morpholino propanesulfonic acid (MOPS), purchased from Melford (Ipswich, U.K).

RNeasy RNA extraction kit, fibrous tissue RNA extraction kit, DNase I, were purchased from Qiagen. Hoechst 33342 purchased from Molecular Probes Europe BV (Leiden, The Netherlands). 96 well semi-skirted PCR plates, 384 well PCR plates, Sealing film for PCR, filter tips 10  $\mu$ l, 20  $\mu$ l, 200  $\mu$ l, 1000  $\mu$ l; gel saver tips 10-200  $\mu$ l purchased from STARLAB. 10 cm dishes; 6-, 12-, 24-, 48-, 96- (clear, black, white) well culture plates; centrifuge tubes 15 ml, 50 ml skirted and un-skirted; Eppendorfs 0.5 ml, 1.5 ml and 2 ml; cell scrapers; pipette tips 10  $\mu$ l, 200  $\mu$ l and 1000  $\mu$ l; stripettes 5 ml, 10 ml and 25 ml were purchased from Greiner Bio-One (Stonehouse, U.K). T75 and T25 cell culture flasks purchased from Corning. Goat and donkey serum, purchased from Jackson Research Laboratories.

### *2.1.2 Cell lines, culture medium and solutions*

<b>Name</b>	<b>Cell Type</b>	<b>Patient Information</b>	<b>Catalogue and Lot Numbers</b>	<b>Source</b>
<b>HDMEC Juvenile</b>	Human Dermal Microvascular Endothelial cells Juvenile Patient	Male, Age 3, Caucasian, isolated from foreskin	C-12210 6060707.1	PromoCell (Heidelberg, Germany)
<b>HDMEC adult</b>	Human Dermal Microvascular Endothelial cells adult patient	Female, Age 32, Caucasian, isolated from abdomen	C-12212 0092101.2	PromoCell (Heidelberg, Germany)
<b>HCMEC #1</b>	Human cardiac Microvascular Endothelial cells patient 1	Male, Age 62, Caucasian, isolated from heart muscle ventricle	C-12285 9090701.2	PromoCell (Heidelberg, Germany)
<b>HCMEC #2</b>	Human cardiac Microvascular Endothelial cells patient 2	Male, Age 35, Caucasian, isolated from heart muscle ventricle, known cardiomyopathy	C-12285 1122702	PromoCell (Heidelberg, Germany)
<b>HCMEC #3</b>	Human cardiac Microvascular Endothelial cells patient 3	Female, Age 54, Caucasian, isolated from heart muscle ventricle	C-12285 3011401	PromoCell (Heidelberg, Germany)
<b>HCAEC #1</b>	Human Coronary Artery Endothelial cells patient 1	Female, Age 62, Caucasian, isolated from coronary artery	C-12221 0113008.7	PromoCell (Heidelberg, Germany)
<b>HCAEC #2</b>	Human Coronary Artery Endothelial cells patient 2	Male, Age 41, Caucasian, isolated from coronary artery	C-12221 1111804.1	PromoCell (Heidelberg, Germany)
<b>HBMEC</b>	Human Brain Microvascular Endothelial cells	Isolated from brain	C-12287 1111603.7	PromoCell (Heidelberg, Germany)
<b>HUVEC</b>	Human Umbilical Vein Endothelial cells	Female, Age 0 Caucasian, isolated from umbilical vein	C-12205 8092901	PromoCell (Heidelberg, Germany)

<b>HCF #1</b>	Human Cardiac Fibroblasts patient 1	Male, Age 48, Caucasian, isolated from heart muscle ventricle	C-12375 1051601.5	PromoCell (Heidelberg, Germany)
<b>HCF #2</b>	Human Cardiac Fibroblasts patient 2	Male, Age 64, Caucasian, isolated from heart muscle ventricle	C-12375 1062201.5	PromoCell (Heidelberg, Germany)
<b>HCF #3</b>	Human Cardiac Fibroblasts patient 3	Male, Age 55, Caucasian, isolated from heart muscle ventricle	C-12375 3040802.1	PromoCell (Heidelberg, Germany)
<b>NHDF Juvenile</b>	Normal Human Dermal Fibroblasts Juvenile patient	Male, Age 5, Caucasian, isolated from foreskin	C-12300 0083002.2	PromoCell (Heidelberg, Germany)
<b>NHDF adult</b>	Normal Human Dermal Fibroblasts Adult patient	Male, Age 60, Caucasian, isolated from Cheek	C12302 2061206.2	PromoCell (Heidelberg, Germany)
<b>RCEC</b>	Rat Cardiac Endothelial Cells			Vec Technologies
<b>rHMVEC</b>	Rat Heart Microvascular Endothelial Cells			Isolated by AstraZeneca
<b>H9c2</b>	Rat Immortalised Cardio-Myocytes			Gifted to Dr. Michael Cross
<b>Rat-1-Fibroblasts</b>	Rat Immortalised Fibroblasts			Gifted to Dr. Michael Cross.
<b>A2780</b>	Human Ovarian Cancer Cells			(Brown et al., 1993)

Table 2.5. ***Cell lines used within this study.***

Media/ solution	Components	Source
<b>Endothelial Cell Basal Medium MV2 C-22221 (C-22226 phenol red free) (Full growth media)</b>	Fetal calf serum 0.05 ml/ml, Epidermal growth factor (recombinant human) 5 ng/ml, Basic fibroblast growth factor (recombinant human) 10 ng/ml, Insulin-like growth factor (long R3 IGF) 20 ng/ml, Vascular endothelial growth factor 165 (recombinant human) 0.5 ng/ml, Ascorbic acid 1 µg/ml, Hydrocortisone 0.2 µg/ml.	PromoCell (Heidelberg, Germany)
<b>Fibroblast Basal Medium 3 C-23230 (Full growth media)</b>	Fetal calf serum 0.1 ml/ml, Basic fibroblast growth factor (recombinant human) 1 ng/ml, Insulin (recombinant human 5 µg/ml.	PromoCell (Heidelberg, Germany)
<b>Dulbecco's Modified Eagle's Medium – High Glucose (DMEM) D6429 (Full growth media)</b>	Glucose, L-glytamine, Sodium pyruvate, Sodium bicarbonate 4500 mg/L, Fetal calf serum 0.1 ml/ml.	Sigma-Aldrich (Poole, U.K)
<b>Endothelial Cell Basal Medium MV2 C-22221 (Low serum media)</b>	Fetal calf serum 0.01 ml/ml.	PromoCell (Heidelberg, Germany)
<b>Dulbecco's Modified Eagle's Medium – High Glucose (DMEM) D6429 (Low serum media)</b>	Glucose, L-glytamine, Sodium pyruvate, Sodium bicarbonate 4500 mg/L, Fetal calf serum 0.01 ml/ml.	Sigma-Aldrich (Poole, U.K)
<b>Opti-MEM®   Reduced Serum Medium 31985-070</b>	L-glutamine.	Invitrogen (Paisley, U.K)
<b>0.05% Trypsin-EDTA solution 25300-054</b>	Trypsin 0.05%, EDTA 0.53 mM in PBS, pH7.4	Invitrogen (Paisley, U.K)
<b>0.5% (w/v) Gelatin solution</b>	0.1% (w/v) gelatin from porcine skin, (type A, cell culture tested) in ddH <sub>2</sub> O and autoclaved.	Sigma-Aldrich (Poole, U.K)



<b>Dulbecco's Phosphate-Buffered Saline with Ca<sup>2+</sup> and Mg<sup>2+</sup> (PBS)</b>	CaCl <sub>2</sub> ·2H <sub>2</sub> O 130 mg/L, KCl 200mg/L, KH <sub>2</sub> PO <sub>4</sub> 200 mg/L, MgCl <sub>2</sub> ·6H <sub>2</sub> O 100 mg/L, NaCl 8,000 mg/L, Na <sub>2</sub> HPO <sub>4</sub> ·7H <sub>2</sub> O 2,160 mg/L	Lonza (Basel, Switzerland)
<b>Dulbecco's Phosphate-Buffered Saline without Ca<sup>2+</sup> and Mg<sup>2+</sup> (PBS) BE17-212F</b>	KCl 200 mg/L, KH <sub>2</sub> PO <sub>4</sub> 200 mg/L, NaCl 8,000 mg/L, Na <sub>2</sub> HPO <sub>4</sub> ·7H <sub>2</sub> O 2,160 mg/L	Lonza (Basel, Switzerland)

Table 2.6. *Cell culture mediums used within this study.*

## 2.1.3 Primary and secondary antibodies

Antibody Name	Source	Catalogue Number	Host Species	Dilution Factor	Application
Anti-ZO-1 (mid)	Invitrogen	40-2200	Rabbit	200	IF
Anti-ZO-1 (mid)	Invitrogen	40-2200	Rabbit	250	WB
Anti-Connexin 43/GJA1	Abcam	Ab11370	Rabbit	5000	WB
GAPDH (D16H11) XP™ mAb	Cell Signalling Technologies	#5174	Rabbit	2000	WB
Collagen 1					
Anti-Cardiac Troponin I	Abcam	Ab47003	Rabbit	200	IF
Mouse monoclonal [284(19C7)] to Cardiac Troponin I	Abcam	Ab19615	Mouse	200	IF
Anti-NG2 Chondroitin Sulfate Proteoglycan	Millipore	#AB5320	Rabbit	100	IF
Anti-Connexin 43/GJA1	Abcam	Ab11370	Rabbit	200	IF
Anti-Endothelial Cell Antibody [RECA-1]	Abcam	Ab9774	Mouse	200	IF
Caspase-3	Cell Signalling Technologies	#9662	Rabbit	1000	WB
AKT	Cell Signalling Technologies	#9272	Rabbit	1000	WB
Human/Mouse ERK5/BMK1	R&D Systems	AF2848	Goat	40	IP
Human/Mouse ERK5/BMK1	R&D Systems	AF2848	Goat	50	IF
EGF Receptor (D38B1) XP®	Cell Signalling Technologies	#4267	Rabbit	1000	WB
HER2/ErbB2 (29D8) mAb	Cell Signalling Technologies	#2165	Rabbit	1000	WB
ERK5	Cell Signalling Technologies	#3372	Rabbit	1000	WB
ERK5	Cell Signalling Technologies	#3372	Rabbit	100	IF
Anti-MEK5 [EP648Y]	Abcam	Ab45146	Rabbit	1000	WB
VEGF Receptor 2 (D5B1) mAb	Cell Signalling Technologies	#9698	Rabbit	1000	WB

<b>VE-Cadherin (D87F2) XP™ mAb</b>	Cell Signalling Technologies	#2500	Rabbit	5000	WB
<b>VE-Cadherin (D87F2) XP™ mAb</b>	Cell Signalling Technologies	#2500	Rabbit	500	IF
<b>Phospho-AKT (Ser473) (D9E) XP™ mAb</b>	Cell Signalling Technologies	#4060	Rabbit	2000	WB
<b>Phospho-p44/42 (ERK1/2) (Thr202/Tyr204) (D13.14.4E) XP™ mAb</b>	Cell Signalling Technologies	#4370	Rabbit	2000	WB
<b>Phospho-EGF Receptor (tyr1068) (D7A5) XP® mAb</b>	Cell Signalling Technologies	#3777	Rabbit	1000	WB
<b>Phospho-ERK5 (Thr218/Tyr220)</b>	Cell Signalling Technologies	#3371	Rabbit	2000	WB
<b>Phospho-HER2/ErbB2 (Tyr1221/1222) (6B12) mAb</b>	Cell Signalling Technologies	#2243	Rabbit	1000	WB
<b>Phospho-SAPK/JNK (Thr183/Tyr185)</b>	Cell Signalling Technologies	#9251	Rabbit	1000	WB
<b>Phospho-p38 MAPK (Thr180/Tyr182) (D3F9) XP™ mAb</b>	Cell Signalling Technologies	#4511	Rabbit	1000	WB
<b>Phospho-VEGF Receptor 2 (Tyr1175) (D5B11) XP™ mAb</b>	Cell Signalling Technologies	#3770	Rabbit	1000	WB

Table 2.7. **Primary antibodies used within this study.** WB – western blotting; IF – immunofluorescence; IP – immunoprecipitation.

<b>Antibody</b>	<b>Source</b>	<b>Catalogue Number</b>	<b>Dilution Factor</b>	<b>Application</b>
<b>Peroxidase-conjugated AffiniPure Goat anti-Rabbit IgG (H+L)</b>	Jackson ImmunoResearch Laboratories	111-035-144	5000	WB
<b>Alexa Fluor® 568 Phalloidin</b>	Invitrogen (Paisley, U.K)	A12380	300	IF
<b>Alexa Fluor® 488 Donkey anti-mouse IgG (H+L)</b>	Invitrogen (Paisley, U.K)	A21202	1000	IF
<b>Alexa Fluor® 568 Donkey anti-rabbit IgG (H+L)</b>	Invitrogen (Paisley, U.K)	A10042	1000	IF
<b>Alexa Fluor® 568 Donkey anti-mouse IgG (H+L)</b>	Invitrogen (Paisley, U.K)	A10037	1000	IF
<b>Alexa Fluor® 680 Donkey anti-mouse IgG (H+L)</b>	Invitrogen (Paisley, U.K)	A10038	1000	IF
<b>Alexa Fluor® 680 Donkey anti-rabbit IgG (H+L)</b>	Invitrogen (Paisley, U.K)	A10043	1000	IF
<b>Alexa Fluor® 488 Donkey anti-rabbit IgG (H+L)</b>	Invitrogen (Paisley, U.K)	A21206	1000	IF

Table 2.8. **Secondary antibodies used within this study.**

*WB – western blotting; IF – immunofluorescence; IP – immunoprecipitation.*

## 2.2 Methods

### 2.2.1 Cell Culture

#### 2.2.1.1 Cell culture techniques

Cells were routinely cultured in a TriMAT<sup>2</sup> class II microbiological safety cabinet under sterile conditions. All equipment used was sterile and media was warmed to 37°C prior to use. All surfaces were wiped with 70% isopropanol to disinfect them prior to use.

#### 2.2.1.2 Coating of culture dishes

All human and rat endothelial cells were cultured on 0.5% (w/v) gelatin coated dishes that had been coated for a minimum of 20 minutes at 37°C in a humidified 5% (v/v) CO<sub>2</sub> atmosphere. Immortalised cell lines and A2780 cells grow on uncoated T75 flasks. Experiments requiring plates coated with fibronectin were coated for 1 hour at 37°C in a humidified 5% (v/v) CO<sub>2</sub> atmosphere. Fibronectin was diluted in 0.1% (w/v) gelatin at 5 µg/ml.

#### 2.2.1.3 Thawing of cryopreserved cells

Cells were cryopreserved at -196°C in liquid nitrogen. Thawing required heating vial to 37°C in a water bath, and diluting in 9 ml of pre-warmed FGM, centrifuging at 1000 RPM for 5 minutes and the cell pellet resuspended in fresh FGM before plating onto desired dish. The dishes were left for 24 hours at 37°C in a humidified 5% (v/v) CO<sub>2</sub> atmosphere to adhere to the dish before removal and replacement of fresh pre-warmed FGM.

#### *2.2.1.4 Passaging of cells*

Passaging cells involved a Versene wash (PBS without calcium and magnesium and with 0.5 mM EDTA), before addition of 0.05% trypsin-EDTA and incubated at 37°C in a humidified 5% (v/v) CO<sub>2</sub> atmosphere for 3 minutes, followed by cell resuspension in an appropriate volume of FGM and plating onto the relevant dishes.

Name	Culture Medium	Split ratio	Frequency	Passages used for experiment (from-to)
<b>HDMEC Juvenile</b>	Endothelial cell basal MV2 medium with supplements (FGM)	1:4	Every 2-3 days	p4-p10
<b>HDMEC adult</b>	Endothelial cell basal MV2 medium with supplements (FGM)	1:5	Every 2-3 days	p4-p10
<b>HCMEC #1-3</b>	Endothelial cell basal MV2 medium with supplements (FGM)	1:2	Every 2-3 days	p4-p10
<b>HCAEC #1-2</b>	Endothelial cell basal MV2 medium with supplements (FGM)	1:5	Every 2-3 days	p4-p10
<b>HBMEC</b>	Endothelial cell basal MV2 medium with supplements (FGM)	1:4	Every 2-3 days	p4-p10
<b>HUVEC</b>	Endothelial cell basal MV2 medium with supplements (FGM)	1:4	Every 2-3 days	p4-p10
<b>HCF #1-3</b>	Fibroblasts basal medium 3 with supplements (FGM)	1:3	Every 2-3 days	p4-p17
<b>NHDF Juvenile</b>	Fibroblasts basal medium 3 with supplements (FGM)	1:5	Every 2-3 days	p4-p17
<b>NHDF adult</b>	Fibroblasts basal medium 3 with supplements (FGM)	1:5	Every 2-3 days	p4-p17
<b>RCEC</b>	Endothelial cell basal MV2 medium with supplements (FGM)	1:2	Every 3 days	p4-p20
<b>rHMVEC</b>	Endothelial cell basal MV2 medium with supplements (FGM)	1:2	Every 3 days	p4-p10
<b>H9c2</b>	DMEM with supplements (FGM)	1:5	Every 2-3 days	p7-p25
<b>Rat-1-Fibroblasts</b>	DMEM with supplements (FGM)	1:10	Every 2-3 days	p7-p25
<b>A2780</b>	RPMI with supplements (FGM)	1:5	Every 2-3 days	

Table 2.9. Cells routine split ratios, frequency and passages.

### *2.2.1.5 Cell counting for experiments*

Cells were trypsinised in the same way outlined in section 2.2.1.4. They were resuspended in 3 ml FGM before a small drop was pipetted on a Neubauer Improved 0.0025 mm<sup>2</sup> and 0.100 mm depth haemocytometer (Hecht-Assostnet, Sondheim/Rhön, Germany) to determine the cell density.

Number (#) of cells counted = cells per 0.1 mm<sup>3</sup>

Therefore: # of cells counted x 10,000 = cells per 1 cm<sup>3</sup> (cells/ml)

Multiplied by the volume of media = total # of cells

Cells were diluted to the desired density in FGM before plating onto the required plates that had been previously processed by using the method described in section 2.2.1.2.

### *2.2.1.6 Cell cryopreservation*

Cells were trypsinised using the method detailed in section 2.2.1.4 and resuspended in 9ml FGM. Cells were counted (as described in section 2.2.1.5) before being centrifuged at 1000 RPM for 5 minutes. The cell pellet was resuspended in 10% (v/v) DMSO/90% (v/v) fetal calf serum mix to the desired cell density and aliquoted into sterile cryovials at 1ml volumes. These were placed in a Mr. Frosty Slow freezer container filled with isopropanol and given 24 hours at -80°C to slowly freeze before transfer to -196°C liquid nitrogen for long-term storage.



### 2.2.1.7 Transfection of cells with small interfering RNA (siRNA)

Cell line	Cell density 6 – well plate	Cell density 24 – well plate with 13mm coverslip
HDMEC adult	$1.6 \times 10^5$	$4 \times 10^4$
HCMEC #3	$1.8 \times 10^5$	$4.5 \times 10^4$
RCEC	$2.4 \times 10^5$	$6 \times 10^4$

Table 2.10. **Cells densities used for 6 and 24 well plates for HDMEC adult, HCMEC and RCEC.** Cell densities used for all further described experiments.

Cells were seeded at the desired density outlined in table 2.10. Cells were given 24 hours to adhere before transfection with siRNA. siRNA duplexes were diluted to 10 nM in Opti-MEM and incubated for 5 minutes at room temperature before addition of 0.2% (v/v) Lipofectamine RNAi MAX for a further 30 minutes to allow formation of the liposomenucleic acid complex prior to transfection of cells. Cells were transfected with 250  $\mu$ l siRNA Lipofectamine RNAi MAX mix /ml FGM for 6 hours incubated at 37°C in a humidified 5% (v/v) CO<sub>2</sub> atmosphere. Following 6 hour incubation cells were washed in PBS with calcium and magnesium twice before addition of fresh FGM. Cells were allowed to grow to confluence for a further 6 days, with additional media changes every 2 days.

### 2.2.1.8 Transfection of cells with adenovirus

Cells were seeded at the desired density outlined in table 2.6. Cells were given 6 days to reach confluence before transduction with adenovirus. The infectious units (IFU) used to determine the volume of adenovirus solution to add for each cell line to each plate are outlined in table 2.11. Virus was added to cells for 24 hours in 1% (v/v) FCS endothelial cell low serum medium.

Adenovirus	IFU/ $\mu$ l
Adeno - control	$1.1 \times 10^7$
Adeno ERK5-WT	$7.72 \times 10^6$
Adeno ERK5-AEF	$8.45 \times 10^6$
Adeno CA-MEK5	$7.2 \times 10^6$

Table 2.11. *Viral titer IFU/ $\mu$ l for each adeno-virus used.*

The virus was titered with use of HEK 293 cells seeded at  $5 \times 10^5$  cells per well of a 12 well plate. Virus was added to cells 24 hours after seeding at 10 fold dilutions, and given 48 hours to infect the cells. Cells were fixed in ice-cold 100% methanol at  $-20^\circ\text{C}$  for 10 minutes. Cells were washed in DPBS before addition of rabbit anti-Hexon antibody for 1 hour at  $37^\circ\text{C}$ . Cells were washed again in DPBS before addition of HRP conjugated goat anti-rabbit secondary antibody for a further 1 hour at  $37^\circ\text{C}$ . Cells were washed again in DPBS before addition of sigmafast™BCIP®/NBT for 10 minutes at  $37^\circ\text{C}$  to allow colour to develop. Cells were washed in DPBS before visualising on the light microscope (Nikon). Cells infected with virus appeared in brown, these cells were counted from 3 images per virus dilution and averaged. To determine the IFU the below calculation was utilised (obtained from Adeno-X™ Rapid Titer Kit user manual):

Positive cells per field x fields per well / volume added to well x dilution

e.g.

- 10 brown cells as the average across the 3 images
- 594 fields per well (outlined in the protocol in the Adeno-X™ Rapid Titer Kit user manual)
- 100  $\mu$ l (=0.1 ml) of virus dilution added to each well
- $10^{-5}$  dilution

$$10 \times 594 / 0.1 \times 10^{-5} = 5.94 \times 10^9 \text{ IFU/ml}$$

Once the virus had been titered and the IFU calculated the optimum MOI was determined. Adenovirus has potential to interfere with FAK which can induce rearrangement of the actin cytoskeleton. For this reason different MOIs were investigated to determine a concentration of control virus that did not induce actin cytoskeleton remodeling. MOIs were tested from 1 to 20. The final MOI to be used was chosen as 5.

$$\begin{aligned} \# \text{ cells} \times \text{desired MOI} &= \# \text{ infectious units required (IFUr)} \\ \# \text{ IFUr} / \text{viral titer (IFU}/\mu\text{l)} &= \# \mu\text{l adenovirus stock required for desired} \\ &\text{MOI} \end{aligned}$$

#### 2.2.1.9 Preparation of total cell lysates

Proteins were extracted from cultured cells grown in FGM in a 10cm dish that were at approximately 80% confluence with the use of 0.5ml radioimmunoprecipitation assay (RIPA: 20 mM Tris pH 7.5, 150 mM NaCl, 2.5 mM EDTA, 10% (w/v) glycerol, 1% (v/v) Triton X-100; 1 mM Na<sub>3</sub>VO<sub>4</sub>; 10 µg/ml aprotinin; 10 µg/ml leupeptin; 10 µg/ml pepstatin A; 1 mM PMSF; 0.5% (v/v) SDS and 0.5% (v/v) sodium deoxycholate) lysis buffer on ice following two washes with ice cold PBS without calcium and magnesium. RIPA was made up on ice and used within 30 minutes. RIPA lysis buffer remained on the cells for 15 minutes on ice before scraping the lysis buffer into a 1.5 ml eppendorf tube and centrifuging at 4°C for 20 minutes at 14,000 RPM. The supernatant was then transferred to a new tube and diluted in 4X LDS (lithium dodecyl sulfate), boiled at 90°C for 5 minutes before freezing.

mRNA was extracted from cells using RLT (Qiagen) lysis buffer containing 2-mercaptoethanol. Cells were washed in PBS with calcium and

magnesium before addition of RLT lysis buffer at room temperature. Cells were scrapped and transferred to Qia-Shredders.

#### *2.2.1.10 Protein measurement of total cell lysates*

Protein standards were prepared from BSA 1 mg/ml stock. The standards were diluted in molecular grade dH<sub>2</sub>O. Standards were plated into desired wells with the same volume of water plated into sample wells. Samples were diluted further in RIPA lysis buffer and plated out, with RIPA lysis buffer to the same volume plated in the standard wells. To this 200µl of BCA (bicinchoninic acid assay) reagent was added and incubated at 37°C for 30 minute plate read on a Vario-Scan plate reader at 570 nm, and the concentration of protein calculated allowing for equal dilution for protein samples in LDS.

#### *2.2.1.11 Cell treatment with growth factors to generate lysates*

Cells were plated onto 12 well plates that had been coated with 0.5% (w/v) gelatin. HDMEC adult cells were seeded at  $3 \times 10^4$ , HCMEC #3 were seeded at  $5 \times 10^4$  and RCEC were seeded at  $8 \times 10^4$ . Cells were plated in FGM and given 2 days growth before washing with PBS with calcium and magnesium and addition of endothelial cell basal medium supplemented with 1% (v/v) FCS for 18 hours prior to growth factor stimulation. Growth factors were initially diluted in sterile filtered PBS containing 0.1% (w/v) BSA to 100 mg/ml and stored. For use in the assay growth factors were diluted to 50 ng/ml in 1% (v/v) FCS basal medium before addition to the well. The growth factors used included: human VEGF-A<sub>165</sub>, VEGF-B, bFGF-2, PDGF-BB, EGF, NRG-1, TGF- $\alpha$ , HGF and IGF; for rat cells rat VEGF-A<sub>164</sub> was used. Growth factors were added for 10 minutes prior to lysis. The lysis buffer used was 1 X LDS solution with 25 µl/ml  $\beta$ -mercaptoethanol. This was added following 2 washes with ice cold PBS without calcium and magnesium, lysis was done on ice using 175 µl/well

of a 12 well plate. Lysates were scraped and boiled at 90°C for 5 minutes before sonication and freezing.

#### *2.2.1.12 Cell treatment with drugs to generation lysates*

Cells were plated onto 6 well plates that had been coated with 0.5% (w/v) gelatin. Cells were seeded at densities outlined in table 2.6. Cells were plated in FGM and given 6 days growth before addition of drugs. Drugs were initially diluted in 100% (v/v) DMSO before be further diluted to 0.1% (v/v) DMSO in FGM for use in experiments. Media was changed every 2 days. Drugs were added for the desired time before washing in ice cold PBS without calcium and magnesium on ice and addition of 250 µl RIPA lysis buffer for 15 minutes prior to scraping and centrifuging at 14,000 RPM for 20 minutes at 4°C. Supernatant was transferred to new tube and diluted in 4 x LDS before boiling at 90°C for 5 minutes then freezing. mRNA was extracted from cells using RLT lysis buffer containing 2-mercaptoethanol. Cells were washed in PBS with calcium and magnesium before addition of RLT lysis buffer at room temperature. Cells were scrapped and transferred to Qia-Shredders.

#### *2.2.1.13 Cell treatment with growth factors to analyse cell proliferation*

Cells were plated onto gelatin coated 48 well plates at the following densities: HDMEC adult  $5 \times 10^3$ , HCMEC  $5 \times 10^3$  and RCEC  $8 \times 10^3$  for 24 hours to allow cell adhesion. Cells were then washed in PBS with calcium and magnesium and 1% (v/v) FCS media was added for 18 hours before addition of growth factors at 50 ng/ml. Growth factors were added for 72 hours before being washed off with PBS with calcium and magnesium and addition of 200 µl PBS with calcium and magnesium with 25 µl Cell Titer Glo® (Promega, G7571), this was left to lyse the cells and allow them to release ATP for 10 minutes at room temperature on a rocker at 100 RPM.

Following this 150µl was transferred to a white bottom 96 well plate before reading on a vario-scan plate reader.

Growth factors used include: human VEGF-A<sub>165</sub>, -B, -E, bFGF-2, PDGF-BB, EGF, NRG-1, TGF- $\alpha$ , HGF and IGF; for rat cells rat VEGF-A<sub>164</sub> was used.

#### *2.2.1.14 Treatment of cells with drugs to analyse cell viability*

Cells were plated onto gelatin-coated 96 well plates at the following densities: HDMEC adult  $5 \times 10^3$ , HCMEC  $5 \times 10^3$  and RCEC  $8 \times 10^3$  for 48 hours to allow cell adhesion. Drugs were added for 72 hours before being washed off with PBS with calcium and magnesium and addition of 100 µl PBS with calcium and magnesium with 10 µl Cell Titer Glo® (Promega, G7571), this was left to lyse the cells and allow them to release ATP for 10 minutes at room temperature on a rocker at a low speed. Following this 100 µl was transferred to a white bottom 96 well plate before reading on a vario-scan plate reader.

#### *2.2.1.15 Cell treatment with drugs to stain for immunofluorescence*

Cells were plated onto gelatin-coated 24 well plates containing 13mm coverslips at densities outlined in table 2.6. Cells were plated in FGM and given 6 days growth before addition of drugs in FGM, media was changed every 2 days. Drugs were added for the desired time before washing with PBS containing calcium and magnesium, and fixing in 2% (w/v) PFA for 15 minutes.

#### *2.2.1.16 Cell treatment with drugs to assess barrier function*

Cells were plated onto fibronectin coated ThinCerts™ 0.4 µM translucent (Greiner, 665640). Cells were plated in FGM at the following densities

HDMEC adult  $4 \times 10^4$ , HCMEC  $4.5 \times 10^4$  and RCEC  $6 \times 10^4$ . Within the ThinCerts™ 0.5ml cells were plated with 1ml media in the surrounding well. Cells were grown for 6 days to ensure confluency was reached with media changes every 2 days, method outlined in figure 2.1. Once cells had reached confluency they were drugged for 6 hours before washing the drug off and addition of 2 mg/ml FITC 4kDa fluorescent dextran diluted in phenol red free endothelial FGM for 25 minutes at 37°C in a humidified 5% (v/v) CO<sub>2</sub> atmosphere, after which a sample was removed from the well and transferred to a black 96 well plate to enable fluorescence levels to be detected on the vario-scan plate reader at Ex 490 nm and Em 525 nm.

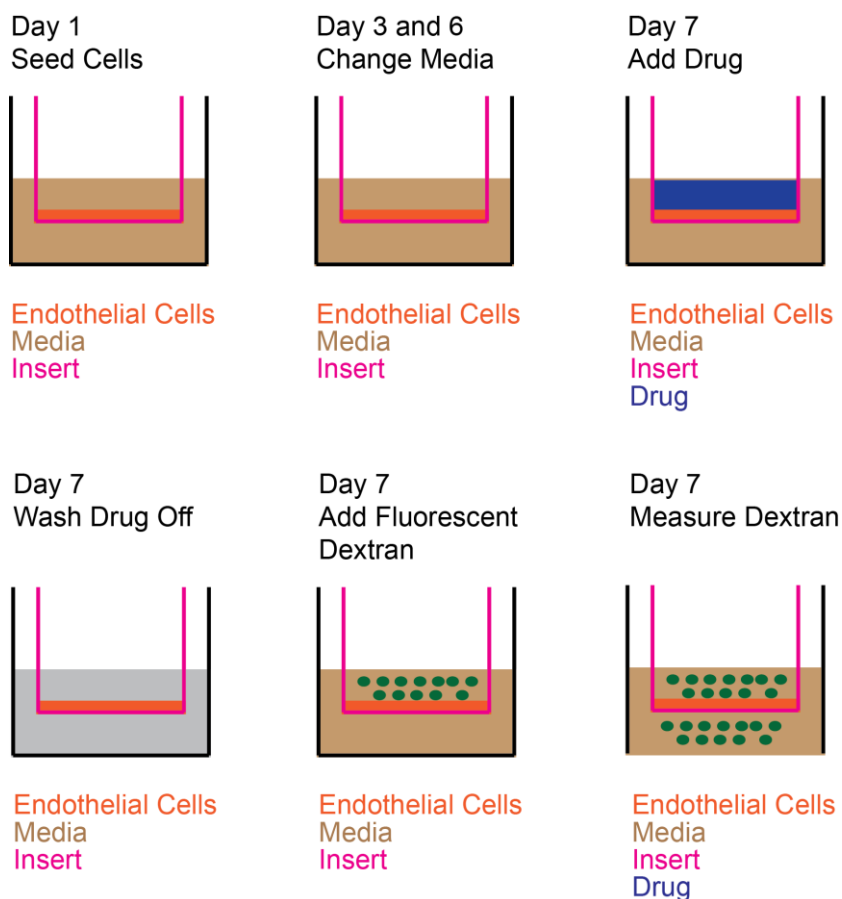


Figure 2.1. **Outline of the method for plating out the barrier function assay on inserts.**

### *2.2.1.16 Cell treatment with growth factors to determine ability to migration*

Cells were plated onto 0.5% (v/v) gelatin coated 24 well plates at densities outlined in table 2.6. Cells were given 24 hours to adhere before washing in PBS with calcium and magnesium and addition of 1% (v/v) FCS low serum endothelial cell medium for 18 hours before scratching down the center of the well with a sterile 200 µl pipette tip then adding to fresh 1% (v/v) FCS basal endothelial cell medium with or without the growth factor of interest. This was incubated for 16 hours at 37°C in a humidified 5% (v/v) CO<sub>2</sub> atmosphere before 2% (w/v) PFA fixation for 15 minutes and washing in 1 X PBS and crystal violet staining for 10 minutes before washing off with water and leaving to dry to enable photos to be taken on a Nikon light microscope.

## **2.2.3 Western Blotting**

### *2.2.3.1 Gel electrophoresis*

Cell lysates were separated on sodium dodecyl sulphate polyacrylamide gel electrophoresis (SDS-PAGE) pre-cast Nu-PAGE 4-12% Bis-Tris polyacrylamide gels in the XCell SureLock™ Mini-Cell electrophoresis system (Invitrogen). Previously prepared lysates were loaded into the wells and resolved at 50 mA, 200 V, 15 W for 1.5 – 3 hours depending on molecular weights of proteins of interest, with 800 ml 1X MOPS running buffer (0.05 M MOPS, 0.05 M Tris, 1 mM EDTA and 0.1% (v/v) SDS). The resolving gel was separated from the stacker and 'foot' of the gel before equilibrating in 1 X Tris-glycine transfer buffer (12 mM Tris, 96 mM glycine, 20% (v/v) methanol). The gels were transferred to 0.2 µm nitrocellulose membrane at 140 mA, 250 V for 2 hours. Membranes were washed in TBS with 0.1% (v/v) Tween-20 to remove the methanol that is present in the transfer buffer, after washed membranes were placed immediately in



blocking solution consisting of 5% (w/v) BSA in TBS with 0.1% (v/v) Tween-20 for 1 hour before addition of primary antibodies in 2% BSA in TBS with 0.1% (v/v) Tween-20 these were incubated overnight at 4°C. They were washed 6 times in TBS with 0.1% (v/v) Tween-20 before addition of relevant secondary antibodies in 2% BSA in TBS with 0.1% (v/v) Tween-20 at 4°C for 1.5 hours and washed in TBS with 0.1% (v/v) Tween-20 6 times before a final TBS wash and addition of ECL viewing solution that the membranes were soaked in for 5 minutes.

Lysates from doxorubicin, sorafenib and sunitinib were run on 8% tris-glycine gels composition outlined in table 2.8, to ensure separation of ERK5 and phosphorylated ERK5. Gels were run for 1 hour at 35 mA, 200 V 15 W with 1 X SDS running buffer (0.025 M Tris-HCl, 0.192 M glycine, 0.1% (v/v) SDS at pH 8.3) and transferred to nitrocellulose membrane for 2 hours at 125 mA, 250 V. All proceeding steps remain the same as with Nu-PAGE gels method described above.

	Resolving gel	Stacking gel
<b>30% (w/v) acrylamide solution</b>	2.7ml	0.7ml
<b>2.0M Tris/HCl pH 8.8, 0.4% (w/v) SDS</b>	2ml	-----
<b>0.5M Tris/HCl pH 6.8, 0.4% (w/v) SDS</b>	-----	0.7ml
<b>87% (v/v) glycerol</b>	0.7ml	-----
<b>dH<sub>2</sub>O</b>	4.6ml	3.6ml
<b>Temed</b>	5µl	5µl
<b>10% (w/v) APS</b>	22.9µl	25µl

Table 2.12. **Composition of 8% tris-glycine gel resolving and stacker.**

### *2.2.3.2 Densitometry quantification of western blots*

Blots were developed on X-ray film before scanning on an Epson® perfection 4490 photo scanner (Epson U.K Ltd, Hemel Hempstead, U.K). Scanned blots were processed in Photoshop, before densitometry analysis using image J to quantify bands relevant to an untreated or vehicle control sample, which was arbitrarily set to 1.0.

Image J software was used to quantify the band intensity. Equal sized boxes were drawn around each band allowing the software to determine the pixels. From this the area under the curve (AUC) was calculated by the software. From the AUC value the background pixel intensity was removed before the values were quantified by converting to fold change in relation to basal/vehicle control.

## **2.2.3 Immunofluorescence**

### *2.2.3.1 Fixing and embedding of tissues*

Upon removal of tissue from the animal, rat hearts were placed into 4% (w/v) PFA (made up by dissolving paraformaldehyde powder in PBS without calcium and magnesium at 55°C and pH to 7.5 with use of NaOH and HCl) for 30 minutes at room temperature they were washed with PBS without calcium and magnesium before addition to 30% (w/v) sucrose overnight at 4°C. Following this they were added to OCT (cryomatrix ThermoScientific, 6769006) in a 12 x 12 x 20 mm embedding mold (ThermoScientific, 1220) and placed on a dry ice/isopropanol bath for about 30 minutes to set before removal and sectioning on the cryostat (Leica) at 7-10µm depth.

### *2.2.3.2 Cultured Cells*

Following drug stimulation for desired time, cells were washed with PBS to remove any cell debris and fixed in 2% (w/v) PFA for 15 minutes at room temperature.

### *2.2.3.3 Immunofluorescence staining*

Following sectioning, rat heart sections on slides were washed in quench solution (50mM ammonium chloride) and incubated at room temperature for 10 minutes. Cell culture dishes containing coverslips were also washed with quench solution in the well. This was washed off with 1X PBS before permeabilising in 0.25% (v/v) Triton X-100 diluted in PBS for 10 minutes at room temperature. This was washed off with TBS before addition of blocking solution 1% (w/v) BSA diluted in TBS with 0.1% (v/v) Tween-20 with 5% (v/v) animal serum for 1 hour at room temperature. Primary antibody was added following the blocking stage for 1 hour at room temperature in 1% (w/v) BSA diluted in TBS with 0.1% (v/v) Tween-20 followed by washes with TBS with 1% (v/v) Tween-20 before addition of secondary antibodies for 50 minutes then addition of Hoechst for the final 10 minutes. This was washed off in TBS with 0.1% (v/v) Tween-20 before mounting in pro-long gold®. Images were taken on the Zeiss Axio Observer inverted fluorescence microscope using X40 and X63 oil emersion objectives.

## **2.2.4 Gene Analysis**

### *2.2.4.1 Cell RNA Extraction*

All steps were carried out using RNase and DNase free filter pipette tips. The cells were scraped using a sterile cell scraper to ensure complete lysis and release of RNA. The Qia-Shredder column was centrifuged for 2 minutes at 14,000 xg. The liquid run through was added to 100% ethanol (RNA and DNA free) this was then added to a spin column centrifuged for

30 seconds at 8,000 xg. The column was then washed with RW1 wash solution before 15 minute DNA digestion with DNase I and RDD mix which was further washed with RW1 wash solution. The final two washes were carried out with RPE wash solution before the column was centrifuged for 1 minute at 8,000 xg with 40µl RNase free water, which collected the RNA. The level of RNA was measured using a nanodrop.

#### *2.4.2 Tissue RNA Extraction*

Following removal of the tissue from the animal, tissues were placed into a small volume of RNAlater. A small section of the tissue in the required area was removed and added to 300 µl RLT lysis buffer with addition of a metal bead to a 2 ml eppendorf tube, the tissue was lysis using a mixer mill MM400 (Retsch.) Following complete lysis samples were spun down for 1 minute before removal of the metal bead and addition of a 600 µl solution containing 590 µl RNase free water and 10 µl proteinase K. This was vortexed to ensure sufficient mixing and incubated at 55°C for 10 minutes. This was centrifuged for 3 minutes on 10,000 xg and the supernatant removed and added to ethanol. All following steps are the same as described in section 2.2.4.1 cell RNA extraction.

#### *2.2.4.3 Reverse transcription of mRNA*

RNA was diluted to 0.1 µg/ml with dH<sub>2</sub>O, Oligo dT (4.1 µg/ml) and dNTP mix (0.08 mM) were added and incubated at 70°C for 5 minutes, following this samples were immediately placed on ice to prevent secondary structure formation. Samples were then added to first strand buffer, DTT, RNaseOUT and M-MLV reverse transcriptase before annealing stage at 25°C for 5 minutes and extended synthesis at 37°C for 60 minutes, inactivation followed this step by heating the sample to 70°C for 15 minutes and diluting with dH<sub>2</sub>O to achieve a cDNA concentration of 6.66ng/µl.

#### *2.2.4.4 Primer Design*

Primers were designed to genes of interest using online tools. The RNA sequence for the gene of interest was determined using Qiagen: <http://www.qiagen.com/products/quantifastprobeassay.aspx>, this sequence was inputted into Invitrogen primer design tools: <http://tools.invitrogen.com/content.cfm?pageid-9716>, where a list of primers using the parameters in table 2.9.

	Minimum	Optimum	Maximum
<b>Primer Size</b>	18	20	27
<b>Primer Tm</b>	57	60	63
<b>Primer %GC</b>	40	50	60
<b>Product Size</b>	100	N/A	150
<b>Salt Concentration</b>	N/A	N/A	50
<b>Primer Concentration</b>	N/A	N/A	50

Table 2.13. *Table of parameters for primer design.*

Primers were finally tested using an online BLAST search to determine their predicted specificity. This was done using PubMed: [http://www.ncbi.nlm.nih.gov/tools/primer-blast/index.cgi?LINK\\_LOC=BlastHome](http://www.ncbi.nlm.nih.gov/tools/primer-blast/index.cgi?LINK_LOC=BlastHome). Primers that were most specific to gene of interest were ordered for testing.

#### 2.2.4.5 Agarose gel electrophoresis for primer testing

Primers were tested by PCR on a 3% agarose gel. This was carried out by making PCR reaction mixes consisting of: 4  $\mu$ l colored GoTaq® Flexi Buffer with 2.4  $\mu$ l MgCl<sub>2</sub> (25 mM, Promega, M8305), 2  $\mu$ l dNTP mix (10 mM, Promega, U1330), 5.8  $\mu$ l PCR grade dH<sub>2</sub>O and 0.2  $\mu$ l GoTaq® Flexi

DNA polymerase. This reaction mix was added to 1.6 µl of relevant cDNA for the gene of interest and then 250 nM of each forward and reverse primers for the gene of interest. The samples were run on PCR for 30 cycles of 10 minutes 95°C, 15 seconds 95°C and 1 minute 60°C. Following completion, samples were run on a 3% agarose (Melford, MB1200) gel with 0.5 µg/ml Ethidium Bromide (VWR, 443922U) for 45 minutes at 100V before viewing on a transilluminator.

#### *2.2.4.6 Quantitative RT-PCR*

Following identification of primers specific for the gene of interest the primers were tested on RT-PCR. The cDNA was diluted with dH<sub>2</sub>O to give 2.22 ng/µl. This was added to 2 X SYBR green, and the primer at 400 nM concentration for both forward and reverse primers. This was run on the ABI700 real time machine at 50°C for 2 minutes, 95°C for 10 minutes and 40 cycles at 95°C for 15 seconds and 60°C for 1 minute. Determination of the specificity of the primers was finally validated at this stage with the dissociation curve.

#### *2.2.4.7 Relative quantitation of expression*

Derivation of the  $2^{-\Delta\Delta C_t}$  method (Livak and Schmittgen, 2001):

#### Exponential amplification of PCR

The exponential amplification of PCR is described by the following equation:

$X_n$  = number of target molecules at cycle  $n$

$X_0$  = initial number of target molecules

$E_x$  = efficiency of target amplification

$n$  = number of cycles

$$X_n = X_0 \times (1 + E_x)^n$$

The fractional cycle number at the point where the amount of amplified target reaches the set threshold is referred to as the threshold cycle (Ct):

$X_t$  = threshold number

$C_{t,x}$  = threshold cycle for target amplification

$K_x$  = constant

$$X_t = X_0 \times (1 + E_x)^{C_{t,x}} = K_x$$

Endogenous reference (internal control gene)

The internal control gene also known as the endogenous reference is defined by the equation:

$R_t$  = threshold number of the reference molecule

$R_0$  = initial number of the reference molecule

$E_r$  = efficiency of the reference amplification

$C_{t,r}$  = threshold cycle for the reference amplification

$K_r$  = constant

Dividing  $X_t$  by  $R_t$  gives the expression:

$$\underline{X_t} = \underline{X_0} \times (1 + E_x)^{C_{t,x}} = \underline{K_x}$$

$$R_t = R_0 \times (1 + E_r)^{C_{t,r}} = K_r$$

$$\underline{X_0} \times (1 + E)^{C_{t,x} - C_{t,r}} = K$$

$$R_0$$

$X_N$  = normalized amount of target ( $X_0/R_0$ )

$\Delta C_t$  = the difference in threshold cycles for target and reference ( $C_{t,x} - C_{t,r}$ )

Rearranging the equation gives:

$$X_n = K \times (1 + E)^{-\Delta C_t}$$

The final step divides the XN for any sample (q) by the calibrator (cb) XN:

$$\frac{X_{N,q}}{X_{N,cb}} = \frac{K \times (1 + E)^{-\Delta C_{t,q}}}{K \times (1 + E)^{-\Delta C_{t,cb}}} = (1 + E)^{-\Delta \Delta C_t}$$

$$X_{N,cb} = K \times (1 + E)^{-\Delta C_{t,cb}}$$

In amplicons designed to be less than 150 bp with optimal primer and  $Mg^{2+}$  concentration, the efficiency is nearing one. This means that the amount of target that has been normalized to an endogenous control and calibrator can be expressed by the following:

$$\text{amount of target} = 2^{-\Delta \Delta C_t}$$

Using the Ct values determined by the PCR machine:

Using Ct values provided by PCR run take the mean of the Ct for both target and reference gene to work out the  $\Delta C_t$  by the following equation:

$$\Delta C_t = C_t \text{ target gene} - C_t \text{ reference gene}$$

Use this value to calculate the  $\Delta \Delta C_t$  by the following equation:

$$\Delta \Delta C_t = \Delta C_t \text{ stimulated samples} - \Delta C_t \text{ Control sample}$$

This can finally be used to determine fold change in relation to the control sample by the use of the equation:

$$\text{Fold change relative to control} = 2^{-\Delta \Delta C_t}$$



Target Gene	Species	Accession number	Forward primer 5' – 3'	Reverse primer 5' – 3'
<b>ACTN2</b>	Rat	NM_001170325.1	TATTGGGGCTGAAGA AATCG	CCTCTGACACCATAG CAGCA
<b>CD31</b>	Rat	NM_031591.1	GTGGAAGTGGGGACAAAGAA	TGGCAGCGAAACACTAACAG
<b>CD90</b>	Rat	NM_012673.2	AGCCAGATGCCTGAAAGAGA	AGCAGCGCTCTCCTATCTTG
<b>cTnl</b>	Rat	NM_017144.1	ACGTGGAAGCAAAG TCACC	CAGTAGTGCCTGCAT CATGG
<b>DDR2</b>	Rat	NM_031764.3	ACTACAGTCGGGATGGCAAC	TGGGATAAGGCGAACAAATC
<b>GAPDH</b>	Rat	NM_017008.3	TGGCCTCCAAGGAGTAAGAA	TGTGAGGGAGAT GCT CAGTG
<b>TOP2a</b>	Rat	NM_022183.2	TGGACCGACCTTCAACTACC	CCACAAATCCGATGGAGTCT
<b>TOP2b</b>	Rat	NM_001100858.1	GGACTGGATGGGCTTGTAAG	CTGGATGGTGCCTTTGAAGT
<b>α-SMA</b>	Rat	NM_031004.2	GCCGAGATCTCACCGACTAC	GTCCAGAGCGACATAGCACA

Table 2.14. *List of rat primers used within this thesis.*

<b>Target Gene</b>	<b>Species</b>	<b>Accession number</b>	<b>Forward primer 5' – 3'</b>	<b>Reverse primer 5' – 3'</b>
<b>EGFR1</b>	Human	NM_005228.3	TATGTTCCCTCCAGGTCAGC	GCACCTGTAAAATGCCCTGT
<b>EGFR2</b>	Human	NM_004448	CTACGGCAGAGAACCCAGAG	CTTGATGCCAGCAGAAGTCA
<b>EGFR3</b>	Human	NM_001982	CTTATCCGAGGGCAAATTCA	TTTCCCTTAGTTCCCCATCC
<b>EGFR4</b>	Human	NM_005235	TGTGTTCCAGTGATGGCTGT	CCATTCTCAAACCTCCCGAAA
<b>P-gp</b>	Human	NM_000927.4	GTGGGGCAAGTCAGTTCATT	TTCCAATGTGTTCCGGCATT
<b>GAPDH</b>	Human	NM_002046.4	GGCCTCCAAGGAGTAAGACC	AGGGGTCTACATGGCAACTG
<b>TOP2a</b>	Human	NM_001067.3	CTCTTGACCTGTCCCCTCTG	CAAATGTTGTCCCCGAGTCT
<b>TOP2b</b>	Human	NM_001068.3	GCAGGAGAAGAGGCATTGAC	CCAAGGATTCCGTTTCTTCA
<b>ABCC1</b>	Human	NM_004996	GCCGGTGAAGGTTGTGTACT	AGGGGTTCCACTCCTTCTGT

<b>SLC22A5</b>	Human	NM_003060.3	CTGGTGGTTCATCCCTGAGT	AGTGGAAGGCACAACAATCC
<b>SLC22A4</b>	Human	NM_003059	CTGCCCAGGCGTTATATCAT	AATTTTCCCAGCATGACCAG

Table 2.15. *List of human primer used within this thesis.*

#### *2.2.4.8 Statistics*

All statistical analysis was performed using SPSS. The statistic test that has been performed through this thesis is the one-way ANOVA.

One-way ANOVA was used to compare differences between more than two groups of unrelated measurements. This test was used to determine if several groups of cells treated with different drugs were different from a vehicle control. ANOVA tests analyse the variability of the data rather than directly assessing the difference in means like t tests. This allows for not only the between group variability but also the within group variability to be assessed.



## **Chapter 3**

### Comparing Endothelial Cell Physiology Between Different Vascular Beds and Species



### 3.1 Introduction

Cardiovascular toxicity has primarily focused on cardiomyocytes as they form the contractile portion of the heart and are non-regenerative (Adamcova et al., 2005). This field has recently shifted to investigating other heart cell types, such as endothelial cells (Chiusa et al., 2012). There is now speculation that drug-induced cardiovascular toxicity may be as a result of effects on multiple cells rather than just the cardiomyocytes. For this reason, this thesis investigates the role of the microvascular endothelial cells in drug-induced cardiovascular toxicity as these cells provide a barrier to myocytes and fibroblasts from the circulating drug. Understanding how the drugs affect the microvasculature will enable a clearer understanding of potential cell targets.

This chapter looks at comparing endothelial cells from different vascular beds and species to determine if their physiological responses are comparable. Currently rodents are used for pre-clinical toxicity screening. If no toxic effects are observed in rodents, drugs are administered to humans in phase I-III clinical trials. It is emerging that toxic effects are occurring in humans that were not previously detected in rodents. The anti-diabetic drug rosiglitazone (Avandia®) has been withdrawn from the market due to its ability to produce cardiovascular toxicity, additionally rofecoxib (Vioxx®) an NSAID was withdrawn in 2004 due to its cardiovascular toxic effect. The fact that drugs are able to advance to market before toxicity is observed suggests that rodents are possibly not an ideal model for toxicity testing. Comparing rat and human cells will allow detection of any *in vitro* differences that could explain why the toxicity has not been observed in rodents during drug development. Alternatively, there is potential for discovering markers to early signs of toxicity. Toxicity is only detectable once patients develop symptoms such as arrhythmias and decreased left ventricle ejection fraction (LVEF), i.e. when long-term potentially irreversible damage has transpired.

Additionally, investigating human endothelial cells from different vascular beds, i.e. HDMEC (human dermal microvascular endothelial cells) and HCMEC (human cardiac microvascular endothelial cells), will determine if the current commonly used *in vitro* human cell model, HDMEC, is providing accurate evidence as to how HCMECs would respond. HDMEC is the classically used human endothelial cell line; comparing this to endothelial cells from the specific area of toxicity will allow a deeper understanding of how relevant HDMECs are for *in vitro* investigations in toxicity. Another commonly used endothelial cell lines is HUVEC, however these are not a microvasculature endothelial cell line so have the potential to respond differently (Damrot et al., 2006). Other studies have used animal endothelial cells for toxicity testing for example BAEC (bovine aortic endothelial cells) (Wolf and Baynes, 2006). As it is already known that vascular beds have different properties, such as the brain microvascular, expresses high levels of transporters and a very tight paracellular barrier in comparison to liver microvasculature (Garg et al., 2015; Sardi et al., 2013). In order to determine if these differences occur in other vasculature this chapter compares HDMEC and HCMEC for their physiological response to growth factors to validate a relevant cell model for *in vitro* toxicity analysis.

Endothelial cell physiology is regulated by a range of growth factors (Holmes et al., 2007). In order to compare rat and human endothelial cells their response to growth factors will be evaluated. Vascular endothelial growth factor (VEGF-A) is considered the most important in endothelial cell physiology (Cudmore et al., 2012; E et al., 2012). This growth factor is known to activate VEGFR-2 on the surface of endothelial cells, which following phosphorylation of intracellular signalling cascades leads to cellular processes such as: proliferation, survival and migration (Bruns et al., 2010; Cudmore et al., 2012; E et al., 2012). Upon agonist binding to the receptor, VEGFR-2 dimerises leading to phosphorylation

of downstream signalling molecules such as ERK1/2 and AKT resulting in cell proliferation and survival (Holmes et al., 2007; Olsson et al., 2006).

This chapter focuses on how endothelial cells from different anatomical locations and species compare. With the use of growth factor stimulation using a range of growth factors known to be involved in endothelial cell regulation and ones that have been shown to have no previous role including: EGF, NRG-1 and TGF- $\alpha$ .

## 3.2 Results

### 3.2.1 *Rat heart structure*

Pathological analysis of rodent tissue commonly used H and E staining to visualise tissue damage following drug treatment. This staining within the heart provides evidence of cardiomyocyte damage but does not provide clear evidence as to effects on other cell types. It is becoming apparent that other cell types as well as the cardiomyocytes could be important in drug-induced cardiovascular toxicity (Wolf and Baynes, 2006). For this reason a more detailed staining method has been used to show the localisation of the other cardiac cell types, this method uses cell specific markers to stain individual cell types for immunofluorescence. H and E staining, of a male wistar rat heart, in figure 3.1A provides evidence that this does not provide a detailed image of the different cells within the heart. H and E staining allows for visualisation of the cardiomyocytes and macrovasculature. In an H and E stained section the microvasculature is not clearly detectable. As the endothelial cells are becoming of increasing interest within the field of cardiovascular toxicity this project has begun to investigate microvascular endothelial cells (Greineder et al., 2011). To initially outline the importance of the microvasculature within the heart immunofluorescence staining was used to show that the heart is highly microvascularised. This was compared to



classical H and E staining where the microvasculature has not previously been observed in detail. As is evident from figure 3.1C and D there are a large number of microvessel within the heart. Endothelial cells isolated from these vessels (cells from PromoCell) will be used to investigate the role of microvessels in cardiovascular toxicity.

This project also investigated the relevance of the rat as a rodent model for cardiovascular toxicity. This was achieved *in vitro* by comparing rat and human cardiac endothelial cells. In order to achieve this the cell lines to be utilised within this study were initially validated.

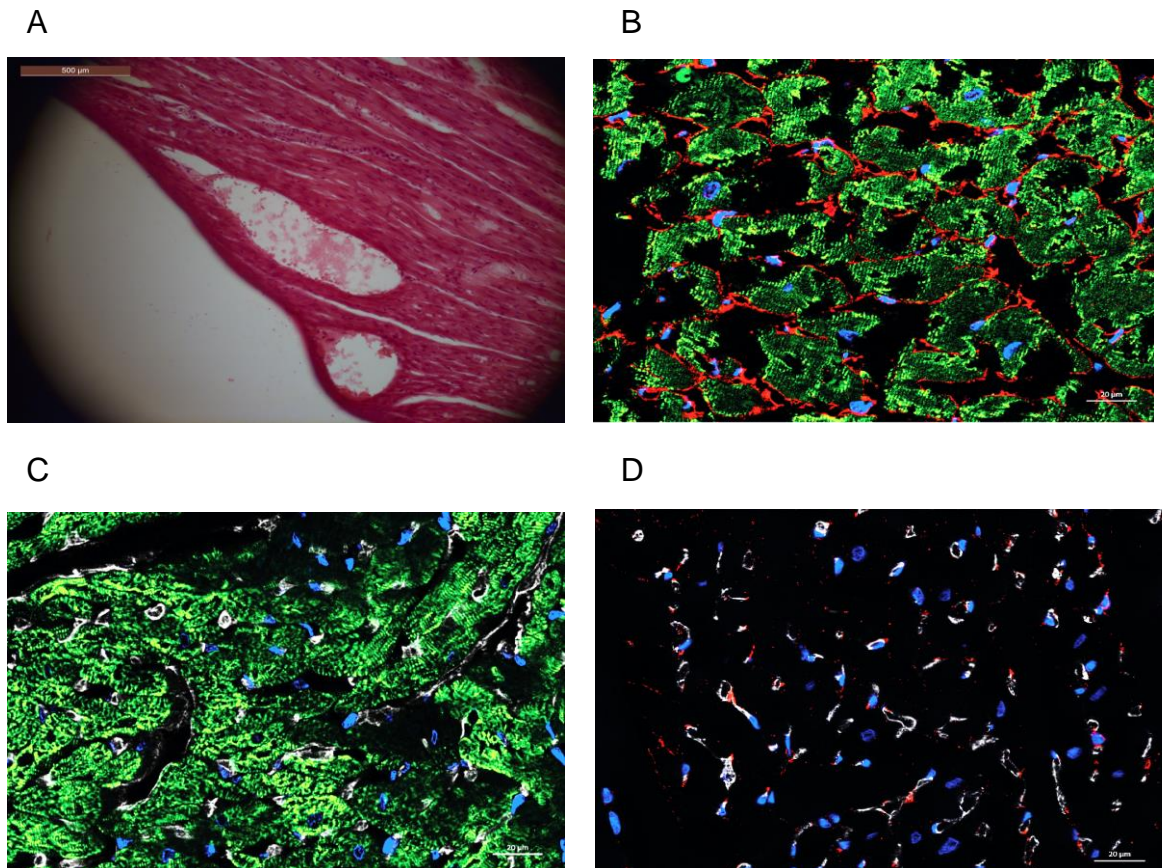


Figure 3.1. **Images of rat heart stained with H and E or immunofluorescence.** Rat hearts were obtained from male wistar rats A. H and E staining, B. cTnI (myocytes, green), collagen 1 (fibroblasts, red) and hoechst (nuclei, blue), C. cTnI (myocytes, green), RECA1 (endothelial cells, white) and hoechst (nuclei, blue) and D. NG2 (pericytes, red), RECA1 (endothelial cells, white) and Hoechst (nuclei, blue).

### 3.2.2 Characterising rat cells

Rat cardiac endothelial cells (RCECs, from male sprague dawley rats) were characterised for their expression of endothelial cell markers. The RCECs were compared to rat heart tissue (from male wistar rats) for expression of known cellular markers using qRT-PCR. The cellular markers being investigated included: *Cd31*, *Vegfr-2*, *Actn2*, *Ctni*, *Ddr2*, *Thy1* and  $\alpha$ -*Sma*. Endothelial cells were characterised as *Cd31* (platelet endothelial cell adhesion molecule 1, PECAM1) and *Vegfr-2* (vascular endothelial growth factor receptor 2) positive (Ulger et al., 2002). *Actn2* (sarcomeric alpha actinin), *Ctni* (cardiac troponin inhibitory), *Ddr2* (discoidin domain receptor 2), *Thy1* (CD90) and  $\alpha$ -*Sma* (smooth muscle actin) negative (Souders et al., 2009), figure 3.2. The endothelial cells were compared against commercially available immortalised rat cardiac myocytes, H9c2 (Will et al., 2008) and immortalised rat fibroblasts, rat-1-fibroblasts.

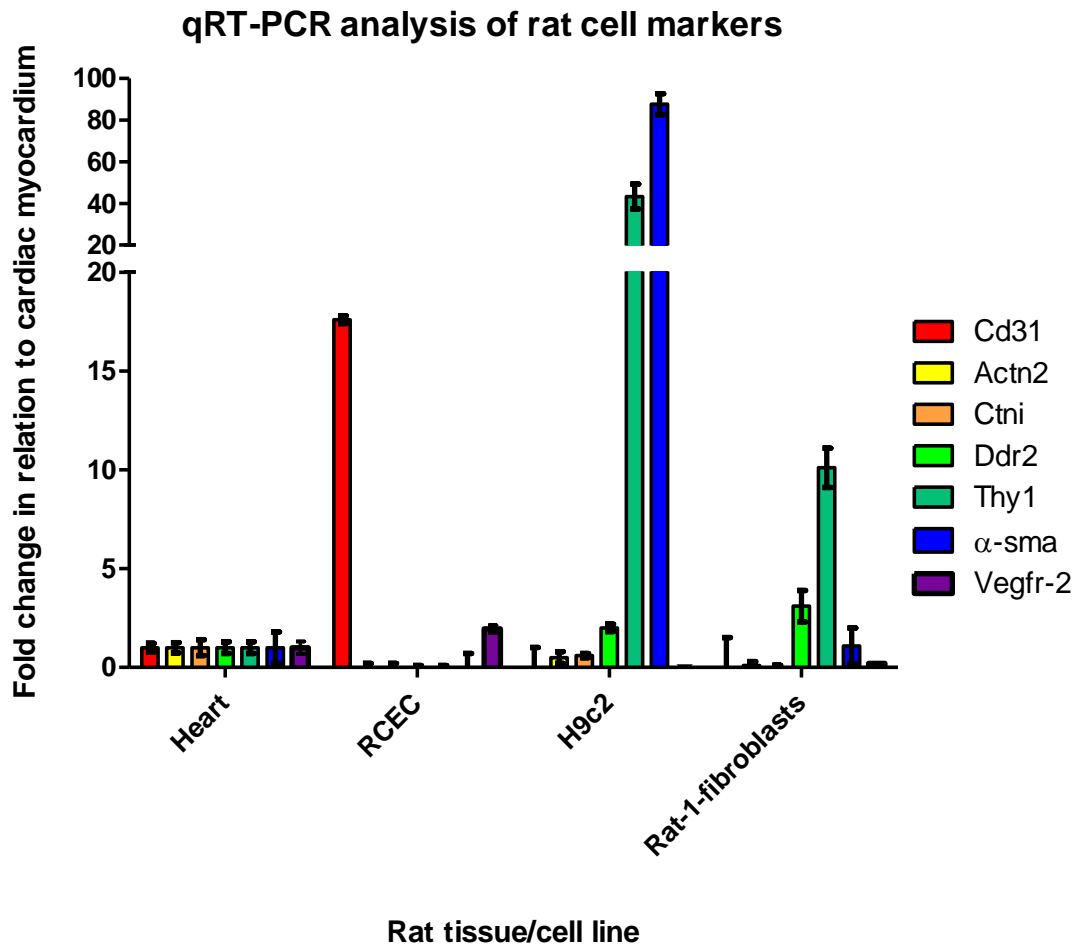


Figure 3.2. **qRT-PCR analysis of rat cellular markers.** qRT-PCR in triplicate for expression of *Cd31*, *Actn2*, *Ctni*, *Ddr2*, *Thy1*,  $\alpha$ -*Sma* and *Vegfr-2* in relation to the housekeeping gene *Gapdh*. Expression represented relative to heart, which was arbitrarily set as 1.00. Data is representative of a single cell extraction analysed in triplicate, mean  $\pm$  SD, data plotted in GraphPad Prism.

### 3.2.3 Comparing intracellular signalling responses to growth factors in endothelial cells

The data outlined in figure 3.2 clearly demonstrated the expression of known endothelial markers *Cd31* and *Vegfr2* (Ulger et al., 2002). The absence of expression for other cellular markers provided evidence that the endothelial cell line is not contaminated with other cell types, as can commonly occur in cell isolation preparations.

Following characterisation of the rat cardiac endothelial cells, the validity of rat cardiac endothelial cells for extrapolation to human models was determined through physiological comparisons. This was performed by investigating the intracellular signalling responses of the different endothelial cell lines to a range of growth factors. This response was analysed to allow the identification of different receptor tyrosine kinases expressed on these cells. Endothelial pathophysiology is regulated by a number of stimuli including growth factor activation of RTKs. Endothelial cell physiology has been demonstrated to be regulated in response to VEGF-A, FGF, PDGF, HGF and EGF to varying degrees (Amin et al., 2008; Barkefors et al., 2008; Sulpice et al., 2009). Currently, the effect of VEGF-A on endothelial physiology has been extensively evaluated, with more recent literature linking HGF and VEGF-A signalling in endothelial cells (Sulpice et al., 2009). Following growth factor activation of RTKs down stream signalling cascades are induced. Within endothelial cells it is known that AKT and ERK1/2 intracellular signalling kinases are important in endothelial survival and proliferation (Mori et al., 2000).

In this screen shown in figure 3.3, it was determined that as expected VEGF-A and HGF stimulation led to phosphorylation of AKT and ERK1/2 in the endothelial cells. This result was expected as it has been previously published that endothelial cells express VEGFR-2 and HGFR and upon stimulation these receptors regulate intracellular signalling kinases to induce cell proliferation, survival and migration (Holmes et al., 2007; Sulpice et al., 2009). However, it was observed that in HCMECs, EGF and TGF- $\alpha$  also led to phosphorylation of AKT and ERK1/2. This showed a difference, not only between species, but also between anatomical locations, as this response was not seen in either RCEC or HDMECs.

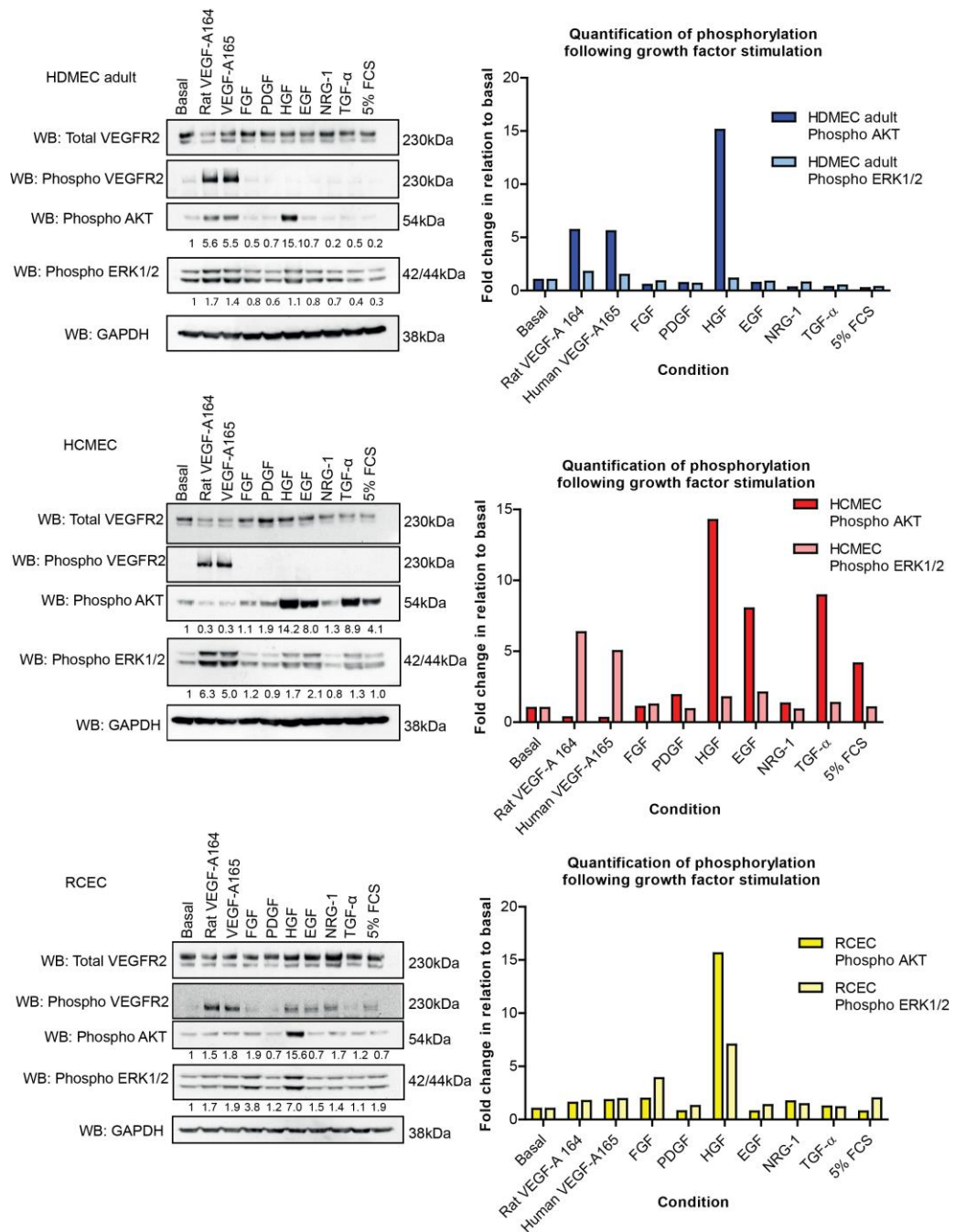


Figure 3.3. **Comparing intracellular signalling responses using western blotting.** Top – HDMEC adult, middle – HCMEC, bottom – RCEC. Blotting for total VEGFR2, phospho VEGFR2, phospho AKT, phospho ERK1/2 and GAPDH.

As it has been demonstrated that endothelial cells respond differently to growth factors the next logical step was to analyse physiological responses of endothelial cell to growth factors. If the different kinase activation profiles observed in the endothelial cells led to the endothelial

cells having different physiological responses this could begin to explain how cardiac endothelial cells are more susceptible to certain drugs than endothelial cells from other anatomical locations.

#### 3.2.4 Physiological relevance of growth factor stimulation

Important physiological responses known to be regulated by growth factors in endothelial cells include: proliferation and angiogenesis (Holmes et al., 2007). The first physiological response to be investigated was cellular proliferation. This was analysed by measuring the level of ATP released from cells using Cell Titer Glo®. Cells were grown to sub-confluence to allow space for proliferation upon stimulation with growth factors for 72 hours. This assay measured the level of ATP released from the cells, as more cells within a well will increase the concentration of ATP upon Cell Titer Glo® lysis as more cells are able to contribute to the level of ATP.

It is outlined in figure 3.4 that endothelial cell proliferation was significantly enhanced by VEGF-A, VEGF-E and HGF. EGF and TGF- $\alpha$  significantly increases proliferation in HCMEC, but not HDMEC adult or RCEC. This provided evidence of differences between endothelial cells from different anatomical locations and species.



### Cellular proliferation following growth factor stimulation

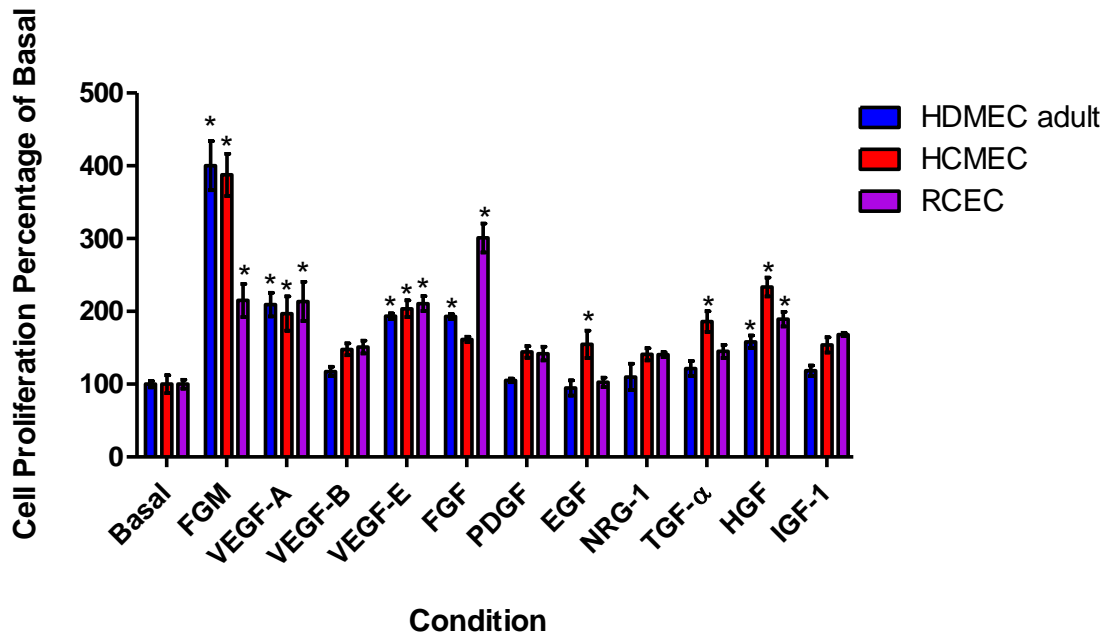
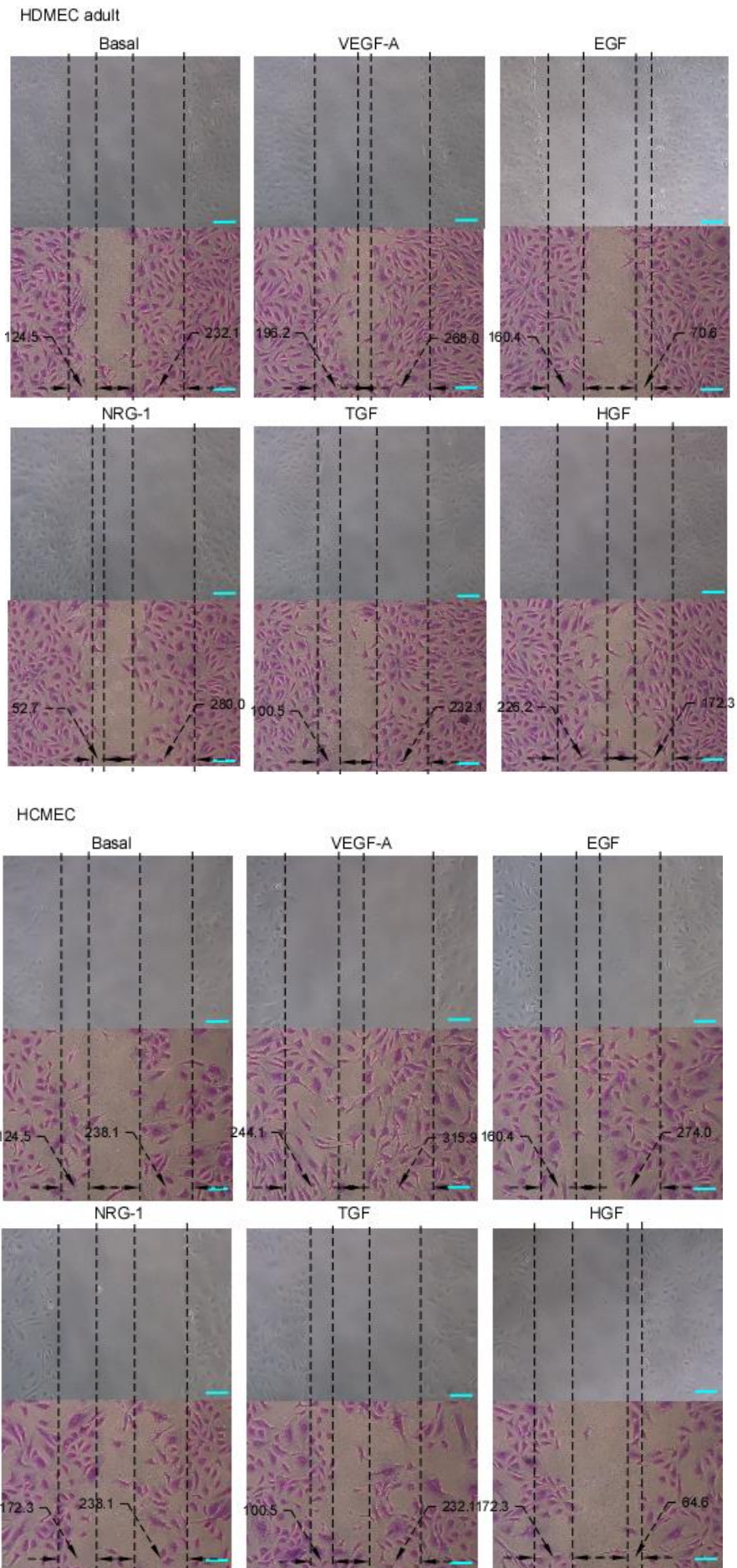


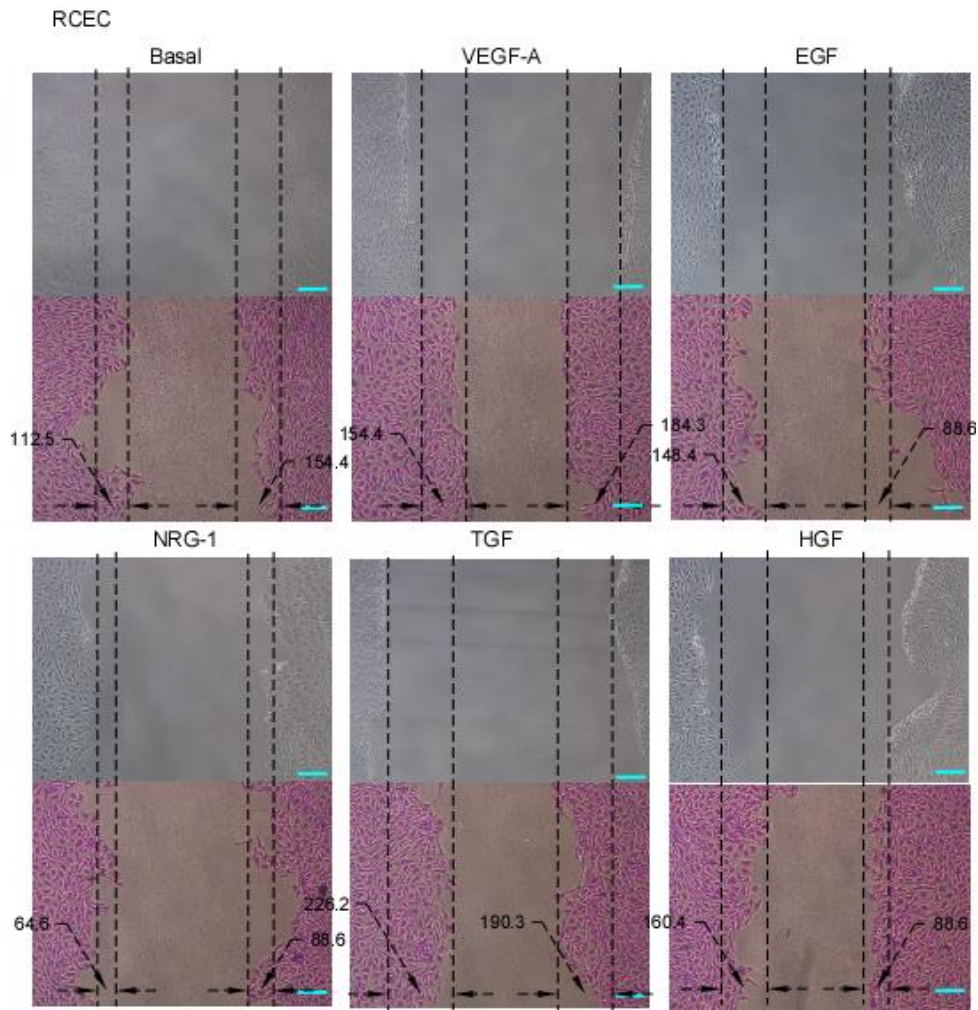
Figure 3.4. **Cellular proliferation following growth factor stimulation.** HDMEC adult, HCMEC and RCEC were stimulated with growth factors at 50ng/ml for 72 hours. Cells were lysed using Cell Titer Glo®. Data representative of 3 individual wells of cells, n=3, mean  $\pm$  SD; \* =  $p \leq 0.05$  one way ANOVA, SPSS, data plotted in GraphPad Prism.

Endothelial cells possess the potential to migrate following formation of a wound. Migration is classed as a form of angiogenesis where the endothelial cells are able to replicate to repair a pre-existing vessel. This response is known to be enhanced by VEGF-A (Holmes et al., 2007). In order to determine if this process is regulated by other growth factors, EGF, NRG-1, TGF- $\alpha$  and HGF were analysed. As HCMEC have been shown to respond to EGF and TGF- $\alpha$  in previous experiments within the Chapter (Figs. 3.3 and 3.4) the effect of these growth factors on migration of endothelial cells was analysed. NRG-1 is known to be a ligand for EGFR4, one of the members of the EGFR family. This growth factor was analysed to determine if several ligands to different EGFRs could induce the same physiological events. Previous data in figures 3.3 and 3.4 suggested that NRG-1 did not activate the kinases AKT and ERK1/2 and

was not involved in endothelial cell proliferation. HGF was used as it had been shown to be linked to VEGF-A signalling (Sulpice et al., 2009). Cells were plated and scratched to make a hypothetical wound and the response to each growth factor was analysed. The results are outlined in figure 3.5.







**Cellular Migration Following Growth Factor Stimulation**

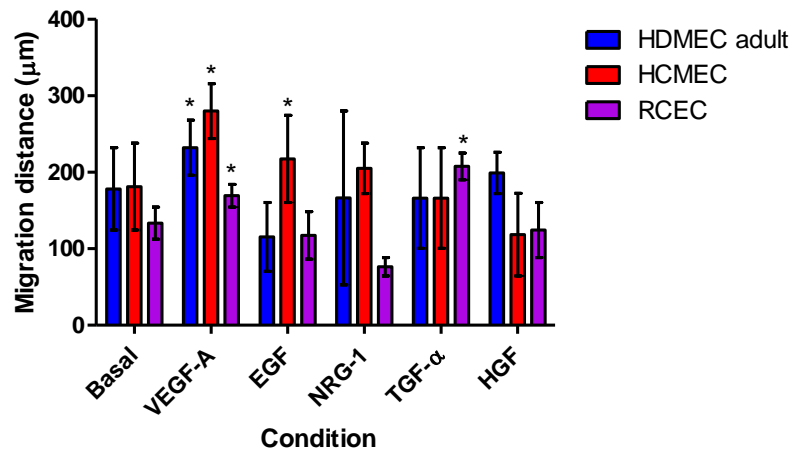


Figure 3.5. **Cellular physiology analysis of migration ability following stimulation.** HDMEC adult, HCMEC and RCEC were scratched before addition of growth factors at 50ng/ml in low serum media for 16 hours,

cells were imaged immediately after scratch for a time 0 image. Images were analysed using canvas and data plotted using graph pad prism n=6, 3 separate wells with measurements taken for each side of the scratch (image from a single well shown), \* =  $p \leq 0.05$  one way ANOVA, SPSS.

The results provided evidence that VEGF-A induces cellular migration, while other growth factors did not appear to affect migration to the same extent that VEGF-A induces migration. The data suggest that EGF was not involved in endothelial angiogenic processes but was involved in proliferation and potentially survival of endothelial cells as shown in figures 3.3 and 3.4.

### *3.2.5 Further differences between endothelial cells*

Moving on from growth factor effects on endothelial cells, the next step in comparing endothelial cells was to assess expression of known targets for the drugs of interest within this project. Of specific interest was to investigate the effects of doxorubicin on endothelial cells, as it had been demonstrated that doxorubicin induces cardiovascular toxicity and decreases barrier function (Wolf and Baynes, 2006). Doxorubicin is known to have several actions on cells, but a recent publication has shown the importance of the topoisomerase II  $\alpha$  and  $\beta$  enzyme (Vejpangsa and Yeh, 2014). Doxorubicin targets the topoisomerase II enzyme, leading to apoptosis induction. It has recently been published that toxicity can be reduced by depleting topoisomerase II  $\beta$  in cardiomyocytes (Vejpangsa and Yeh, 2014). This section investigates if the level of topoisomerase II  $\beta$  is higher in cardiac endothelial cells in comparison to dermal endothelial cells.

Since topoisomerase II levels differ between the different tissues, and doxorubicin targets topoisomerase II, different topoisomerase II levels across the range of cells could be an indicator of cell type-specific susceptibility to toxicity. Figure 3.6 outlines the two types of

topoisomerase II that are known to be inhibited by doxorubicin, these results show that both TOP2 $\alpha$  and TOP2 $\beta$  were expressed at higher levels within the heart compared to other tissues.

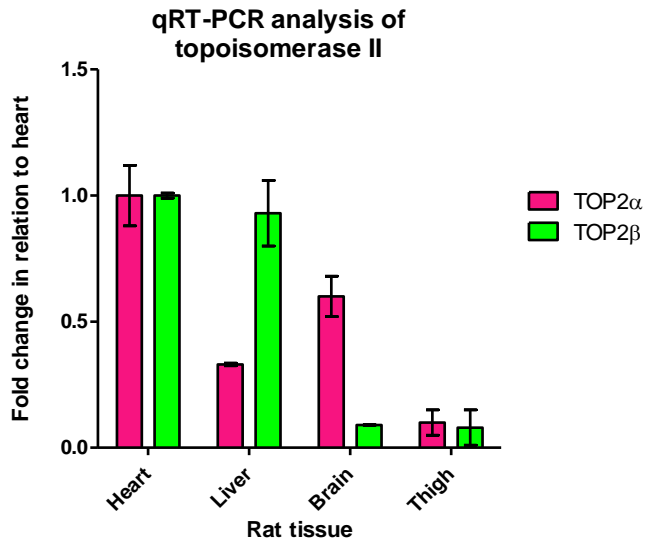


Figure 3.6. ***qRT-PCR expression of TOP2 $\alpha$  and TOP2 $\beta$  across rat tissues.*** qRT-PCR in triplicate for expression of *Top2 $\alpha$*  and *Top2 $\beta$*  in relation to the housekeeping gene *Gapdh*. Expression represented relative to heart, which was arbitrarily set as 1.00. Data is representative of a single tissue extraction analysed, mean  $\pm$  SD, data plotted in GraphPad Prism.

As the expression of topoisomerase II differed between rat tissues it was next evaluated if this was also true in human endothelial cells from different vascular beds.

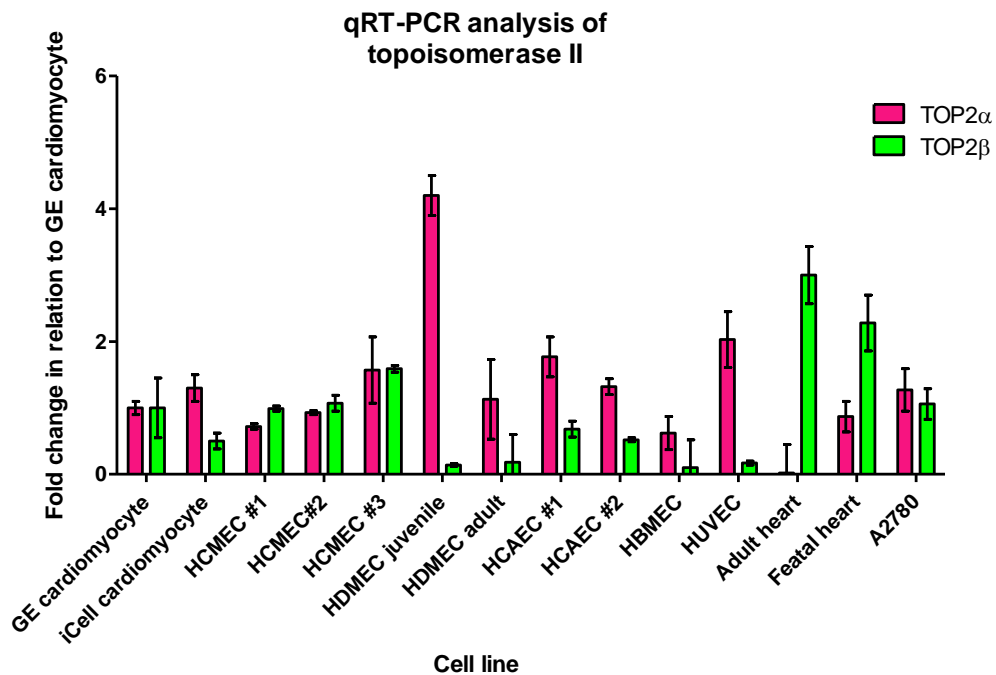


Figure 3.7. **qRT-PCR analysis of TOP2 across different human endothelial cells.** qRT-PCR in triplicate for expression of *TOP2 $\alpha$*  and *TOP2 $\beta$*  in relation to the housekeeping gene *GAPDH*. Expression represented relative to HDMEC juvenile, which was arbitrarily set as 1.00. Data is representative of a single cell extraction analysed in triplicate, mean  $\pm$  SD, data plotted in GraphPad Prism.

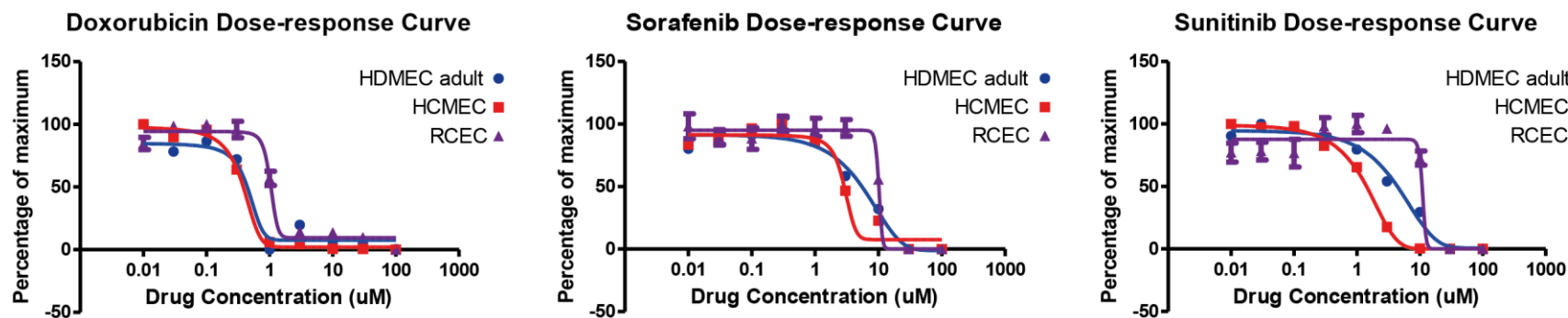
Figure 3.7 details that topoisomerase II b had higher expression in HCMEC than other endothelial cell types (representative of HCMEC from 3 different patients). Topoisomerase II  $\alpha$  levels remained constant across the range of adult endothelial cells screened. Interestingly, there appeared to be a higher level of topoisomerase II  $\alpha$  in juvenile cells (HDMEC and HUVEC) in comparison to adult endothelial cells screened (HCMEC, HDMEC and HCAEC). Topoisomerase II  $\alpha$  is the known clinical target for doxorubicin whereas topoisomerase II  $\beta$  is predicted to be associated with cardiovascular toxicity events. The evidence from figure 3.7 shows that cardiac endothelial cells expressed a higher level of topoisomerase II  $\beta$  than other endothelial cells. The increase in topoisomerase II  $\beta$  could contribute to the cardiovascular toxicity observed following doxorubicin treatment.



The findings thus far in this Chapter suggested differences in endothelial cells from different anatomical regions and between species. The next step in comparing the endothelial cells led to comparing how the endothelial cells respond to three anti-cancer drugs known to induce cardiovascular toxicity that will be investigated further within this thesis.

### *3.2.6 Comparison of cellular viability across endothelial cells*

Emerging research has shown that anti-cancer drugs doxorubicin, sorafenib and sunitinib affect the endothelium, which could contribute to cardiovascular toxicity (Wolf and Baynes, 2006; Chiusa et al., 2012). The IC<sub>50</sub> of these drugs across HDMEC adult, HCMEC and RCEC was analysed to determine if any cells are more sensitive (Fig. 3.8).



	Doxorubicin IC50 ( $\mu\text{M}$ )	Sorafenib IC50 ( $\mu\text{M}$ )	Sunitinib IC50 ( $\mu\text{M}$ )
HDMEC adult	$0.45 \pm 0.05$	$3.05 \pm 0.09$	$2.86 \pm 0.11$
HCMEC	$0.36 \pm 0.03$	$2.89 \pm 0.07$	$1.3 \pm 0.08$
RCEC	$1.03 \pm 0.10$	$10.12 \pm 0.15$	$10.98 \pm 0.21$

Figure 3.8. **Cell viability following treatment with doxorubicin, sorafenib or sunitinib.** Measurement of cell viability following treatment with drugs doxorubicin, sorafenib or sunitinib at concentrations ranging from 100 $\mu\text{M}$  to 0.01 $\mu\text{M}$ . Viability analysis was measured with Cell Titer Glo®. The IC50 was calculated using GraphPad Prism.

## 3.3 Discussion

### *3.3.1 Rat heart structure and characterising rat cells*

This project aimed to investigate cardiovascular toxicity *in vitro*. In order to do this cell models were initially validated. The field of cardiovascular toxicity has primarily focused on cardiomyocytes, until recently when other cardiac cell types have been investigated for their role in cardiovascular toxicity (Greineder et al., 2011). This section of work began by visualising the rat heart. Here, this project confirmed that macrovessels and cardiomyocytes could be observed with classical H and E staining, which has been used to study cardiovascular toxicity. Immunofluorescence staining provided evidence of the high level of microvasculature within the heart. As the vasculature is becoming increasingly investigated within the field of cardiovascular toxicity this is the area this project has focused on.

In order to compare between species a cell model for rat cardiac endothelial cells was validated. Data is presented for RCEC, however, other rat endothelial cells were tested but these did not express cell specific markers so were ruled out from further testing. The results from this Chapter identified RCECs to be endothelial in origin so these cells could be carried forward for future experiments.

### *3.3.2 Comparing intracellular signalling responses to growth factors in endothelial cells*

The vasculature is known to provide a barrier to the underlying cells so understanding how drugs affect the endothelial cells lining the vasculature will provide an understanding of potential cellular targets. The endothelial barrier is comprised of junctions between adjacent cells and



the plasma membrane containing proteins that regulate the movement into and out of the cell. The barrier is known to be regulated by a range of intracellular signalling kinases with recent evidence showing MAPKs and RTKs are involved in the regulation (Liu et al., 2014). The barrier is known to have different levels of permeability depending on the anatomical location, for example the blood brain barrier (BBB) is considered highly impermeability; whereas the kidney and liver and considered highly permeable as these are the sites of removal and metabolism of compound within the body (Sardi et al., 2013; Gonzalez-Mariscal et al., 2005).

This project began by investigating if endothelial cells from different anatomical locations respond differently to growth factors. Endothelial cells express a range of RTKs that are known to modulate several physiological responses of endothelial cells. It is generally assumed that endothelial cells respond in a similar fashion. However, the knowledge that endothelial permeability differs between vascular beds and that this process is regulated by MAPKs and potentially RTKs provided the question: do all endothelial cells respond to growth factors identically? While investigating this question it was also analysed if endothelial cells from different species have similar growth factor activation profiles. Currently immortalised brain endothelial cells have been studied for junction regulation and a link has been demonstrated between junctions and EGFRs (Cameron *et al.*, 2003).

### *3.3.3 Physiological relevance of growth factor stimulation*

The results detailed in figure 3.3 provided evidence that HCMEC are able to respond to EGF and TGF- $\alpha$ . As EGFRs have begun to be linked to endothelial barrier regulation this is an interesting observation (Samak et al., 2011; Liu et al., 2014). Given that doxorubicin is able to reduce barrier

function this observation could be useful in understanding cardiovascular toxicity (Wolf and Baynes, 2006).

Determining the role of EGF induced phosphorylation of AKT and ERK1/2 on endothelial physiology in HCMEC proliferation and angiogenic migration were assessed (Figs. 3.4 and 3.5). Here it is clear that EGF and TGF- $\alpha$  were able to significantly induce proliferation, suggesting a role potentially in cellular survival.

#### *3.3.4 Further differences between endothelial cells*

As has been demonstrated thus far within this Chapter, there are differences in endothelial cell responses to growth factors. To further determine if there were differences between endothelial cells this section of work looked at the expression of topoisomerase II across a range of cells. It has been recently observed that increased levels of topoisomerase II  $\beta$  are associated with doxorubicin cardiovascular toxicity (Vejpongsa and Yeh, 2014).

Doxorubicin works by inhibition of topoisomerase II which prevents DNA replication leading to cell death (Kik et al., 2009; Mizutani et al., 2005; Pommier et al., 2010). It has been demonstrated that topoisomerase II  $\alpha$  is highly expressed in proliferating cells where as topoisomerase II  $\beta$  is expressed in quiescent cells (Vejpongsa and Yeh, 2014). Topoisomerase II  $\beta$  has been detected in the heart and has been implicated to be involved in cardiovascular toxicity (Vejpongsa and Yeh, 2014). Data from figure 3.7 provides evidence that topoisomerase II  $\beta$  has higher expression levels in the cardiac endothelial cells than endothelial cells from other anatomical locations, such as HDMEC. As it has been demonstrated that depleting topoisomerase II  $\beta$  in cardiomyocytes leads to reduced cardiovascular toxicity (Vejpongsa and Yeh, 2014). This provides the question whether depleting topoisomerase II  $\beta$  in cardiac endothelial cells as well as cardiomyocytes could further

reduce the toxicity observed? This is a potential hypothesis for reduced cardiovascular toxicity.

### *3.2.5 Comparison of cellular viability across endothelial cells*

As it has been demonstrated that the anticancer drugs doxorubicin, sorafenib and sunitinib exert toxicity on the endothelial cells as well as the cardiomyocytes, these drugs were investigated within this study (Wolf and Baynes, 2006; Schmidinger et al., 2008).

It is clear that for the three drugs of interest that HDMEC adult and HCMEC have similar IC<sub>50</sub> values whereas RCEC has a higher IC<sub>50</sub> value suggesting that the drugs are less toxic to rat cells. This difference could account for the fact that cardiovascular toxicity is missed in preclinical trials along with the fact that toxicity only occurs at later stages of drug treatment.

This project will move on to investigate how anti-cancer drugs known to induce cardiovascular toxicity affect endothelial cell barrier formation.



## **Chapter 4**

Herceptin® and Doxorubicin Affect Cardiac  
Microvascular Endothelial Cell Barrier  
Formation Leading to Increased Drug  
Permeability and Cardiac Toxicity



## 4.1 Introduction

The previous Chapter provided evidence to show that endothelial cells from different anatomical locations respond differently to EGF stimulation. Combining this knowledge with the published data showing a role for EGFRs in the regulation of tight junctions (Samak et al., 2011; Liu et al., 2014), here the expression of the EGFRs across a range of endothelial cells was investigated. It was of particular interest to analyse the effects of Herceptin® and doxorubicin on the tight junction barrier. Herceptin® is an inhibitor for EGFR2 (HER2) and has been demonstrated to induce cardiovascular toxicity in the clinic. Herceptin® has been used here to investigate if tight junctions are regulated by EGFRs in endothelial cells and if there is a difference in endothelial cells from different anatomical locations. However, as Herceptin® only inhibits EGFR2 in human endothelial cells (data not being presented in this Chapter), its effect was studied on different human endothelial cells. Furthermore, the effects of doxorubicin on endothelial tight junctions in different human endothelial cells were analysed. Doxorubicin has been investigated as it has shown to decrease barrier function (Wolf and Baynes, 2006). Herceptin® and doxorubicin were used here both individually and in combination, as clinically the drug combination is becoming increasingly popular (Baselga et al., 1998).

The microvasculature is comprised of a monolayer of endothelial cells, which function to provide a barrier between the circulation and other cells within specific tissues (Bazzoni and Dejana, 2004; Dejana et al., 1995; Vandenbroucke et al., 2008; Wang and Alexander, 2011). Endothelial cell homeostasis is regulated by growth factors and receptors (Harhaj et al., 2006). Endothelial homeostasis includes: proliferation, migration, survival and permeability (Bazzoni and Dejana, 2004).

The endothelial barrier regulates the paracellular movement of oxygen, free fatty acids and toxins from the circulation. This barrier is comprised of tight and adherens junctions, that are thought to regulate permeability regulation in different vascular beds (Gunzel and Yu, 2013). Tight junctions are comprised of transcellular proteins claudins, occludins and JAMs connecting the intracellular proteins ZO-1, -2 and -3 which connect the junction to the actin cytoskeleton (Fig. 1.7) (Bazzoni and Dejana, 2004; Dejana et al., 1995; Gunzel and Yu, 2013; Le Guelte and Gavard, 2011; Li and Poznansky, 1990; Niessen, 2007; Vandenbroucke et al., 2008). Adherens junctions comprise of transcellular proteins cadherins connecting to intracellular catenins which connect the junction to the actin cytoskeleton (Fig. 1.7) (Bazzoni and Dejana, 2004; Le Guelte and Gavard, 2011; Niessen, 2007; Vandenbroucke et al., 2008; Wang and Alexander, 2011).

Tight junctions play a critical role in the regulation of paracellular permeability, and have been investigated for their role in the blood brain barrier (BBB), which is considered highly impermeable to drugs and their metabolites (Liu et al., 2014; Sardi et al., 2013). This Chapter investigates how the paracellular permeability of endothelial cells from different anatomical locations alters in response to doxorubicin and Herceptin®.

Doxorubicin is an anti-cancer drug belonging to the anthracycline antibiotic class of drugs (Kik et al., 2009; Mizutani et al., 2005; Perez-Arnaiz et al., 2014; Pommier et al., 2010; Sartiano et al., 1979; Wojcik et al., 2014). Doxorubicin's clinical efficiency has been limited by its dose-dependent cardiovascular toxicity observed (Heger et al., 2013; Wolf and Baynes, 2006; Zhang et al., 2012). It has been observed that doxorubicin increases permeability when endothelial cells are treated with doxorubicin, suggesting that this could contribute to overall toxicity (Wolf and Baynes, 2006).

Herceptin® is a humanised monoclonal antibody that specifically targets EGFR2 (Baselga et al., 1998). This drug has clinical efficacy in around 20% of human breast cancers which over express EGFR2. Breast cancer patients have a biopsy taken which is tested for expression of EGFR2 to determine which subset of patients are likely to respond to Herceptin®. Herceptin® has been shown to induce cardiovascular toxicity in patients (Valabrega et al., 2007). Herceptin® has been trialled in combination therapies and has shown success with doxorubicin (Baselga et al., 1998). Combinations initially involved the drugs been administered together, however, after observed toxicity doxorubicin is administered before Herceptin® (Baselga et al., 1998).

This Chapter investigates how doxorubicin and Herceptin® combination therapy affect endothelial permeability as it has previously been observed that doxorubicin increases endothelial permeability (Wolf and Baynes, 2006). This Chapter investigates the effects of these drugs in combination across multiple vascular beds on paracellular permeability.

## 4.2 Results

### *4.2.1 Investigation of kinase phosphorylation following growth factor stimulation*

In order to investigate the effects of doxorubicin and Herceptin® combinations, to try to understand drug-induced cardiovascular toxicity a range of human cell lines were investigated: HCMECs (human cardiac microvascular endothelial cells), HDMECs (human dermal microvascular endothelial cells), HBMECs (human brain microvascular endothelial cells) and the A2780 ovarian cancer cell line. HCMEC (human cardiac microvascular endothelial cells) have been shown in chapter 3 to respond differently to HDMEC (human dermal microvascular endothelial cells). The difference observed was due to HCMEC expressing EGFR1 and 2 at higher levels than HDMEC. As EGFR2 is the target for Herceptin® this

could also be important for drug-induced cardiovascular toxicity observed following Herceptin® treatment. These two cell types were further compared to HBMEC (human brain microvascular endothelial cells), as Herceptin® and doxorubicin are unable to cross the BBB (Garg et al., 2015; Sardi et al., 2013). This allows HCMEC to be compared to two cell lines that do not undergo Herceptin® induced toxicity to provide an understanding of how Herceptin® affects HCMEC different to HDMEC and HBMEC. The response of HCMEC was further compared to a cancer cell line known to express high levels of EGFR2, A2780 ovarian cancer cell line (Villa-Moruzzi, 2011).

Endothelial cells are known to respond to growth factors with much focus on VEGF-A (Holmes et al., 2007). A panel of growth factors known to be important in survival and proliferation were investigated to determine if endothelial cells from different anatomical locations responded to different growth factors. Endothelial cells express receptors to VEGF, FGF, PDGF and HGF. These growth factors along with EGF, NRG-1 and TGF- $\alpha$  were analysed for their activation of intracellular kinases AKT and ERK1/2. The results in figure 4.1 demonstrated that stimulation of HCMEC with EGF induced phosphorylation of AKT and ERK1/2. These kinases signal downstream of the individual growth factor receptors so give an indication which growth factor receptors are functional on the endothelial cells. Endothelial cell survival and proliferation are regulated by AKT and ERK1/2 signalling cascades.

Cardiac endothelial cells (HCMEC) responded to EGF stimulation (Fig. 4.1 B), whereas dermal endothelial cells (HDMEC) did not respond to EGF stimulation (Fig. 4.1 A), and brain microvascular endothelial cells (HBMEC) showed minor phosphorylation following EGF stimulation (Fig. 4.1 C). This result suggested that endothelial cells from different anatomical locations express different growth factor receptors giving them the potential to respond differently from each other. All cell types responded similarly to VEGF-A and HGF which had been previously



reported (Ding et al., 2003; Sulpice et al., 2009). A2780 cancer cells show phosphorylation in response to NRG1 which is the known ligand for EGFR2/EGFR4 receptor dimer.

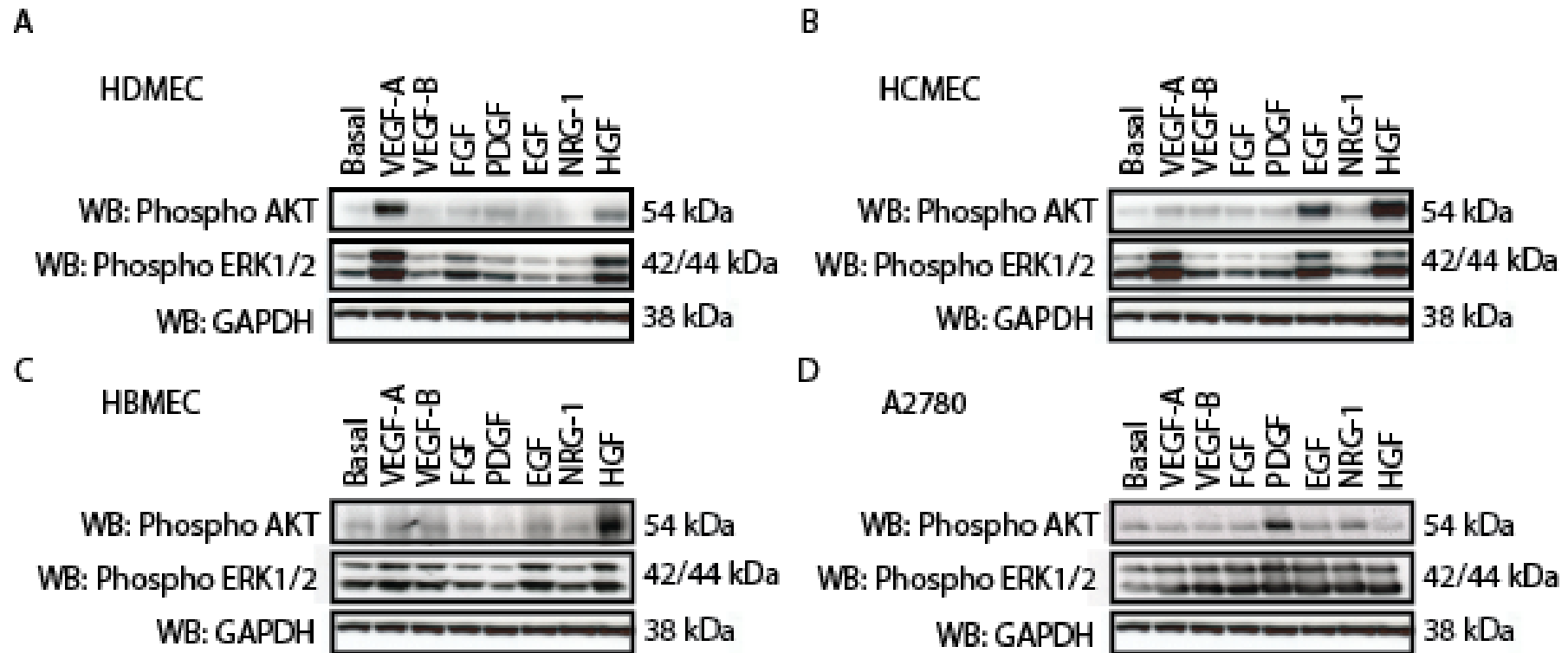
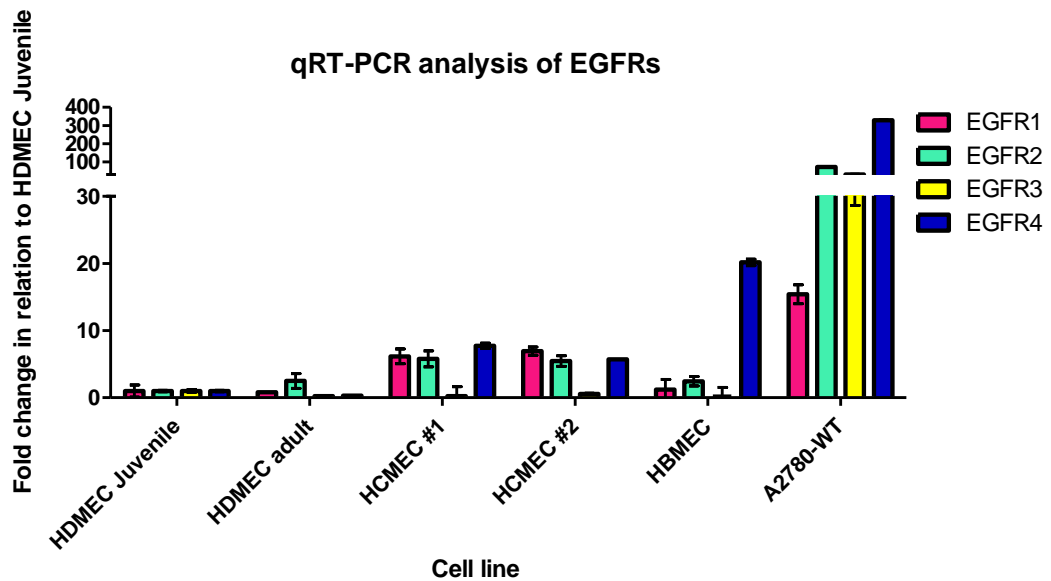


Figure 4.1. **Intracellular kinase response to growth factor stimulation.** (A) HDMEC adult, (B) HCMEC, (C) HBMEC and (D) A2780 WT. Intracellular signalling responses were analysed focusing on phosphorylation of AKT and ERK1/2.

#### 4.2.2 Analysis of growth factor receptor expression in different endothelial cells

The expression of EGF growth factor receptors on endothelial cells from different anatomical locations was analysed by qRT-PCR to determine if they differed between vascular beds. This was designed to determine the difference between HDMEC adult and HCMEC observed in figure 4.1, detailing that HCMEC stimulation with EGF leads to phosphorylation of the intracellular kinase AKT and ERK1/2. Cells were analysed for expression of *EGFR1*, *EGFR2*, *EGFR3* and *EGFR4*. Cell lines were compared to HDMEC juvenile cells for receptor expression, A2780s were used as a control to determine how relative EGFR expression in endothelial cells compares to cancer cells.



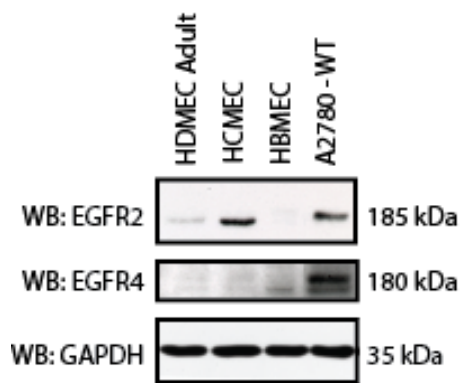


Figure 4.2. **Gene expression of growth factor receptors in different human cell lines.** Blotting for EGFR2 and EGFR4 with GAPDH used as a loading control. qRT-PCR for expression of receptors EGFR1, EGFR2, EGFR3 and EGFR4. Data plotted as fold change relative to HDMEC juvenile cells which was arbitrarily set as 1.00. Data is representative of mean  $\pm$  SD, data plotted in GraphPad Prism.

It can clearly be deduced from figure 4.2 that there is a difference in expression of the EGFRs across the different endothelial cell lines. HCMEC clearly demonstrated higher levels of EGFR1 and 2 than HDMEC, however in comparison to ovarian cancer cells, A2780, this is minimal expression.

#### 4.2.3 Herceptin® and doxorubicin combination therapy in endothelial cells

The primary focus of this Chapter was to assess if endothelial cell tight junctions are regulated by EGFRs, as well as determining if there are differences in the endothelial cells. Therefore, it was also investigated how Erbitux® and lapatinib affect the tight junctions.

Erbitux® is a humanised monoclonal antibody known to specifically target EGFR1 (Buchsbaum et al., 2002). Erbitux® has been used to determine if inhibition of EGFR1 affects endothelial cells in a similar way to inhibition of EGFR2 using Herceptin®. Lapatinib is a RKT that is able to inhibit both EGFR1 and 2. The idea behind utilising this drug was to determine if any changes are specific to monoclonal antibodies or if the effects can be observed with other classes of drugs that are known to target EGFRs.

Lapatinib was also used to provide evidence to determine if dual inhibition of the EGFRs was able to induce further barrier perturbation.

In order to effectively use these drugs the IC<sub>50</sub>s were determined to ensure that the drugs were being used at concentration that did not exert any cytotoxicity to the cells. This aimed to rule out any effects linked to apoptosis.

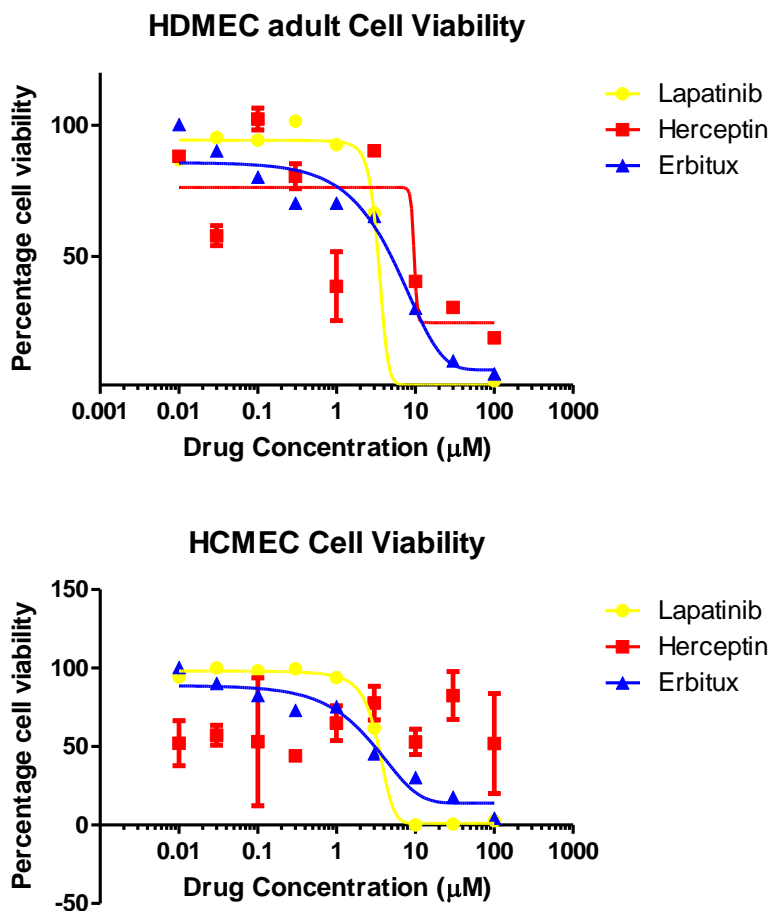


Figure 4.3. **Cell viability of lapatinib, Herceptin and Erbitux.** HDMEC adult and HCMEC cell viability for lapatinib, Herceptin® or Erbitux® at concentrations ranging from 100 µM to 0.01 µM for 72 hours. Viability was measured with Cell Titer Glo®.

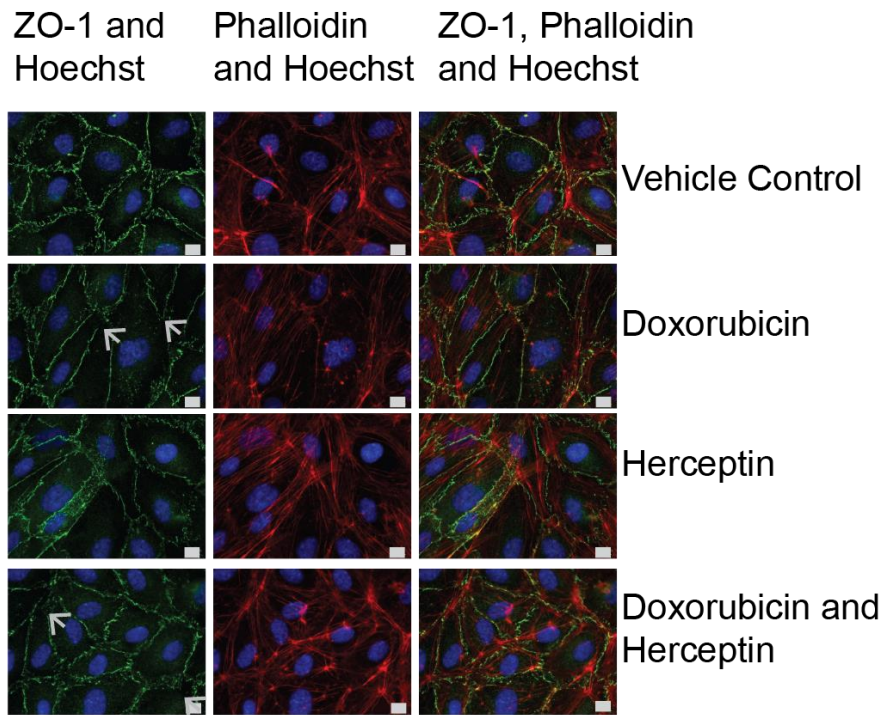
The IC<sub>50</sub> of Herceptin® in HDMEC adult was 10 µM which is 1.5mg/ml (Fig. 4.3). Herceptin® has been utilised at 100 µg/ml in the literature (Baselga et al., 1998). An IC<sub>50</sub> for HCMEC was undetermined at the

concentrations tested, suggesting that Herceptin® is unable to induce cell death in HCMEC. This could be as a result of the absence of the immune system. Herceptin® is known to be able to induce cell death by sequestering the immune system, which is known to be a major contributor to Herceptin®'s mechanism of action. Herceptin® was used at 100 µg/ml for further experiments to match already published data as this concentration has been shown to exert cytotoxic effects on the cells.

Herceptin® is being used in combination therapies commonly administered to patients with doxorubicin (Baselga et al., 1998), for this reason the effects of the drugs alone and in combination were analysed. As both drugs induce cardiovascular toxicity the effect on the endothelial barrier was initially analysed to determine potential cellular targets. It is outlined in figure 4.4, through immunofluorescent staining of the tight junction barrier and actin cytoskeleton, that doxorubicin induced barrier perturbation in HDMEC and HCMEC whereas Herceptin only induced barrier perturbation in HCMEC. HBMEC tight junction barrier was unaffected by both the chemotherapeutic agents alone and in combination. These results suggest that Herceptin has a specific cardiac effect, allowing the drug to gain access to underlying cells, such as cardiomyocytes, that could result in the observed cardiovascular toxicity.

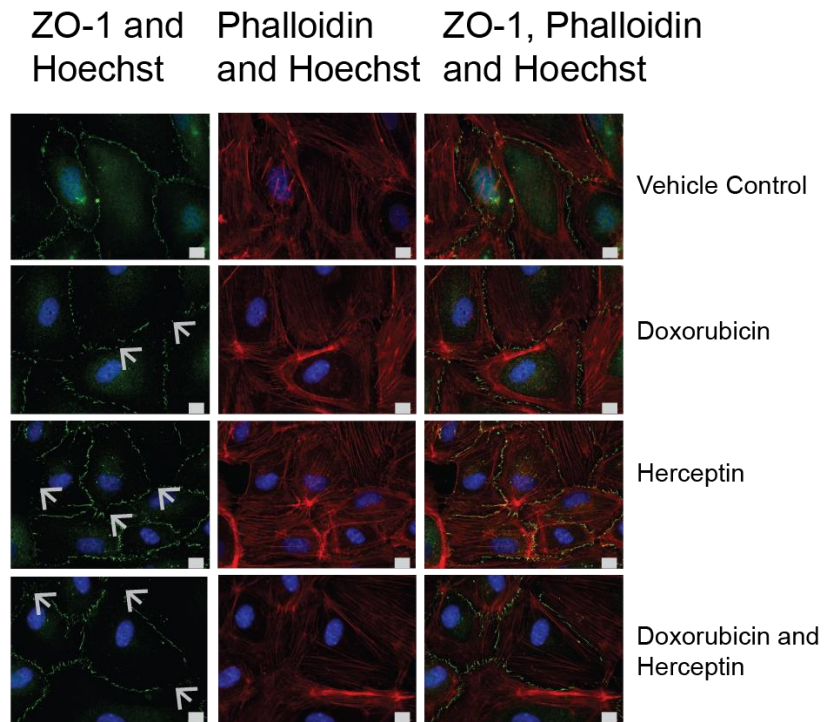
A

HDMEC adult



B

HCMEC



C

HBMEC

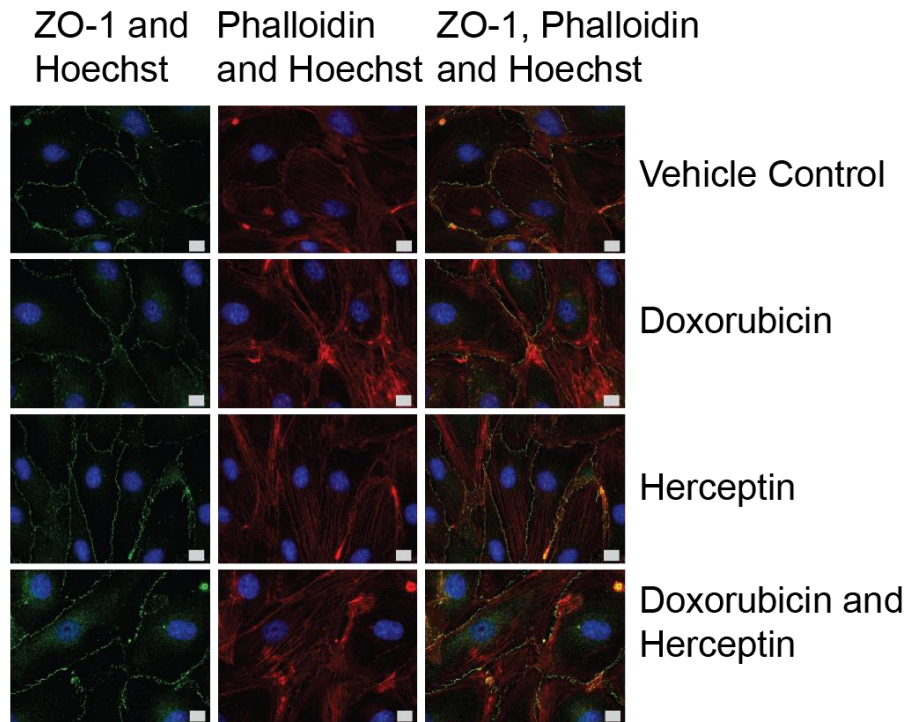


Figure 4.4. **Effects on the tight junction barrier following drug treatment.** (A) HDMEC adult, (B) HCMEC and (C) HBMEC were treated with 0.1  $\mu$ M doxorubicin and/or 100  $\mu$ g/ml Herceptin®. Cells were stained for tight junctions (ZO-1, green), actin fibers (phalloidin, red) and nuclei (Hoechst, blue).

The observation from figure 4.4 showed differences in tight junction barrier perturbation between the endothelial cells following doxorubicin and/or Herceptin® treatment. These differences were next quantified using a barrier function assay. The barrier function assay used ThinCerts with 0.4  $\mu$ m pores in the membrane. Cells were plated onto the membrane and grown to confluence. Following drug treatment, fluorescent dextran was added to the ThinCert and the flow through was measured by taking a sample from the well below the ThinCert. This assay allowed quantification of the barrier perturbation to define significance.



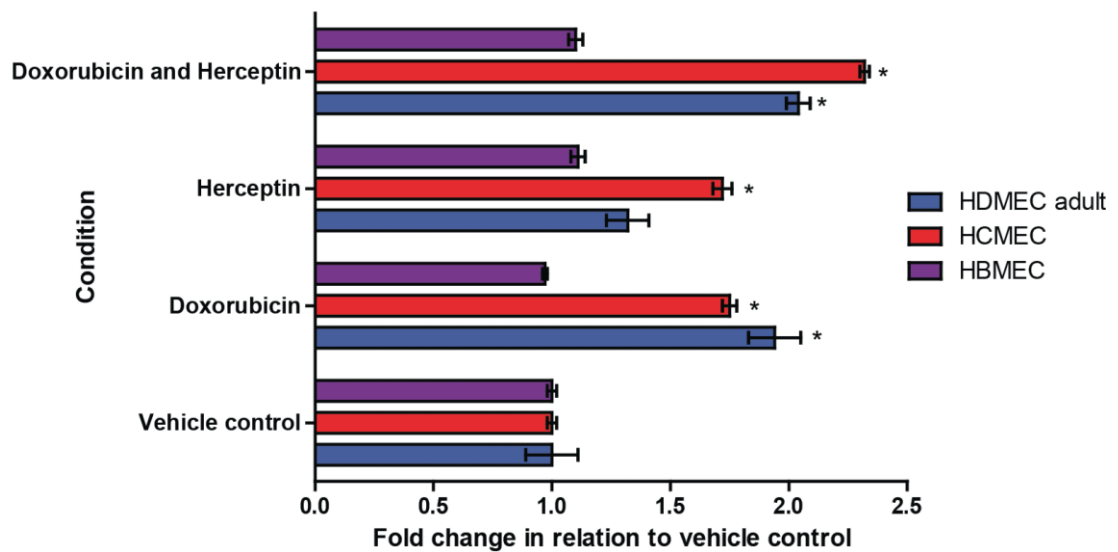


Figure 4.5. **Barrier function following doxorubicin and Herceptin® treatment.** HDMEC adult, HCMEC and HBMEC were treated with 0.1  $\mu$ M doxorubicin and/or 100  $\mu$ g/ml Herceptin®. Inserts were drugged for 6 hours before addition of fluorescent dextran. N=4 ThinCerts, mean  $\pm$  SD, \* =  $P \leq 0.05$  one way ANOVA, SPSS.

The data in figure 4.5 complimented what was previously observed in figure 4.4. The immunofluorescence images in figure 4.4 provided evidence that doxorubicin induced barrier perturbation in HDMEC adult and HCMEC but not HBMEC. Further to this it was observed in figure 4.5 that in HDMEC adult and HCMEC doxorubicin induced a significant decrease in barrier function. Additionally, figure 4.5 also quantified that Herceptin® only significantly reduced barrier function in HCMEC, complementing the data in figure 4.4 that showed Herceptin® only induced barrier perturbation in HCMEC. When the drugs were applied in combination it was observed that barrier function was significantly reduced in HDMEC adult and HCMEC (Fig. 4.5). It is interesting to note that in combination doxorubicin and Herceptin® increased permeability in HCMEC more than either drug alone, which suggested a more profound effect in combination.

This data had demonstrated that inhibition of EGFR2 (with Herceptin®) resulted in a significant reduction in barrier function accompanied by observed tight junction barrier perturbation in HCMEC. The next step was to determine if the EGFR1 inhibitor, Erbitux® showed similar effects on the tight junctions, using immunofluorescent staining of the tight junctions and actin cytoskeleton. It was observed in figure 4.2 that there is higher expression of EGFR1 and EGFR2 in HCMEC compared to other endothelial cells. In order to assess if both these receptors were potentially involved in tight junction regulation Erbitux® was added to HCMEC and HDMEC adult to determine the effect on the tight junction barrier. Lapatinib was also tested to determine the effect of a different class of drugs also known to inhibit EGFRs. Lapatinib is able to inhibit both EGFR1 and EGFR2, so can also show if the effect can be enhanced with inhibition of both receptors.

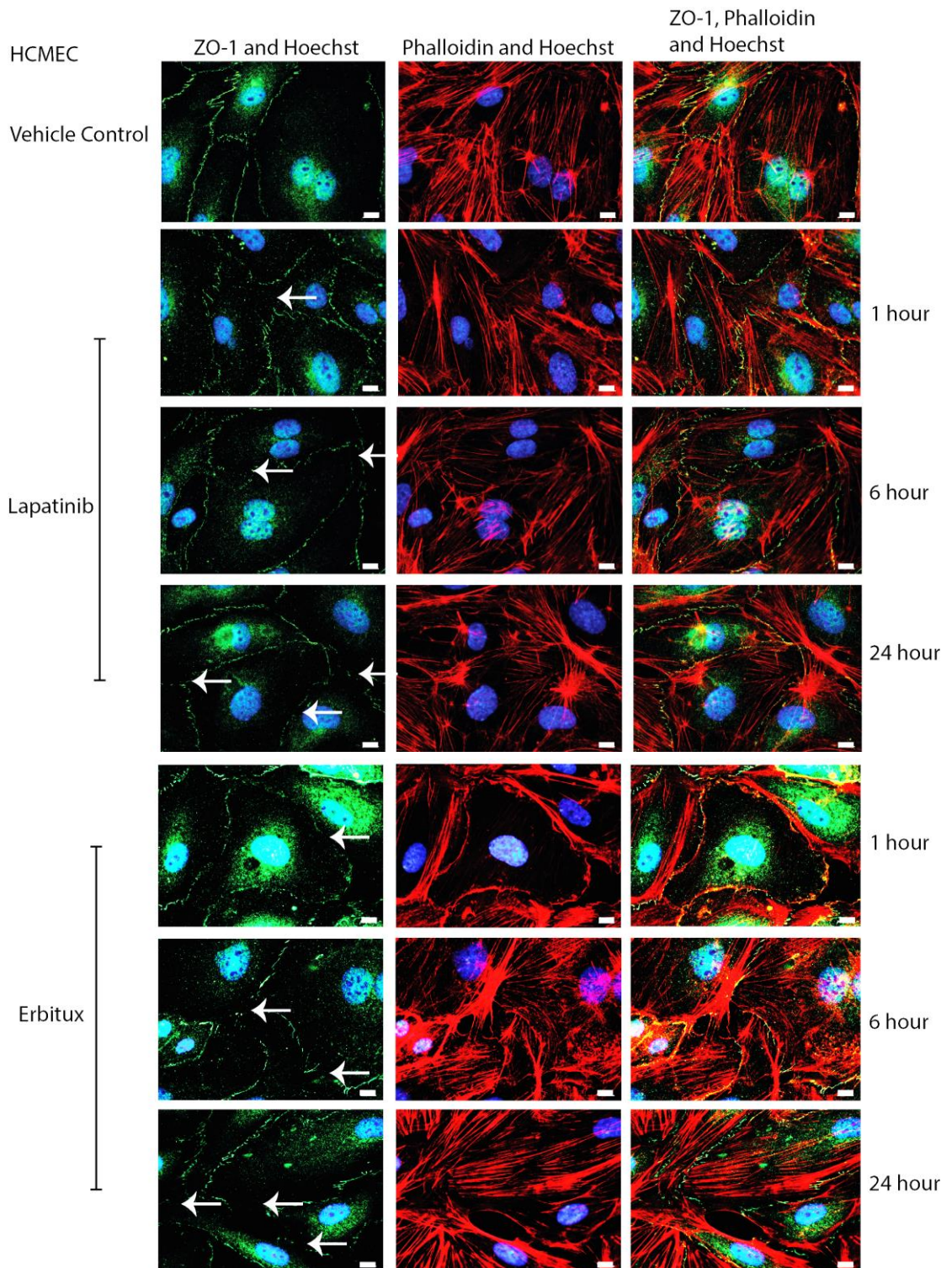


Figure 4.6. **Immunofluorescence analysis of Erbitux® and lapatinib treatment in HCMEC.** HCMEC were treated with 3  $\mu$ M lapatinib or 10  $\mu$ g/ml Erbitux. Cells were stained for tight junctions (ZO-1, green), actin fibers (phalloidin, red) and nuclei (Hoechst, blue).



Lapatinib and Erbitux® were both able to induce barrier perturbation in HCMEC, similar to Herceptin® (Fig. 4.6). By contrast, lapatinib and Erbitux® only showed a small amount of barrier perturbation at 24 hours in HDMEC adult, which again suggested that the drugs are acting differently on the cells (Fig. 4.7).

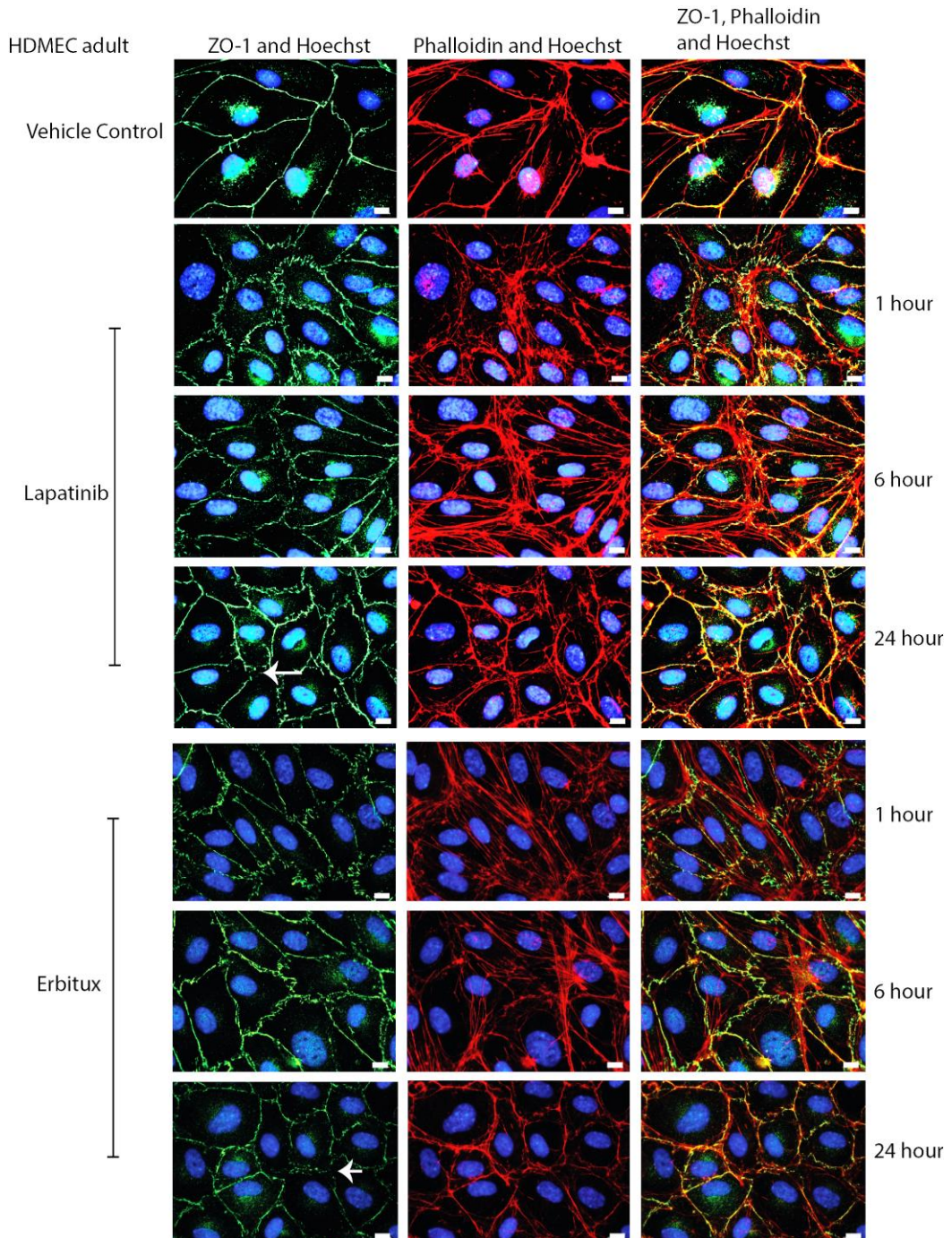
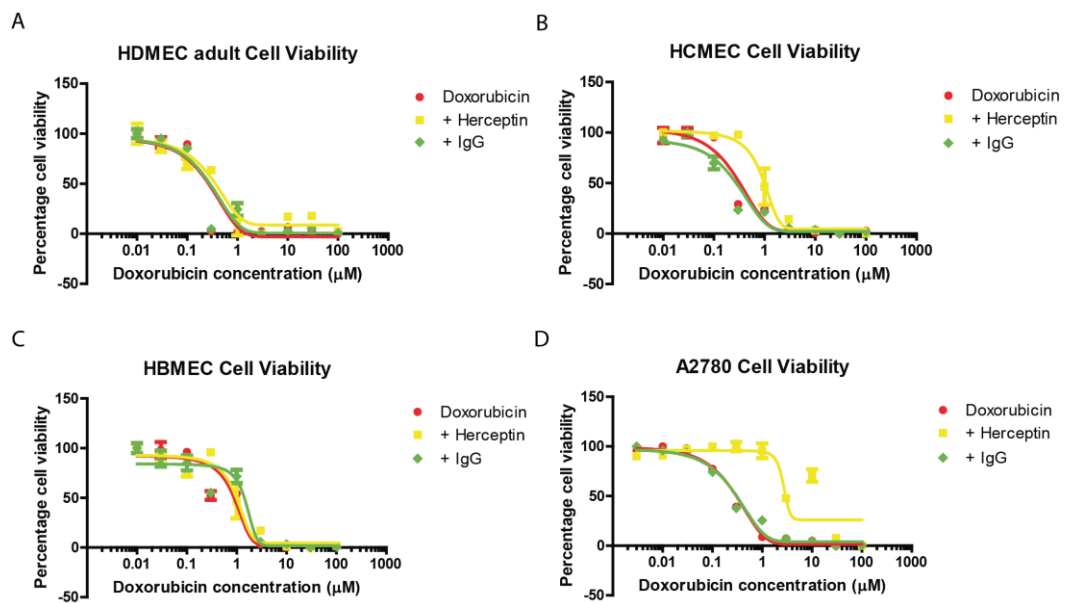


Figure 4.7. **Immunofluorescence analysis of Erbitux and lapatinib treatment in HDMEC adult.** HDMEC adult were treated with 3  $\mu$ M lapatinib or 10  $\mu$ g/ml Erbitux. Cells were stained for tight junctions (ZO-1, green), actin fibers (phalloidin, red) and nuclei (Hoechst, blue).

The data showed that the drugs are able to affect the endothelial tight junction barrier differently across the range of endothelial cells tested. The findings indicate that inhibition of EGFR1 and 2 was more severe in HCMEC as treatment with all three EGFR inhibitors (Erbbitux®, Herceptin® and lapatinib) induced tight junction barrier perturbation.

The next step was to investigate how inhibition of EGFR2 with Herceptin® affected cell viability following doxorubicin treatment. These drugs were investigated as Herceptin® and doxorubicin are given to patients in combination. Since in Chapter 3 it had been shown that EGF and TGF- $\alpha$ , which are ligands for EGFRs, were able to significantly increase cell proliferation in HCMEC, this suggested that the EGFRs have a role in HCMEC proliferation/survival.



	HDMEC adult	HCMEC	HBMEC	A2780
Doxorubicin (IC50, μM)	0.23 ± 0.05	0.24 ± 0.03	0.87 ± 0.1	0.35 ± 0.05
Doxorubicin (IC50, μM) + Herceptin®	0.24 ± 0.09	0.68 ± 0.07	0.89 ± 0.09	2.64 ± 0.07
Doxorubicin (IC50, μM) + IgG control	0.23 ± 0.04	0.26 ± 0.03	0.91 ± 0.08	0.34 ± 0.08

Figure 4.8. **Cellular viability of doxorubicin.** (A) HDMEC adult, (B) HCMEC, (C) HBMEC and (D) A2780 were treated with doxorubicin at concentrations ranging from 100 – 0.0003 μM, and presence of 100 μg/ml Herceptin or IgG control. Viability was analysed with Cell Titer Glo® (E) IC50s ± SD, N= 4.

Therefore, the cell types were treated with doxorubicin and the effect of Herceptin® on cell viability was assessed. The data presented in figure 4.8 show that Herceptin® had a protective effect on HCMEC and A2780 against doxorubicin. A possible explanation for this is that Herceptin® binding to EGFR2 induced receptor internalisation. Receptor internalisation can stimulate synthesis of growth factors as a protective mechanism employed by the cell. This could potentially be NRG-1, which is known to be released by endothelial cells (Pentassuglia and Sawyer, 2009). NRG-1 has been shown to protect against cytotoxic stimuli such

as doxorubicin treatment in cardiomyocytes (Pentassuglia and Sawyer, 2009). The theory is that as endothelial cells also express the EGFRs there is potential that NRG-1 is able to reach levels within the growth medium that are sufficient to stimulate the EGFRs to activate survival signalling, hence protect against doxorubicin cytotoxicity.

#### *4.2.4 Doxorubicin cellular uptake*

The final part of this section of work looked at how doxorubicin is able to enter the different endothelial cells. Doxorubicin naturally fluoresces at Ex 535 nm and Em 595 nm so can be visualised within the cell. To assess doxorubicin uptake within the cell the first thing to compare is the expression of influx and efflux transporters that have been reported to be involved in doxorubicin uptake (Okabe et al., 2005).

In order for any drug to affect the cells they must gain entry to the cell. This involved crossing the plasma membrane (Zhang et al., 2014). Doxorubicin cellular uptake is known to be affected by several membrane transporters; efflux transporters: p-glycoprotein (p-gp), ABCC1 and ABCC4, and influx transporters: SLC22A5, SLC22A2 and SLC22A4 (Okabe et al., 2005). Doxorubicin removal from the cells is strongly associated with p-glycoprotein. The expression levels of several transporters were analysed across the range of endothelial cells and compared to an ovarian cancer cell line.

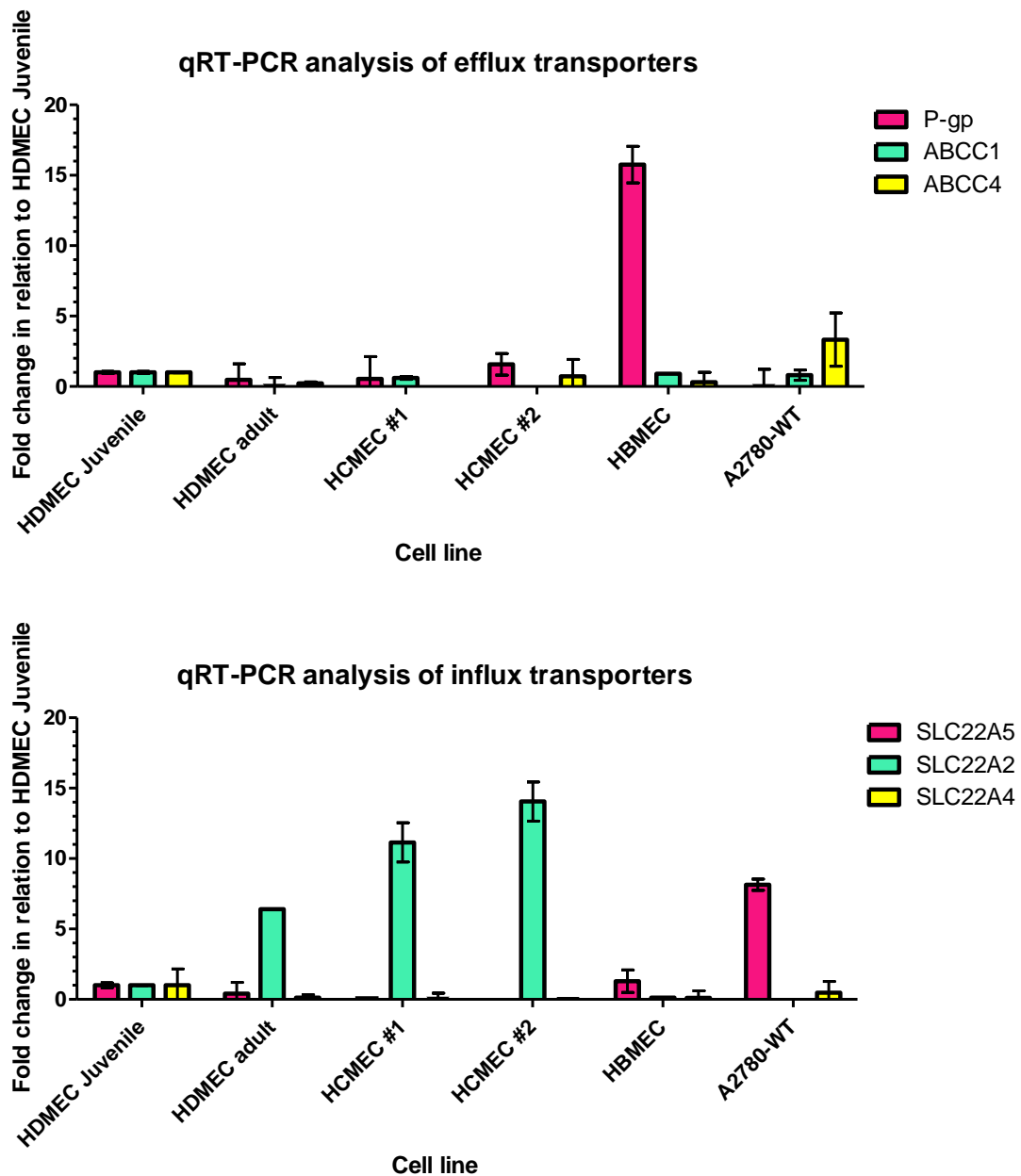


Figure 4.9. ***qRT-PCR analysis of transporters across a selection of human endothelial cells.*** qRT-PCR for expression of transporters p-gp, ABCC1, ABCC4, SLC22A5, SLC22A2 and SLC22A4. Data is plotted as fold change relative to HDMEC juvenile cells which was arbitrarily set as 1.00. Data is representative of mean  $\pm$  SD, data plotted in GraphPad Prism.

Results in figure 4.9 show that HBMEC had the highest expression of p-glycoprotein when compared to the HDMEC, HCMEC and A2780.



Interestingly, doxorubicin influx transporters differed more strongly between cell lines. HCMEC and HDMEC adult expressed higher levels of *SLC22A2* whereas HBMEC and A2780 cell lines expressed higher levels *SLC22A5*. This could further provide an explanation as to why the different cell lines respond differently to doxorubicin.

The cellular uptake of doxorubicin was further analysed by fluorescent uptake into the nucleus. Doxorubicin is a naturally fluorescent compound allowing for its intracellular translocation to be visualised. It can clearly be deduced from figure 4.10 that doxorubicin accumulates within the nucleus of the cells and the concentration of doxorubicin increases over the time course, indicated by the fluorescence intensity. This work has been further quantified to demonstrate the doxorubicin uptake relative to the concentration of protein in order to compare between cell lines. It can be observed from figure 4.11 that the highest level of doxorubicin appeared to be in the HBMECs.

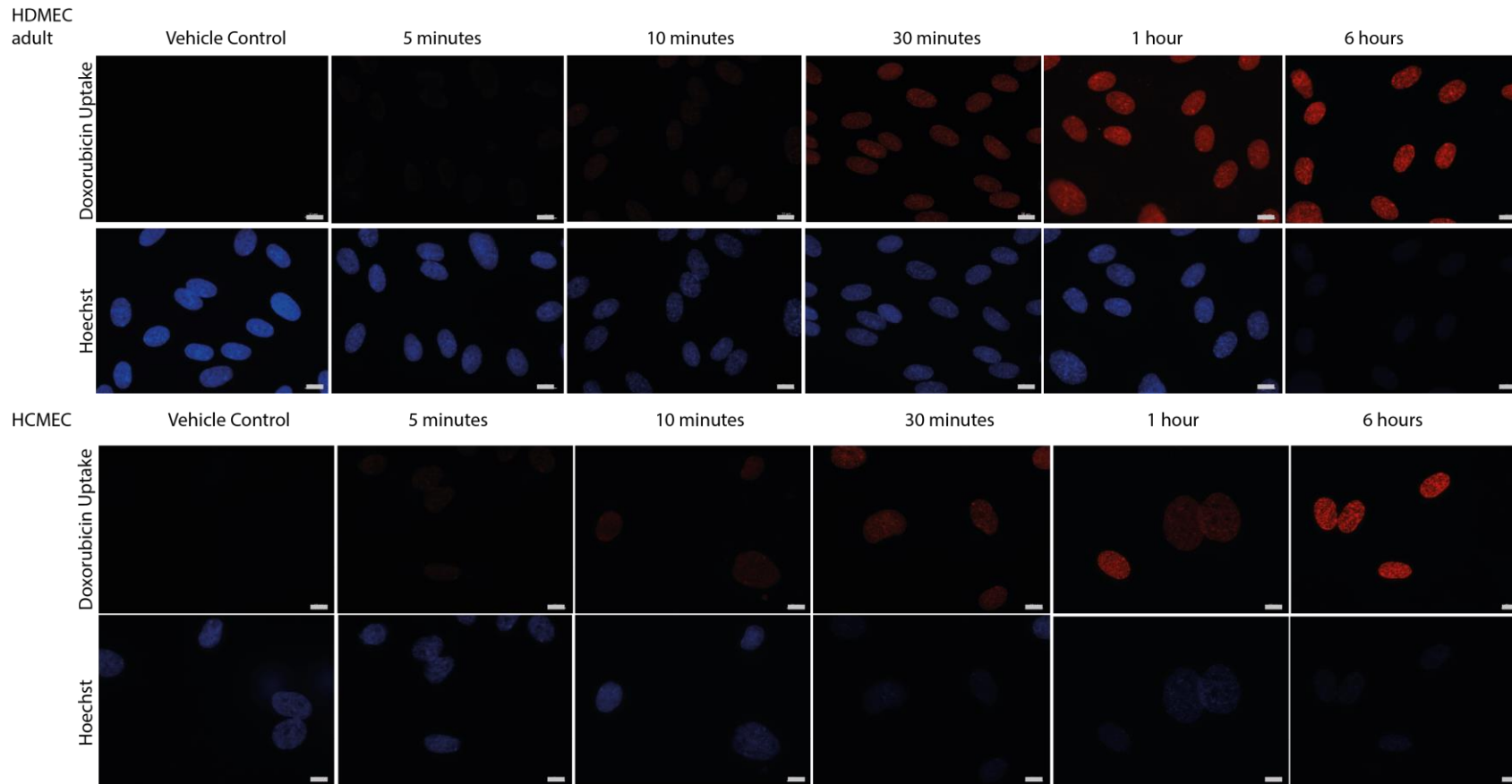


Figure 4.10. ***Immunofluorescence analysis of doxorubicin intracellular translocation.*** (A) HDMEC adult, (B) HCMEC and (C) RCEC were treated with doxorubicin 10  $\mu$ M (dose required for intracellular visualisation) for 5 minutes to 6 hours. Doxorubicin naturally fluoresces at around Ex 535 nm and Em 595 nm and appears in red in the image.

The results in figure 4.10 provided evidence that doxorubicin was able to gain access to the nucleus and accumulate over time. This panel shows images with the same exposure time and graphical manipulations to ensure the images are comparable. Doxorubicin was able to access the nucleus at time points as early as 5 minutes (data not shown). Since doxorubicin was able to gain entry to the cell at such early time point this suggested that doxorubicin has potential to gain access to the cells in a transporter-independent manner, as transporter mediated uptake would require a longer duration. To further assess this the level of doxorubicin that accumulated over time in the cells was assessed.

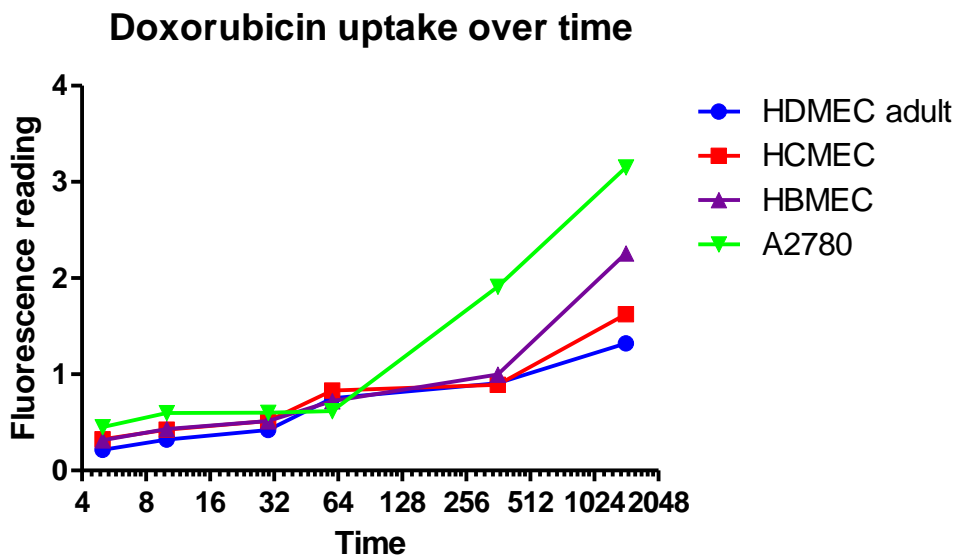


Figure 4.11. **Quantification of doxorubicin cellular uptake.** HDMEC adult, HCMEC I, HBMEC and RCEC were treated with doxorubicin 10  $\mu$ M before RIPA lysing and the fluorescence analysed. Data expressed as fluorescence intensity.

This was achieved by treating the cells with doxorubicin over time before lysis and measurement of the fluorescent expression within the sample to determine the level of doxorubicin within the cell. The results in figure

4.11 demonstrated that the transporters were not solely responsible for doxorubicin cellular accumulation. Here it is clear that the level of doxorubicin within the HBMEC was higher than in other endothelial cells. HBMEC had the highest level of p-gp (Fig. 4.9), which was thought to be efficient in doxorubicin removal from the cells. The data from figures 4.9 – 4.11 provide evidence that doxorubicin has the potential to passively diffuse across the plasma membrane to gain access to the cells.

## 4.3 Discussion

### *4.3.1 Investigation of kinase phosphorylation following growth factor stimulation*

The data outlined in Chapter 3 showed that endothelial cells responded differently to growth factor stimulation. This Chapter has built on this data through analysing the expression of EGFRs in different endothelial cells to begin to understand the physiological implications of this difference. EGFRs have been shown to regulate junctions through MAPKs (Liu et al., 2014). Junctions play an important physiological role in endothelial cells, to regulate paracellular permeability. This Chapter demonstrated (Fig. 4.2) that EGFR1 and 2 were expressed at a higher levels in HCMEC than in other endothelial cells. Having increased EGFR expression levels has the potential to make HCMEC more susceptible to EGFR inhibitors. Herceptin® is an anticancer drug known to inhibit EGFR2, and has been linked to cardiovascular toxicity in the clinic. The data had demonstrated that EGFRs regulate tight junctions, and that HCMEC expressed higher levels of EGFR1 and EGFR2; together these observations provided evidence to suggest that HCMECs were more susceptible to EGFR inhibitors which provided a potential explanation for cardiovascular toxicity. This Chapter has investigated how Herceptin® affects the endothelial tight junctions in a range of endothelial cells.

This project had been able to investigate multiple aspects of EGFR biology. With the use of Herceptin® to inhibit EGFR2, Erbitux® to inhibit EGFR1 and lapatinib to investigate the effects of inhibition of EGFR1 and 2 from a different class of anticancer drugs, a clearer understanding of EGFRs in tight junction regulation had been achieved.

#### *4.3.3 Herceptin® and doxorubicin combination therapy in endothelial cells*

Analysis of the data suggests that EGFR1 and 2 played a critical role in the regulation of tight junctions in HCMEC (Figs. 4.4 and 4.6). Inhibition of these receptors with drugs induced barrier perturbation and a significant increase in permeability (Fig. 4.5). This data built on the data from Chapter 3 that showed differences between endothelial cells. In this Chapter it was observed that EGFR inhibitors do not appear to affect the tight junction barrier in HDMEC adult or HBMEC (Figs. 4.4 and 4.6), and no significant changes in barrier function were observed following drug treatment (Fig. 4.5).

Research that analysed the effects of Herceptin® on cardiomyocytes had investigated how inhibition of EGFR2 could play a role in cardiovascular toxicity (Pentassuglia and Sawyer, 2009). The data observed in this Chapter further built on this and detailed how inhibition of EGFR2 on endothelial cells could also contribute to cardiovascular toxicity.

Targeting EGFR2 had proven successful in cancer therapy. However, the development of cardiovascular toxicity is beginning to limit the success. This outlines the need to understand the mechanism for toxicity and determine a way to prevent toxicity. As it appeared to be 'on-target' toxicity, i.e. toxicity induced by the desired target for the drug, this complicates the ability to avoid toxicity. Toxicity induced by 'off-target' effect can be overcome through development of a drug to be more specific to the target molecule. This project aimed to move forward in subsequent Chapters to understand the mechanism for how tight

junctions are regulated at the intracellular level, with the aim to be able to use an agonist to this pathway which can overcome the drug-induced barrier perturbation.

The data from figure 4.8 shows how the IC<sub>50</sub> of doxorubicin is affected with Herceptin® treatment. This assay uses a monolayer of cells treated with doxorubicin in the presence and absence of Herceptin®. It can be seen that addition of Herceptin® in HCMEC and A2780 produces an increase in the IC<sub>50</sub>. This goes against published data to suggest that these drugs in combination provide better tumour suppression (Baselga et al., 1998). A possible explanation for this is the absence of immune cell in the *in vitro* assay. When there are no immune cells present this removes one of the mechanisms for Herceptin® antibody directed cell cytotoxicity (ADCC) (Jones and Buzdar, 2009; Kute et al., 2009). ADCC relies on the immune system to target Herceptin® bound to EGFR2 and induce apoptosis specifically killing the tumour cells (Kute et al., 2012; Collins et al., 2012; Kawaguchi et al., 2009; Yoshida et al., 2012). Although there are still two alternative mechanisms for Herceptin® induced cell death, such as receptor internalisation and degradation as well as alterations in signalling pathways, it appears that the immune system plays a critical role in cell death. The work by Clynes *et al* details how inhibiting the Fc region of Herceptin® reduces its ability to suppress tumour growth. The Fc region on Herceptin® is known to interact with the immune system, inhibition prevents ADCC induced apoptosis. There is a profound difference between Herceptin® with and without inhibition of the Fc region, this suggests that the immune response to Herceptin® plays a vital role in apoptosis.

#### 4.3.4 Doxorubicin cellular uptake

Doxorubicin naturally fluoresces around 568 nm allowing for its intracellular localisation to be visualised. Doxorubicin is known to target the enzyme topoisomerase II which is located within the nucleus

(Vejpongsa and Yeh, 2014; Nitiss, 2009b; Zhang et al., 2012; Pommier et al., 2010; Nitiss, 2009a; Dewese and Osheroff, 2009; Kik et al., 2009). Figure 4.10 demonstrates that doxorubicin is able to gain access to the nucleus as it appears to be the only intracellular compartment that doxorubicin is able to be visualised within. The optimum exposure images provide evidence that doxorubicin is present intracellular at 5 minutes indicating that doxorubicin is able to diffuse across the cell membrane, as transporter mediated uptake requires more time. As the fluorescent intensity of doxorubicin increases over time this provides evidence to suggest that doxorubicin crosses the cell membrane via transporters as well as passive diffusion (Feng et al., 2014; Sardi et al., 2013; Zhang et al., 2014). In order to test this theory siRNA or inhibitors to transporters could be used to test the concentration of doxorubicin uptake with active and inhibited transporters.

Figure 4.9 demonstrates that there are differences in the expression of transporters across a range of endothelial cells. This allows for different concentrations of drug to be taken up into the cells, providing more evidence that the different endothelial cells are able to respond to doxorubicin differently. HBMEC express a higher level of p-gp, an efflux transporter known to be important in doxorubicin removal from the cell (Garg et al., 2015; Sardi et al., 2013). This data suggests a physiological advantage to HBMEC as they have the potential to efficiently remove doxorubicin and prevent toxicity. As HCMEC express a relatively low level of p-gp in comparison to HBMEC this suggests they are more susceptible to doxorubicin intracellular accumulation. This becomes contradicted when the level of doxorubicin within the cell is assessed. The data from figure 4.11, clearly outlined that the level of doxorubicin accumulation in HBMEC is greater than other endothelial cells. This suggested that doxorubicin entry and removal from the cells is not solely dependent on transporters. This further provided evidence to the hypothesis gained from figure 4.10, where it was observed that

doxorubicin can be detected within the nucleus at 5 minutes after treatment.

Interestingly the influx transporters expression (Fig. 4.9) appeared to be different between cells. HDMEC and HCMEC expressed higher levels of *SLC22A2*, and HBMEC and A2780 expressed higher levels of *SLC22A5*. This suggested that the uptake of doxorubicin into the cells differs. As there are no current reports to determine if either influx transporter has a more dominant effect on doxorubicin uptake, it cannot be determined if this difference plays a role in the observed differences in how endothelial cells respond to doxorubicin, but this did suggest that the expression of transporters on endothelial cells from different anatomical locations could play a role in combination with doxorubicin passive diffusion.

This work will proceed to understand the role of ERK5 in the regulation of junctions as it has been demonstrated that ERK5 is involved in EGFR regulation of junctions (Cameron et al., 2003).





## **Chapter 5**

ERK5 Regulates Endothelial Junction  
Formation: Statin Mediated Activation of  
ERK5 Stimulates Tight Junction Formation



## 5.1 Introduction

The previous Chapter provided evidence that anti-cancer drugs, doxorubicin and Herceptin®, induced endothelial barrier perturbation and ultimately decreased barrier function. Current literature indicated that intracellular signalling molecules, specifically MAPKs such as ERKs, are involved in junction regulation (Liu et al., 2014; Cameron et al., 2003; Samak et al., 2011). Research has provided a link between ERK5 and gap junction regulation, with specific focus on connexin 43 (CX43) (Cameron et al., 2003), however no link to other junction regulation has been evaluated within the literature. Based on these findings, here I aim to investigate if ERK5 regulates all endothelial junctions. This Chapter also builds on the data presented in Chapter 4 demonstrating a difference in EGFR expression across a range of endothelial cells from different anatomical locations. EGFRs have been linked to ERK5 regulation of junctions, providing the hypothesis that as endothelial cells from different anatomical locations express different levels of EGFRs, these potentially regulate junctions to different degrees.

The effects of ERK5 inhibitors on the maintenance of endothelial junctions was assessed with the use of commercially available ERK5 inhibitors XMD8-92 and BIX02189 (Yang and Lee, 2011; Yang et al., 2010; Tataka et al., 2008). XMD8-92 has been demonstrated to directly inhibit ERK5 (Yang et al., 2010), whereas BIX02189 inhibits MEK5 upstream of ERK5, which prevents MEK5 phosphorylation of ERK5 at the T218/Y220 phosphorylation site (Tataka et al., 2008). Over the last decade, siRNA technology to transiently silence gene expression has been developed (Woo et al., 2010). Previous research within the group has validated the ERK5 siRNA knock down in endothelial cells (Roberts et al., 2010).

ERK5 knockout mice show irregular endothelial cells that have gaps between them (Hayashi et al., 2004), suggesting a potentially “leaky”

vascular phenotype. This was predicted to be due to the transcription factors downstream of ERK5 such as KLF2/4 (Hayashi et al., 2004), known to regulate proliferation, differentiation and survival.

It has recently been demonstrated that statins are able to induce ERK5 phosphorylation (Wu et al., 2013; Le et al., 2014). As ERK5 has a vital role within endothelial cell homeostasis this could provide a potential hypothesis for statin induced cardio-protective effects observed clinically (Riad et al., 2009; Bardeleben et al., 2003; Bardeleben et al., 2002; Damrot et al., 2006; Fritz et al., 2003; Henninger et al., 2012; Henninger et al., 2015; Huelsenbeck et al., 2011; Nubel et al., 2006; Nubel et al., 2004a; Nubel et al., 2004b; Nubel et al., 2005; Ostrau et al., 2009). Statins are being investigated for use in combination therapies, with known cardio-toxic drugs to determine if they can reduce the toxicity observed. Reports have identified that statins are able to protect against anti-cancer drug induced toxicity both *in vivo* and *in vitro*, these effects include protective effects on endothelial cells that are predicted to be regulated through eNOS and KLF2/4 as well as increasing sensitivity of the HeLa ovarian cancer cell line to chemotherapeutic drugs (Bardeleben et al., 2003; Bardeleben et al., 2002; Damrot et al., 2006; Fritz et al., 2003; Henninger et al., 2012; Henninger et al., 2015; Huelsenbeck et al., 2011; Nubel et al., 2006; Nubel et al., 2004a; Nubel et al., 2004b; Nubel et al., 2005; Ostrau et al., 2009). Investigations *in vivo* using mice and rat models have demonstrated how statin pre-treatment can reduce the cardiotoxicity observed following doxorubicin treatment (Kim et al., 2012; Riad et al., 2009). This work proceeded to investigate the role of ERK5 in barrier regulation, which focused on addressing the hypothesis that ERK5 regulates the junctions in endothelial cells from different anatomical locations differently. This hypothesis was built on the knowledge that EGFRs regulate junctions through ERK5 (Cameron et al., 2003). The results in Chapter 4 have demonstrated that the expression of EGFRs difference across endothelial cells from different anatomical locations.

## 5.2 Results

### 5.2.1 ERK5 inhibition alters endothelial tight junction, adherens junction and gap junction formation

In order to analyse the role of ERK5 in the regulation of endothelial cell barrier formation, recently developed small molecule inhibitors were utilised. XMD8-92 (inhibits ERK5 directly) and BIX02189 (inhibits MEK5 preventing T218/Y220 phosphorylation of ERK5) were added to HDMEC adult and HCMEC to determine the cellular viability and to ensure no cytotoxic events occurred at the concentrations being used in further assays (Fig. 5.1 A-C). Additionally, the specificity of the inhibitors was assessed by western blotting for closely related kinases. The results show that small molecule ERK5 inhibitors reduced ERK5 phosphorylation while AKT and ERK1/2 phosphorylation remained unaffected (Fig. 5.1 D). AKT has been demonstrated to be linked the ERK5 signalling (Roberts et al., 2010), while ERK1/2 is a structurally related MAPK.

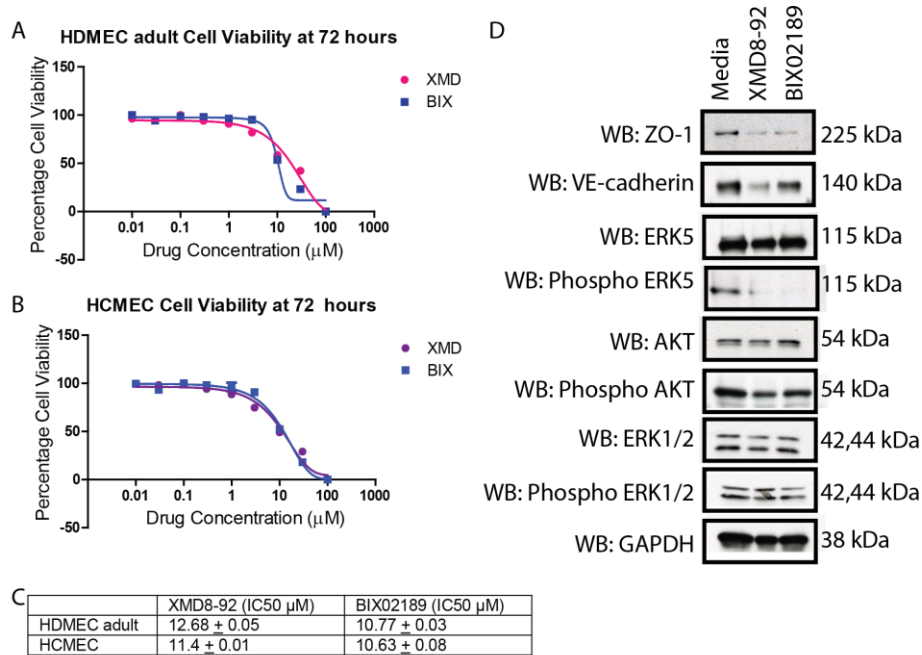


**Figure 5.1. Cell toxicity and specificity of ERK5 inhibitors XMD8-92 and BIX02189.** (A) HDMEC adult, (B) HCMEC were treated with inhibitors XMD8-92 or BIX02189 for 72 hours. Viability analysis was measured with Cell Titer Glo®. (C) The IC<sub>50</sub> was calculated using GraphPad Prism. (D) HCMEC were treated with (3 µM) XMD8-92 or (3 µM) BIX02189 for 6 hours before being run on western blot and probed for: ZO-1, VE-cadherin, ERK5, phospho ERK5, AKT, phospho AKT, ERK1/2, phospho ERK1/2 and GAPDH was used as a loading control.

### 5.2.2 Inhibition of ERK5 induced barrier perturbation

Following viability analysis, a concentration of 3 µM for both XMD8-92 and BIX02189 was used for all further experiments. Since this concentration showed no cytotoxicity in the cells, any events observed with the inhibitors with acute dosing were unlikely to be due to cellular toxicity.

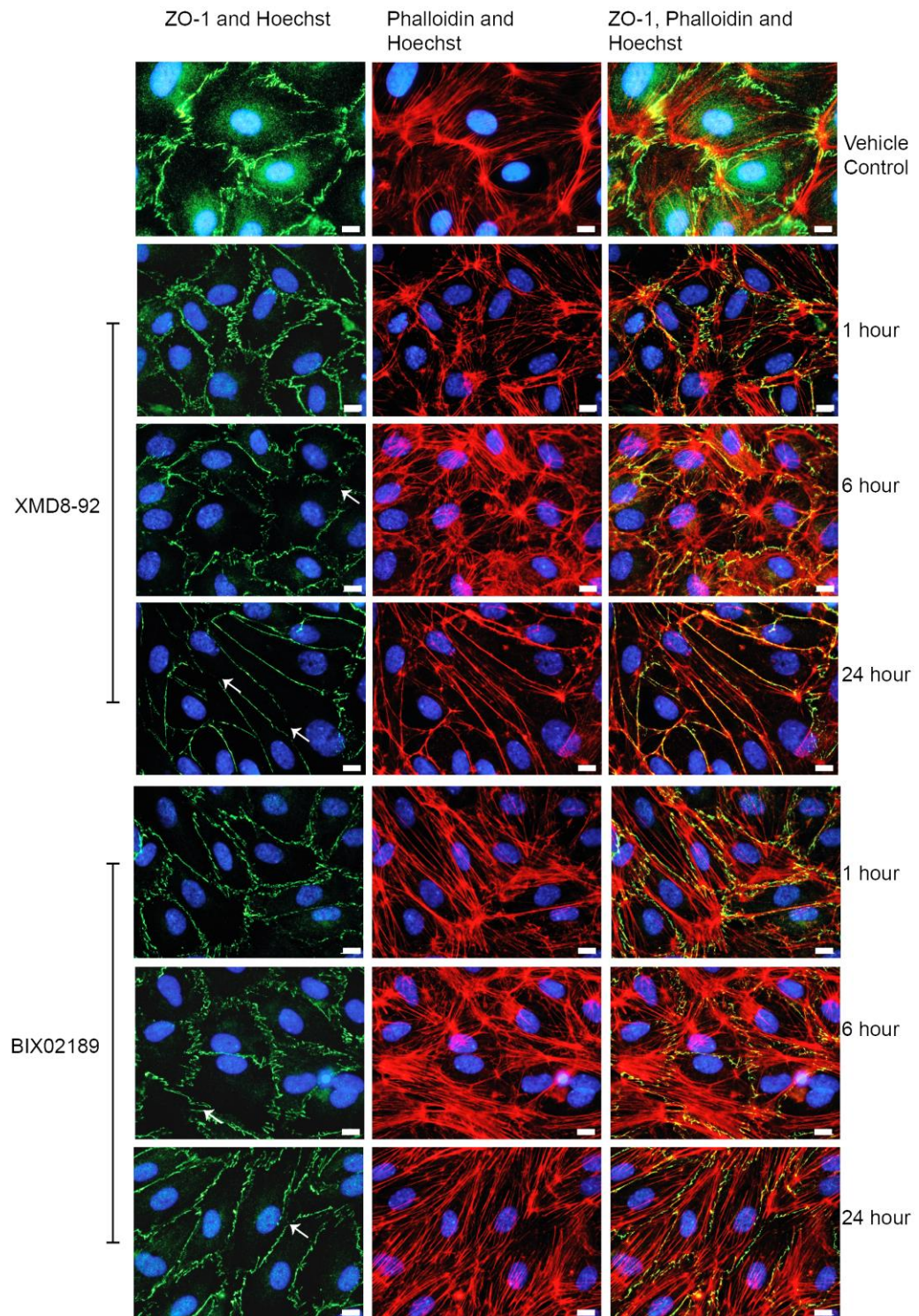
The effects of XMD8-92 (direct ERK5 inhibitor) and BIX02189 (MEK5 inhibitor) on the endothelial tight junction barrier were analysed using immunofluorescence. Cells were treated with XMD8-92 or BIX02189 for 1, 6 or 24 hours to determine the effect on the barrier over time. The effect of inhibition on endothelial tight (Fig. 5.2) and adherens (Fig. 5.3)

junctions, was analysed by immunofluorescence. Following treatment cells were stained with ZO-1 for tight junctions and VE-cadherin for adherens junctions. The assay was sufficiently validated to ensure the barrier formed between the endothelial cells on the coverslip was consistent.

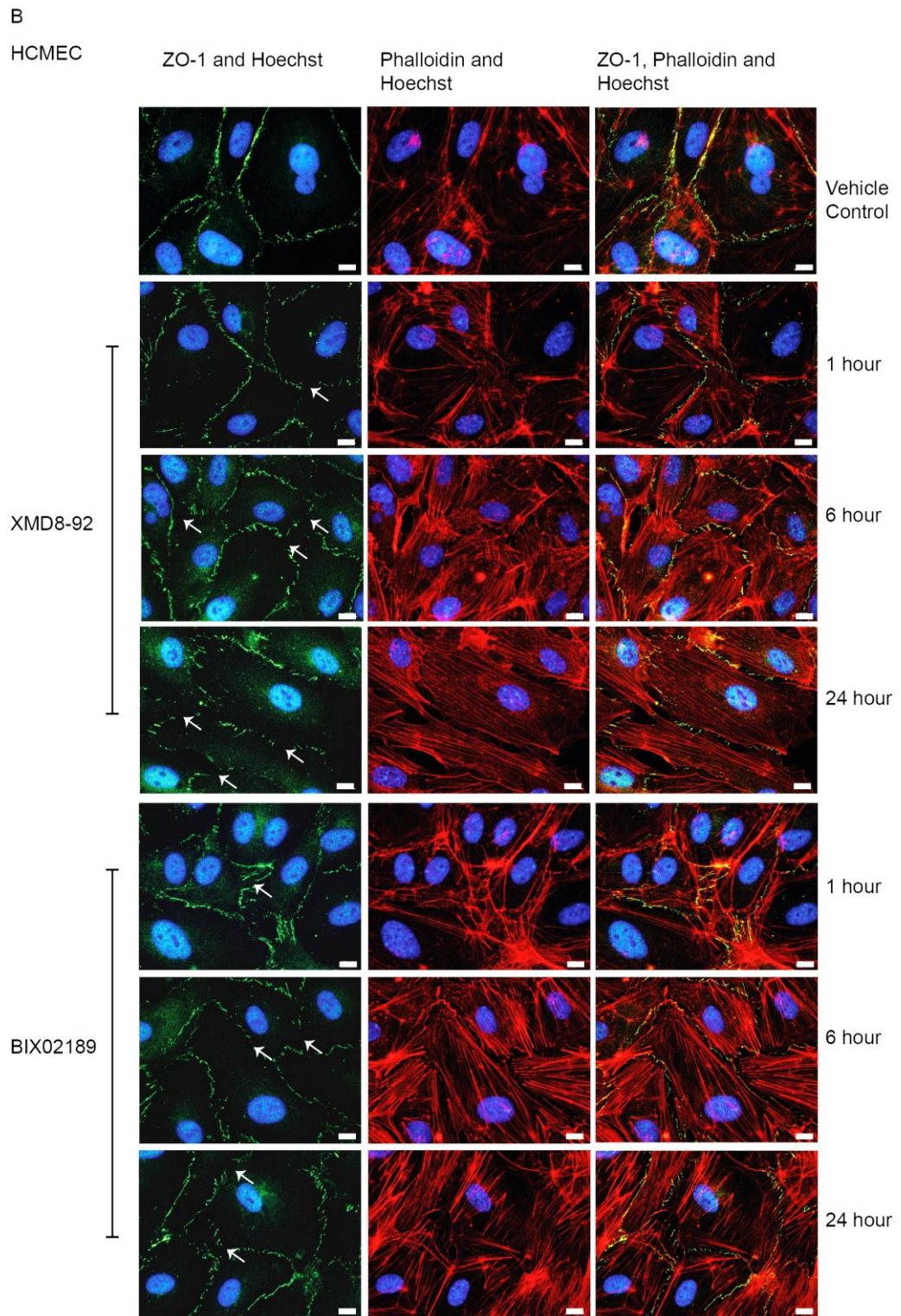


A

HDMEC adult









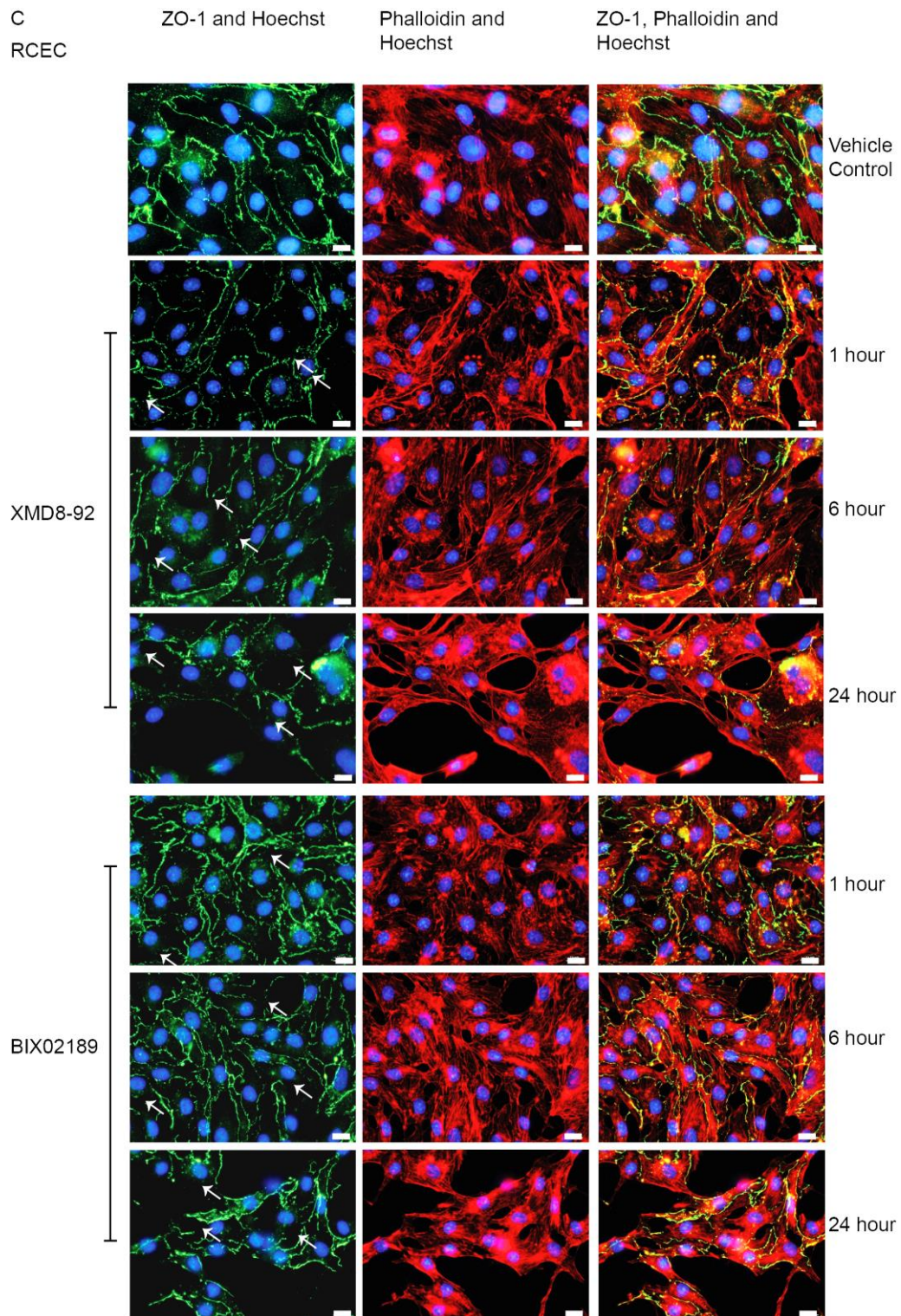
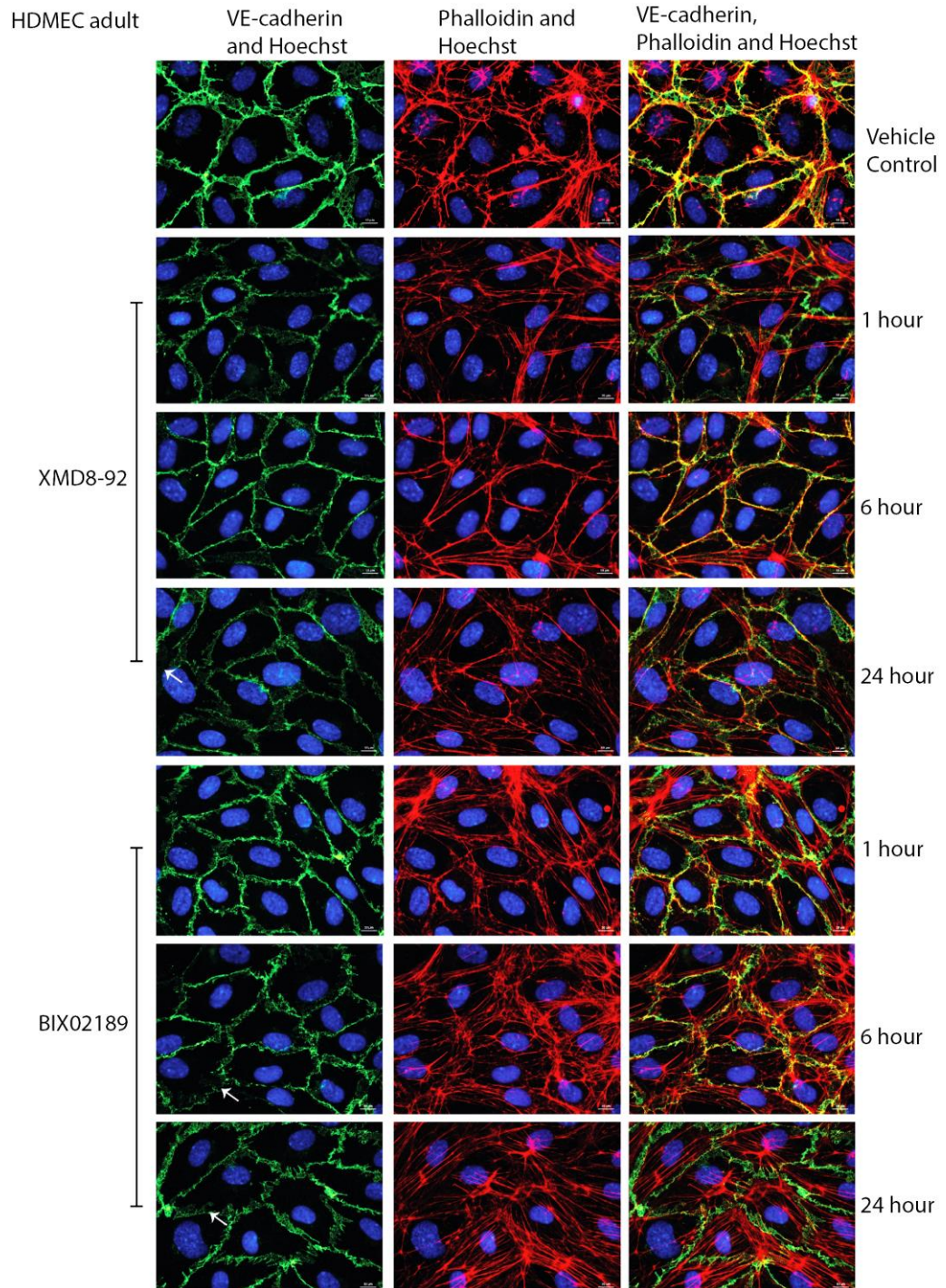


Figure 5.2. **Analysis of the tight junction barrier following XMD8-92 and BIX02189 treatment.** (A) HDMEC adult, (B) HCMEC and (C) RCEC were treated with XMD8-92 (3  $\mu$ M, ERK5 inhibitor) or BIX02189 (3  $\mu$ M, MEK5 inhibitor) for 1, 6 or 24 hours. Immunofluorescence staining with ZO-1 (green), phalloidin (red) and Hoechst (blue). Arrows indicate barrier disruption, scale bar represents 10  $\mu$ m.





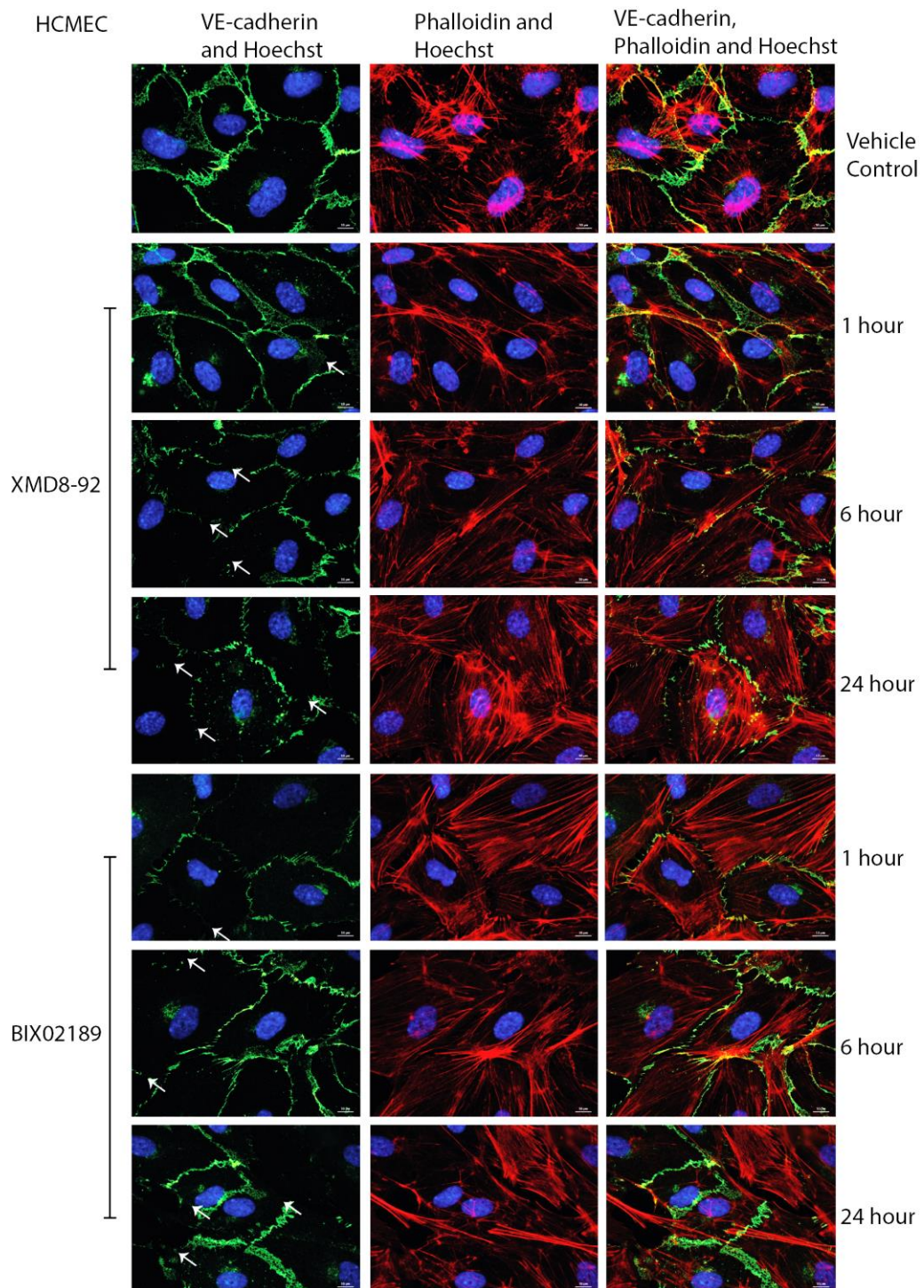


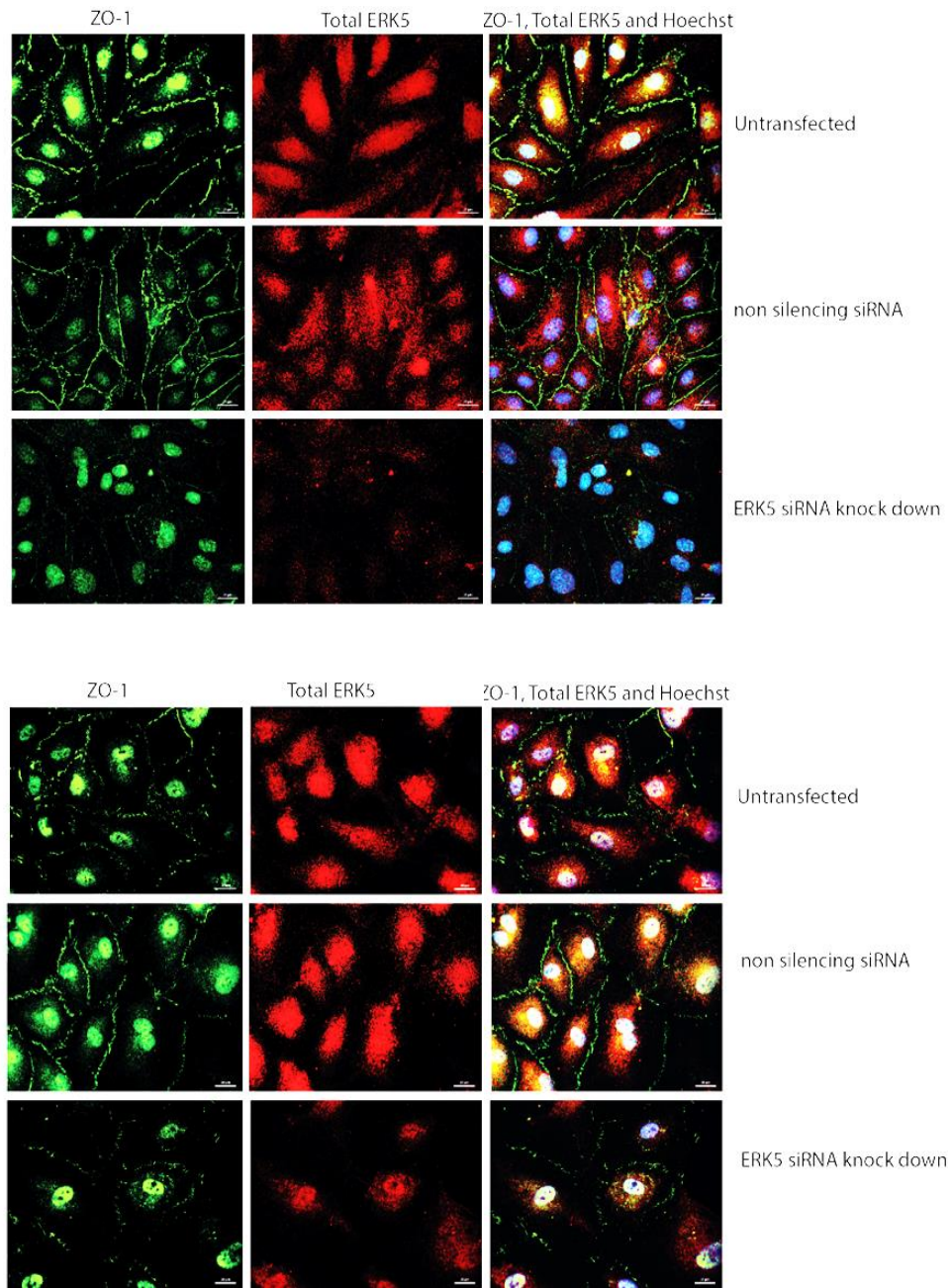
Figure 5.3. **Analysis of the adherens junction barrier following XMD8-92 and BIX02189 treatment.** (A) HDMEC adult and (B) HCMEC were treated with XMD8-92 (3  $\mu$ M, directly inhibits ERK5) or BIX02189 (3  $\mu$ M, inhibits MEK5) for 1, 6 or 24 hours. Cells were stained with VE-cadherin (green), phalloidin (red) and Hoechst (blue). Arrows indicate barrier disruption, scale bar represents 10  $\mu$ m.



It can be concluded from figures 5.2 and 5.3 that barrier perturbation occurred at both tight (ZO-1) and adherens (VE-cadherin) junctions following ERK5 inhibition with small molecule inhibitors. The perturbation appeared to be at a greater extent in HCMEC and RCEC than in HDMEC adult suggesting that there is a potential difference in ERK5 regulation between endothelial cells from different anatomical locations.

### 5.2.3 Small interfering RNA mediated ERK5 silencing reduces endothelial cell barrier function

The previous data utilised small molecule inhibitors of the ERK5 signalling axis. To confirm this data and rule out any possible non-specific off-target effects with the compounds, siRNA mediated gene silencing was performed using two separate oligonucleotide duplexes targeting human *ERK5*, followed by immunofluorescence for ZO-1 and ERK5 (Fig. 5.4). Endogenous ERK5 was transiently silenced in cells using siRNA, this was initially validated to confirm gene silencing.



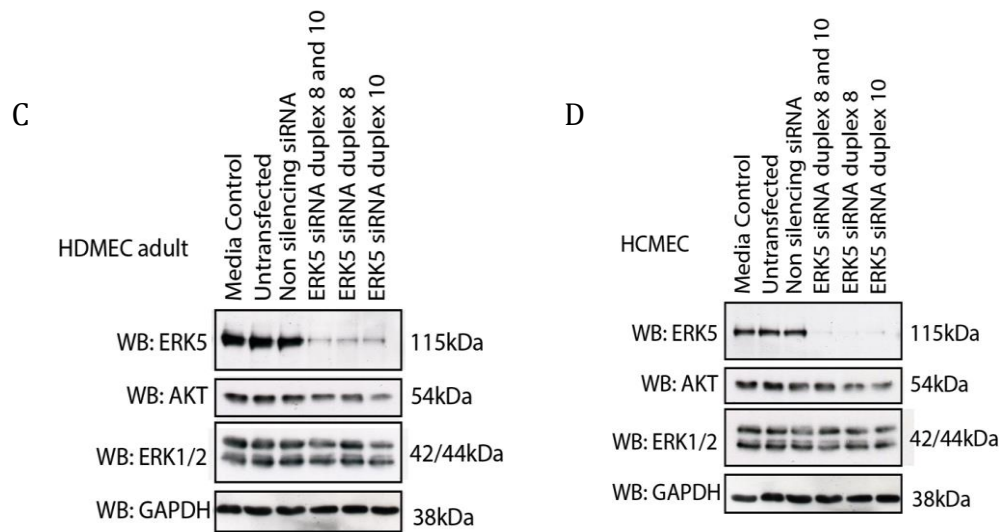
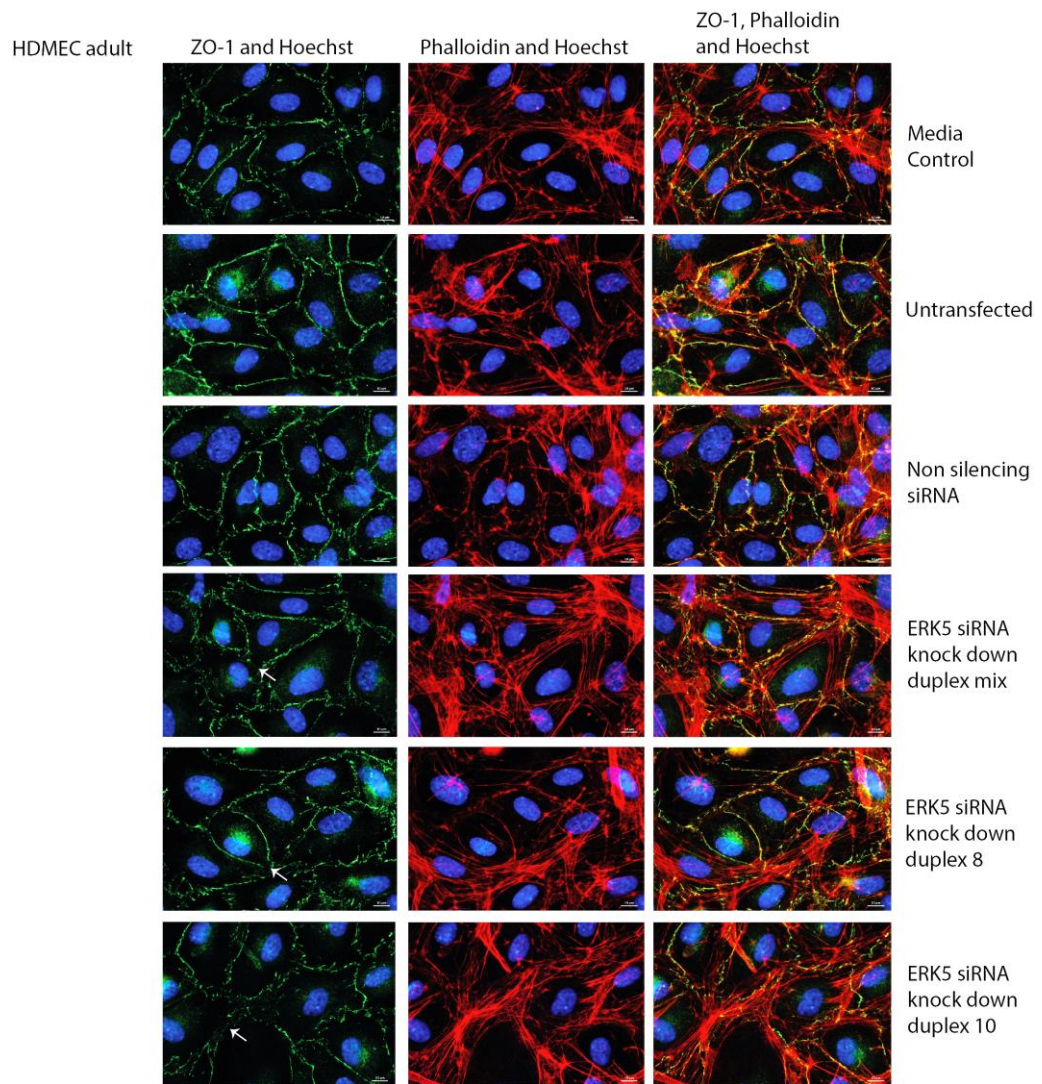


Figure 5.4. **Small interfering RNA transfection.** (A,C) HDMEC adult, (B,D) HCMEC. siRNA transfection with mixed duplexes or individual preceded staining with ZO-1 (green, this is a different antibody to previous staining to allow for use of two antibodies), ERK5 (red) and Hoechst (blue). Western blots were probed for intracellular signalling molecules: ERK5, AKT and ERK1/2; GAPDH is used as a loading control.

The observation from figure 5.4 gives a clear indication that the siRNA specifically knocks down ERK5 levels, as other kinases with similar sequence homology, such as ERK1/2 expression remained unchanged (Fig. 5.4 C and D).

Next, a more detailed analysis of ERK5 knockdown on endothelial junctions was conducted with particular focus on the three cellular junctions known to be present in endothelial cells. I analysed cells after treatment with siRNAs/control conditions, for perturbation of tight junctions (Fig. 5.5), adherens junctions (Fig. 5.6) and gap junctions (Fig. 5.7) using immunofluorescence methods.





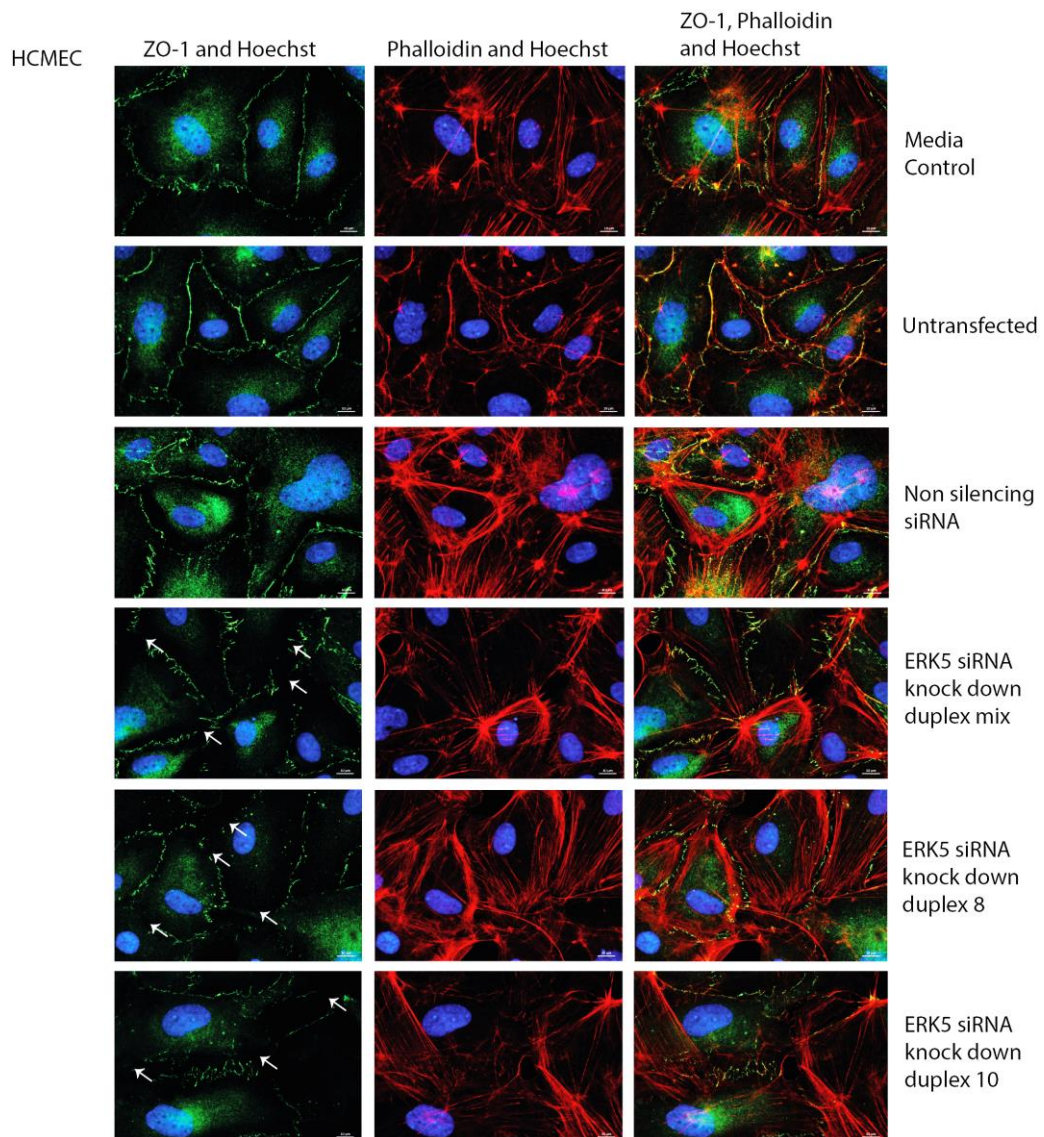
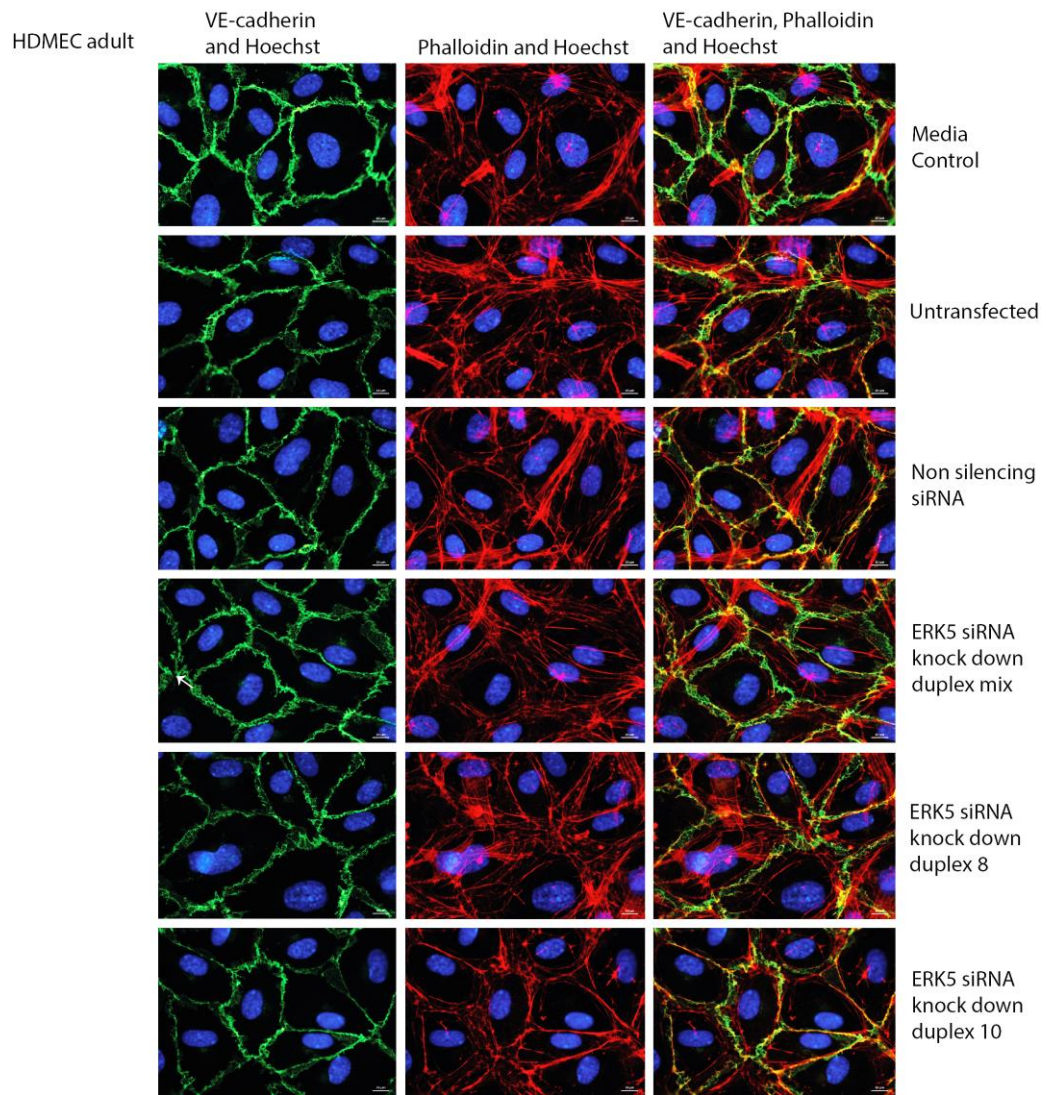


Figure 5.5. **Immunofluorescence analysis of endothelial cell tight junctions following small interfering RNA transfection.** (A) HDMEC adult and (B) HCMEC were transfected with siRNA and stained with ZO-1 (green), phalloidin (red) and Hoechst (blue). Arrows indicate barrier disruption, scale bar represents 10  $\mu$ m.





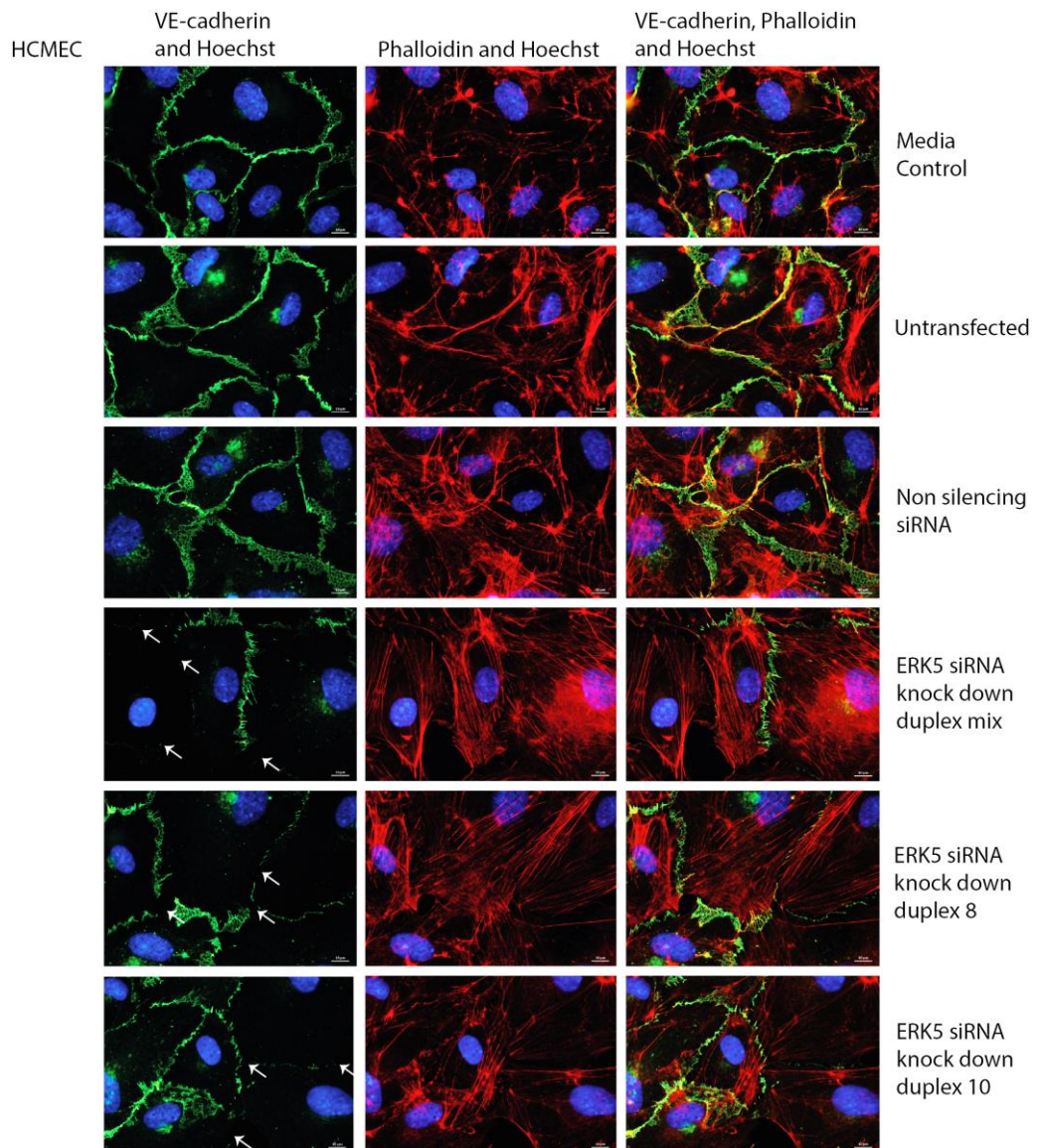
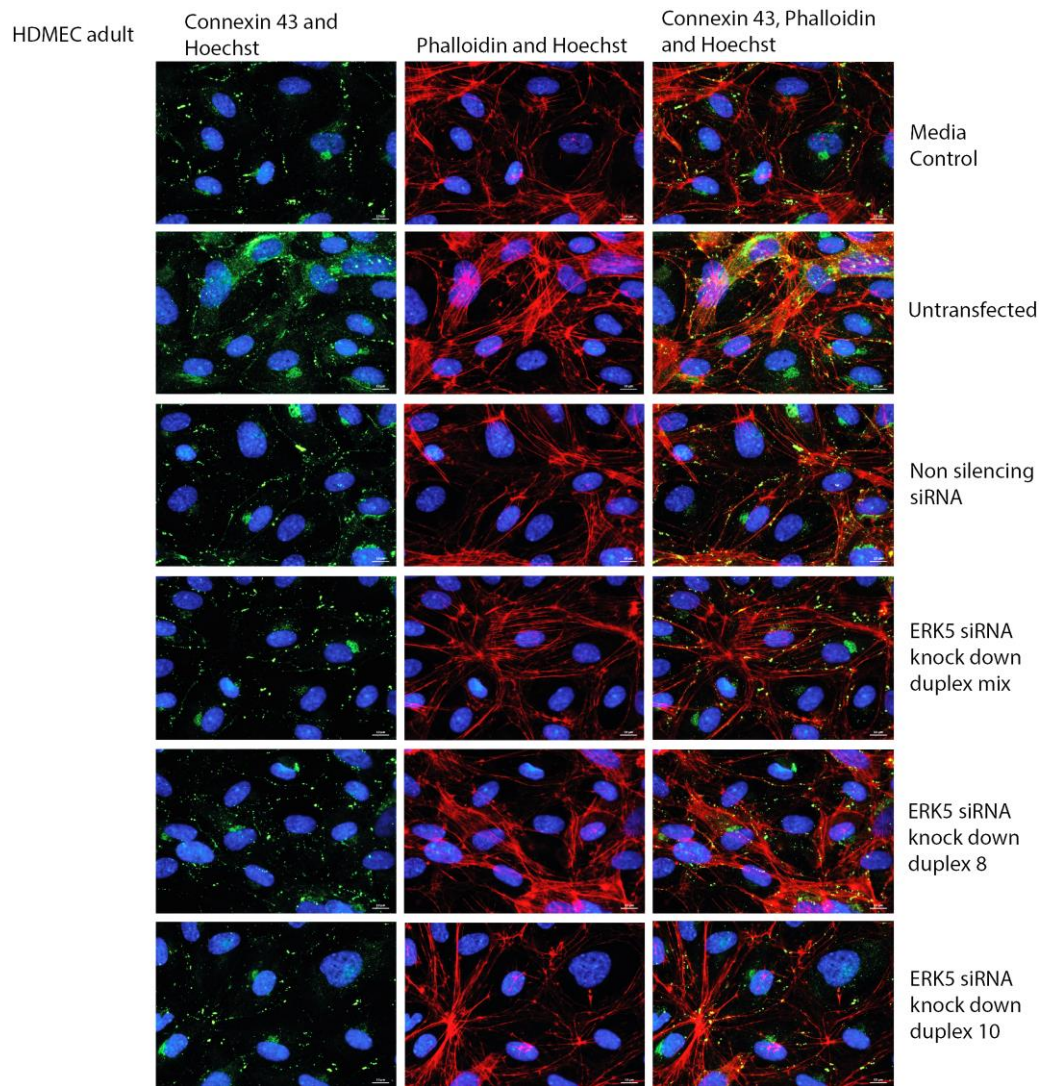


Figure 5.6. **Immunofluorescence analysis of endothelial cell junctions following small interfering RNA ERK5 silencing.** (A) HDMEC adult and (B) HCMEC were transfected with siRNA and stained with VE-cadherin (green), phalloidin (red) and Hoechst (blue). Arrows indicate barrier disruption, scale bar represents 10  $\mu$ m.





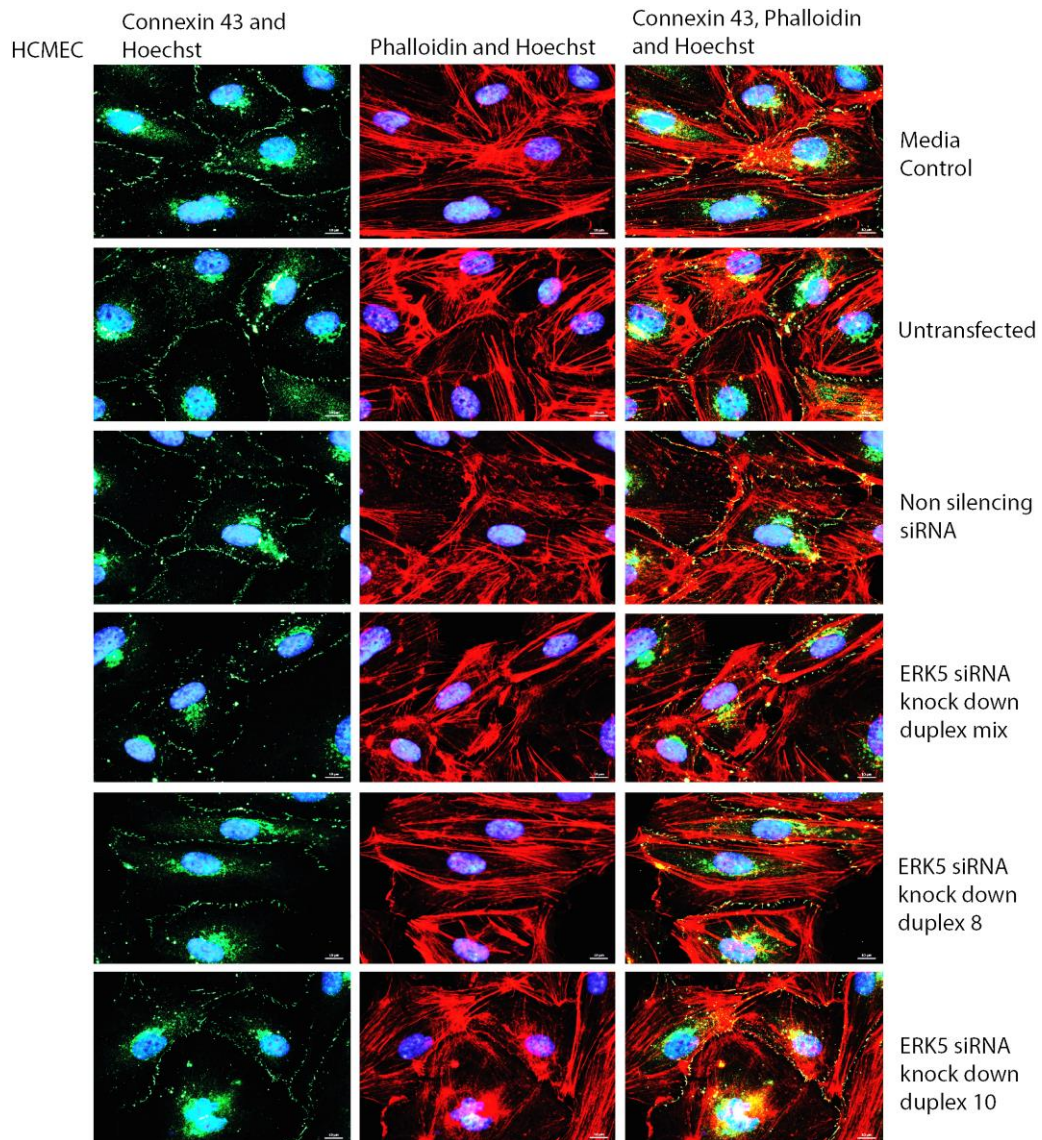


Figure 5.7. **Immunofluorescence analysis of endothelial gap junctions following small interfering RNA ERK5 silencing.** (A) HDMEC adult and (B) HCMEC were transfected with siRNA and stained with CX43 (green), phalloidin (red) and Hoechst (blue). Arrows indicate barrier disruption, scale bar represents 10  $\mu\text{m}$ .

The data in figures 5.5 – 5.7 clearly demonstrated that ERK5 is required for regulation of tight, adherens and gap junctions. The physiological relevance of the observed barrier perturbation on paracellular permeability was further analysed using a FITC dextran barrier function assay to measure the flow of dextran through a ThinCert with 0.4  $\mu\text{m}$  pore covered with a monolayer of endothelial cells. Figure 5.8 shows that

ERK5 inhibition significantly reduced barrier function leading to an increased flux of dextran across the endothelial cells.

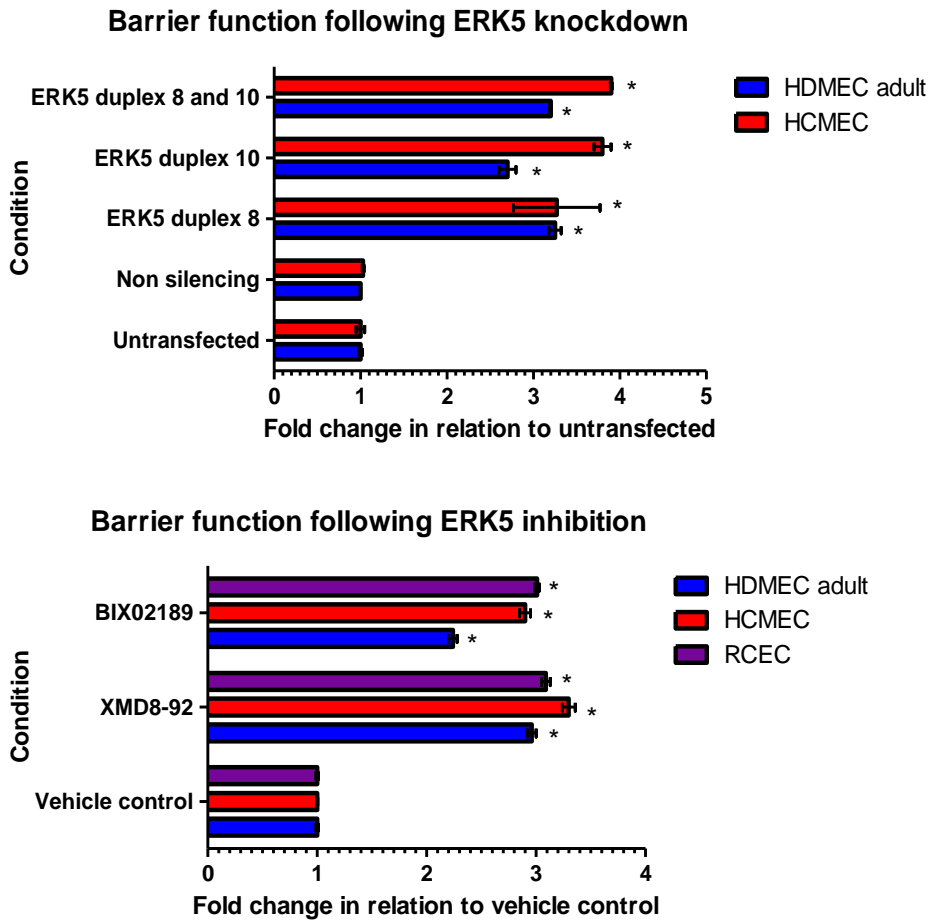


Figure 5.8. **Barrier function assessment of HDMEC adult, HCMEC and RCEC following ERK5 inhibition.** (Top) HDMEC adult and HCMEC were transfected with siRNA, (Bottom) XMD8-92 (3  $\mu$ M) or BIX02189 (3  $\mu$ M) for 6 hours. Addition of 4kDa FITC dextran to the ThinCert. The flow through was measured on a fluorescence plate reader. N=4 separate inserts  $\pm$  SD, \* =  $P \leq 0.05$ , one-way ANOVA, SPSS, data plotted in GraphPad Prism.

#### 5.2.4 Activation of ERK5 by statins

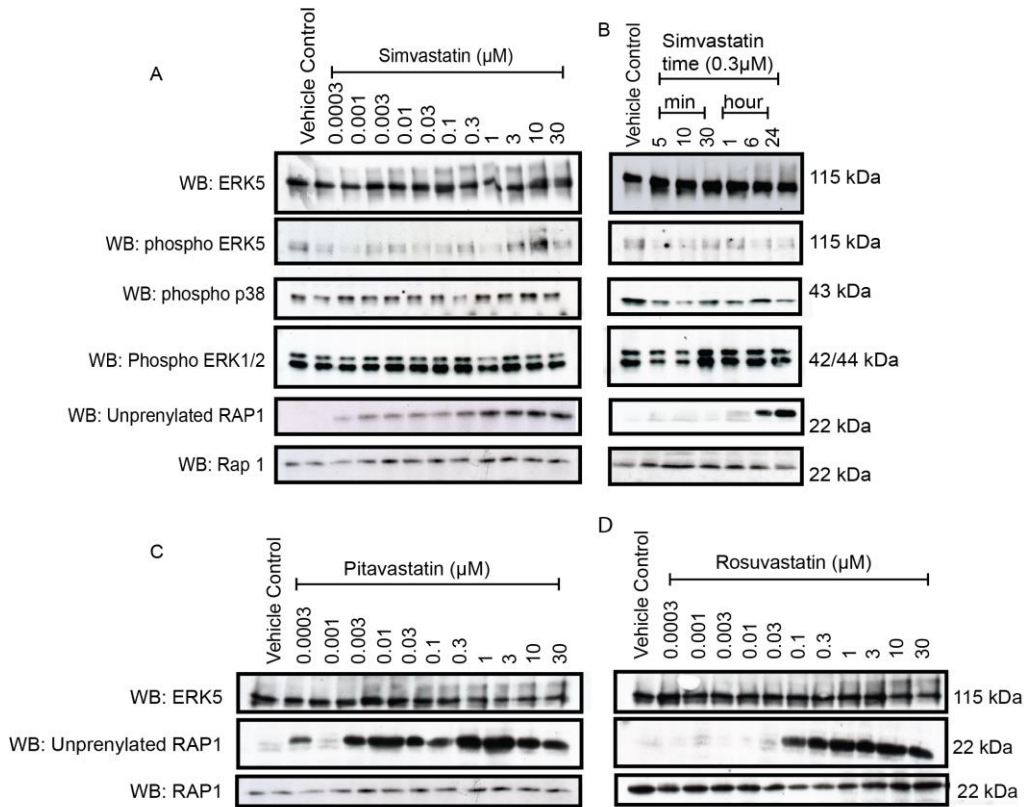
Thus far the data outlines how inhibition of ERK5 induced barrier perturbation and decreased barrier function. This led to the next hypothesis: can activation of ERK5 stimulate the junctions? In order to achieve this an activator of ERK5 needed to be identified. Reports have



shown that statins are able to activate ERK5 in endothelial cells (Wu et al., 2013; Le et al., 2014). Statins have different physico-chemical properties; for this reason three different statins were investigated to determine their ability to activate ERK5. These included the lipophilic statins: simvastatin and pitavastatin, as well as the hydrophilic statin rosuvastatin (statin properties are outlined in table 1.4). Using western analysis, the three statins were analysed for their ability to induce ERK5 phosphorylation. As shown in figure 5.9, the three drugs tests were all able to induce ERK5 phosphorylation. ERK5 phosphorylation can be measured by a band shift on a conventional SDS-PAGE gel. This phenomenon occurs due to the phosphorylated species of the protein running at a slightly higher molecular weight, allowing two bands to be detected for the given protein. The lower band identifies the level of protein within the sample and the higher band identifies the phosphorylated version of the protein. This method has been utilised in studying ERK5 phosphorylation in the absence of specific phospho antibodies. Antibodies to phospho ERK5 tend to be nonspecific and also detect other phosphorylated proteins, such as ERK1/2, so using the two methods for phosphorylation detection is advised when assessing ERK5.

The phosphorylation of ERK5 was compared to the prenylation of RAP1, as this protein becomes unprenylated following inhibition of cholesterol biosynthesis by statins. My results show that simvastatin was able to induce ERK5 phosphorylation at nM concentrations and the phosphorylation mirrored the unprenylation of RAP1, providing evidence that ERK5 phosphorylation occurred at physiologically relevant concentrations (Fig. 5.9 A). The antibody used in these experiments and future experiments within this Thesis, specifically recognised unprenylated RAP1, as previously described (Antoine et al., 2010). This response was observed both dose (Fig. 5.9 A) and time (Fig. 5.9 D) dependently suggesting that ERK5 phosphorylation occurred as a consequence of the ability of statins to inhibit cholesterol biosynthesis. Figure 5.9 C outlined how pitavastatin has a similar activation profile for

ERK5 to simvastatin but figure 5.9 D provided evidence that rosuvastatin was a less potent ERK5 activator.





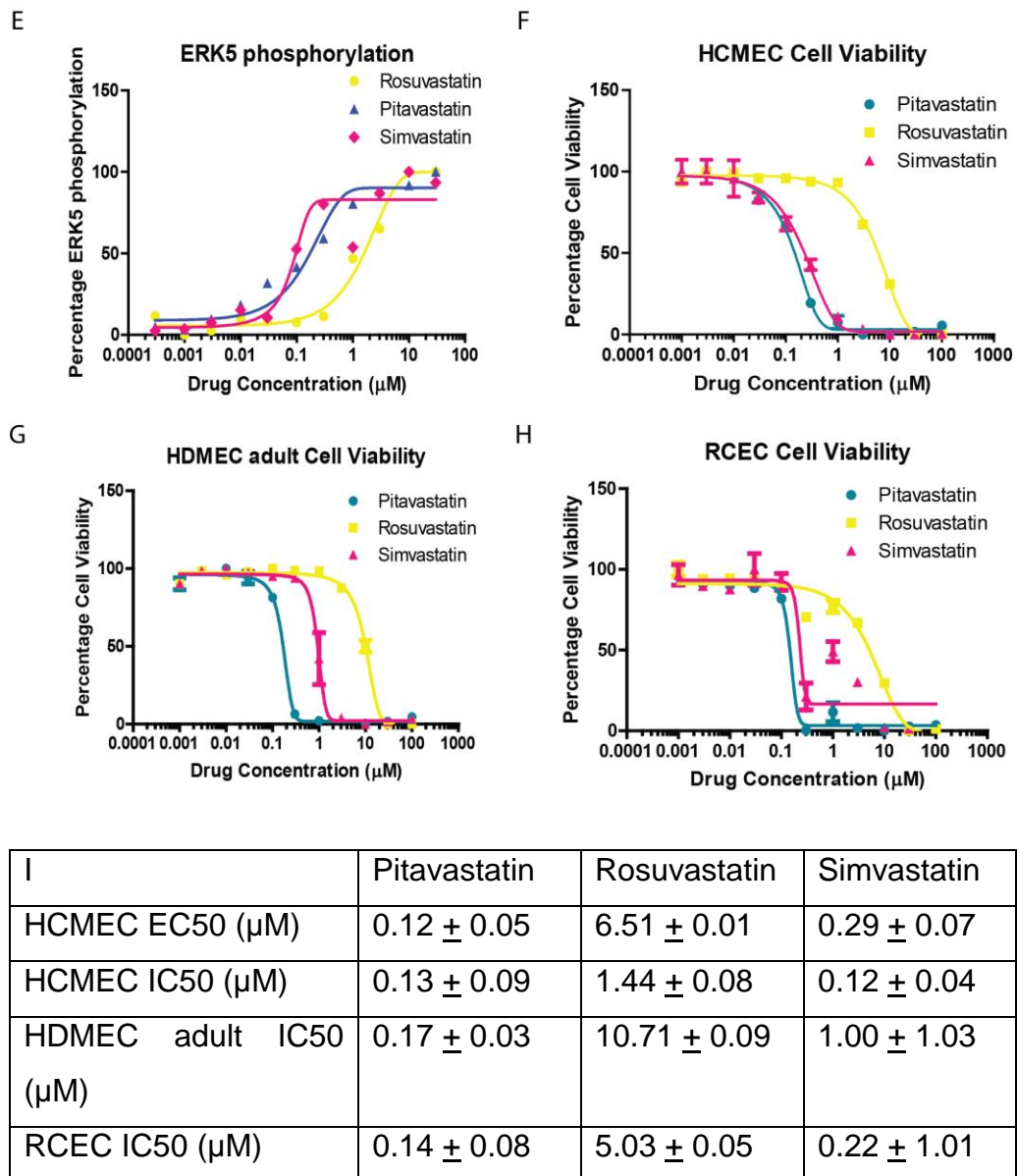


Figure 5.9. **Dose-response for statin affects.** HCMEC (A) simvastatin, (B) Rosuvastatin, (C) Pitavastatin at concentrations ranging from 0.0003 – 30  $\mu\text{M}$  for 6 hours. (D) Simvastatin 0.3  $\mu\text{M}$  over a time course ranging from 0 minutes – 24 hours. Western blots probed for ERK5, phosphorylated ERK5, p38 and ERK1/2, unphosphorylated RAP1 and RAP1 is used as a loading control. Quantification was done using image J with band intensity represented as percentage ERK5 phosphorylation and (E) dose response was plotted in GraphPad Prism. (F) HCMEC, (G) HDMEC adult and (H) RCEC were treated with simvastatin, pitavastatin or rosuvastatin at concentrations ranging from 100  $\mu\text{M}$  to 0.01  $\mu\text{M}$ . Viability analysis was measured with Cell Titer Glo<sup>®</sup>. The IC50 was calculated using GraphPad prism. (I) Table outlining EC50s for ERK5 phosphorylation and IC50s for cell viability.

The IC<sub>50</sub> was determined for the statins to ensure that the concentrations used were below the toxic dose. Figure 5.9 G details the IC<sub>50</sub> for statins after 72 hour treatment in HCMEC.

### 5.2.5 Analysis of ERK5 signalling cascade

ERK5 is known to be activated as part of a linear signalling cascade involving MEKK2/MEKK3 – MEK5 – ERK5. To determine where in this cascade the statins act siRNA mediated gene silencing was used to knock down each of the signalling kinases individually to determine where in the pathway simvastatin acts to ultimately activate ERK5. These cells could then be analysed by western blotting to determine at which point in the cascade the siRNA prevented ERK5 phosphorylation, and in turn this led to the determination of where statins act.

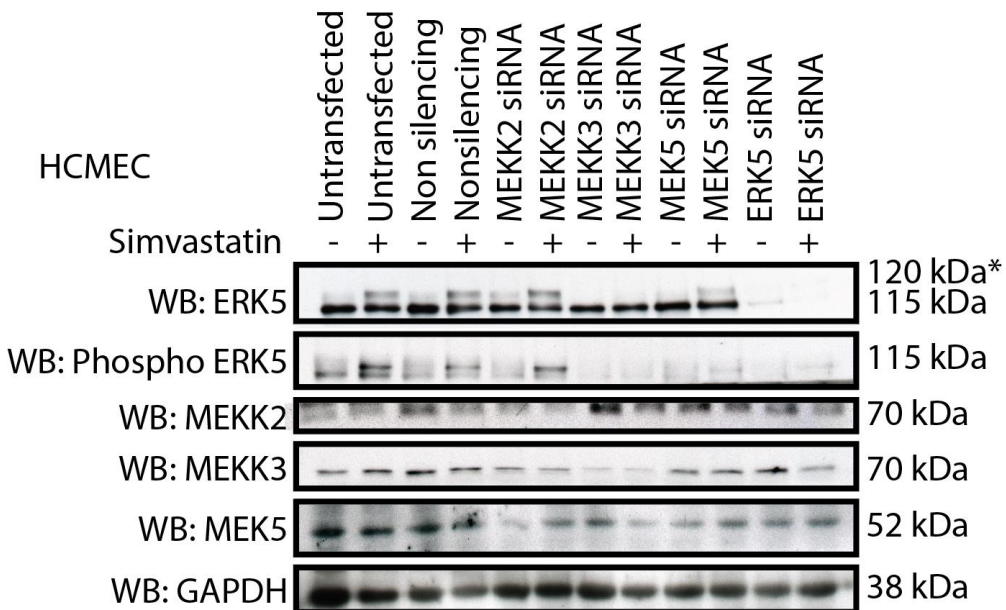


Figure 5.10. **Small interfering RNA transfection to determine the molecular target for simvastatin.** HCMEC were transfected with siRNA to MEKK3, MEKK2, MEK5 and ERK5 as well as non silencing control. Blots were probed for: ERK5, MEKK2, MEKK3, MEK5 and RAP1A, GAPDH is used as a loading control.

The western blot analysis showed that siRNA gene silencing of MEKK2 led to ERK5 phosphorylation by statins at normal levels, while siRNA

silencing of MEKK3 resulted in loss of ERK5 phosphorylation after statin treatment (Fig. 5.10). This suggests that simvastatin acted upstream of ERK5 at the level of MEKK3. The reduction in ERK5 phosphorylation following MEK5 siRNA gene silencing indicates that this kinase was also involved in the pathway. Taken together, these findings suggest that statins induced phosphorylation of MEKK3, which in turn led to MEK5 phosphorylation, which subsequently induced ERK5 phosphorylation. The next step was to determine which molecule in the cholesterol biosynthesis pathway regulated the statin mediated barrier regulation. This was achieved by addition of the inhibited products to determine which prevented ERK5 phosphorylation.

#### *5.2.6 Linking cholesterol biosynthesis to barrier protection*

Statins prevent cholesterol biosynthesis by inhibition of HMG Co-A reductase resulting in an intracellular decrease in the number of biosynthetic precursors (Fig. 1.21). To determine which precursors were responsible for ERK5 phosphorylation and hence barrier preservation the major downstream molecules in the cholesterol biosynthesis process were added back to cells treated with simvastatin. The results of this analysis are shown in Figure 5.11. Addition of mevalonate reduced the phosphorylation of ERK5 observed with statin treatment at 24 hours (Fig. 5.11 A) suggesting that two pathways could be responsible for ERK5 phosphorylation, namely the GGPP and FPP pathways (Stancu and Sima, 2001). Addition of GGPP prevented the phosphorylation of ERK5 (Fig. 5.11 B) (Sundararaj et al., 2008). ERK5 phosphorylation remained with the addition of FPP in the presence of simvastatin (Fig. 5.11 B) (Miura et al., 2004). These results suggested that the ERK5 phosphorylation was a result of the GGPP pathway rather than the FPP. This was further analysed by addition of squalene and cholesterol, synthesised downstream of FPP, both of which also failed to prevent ERK5 phosphorylation (Fig. 5.11 C).

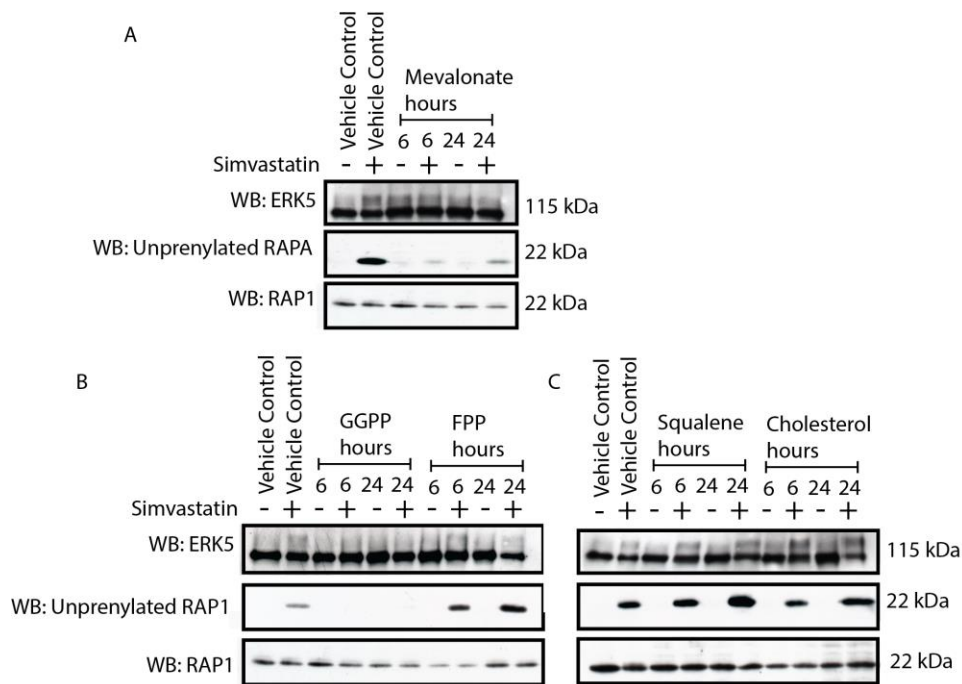


Figure 5.11. **Add back of the downstream cholesterol biosynthesis products following statin inhibition.** HCMEC were treated with (A) mevalonate (100 μM), (B) GGPP (10 μM), FPP (10 μM), (C) Squalene (10 μM) or cholesterol (10 μM) for 6 or 24 hours in the presence and absence of simvastatin. Blots were probed for ERK5, unprenylated RAP1 and RAP1 is used as a loading control.

In summary, statins prevent formation of a number of biosynthetic precursors through inhibition of HMG-Co A. Here I investigated, through addback experiments, which of these precursors were responsible for ERK5 phosphorylation. The addback recovery experiments (Fig. 5.10) provided evidence that ERK5 phosphorylation was due to GGPP inhibition, as addition of GGPP prevented ERK5 phosphorylation. In order to further evaluate this result an inhibitor to GGPP was used. Unlike statins, GGTI-298 specifically inhibits the GGPP pathway with no effect on the FPP pathway. It can be observed from figure 5.12 A that the GGPP inhibitor GGTI-298 induced ERK5 phosphorylation at 6 hours producing similar results to what was observed in figure 5.9 with simvastatin treatment.

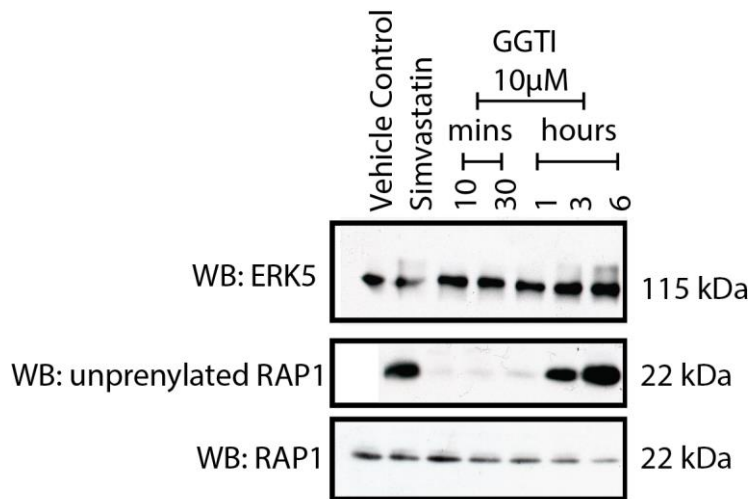


Figure 5.12. ***Inhibition of GGPP affects ERK5 phosphorylation in an identical manner to simvastatin.*** HCMEC were treated with GGTI-298 (10 µM) over time from 5 minutes to 6 hours. Blots were probed for ERK5, unphosphorylated RAP1 and RAP1 is used as a loading control.

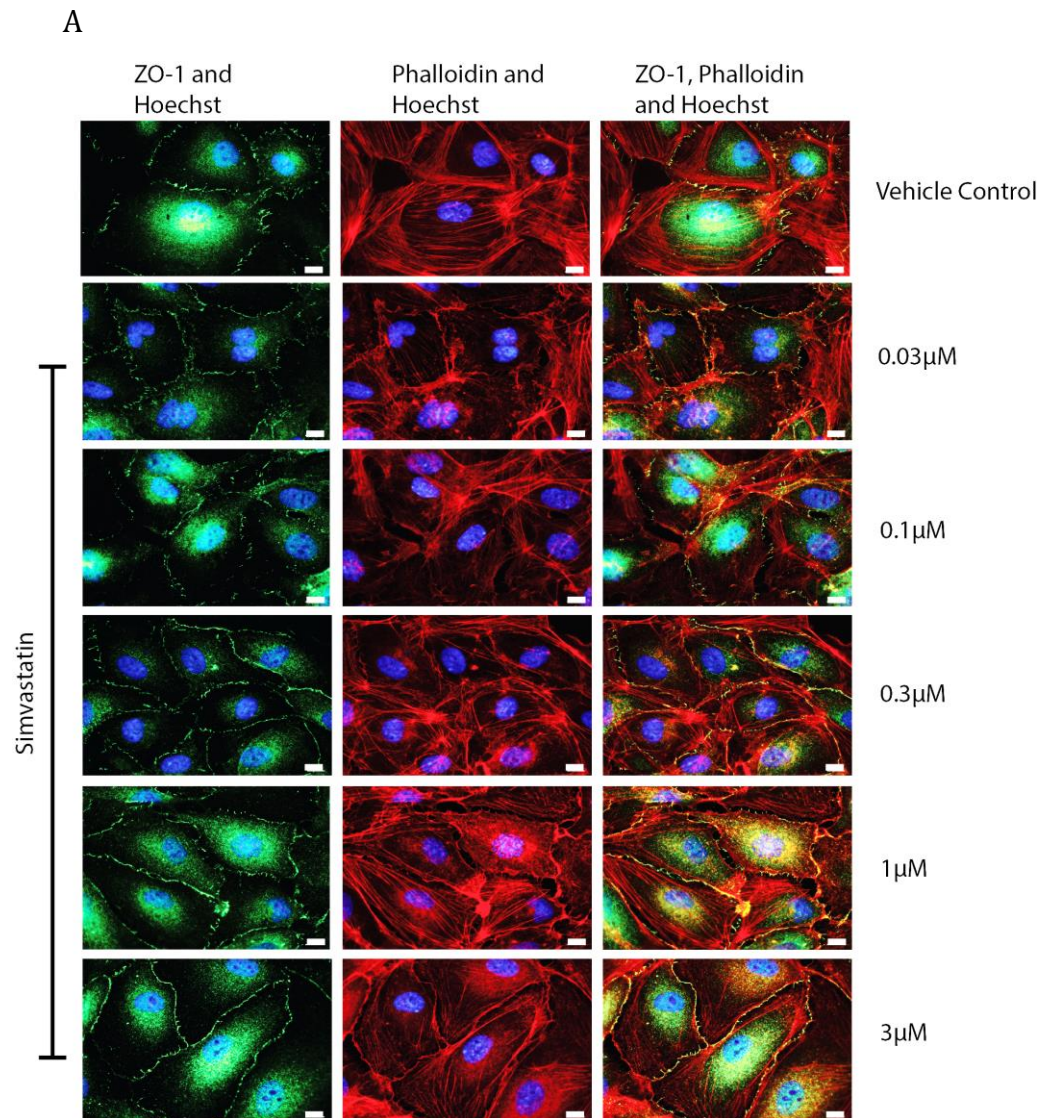
### 5.2.7 Simvastatin regulates tight junction formation in endothelial cells in an ERK5 dependent manner

Simvastatin is one of the top three commonly used statins in the clinic, so this statin was further investigated in this thesis. A range of concentrations of simvastatin were analysed for their ability to stimulate the endothelial tight junction barrier in HCMEC using immunofluorescent staining for ZO-1 (tight junctions). The results show that simvastatin stimulated the endothelial tight junction barrier (Fig. 5.13 A). Furthermore, simvastatin treatment led to ERK localisation to the membrane and nucleus as shown by immunofluorescent staining in figure 5.13 B. Increasing simvastatin concentrations correlated with increased intensity of ERK5 in the nucleus and at the plasma membrane (images with same exposure times).

To conclude, simvastatin was able to stimulate the endothelial barrier in a dose dependent manner showing effective stimulation from 0.1 µM, which coincided with ERK5 translocation to the membrane. As has been outlined in figure 5.9 E-G the IC<sub>50</sub> of simvastatin is 0.3 µM and the EC<sub>50</sub>



is 0.1  $\mu\text{M}$ . A concentration of 0.3  $\mu\text{M}$  was carried forward for all further investigation as it was able to induce ERK5 phosphorylation, stimulate the endothelial tight junction barrier and induce ERK5 translocation to the membrane.



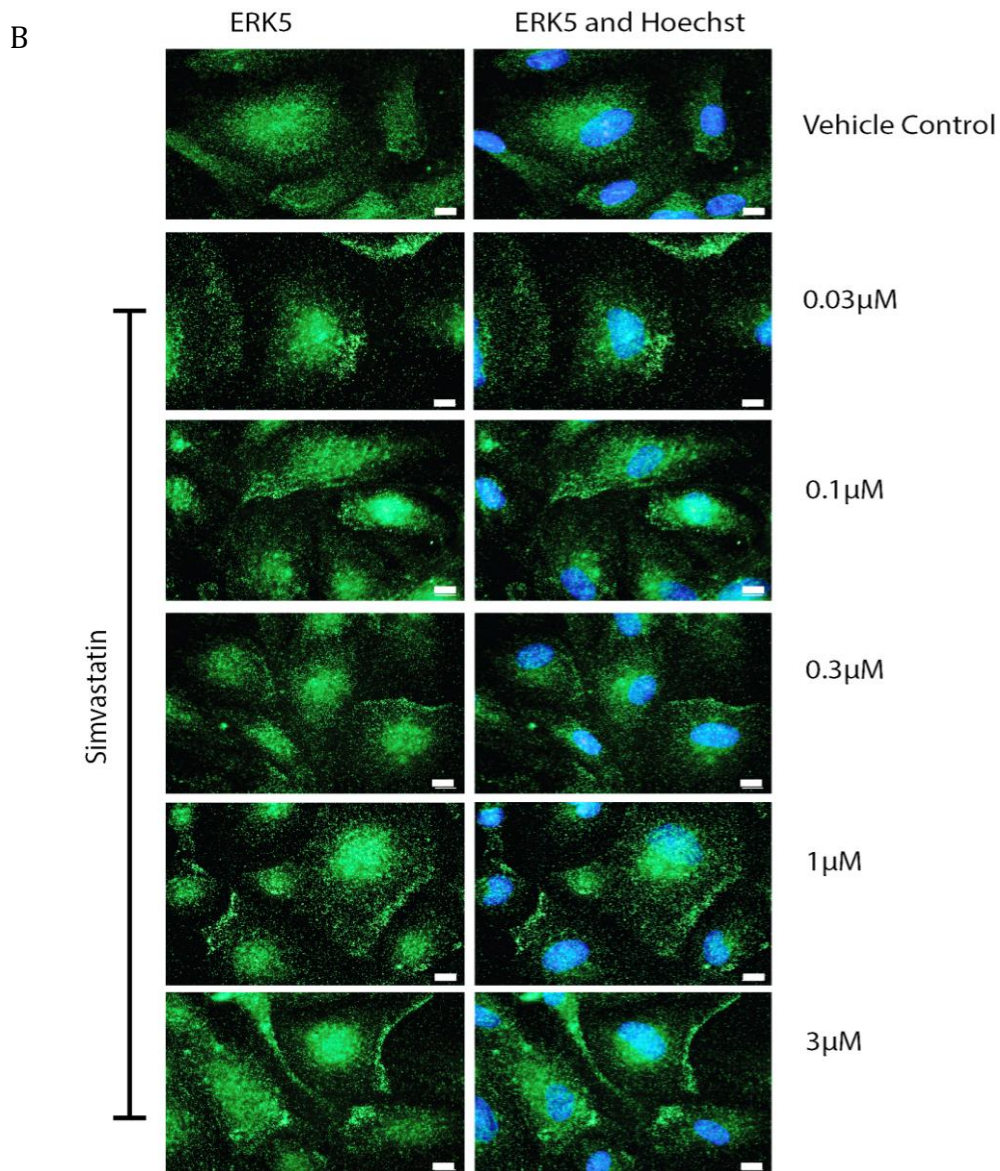


Figure 5.13. **Immunofluorescence analysis of simvastatin barrier protection and ERK5 localisation.** HCMEC were treated with simvastatin at concentrations ranging from 0.03 – 3  $\mu$ M for 6 hours. (A) Staining with ZO-1 (tight junctions, green), phalloidin (actin fibers, red) and Hoechst (nuclei, blue), (B) Staining with ERK5 (green) and Hoechst (blue). Scale bar represents 10  $\mu$ m.

### 5.2.8 Simvastatin is able to overcome XMD8-92 induced barrier perturbation but not BIX02189 induced barrier perturbation

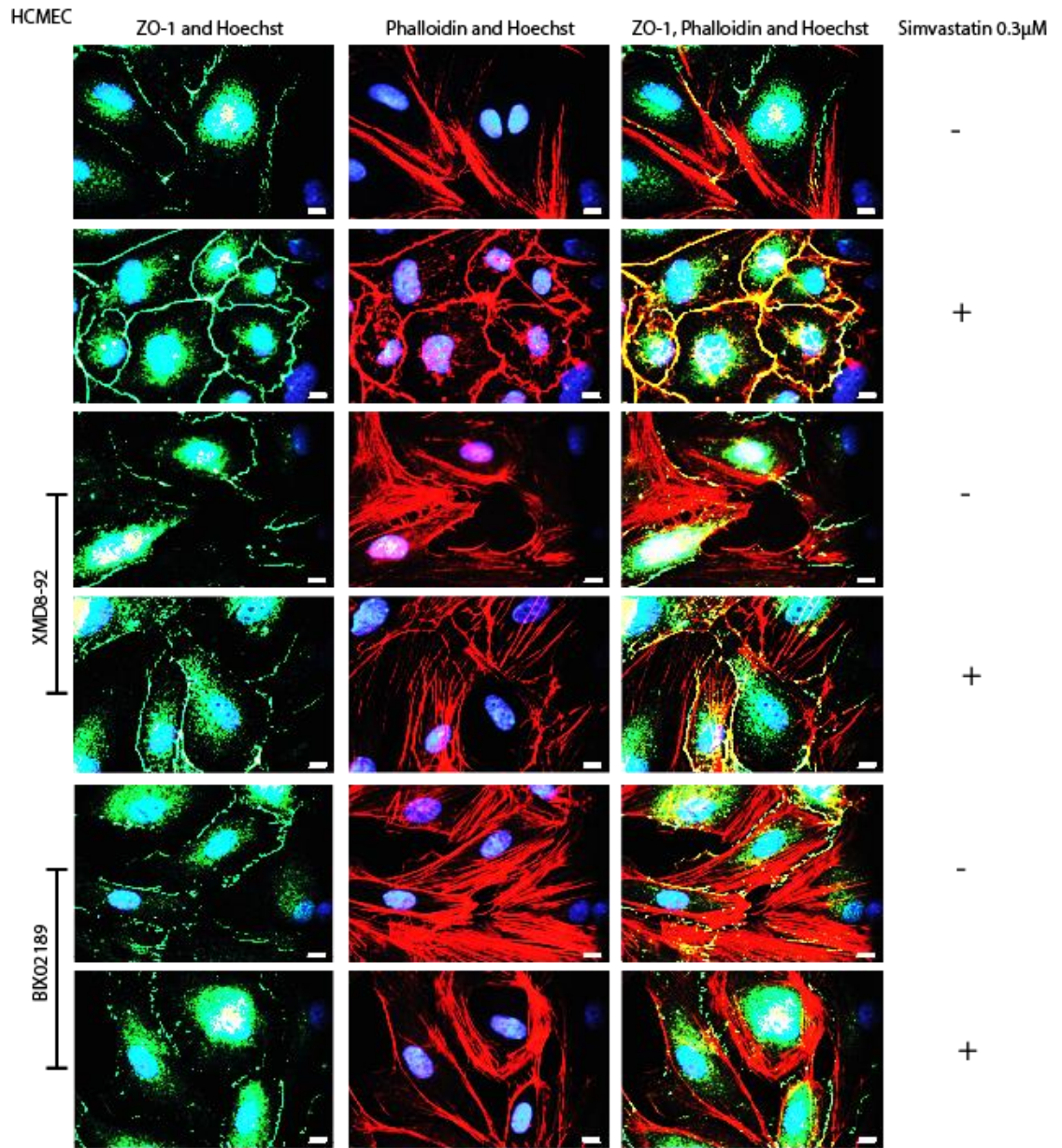
As it had been demonstrated that simvastatin was able to stimulate the tight junction barrier, the next aim was to analyse if simvastatin pretreatment could reverse the barrier perturbation induced by ERK5



inhibitors XMD8-92 and BIX02189 (Fig. 5.14). Cells were pretreated with the small molecule inhibitors XMD8-92 (direct ERK5 inhibitor) and BIX02189 (MEK5 inhibitor) for 30 minutes prior to addition of simvastatin, followed by immunofluorescent analysis for ZO-1 and ERK5. The results demonstrated that simvastatin could overcome ERK5 inhibition with XMD8-92 but not BIX02189 (Fig. 5.14). XMD8-92 has been previously shown to directly inhibit ERK5 without preventing phosphorylation of the T218/Y220 (MEK5) phosphorylation site on ERK5, which is thought to work through inhibition of C terminal phosphorylation (Unpublished data by Jones GN *et al*). By contrast, BIX02189 has been shown to inhibit phosphorylation of ERK5 on the T218/Y220 (MEK5) phosphorylation site (Tatake et al., 2008). The results from the inhibitor experiment therefore suggest that the T218/Y220 is key in simvastatin induced tight junction barrier stimulation.

The difference in the response of simvastatin to overcome ERK5 inhibitor induced barrier perturbation provides a key result in understanding how statins stimulate the tight junction barrier.

A



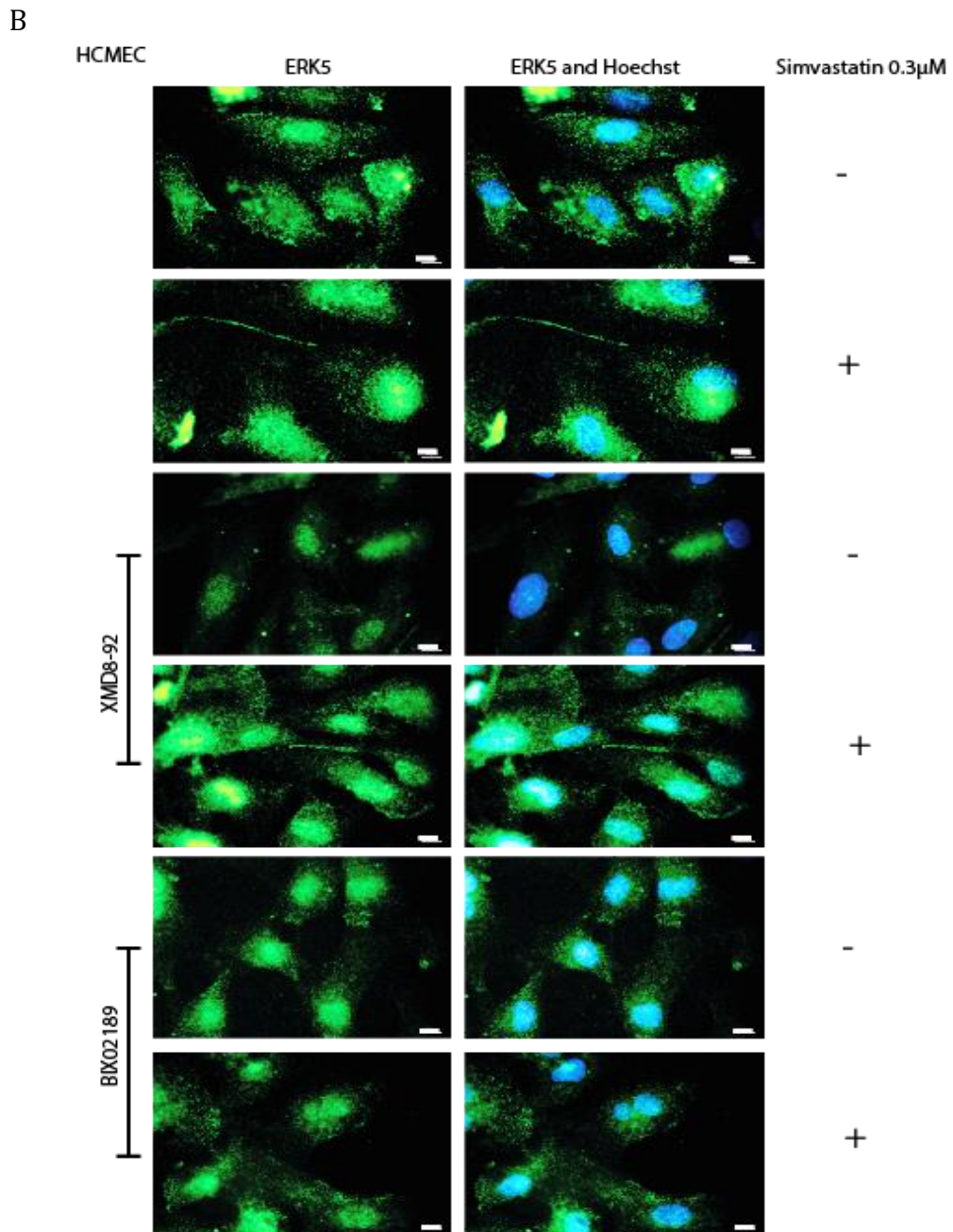
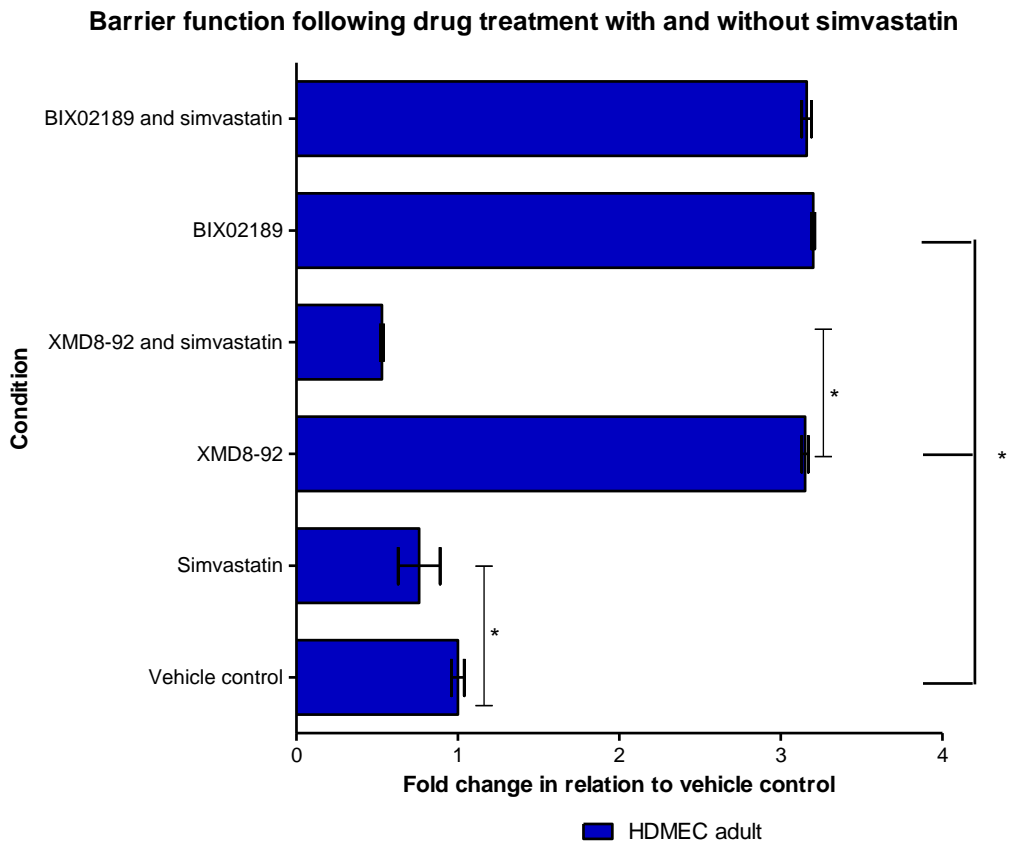
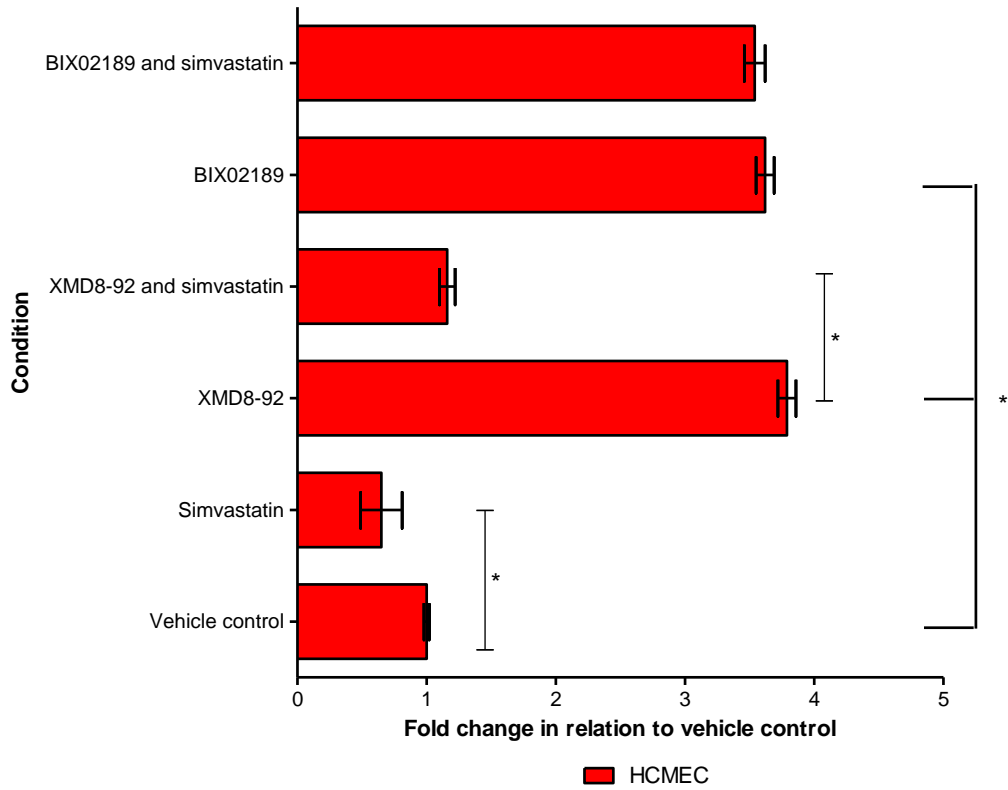


Figure 5.14. ***BIX02189 prevents simvastatin from stimulating the endothelial tight junction barrier.*** HCMEC were treated with XMD8-92 (3  $\mu$ M) or BIX02189 (3  $\mu$ M) for 30 minutes prior to addition of simvastatin 0.3  $\mu$ M for a further 6 hours. (A) Staining with ZO-1 (tight junctions, green), phalloidin (actin fibers, red) and Hoechst (nuclei, blue), (B) Staining with ERK5 (green) and Hoechst (blue). Scale bar represents 10  $\mu$ m.

It is clearly evident that simvastatin was able to overcome the XMD8-92 barrier perturbation but not the BIX02189 barrier perturbation. The physiological implications on barrier perturbation are further assessed using a FITC dextran barrier function assay to measure flux across an endothelial cell monolayer seeded on inserts with 0.4 μm pores (Fig. 5.15). The results provided evidence that simvastatin significantly reduced the level of dextran able to permeate through the endothelial cells following XMD8-92 treatment but not BIX02189 treatment. This result provides an indication that simvastatin was activating ERK5 in a mechanism dependent of MEK5 as it could not be overcome with BIX02189.



**Barrier function following drug treatment with and without simvastatin**



**Barrier function following drug treatment with and without simvastatin**

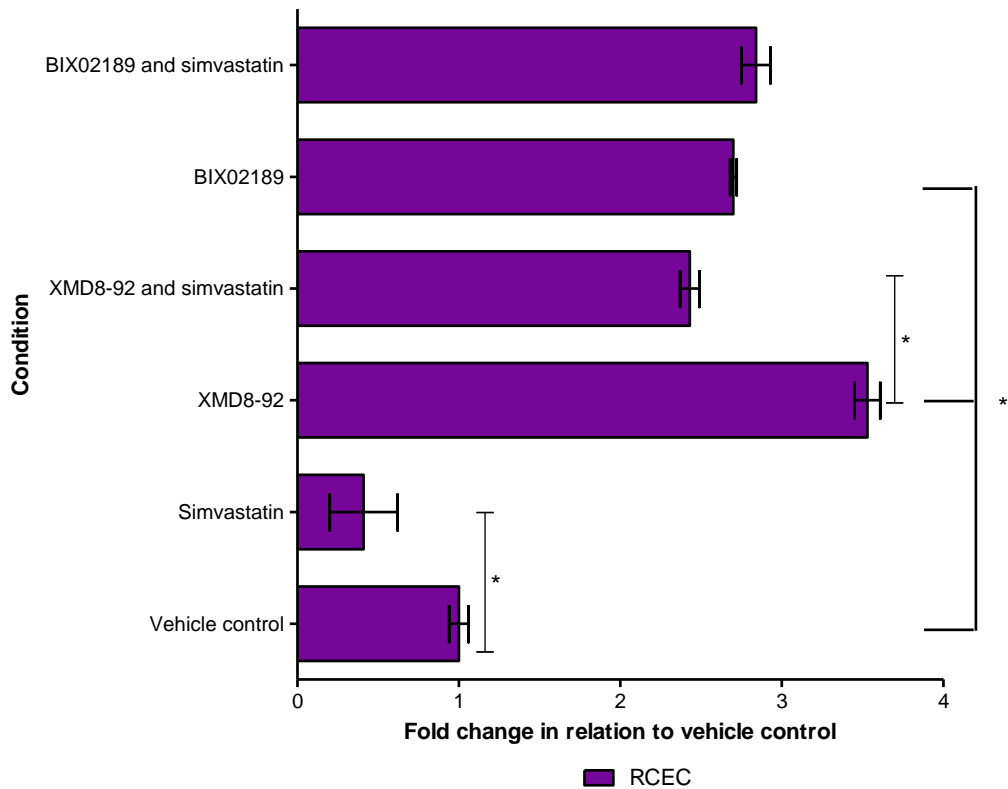
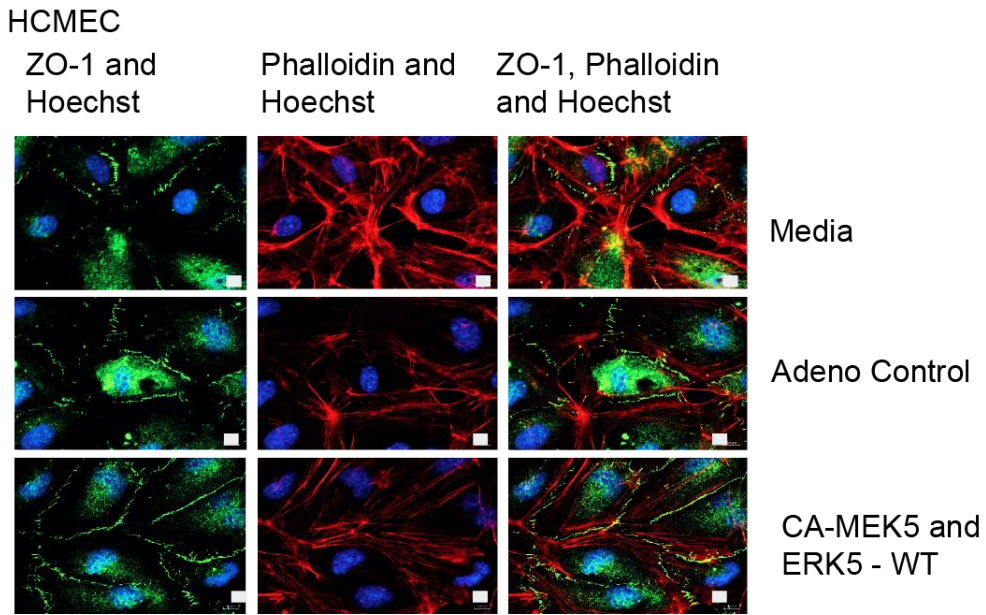


Figure 5.15. **Barrier function following drug treatment with and without simvastatin.** (A) HDMEC adult, (B) HCMEC and (C) RCEC were pretreated with simvastatin 0.3  $\mu$ M for 6 hours prior to treatment with doxorubicin 0.1 $\mu$ M, XMD8-92 3  $\mu$ M or BIX02189 3  $\mu$ M for 6 hours following treatment addition of 4 kDa FITC dextran to the ThinCert and the flow through was measured on a fluorescence plate reader. N=4 inserts. Data plotted as mean  $\pm$  SD, \* =  $P \leq 0.05$  with connections indicating comparisons, one-way ANOVA, SPSS, data plotted in GraphPad Prism.

As the data demonstrated, activation of ERK5 by simvastatin stimulated the tight junction barrier resulting in significant increased barrier function outlined by a decrease in dextran permeation through the endothelial cells. It was next analysed if the same barrier stimulation could be achieved with ERK5 activation using adenovirus. Adenovirus to overexpress ERK5 had been previously created within the group and sequenced to determine specificity for ERK5. It is known that adenovirus can regulate the actin cytoskeleton. In order to reduce this effect the virus was titrated to determine an optimum MOI that did not produce actin cytoskeleton rearrangement using adeno-control. A MOI of 2 was determined optimal for analysing the effects on the barrier. It can be observed in figure 5.16 that ERK5-WT adenovirus stimulated the tight junction barrier and significantly increased barrier function in comparison to Adeno-control. There was a small barrier stimulation indicated by an increase in barrier function with adeno-control, however, this was not a significant effect in comparison to media control.





**Barrier function following ERK5 activation with adeno-virus**

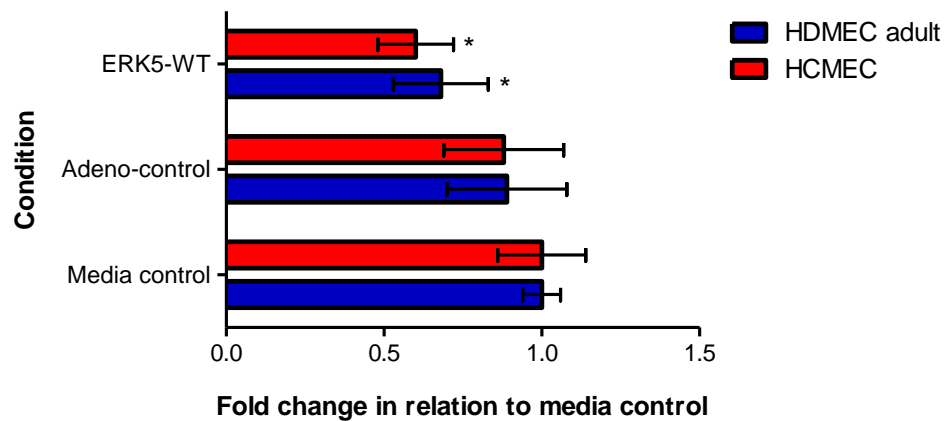


Figure 5.16. **ERK5 activation with adeno-virus.** HCMEC were transfected with ERK5 adeno-virus. Cells were stained for ZO-1 (tight junctions, green), phalloidin (actin fibers, red) and Hoechst (nuclei, blue). Barrier function was measured using ThinCerts with 4 kDa FITC dextran and the flow through was measured on a fluorescence plate reader. N=4 inserts. Data plotted as mean  $\pm$  SD, \* =  $P \leq 0.05$  compared to Adeno-control, one-way ANOVA, SPSS, data plotted in GraphPad Prism.



## 5.3 Discussion

### 5.3.1 ERK5 regulates the tight junction barrier in endothelial cells

ERK5 has been established to play an important role in endothelial cells. It is vital for the initial development of the vasculature during embryogenesis, with knockout mice showing a lethal phenotype at E9.5 - 11.5 (Hayashi et al., 2004). After vasculature development ERK5 has been shown to be critical for endothelial cell survival as it is able to regulate AKT (Roberts et al., 2010). As vascular permeability is a key physiological process in endothelial cells the role of ERK5 in its regulation was investigated. It was initially identified from the literature that the ERK5 knockout mice had gaps in the vasculature (Hayashi et al., 2004). This would suggest a leaky phenotype and potential barrier function regulation. ZO-1 knockout mice also showed a similar phenotype and embryonic lethality at around E10.5 (Katsuno et al., 2008) similar to ERK5 knockout mice.

There are several tools available to manipulate ERK5 activity and protein level; these include small molecule inhibitors, siRNA and adenovirus. Two well established small molecule inhibitors of ERK5 were validated, XMD8-92 and BIX02189. In order to determine if ERK5 plays a role in barrier regulation, inhibitors were validated against the cell lines of interest to define a non-toxic concentration of drug to be used to assess the effects on the endothelial barrier following ERK5 inhibition. BIX02189 is considered a MEK5 inhibitor by preventing phosphorylation of the MEK5 T218/Y220 binding site on the ERK5 protein (Tatake et al., 2008). XMD8-92 is considered to inhibit ERK5 directly (Yang and Lee, 2011; Yang et al., 2010). The use of both inhibitors allowed both direct and indirect inhibition of ERK5 to be investigated for potential induction of endothelial barrier perturbation.

ERK5 small molecule inhibitors XMD8-92 and BIX02189 were used at concentrations shown to induce no cytotoxicity (3  $\mu$ M). These results indicated that ERK5 inhibition not only led to tight junction barrier perturbation but also adherens junction barrier perturbation. This suggests a role for ERK5 in junction regulation. The barrier perturbation appeared more prominent in HCMEC and RCEC (for tight junctions) than HDMEC adult. This begins to identify differences between cardiac and dermal vasculature and could progress to determine a mechanism for cardiovascular sensitivity to the anti-cancer drugs in comparison to alternative vascular beds.

It is well known small molecule inhibitors have the potential to produce off target effects. In order to determine if this was a specific effect of ERK5 inhibition siRNA technology to transiently silence ERK5 was utilised. The observation following siRNA gene silencing of ERK5 provided concluding evidence through immunofluorescent imaging and western blotting that ERK5 levels decreased within the cells. This ERK5 decrease was accompanied by reduction in gap junctions, indicated by use of CX43 (Cameron et al., 2003). This barrier perturbation is not limited to gap junctions, there is evidence to suggest that adherens and tight junctions are regulated by ERK5 as siRNA gene silencing induces perturbation in both these junctions (Fig. 5.5 – 5.7). This effect, similar to the inhibitors, produced a more prominent barrier perturbation in HCMEC than HDMEC adult. The more prominent barrier perturbation in HCMEC again provided evidence of potential vascular bed individuality and could lead to a potential explanation for cardiovascular toxicity. Barrier perturbation was physiologically quantified to provide evidence that ERK5 inhibition significantly decreased barrier function as dextran permeation through the endothelial cells increased following ERK5 inhibition.

This work provided evidence that ERK5 is able to regulate junctions. It has been demonstrated in the literature that ERK5 regulates CX43 (Cameron et al., 2003). It can also be identified that CX43 regulates ZO-

1 (Tien et al., 2013). These two published links along with the data in this Chapter suggest a link between ERK5 – CX43 – ZO-1 which is how ERK5 may be able to regulate the endothelial junctions.

The third tool available to study ERK5 is adenovirus. This is used to over express ERK5 within cells. It is known that adenovirus can regulate FAK leading to actin cytoskeleton remodeling, so titration of the adenovirus to validate the concentration of virus particles per cell was conducted. This data showed that ERK5 overexpression can also stimulate the barrier providing evidence that there is potential through activation of ERK5 to stimulate the tight junction barrier. As the use of adenovirus is not clinically beneficial a search for an ERK5 activator was conducted. There have been reports that link statins to ERK5 activation (Le et al., 2014). As statins are currently considered a relatively safe drug these were investigated for their effects on ERK5 and tight junction stimulation.

### 5.3.2 Activation of ERK5 by statins stimulates endothelial tight junctions

Statins have been demonstrated to induce intracellular ERK5 kinase phosphorylation in vascular endothelial cells such as human aortic endothelial cells (HAEC) (Le et al., 2014; Wu et al., 2013; Ahmed et al., 2014; Chen et al., 2010; Fang et al., 2013; He et al., 2008; Huang et al., 2010; Lee et al., 2012; Miura et al., 2004; Sundararaj et al., 2008; Takayama et al., 2011). The ERK5 phosphorylation is observed in addition to effects on HMG Co-A reductase and the resulting decreased LDL plasma cholesterol levels, since statins have been shown to have a number of pleiotropic effects. Here, I have analysed if these pleiotropic effects were attributal to ERK5 phosphorylation, including endothelial projection through signalling involving eNOS (Chen et al., 2013). These publications along with the data in this Chapter demonstrated that ERK5 inhibition induced endothelial barrier perturbation, resulting in the

question whether statin can induce activation of ERK5 stimulate endothelial tight junction formation?

This Chapter investigated the effects of simvastatin on the endothelial tight junction barrier. The results clearly demonstrated that statins stimulate the endothelial barrier at a concentration that induces ERK5 phosphorylation but does not induce cellular toxicity. The use of simvastatin and small molecule ERK5 inhibitors provided key information about the mechanism of simvastatin induced ERK5 activation. It has been demonstrated at the start of this Chapter that both XMD8-92 and BIX02189 induce barrier perturbation leading to the conclusion: inhibition of ERK5 phosphorylation was important for barrier perturbation. This section has demonstrated that simvastatin treatment can overcome barrier perturbation with XMD8-92 but not BIX02189. This suggests that MEK5 phosphorylation of the T218/Y220 phosphorylation site on ERK5 is crucial for simvastatin induced ERK5 phosphorylation. This provided a further question; does simvastatin directly phosphorylate ERK5 or does it act upstream in the signalling cascade?

This question was addressed with use of siRNA gene silencing to the known kinases in the ERK5 signalling axis. This data has provided evidence that gene silencing of MEKK3 led to prevention of statin induced ERK5 activation suggesting that this is the target kinase for statins. Gene silencing of MEKK2 does not affect statins ability to activate ERK5. Gene silencing of downstream signalling kinases from MEKK3 also demonstrate prevention of ERK5 activation. Since statins work upstream of MEK5, barrier perturbation with BIX02189 cannot be overcome with use of statins, as BIX02189 inhibits MEK5. XMD8-92 inhibits ERK5 directly, it is predicted to work directly on the C termini preventing phosphorylation (Yang and Lee, 2011; Yang et al., 2010; Tataka et al., 2008). As statins are able to overcome XMD8-92 barrier perturbation and siRNA gene silencing of MEKK3/MEK5/ERK5 prevents ERK5 phosphorylation this suggests that it is the TEY motif on ERK5 that is

important for statin induced ERK5 phosphorylation leading to barrier protection.

While analysing this signalling axis it is also interesting to note that the MEKK3 – MEK5 – ERK5 signalling kinases produce similar phenotypical defects and lethality in knockout mice during embryogenesis (Yang et al., 2000; Kato et al., 1997; Hayashi et al., 2004). Knockout mice of MEKK2, which is also known to activate this cascade, do not produce a lethal phenotype suggesting that MEKK2 and MEKK3 activate the pathway in independent manners (Garrington et al., 2000). A difference in MEKK2 and MEKK3 siRNA transient gene silencing had shown that these kinases work independently to activate ERK5. MEKK2 gene silencing does not affect statin induced ERK5 phosphorylation but MEKK3/MEK5/ERK5 siRNA transient gene silencing prevents statin induce ERK5 phosphorylation, suggesting that statins induce ERK5 phosphorylation through MEKK3 – MEK5 – ERK5 and not through MEKK2.

### 5.3.3 Linking cholesterol biosynthesis to barrier protection

The cardio protective ability of statins has not yet been fully understood (Henninger et al., 2012; Huelsenbeck et al., 2011; Nubel et al., 2006; Nubel et al., 2004b). In this thesis I have started to outline how statins are able to induce barrier protection through inhibition of the conventional cholesterol biosynthesis pathway. Statins act to inhibit HMG Co-A reductase (Stancu and Sima, 2001) reducing downstream precursors including mevalonate, which prevented ERK5 phosphorylation in the presence of statins when endogenous mevalonate was added back to cells. As mevalonate prevents ERK5 phosphorylation this means that either FPP or GGPP inhibition could be responsible for ERK5 phosphorylation. Addition of FPP did not induce any changes to the ERK5 phosphorylation, however, addition of GGPP removed the ERK5 phosphorylation. This suggests that the barrier is regulated by the GGPP

pathway not the FPP pathway. RAP1A is a small GTPase that in the absence of GGPP and FPP remains in an unprenylated conformation. This can be confirmed using an antibody specific to the unprenylated RAP1 conformation. Small GTPases are beginning to be linked to ERK5 and barrier regulation so could be a key part in statin induced ERK5 activation and barrier regulation (Zuo et al., 2015; English et al., 1999). It is known that the FPP pathway is responsible for cholesterol production. To further confirm that the FPP pathway is not involved in statin induced ERK5 activation, downstream molecules from FPP are endogenously added back to cells. These results showed that both squalene and cholesterol have no effect on ERK5 phosphorylation.

To definitively test that GGPP is responsible for ERK5 phosphorylation and barrier protection, an inhibitor to GGPP was added to cells. GGTI - 298 showed ERK5 phosphorylation at time points identical to simvastatin. This provided the conclusion that simvastatin inhibition of GGPP led to endothelial barrier stimulation, a potential preventative mechanism for cardiovascular toxicity (Chu et al., 2015). The GGPP pathway has been linked to pleiotropic effects of statins (Ito et al., 2006; Chen et al., 2013). This leaves the question could ERK5 be attributed to all pleiotropic effects of statins? The pleiotropic effects of statins include: endothelial protection, smooth muscle cell proliferation, reduced vascular inflammation, plaque stability and reduced vasoconstriction. It is known that ERK5 can regulate endothelial function (Roberts et al., 2010), and ERK5 can regulate the transcription factors thought to be involved in statins pleiotropic effects on endothelial cells (Chu et al., 2015). However, it has been demonstrated that ERK5 is less important in other cardiac cells such as myocytes and pericytes as these cells appeared to have a normal phenotype in knockout mice (Hayashi et al., 2004). These papers suggest that ERK5 could play a key role in statin induce pleiotropic effects in endothelial cells but is not likely to be involved in the pleiotropic effects observed in other cardiac cells.



## **Chapter 6**

### Anti-Cancer Drug Induced Barrier Perturbment





## 6.1 Introduction

Through the barrier, which is comprised of the plasma membrane and junctions, endothelial cells provide protection to underlying myocytes, fibroblasts and smooth muscle cells in the heart, by preventing drugs and toxins from gaining access to these cells (Birukova et al., 2012; Garcia et al., 2011; Gonzalez-Mariscal et al., 2005; Kevil et al., 1998; Niessen, 2007; Vandenbroucke et al., 2008; Wang and Alexander, 2011). Endothelial cells have three junctions: tight, adherens and gap junctions. Gap junctions are involved in cell-cell communication predominantly and to a lesser extent paracellular barrier function, tight and adherens junctions are primarily involved in paracellular barrier function. Transporters including: influx and efflux regulate transcellular movement utilising ion concentration gradients to transport ions, free fatty acids, drugs and toxins into and out of the cell (Birukova et al., 2012; Fazakas et al., 2011; Garcia et al., 2011; Gonzalez-Mariscal et al., 2005; Ishiguro et al., 2004; Kevil et al., 1998; Lazarowski et al., 2004; Niessen, 2007; Sharma et al., 2012; Sharma et al., 2013; Spudich et al., 2006; Vandenbroucke et al., 2008; Wang and Alexander, 2011).

The potential role of endothelial cells in drug-induced cardiovascular toxicity is becoming evident (Greineder et al., 2011; Chiusa et al., 2012; Duran et al., 2014; Mao et al., 2012). It has been demonstrated in Chapter 4 that anti-cancer drugs doxorubicin and Herceptin® led to endothelial barrier perturbment. Chapter 6 builds on these findings to investigate if barrier perturbment observed following doxorubicin treatment is specific to the anthracycline antibiotic class of drugs, or if other drugs known to induce cardiovascular toxicity also exert the same barrier perturbment. Anthracycline antibiotic doxorubicin was compared to protein kinase inhibitors (PKIs) sorafenib and sunitinib to determine if barrier perturbment occurred following treatment with different classes of anticancer drugs (Cheng and Force, 2010; Mego et al., 2007; Will et al.,

2008; Schmidinger et al., 2008). Lastly, I aimed to determine if barrier perturbment induced by anticancer drugs can be overcome with simvastatin treatment. It was observed in Chapter 5 that simvastatin stimulated the tight junction barrier. This provided a potential hypothesis to explain the cardio protection observed in the clinic following statin treatment (Liao, 2005).

## 6.2 Results

Within this section of work many of the experiments were conducted at the same time in order to minimise experimental variation in the immunofluorescence staining procedure. These experiments can be identified by having the same control images.

### 6.2.1 Drug screen

A range of anti-cancer drugs known to induce cardiovascular toxicity were screened to determine their effects on the endothelial cell barrier. This screen specifically focused on tight junctions as they play a key role in the regulation of paracellular permeability (Bazzoni and Dejana, 2004). The drugs screened included: anthracycline antibiotics doxorubicin and epirubicin, to ensure the barrier perturbment observed with doxorubicin (Chapter 4) occur in other members of this drug class, the PKIs: lapatinib, sorafenib, imatinib, nilotinib and sunitinib; this range included drugs that inhibit multiple RTKs. For each drug, four concentrations were used that ranged from plasma C<sub>max</sub> (data from pharmapendium) to 10-fold below to compare dose-dependent changes in the endothelial barrier. Presence of the cell barrier was assessed using immunofluorescence for ZO-1. Figure 6.1 details the results from a single concentration of drug in HCMEC to outline that all the drugs have disruptive effects on the endothelial barrier 6 hours after drug administration.

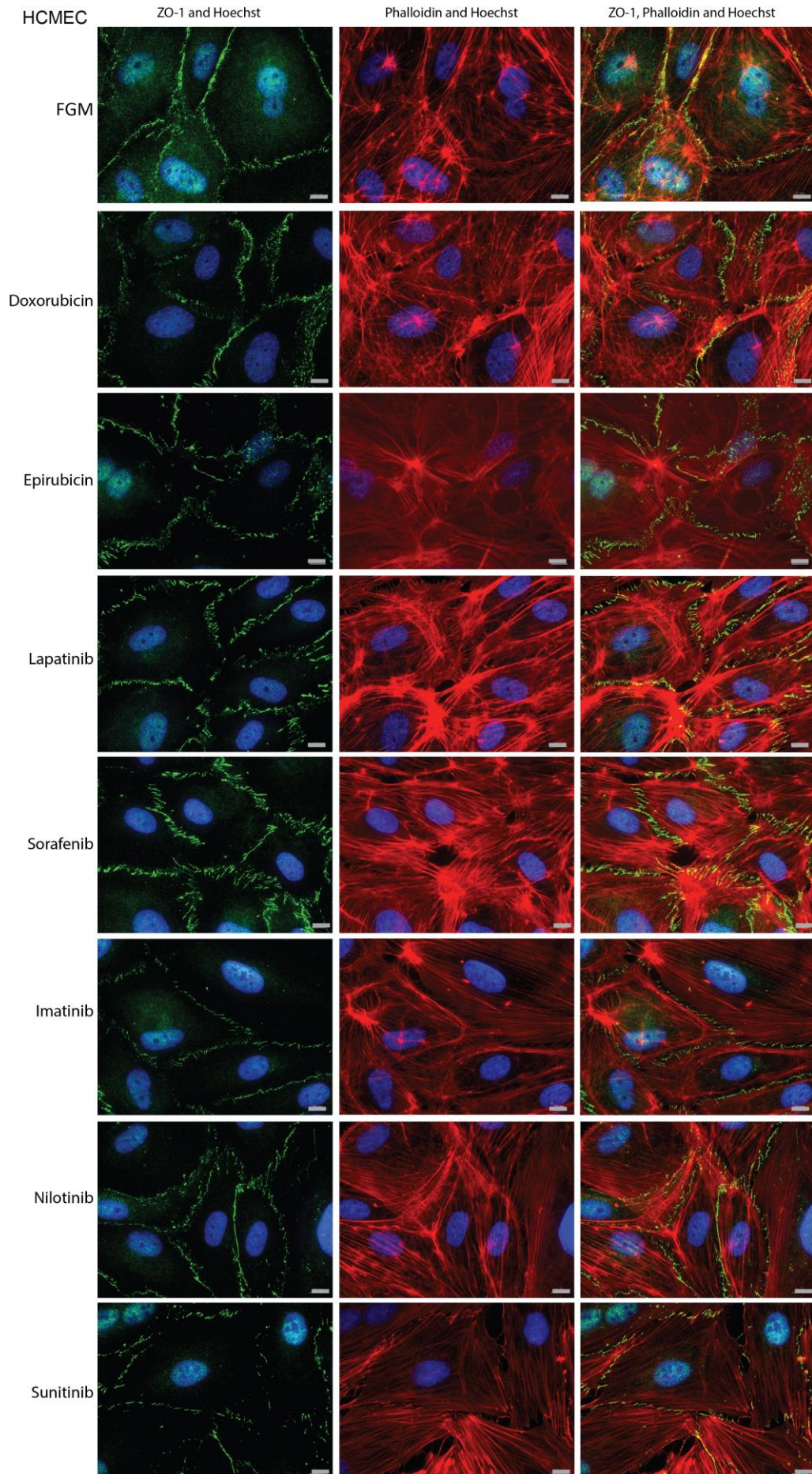
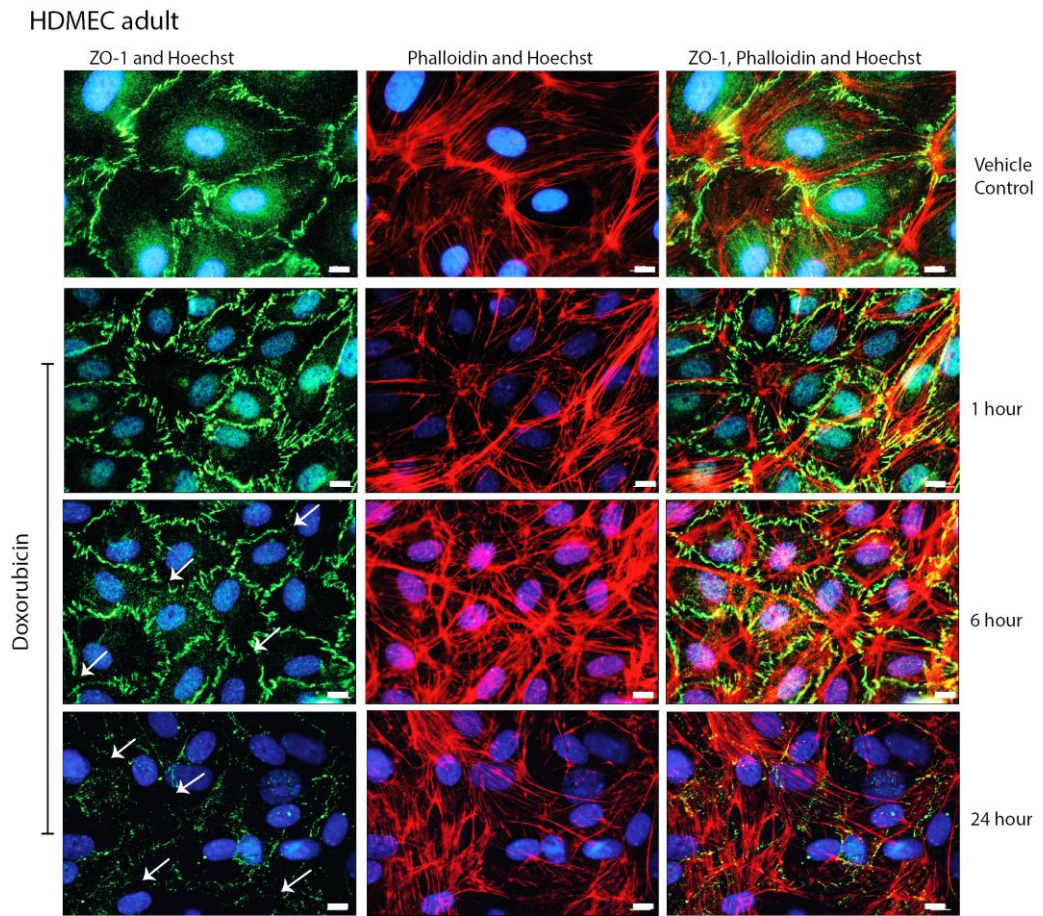


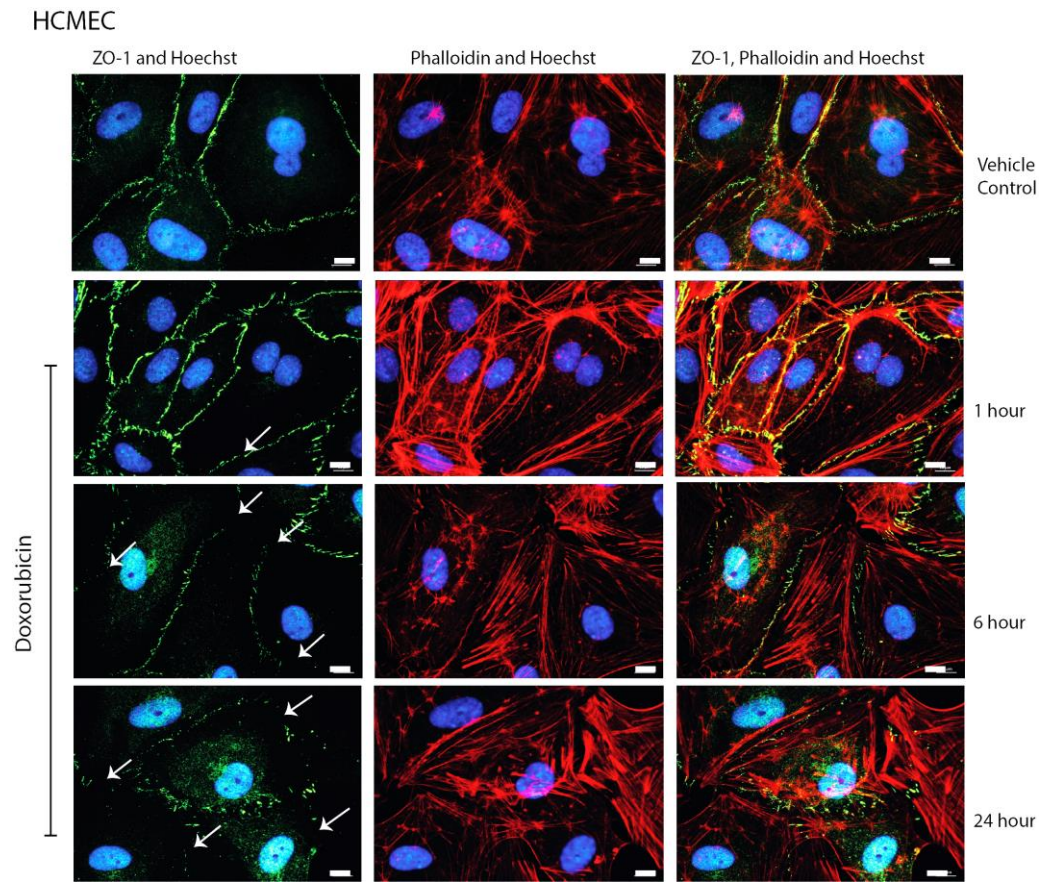
Figure 6.1. **Drug screen to determine which drugs induce barrier perturbment.** HCMEC were treated with doxorubicin 0.1  $\mu\text{M}$ , epirubicin 0.1  $\mu\text{M}$ , lapatinib 3  $\mu\text{M}$ , sorafenib 1  $\mu\text{M}$ , imatinib 1  $\mu\text{M}$ , nilotinib 1  $\mu\text{M}$  or sunitinib 1  $\mu\text{M}$  for 6 hours. Cells were stained with ZO-1 (tight junctions, green), phalloidin (actin fibers, red) and Hoechst (nuclei, blue). Scale bar represents 10  $\mu\text{m}$ .

Preliminary studies had shown that doxorubicin, sorafenib and sunitinib led to the greatest visible disruption across the range of concentrations tested (partial data shown in Fig. 6.1). These drugs had been screened on a panel of different endothelial cells: (i) HCMEC from 3 different patients, to rule out effects specific to an individual patient (lot 9090701.2, 1122702, 3011401); (ii) HDMEC juvenile (lot 6060707.1); (iii) HDMEC adult (lot 0092101.2) and (iiii) RCEC (full data not shown). Because I found no obvious differences between the HCMECs from the 3 patients, HCMEC (lot 3011401) were used for all further experiments. In order to compare vascular beds an endothelial cell line from an alternate anatomical location was required. In order to ensure these can be compared to HCMEC, which were isolated from an adult patient, HDMEC also isolated from an adult patient were used to minimise age as a factor for differences. Additionally, this study investigated the physiological relevance of rat cell models so RCEC cells were used to compare cardiac cells from human and rat to determine if the effects observed in rat can be extrapolated to humans.

Therefore, following the screening of the panel of drugs for those causing the most obvious barrier disruption, doxorubicin, sorafenib and sunitinib were carried forward for further analysis.









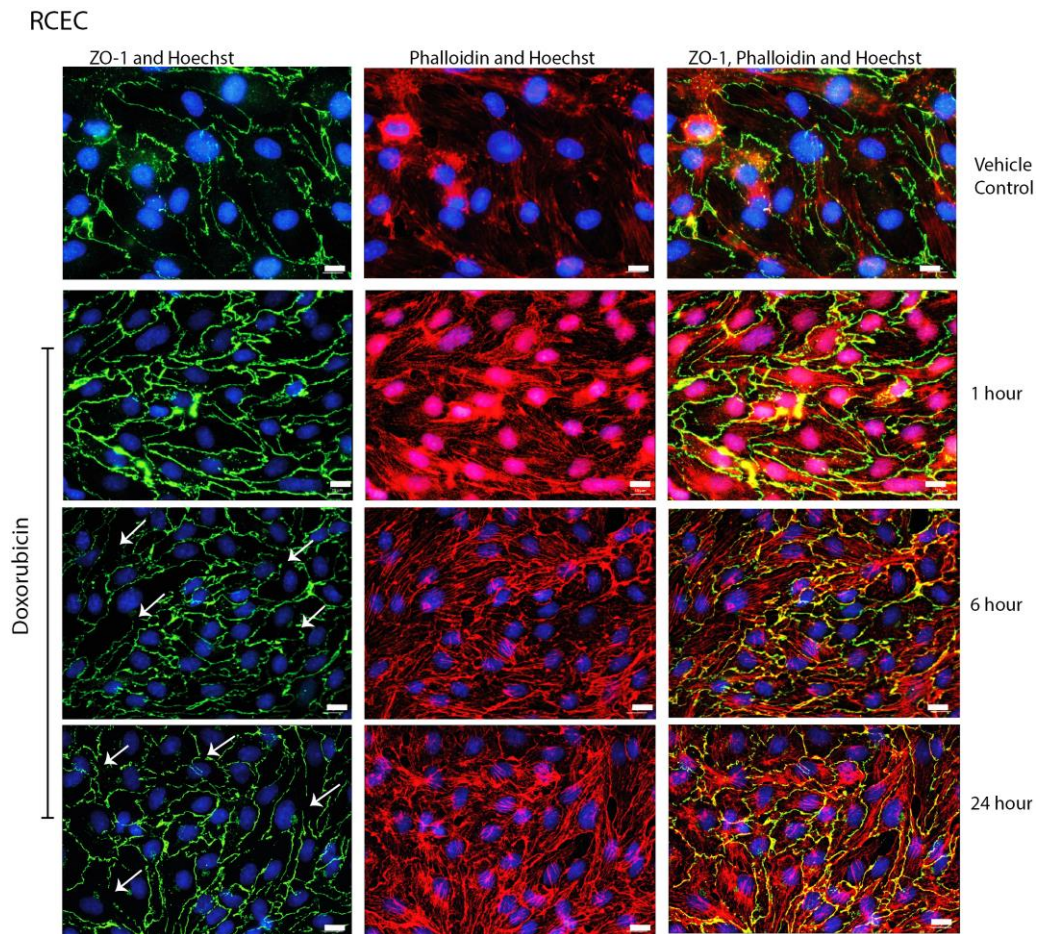
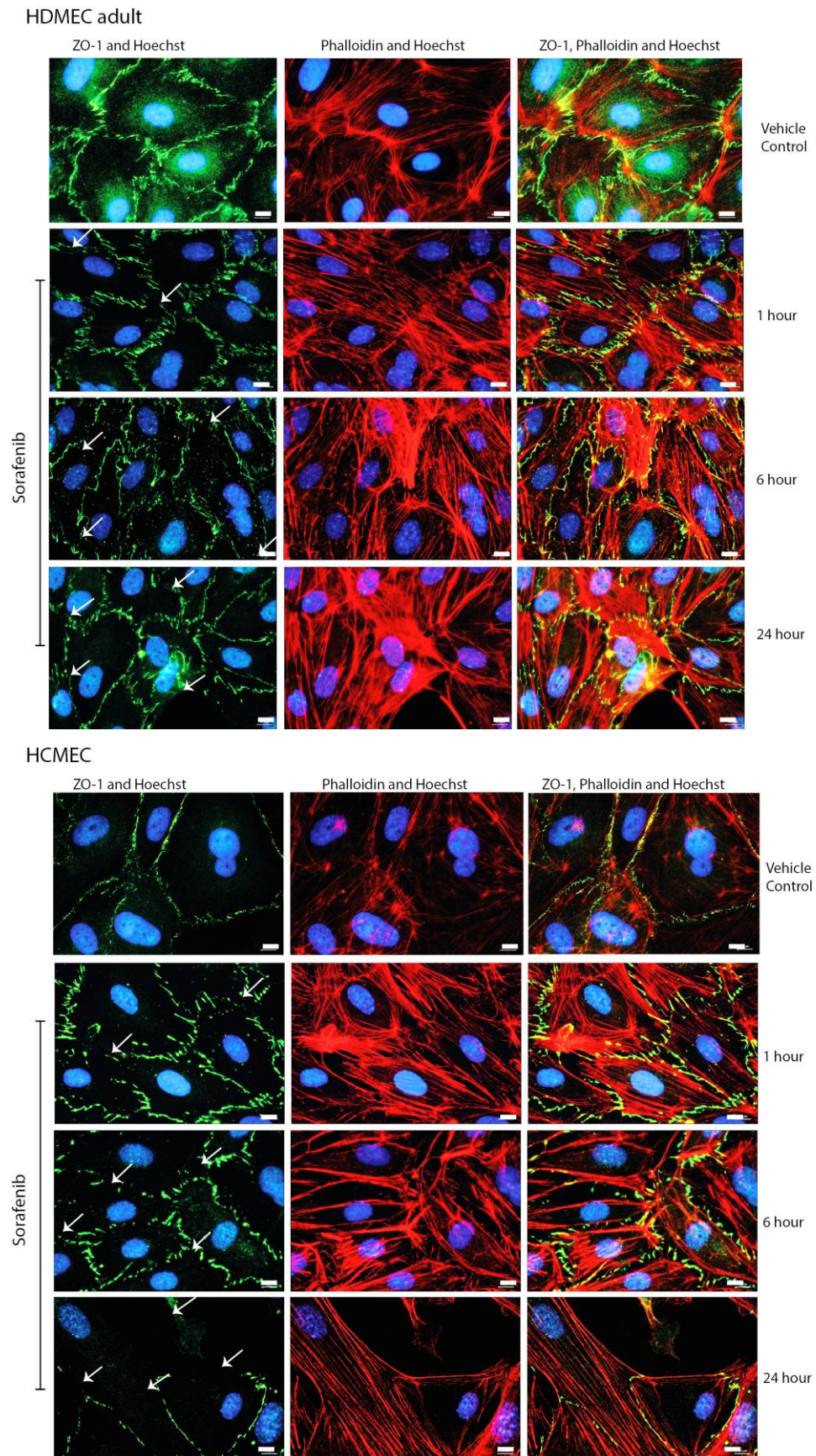


Figure 6.2. **Immunofluorescence staining of cells following doxorubicin treatment over time.** (A) HDMEC adult, (B) HCMEC and (C) RCEC were treated with doxorubicin 0.1  $\mu$ M for 1, 6 or 24 hours. Cells were stained with ZO-1 (tight junctions, green), phalloidin (actin fibers, red) and Hoechst (nuclei, blue). Arrows indicate barrier disruption, scale bar represents 10  $\mu$ m.







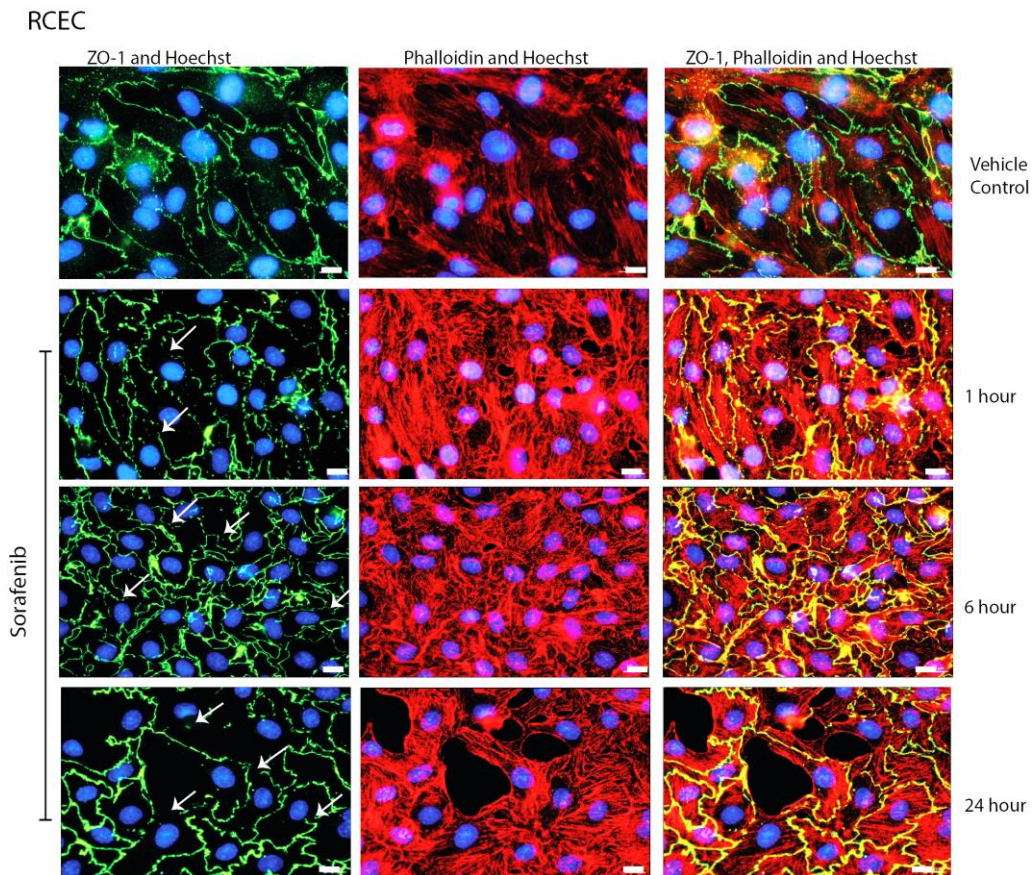
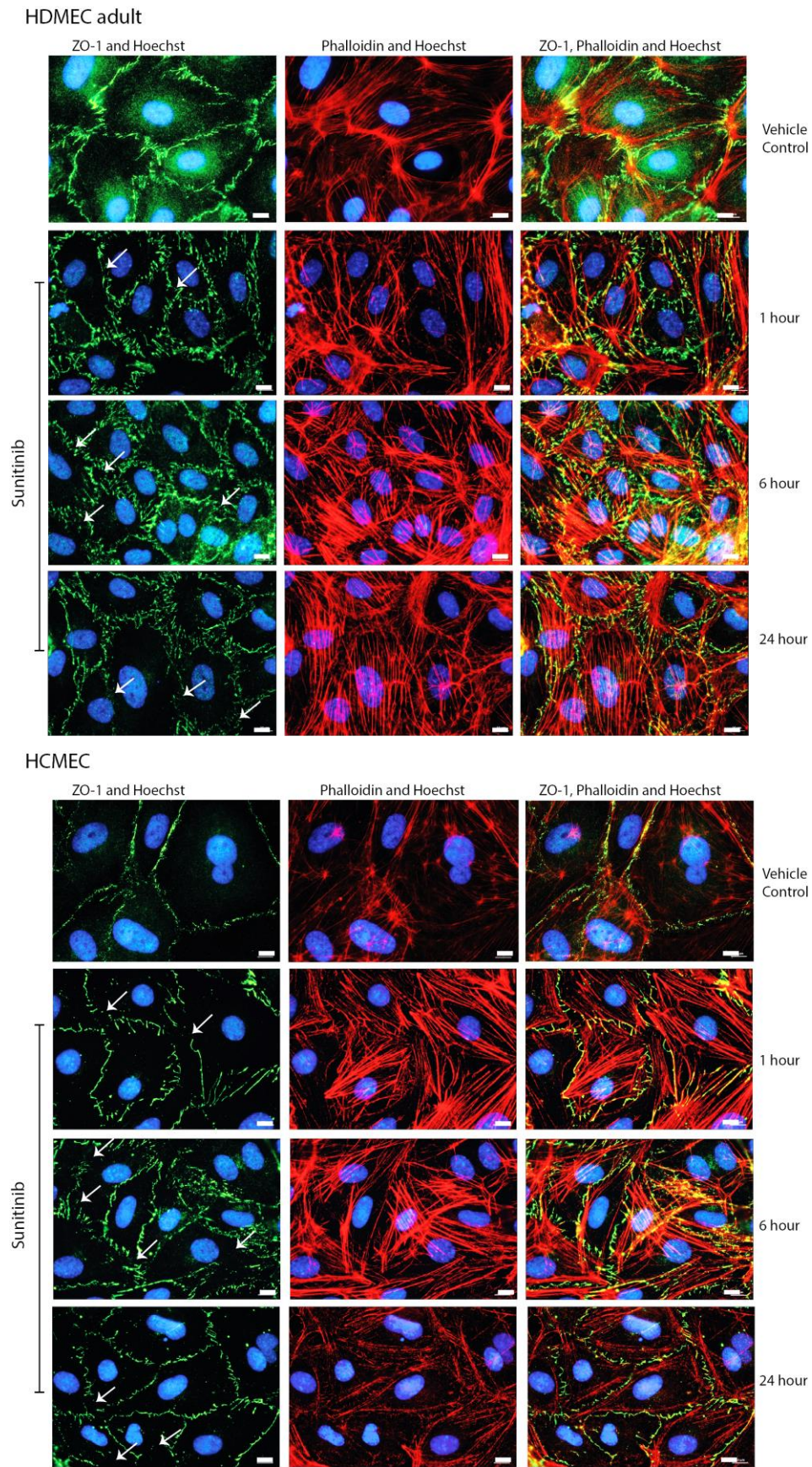


Figure 6.3. **Immunofluorescence staining of cells following sorafenib treatment over time.** (A) HDMEC adult, (B) HCMEC and (C) RCEC were treated with sorafenib 1  $\mu$ M for 1, 6 or 24 hours. Cells were stained with ZO-1 (tight junctions, green), phalloidin (actin fibers, red) and Hoechst (nuclei, blue). Arrows indicate barrier disruption, scale bar represents 10  $\mu$ m.







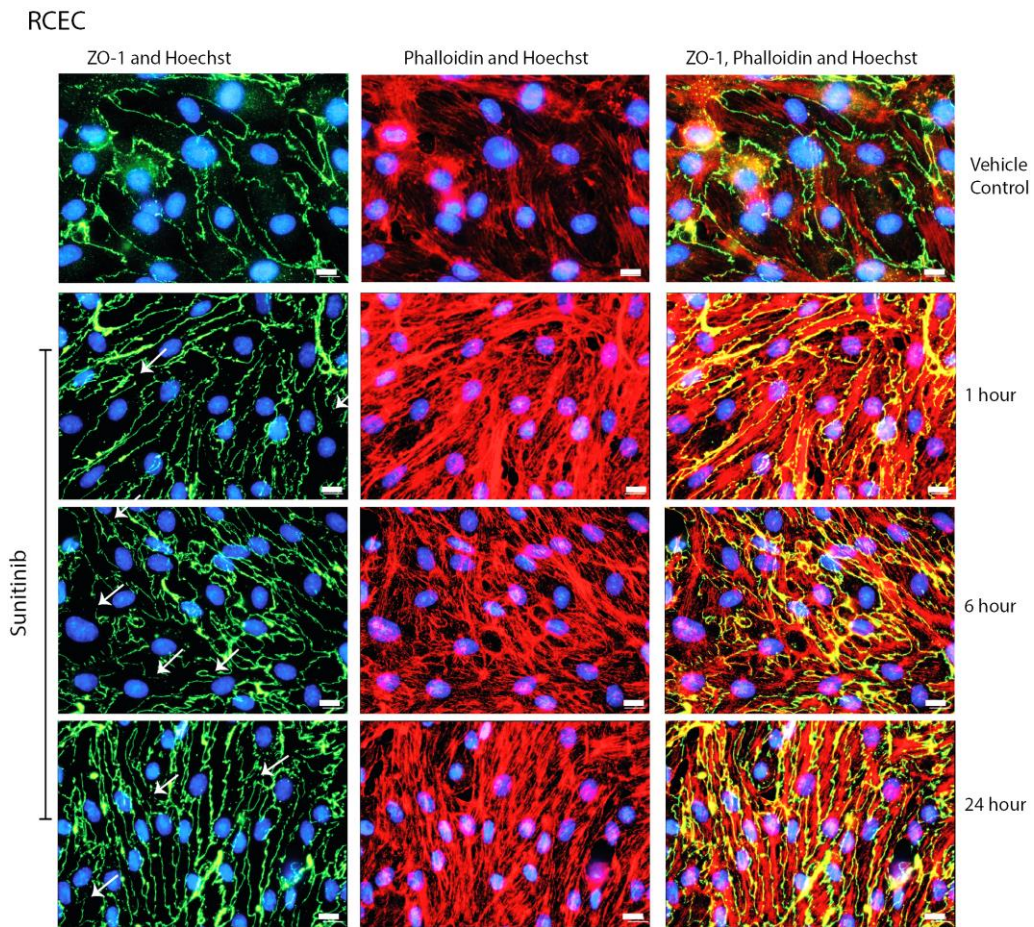


Figure 6.4. **Immunofluorescence staining of cells following sunitinib treatment over time.** (A) HDMEC adult, (B) HCMEC and (C) RCEC were treated with sunitinib 1  $\mu\text{M}$  for 1, 6 or 24 hours. Cells were stained with ZO-1 (tight junctions, green), phalloidin (actin fibers, red) and Hoechst (nuclei, blue). Arrows indicate barrier disruption, scale bar represents 10  $\mu\text{m}$ .

The results outlined in figures 6.2, 6.3 and 6.4 showed that doxorubicin, sorafenib and sunitinib, respectively, induced barrier perturbment in a time-dependent manner. At the 1-hour time point, disruption to the tight junction barrier began to appear, this disruption increased at 6 hours and further at 24 hours, showing that drug-induced barrier perturbment increased over time.

Following confirmation that the anti-cancer drugs induce barrier perturbment the physiological implications on endothelial cell permeability were investigated. A fluorescence dextran barrier function assay was

used to determine the permeability across an endothelial monolayer grown on inserts containing 0.4  $\mu\text{m}$  pores. The cells were grown to confluence before addition of drugs to allow for the effect on the barrier to be investigated. This assay utilises fluorescent dextran to measure the paracellular flux across the endothelial cells. The results are shown in figure 6.5.

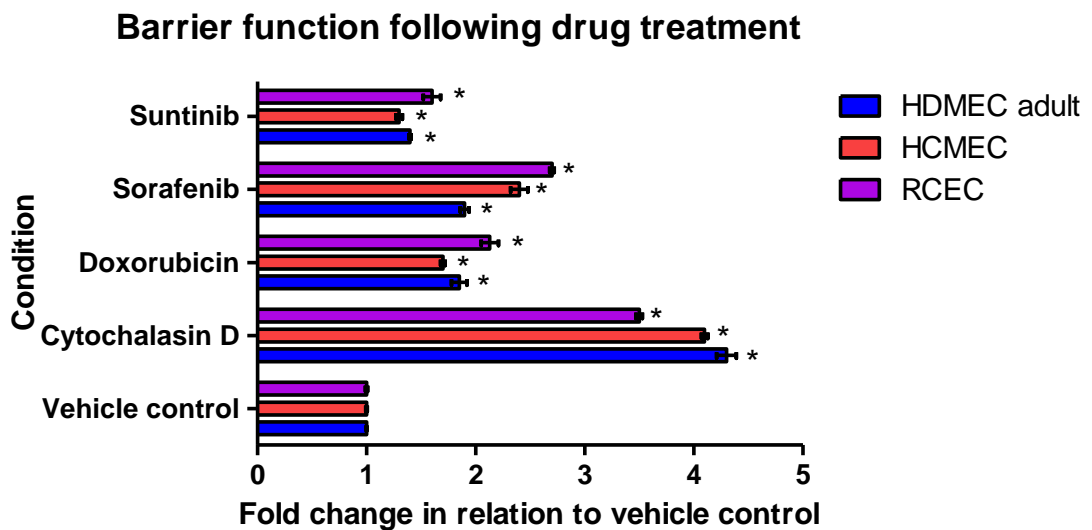


Figure 6.5. **Barrier function assessment of HDMEC adult, HCMEC and RCEC following drug treatment for 6 hours.** HDMEC adult, HCMEC and RCEC were treated with doxorubicin 0.1  $\mu\text{M}$ , sorafenib 1  $\mu\text{M}$  or sunitinib 1  $\mu\text{M}$  for 6 hours prior to addition of 4 kDa FITC dextran the flow through was measured on a fluorescence plate reader. N=4 separate inserts  $\pm$  SD, \* =  $P \leq 0.05$ , one-way ANOVA, SPSS, data plotted in GraphPad prism.

The fluorescence increase following drug treatment confirmed that the barrier perturbment observed by immunofluorescence significantly impacted barrier function. As significantly more drug was able to pass between endothelial cells this implied that *in vivo* when multiple cell types are present within the tissue the underlying myocytes are exposed to higher concentrations of drugs. As it is predicted that cardiotoxicity results from an effect on cardio myocytes, this could be a potential mechanism for induction of cardiovascular toxicity. Current theories for cardiovascular toxicity revolve around cardiomyocytes, involving changes

in contraction and cell death. These theories do not investigate how the drug is able to gain access to the cardiomyocytes to induce the toxicity. The work in this chapter has shown that the anti-cancer drugs doxorubicin, sorafenib and sunitinib induce barrier perturbment allowing the drug access to the underlying cardiomyocytes.

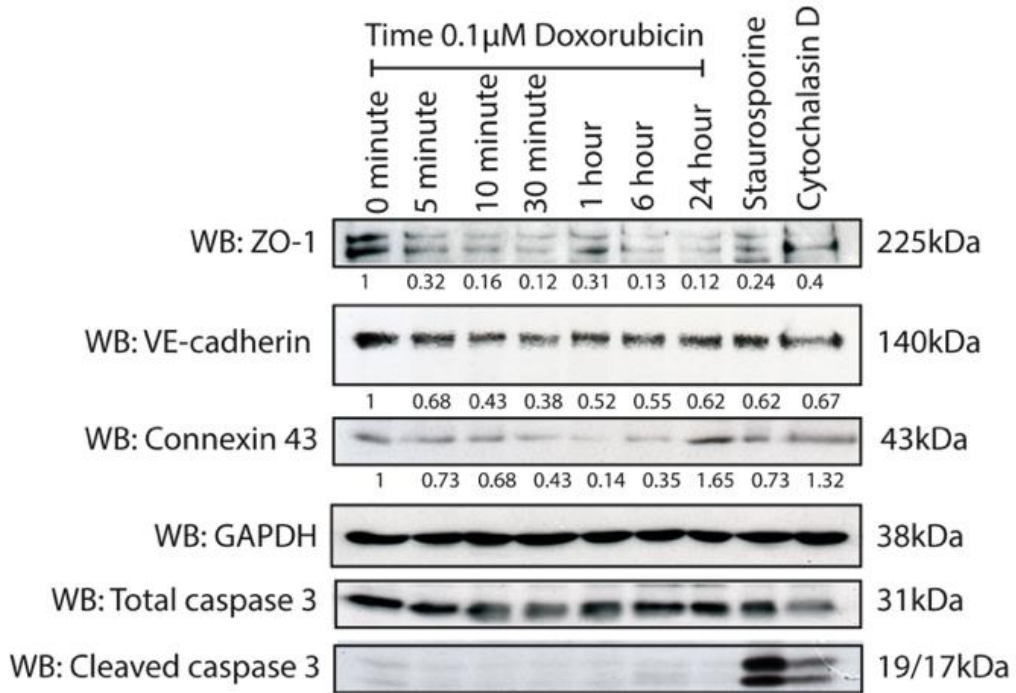
In order to gain a better understanding of the barrier perturbment induced by the drugs western blotting was used to determine the effect on other endothelial junctions and determine if the effect is tight junction specific or if perturbment is induced across the range of junctions.

### 6.2.2 Protein expression changes in junctions following drug treatment

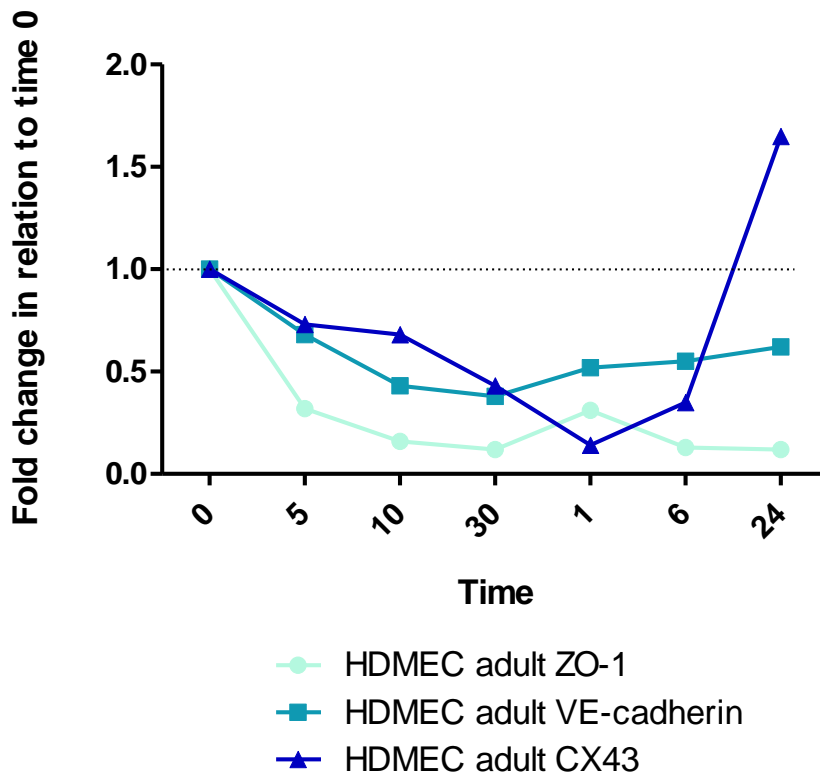
The endothelial barrier perturbment observed following drug treatment was further analysed at the protein level to determine over a greater time frame when the onset of barrier perturbment occurs and if this was specific to tight junctions or could be observed across the adherens and gap junctions expressed by endothelial cells. Additionally the levels of caspase 3 were analysed to rule out the possibility that barrier perturbment was an effect resulting from apoptosis, and that barrier perturbment precedes apoptosis.

The protein levels following doxorubicin, sorafenib and sunitinib treatment were also investigated to determine if the two drugs have the same effects at the protein level. Results are shown in figures 6.6, 6.7 and 6.8, respectively.

HDMEC adult

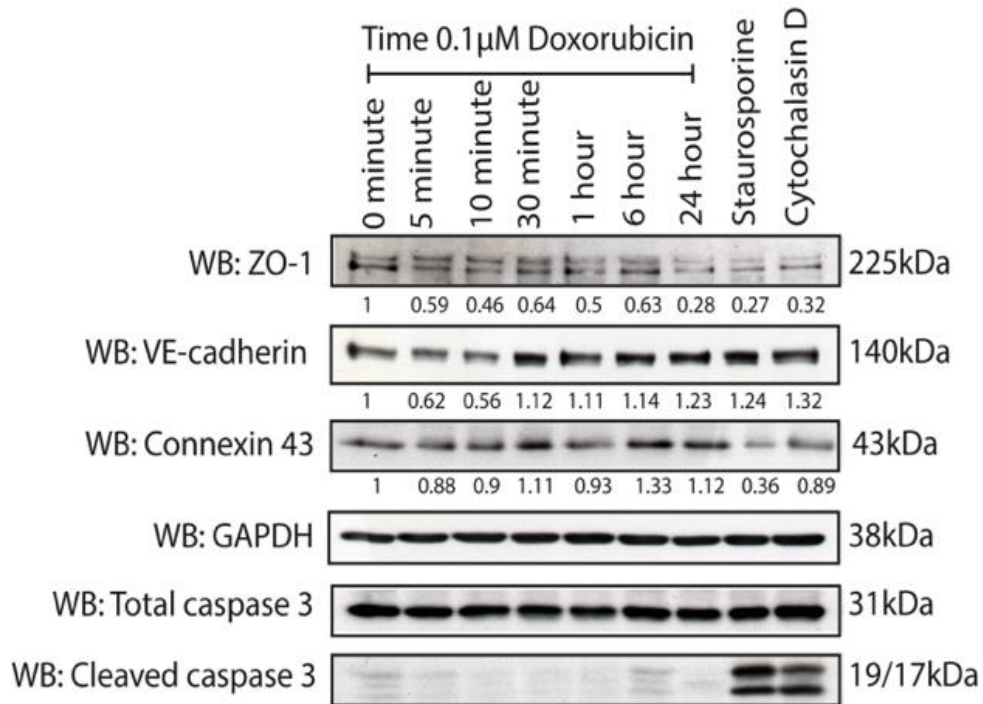


### Quantification of protein expression following doxorubicin treatment

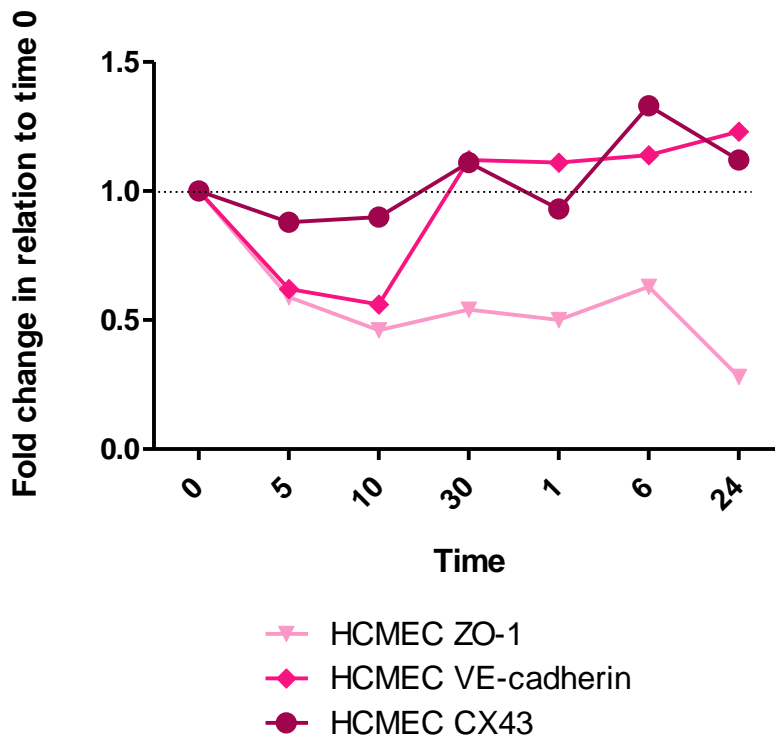




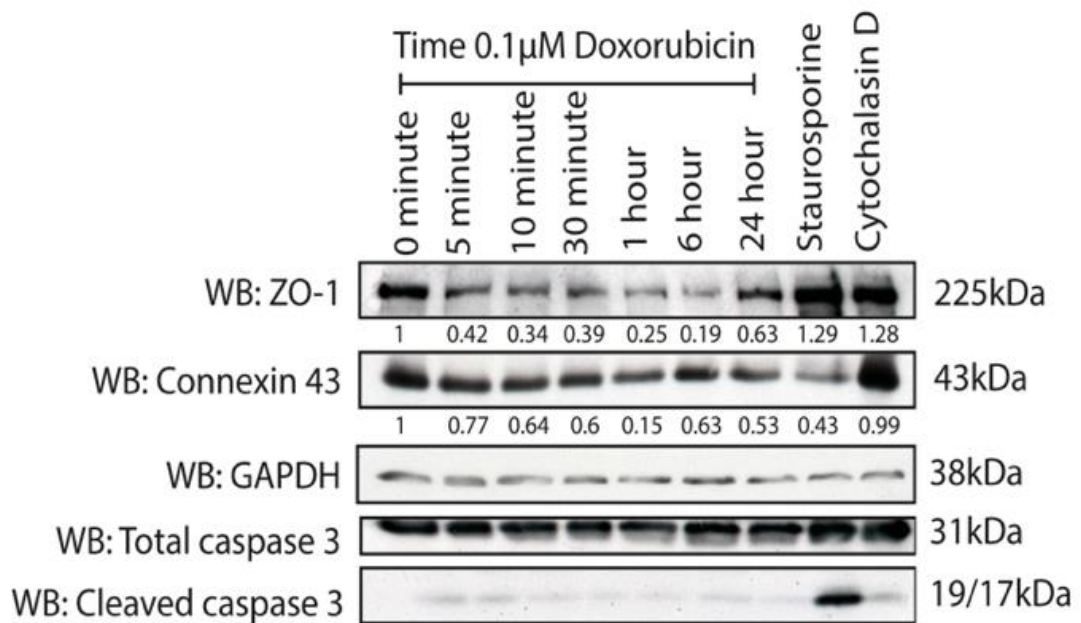
HCMEC



**Quantification of protein expression following doxorubicin treatment**



RCEC



### Quantification of protein expression following doxorubicin treatment

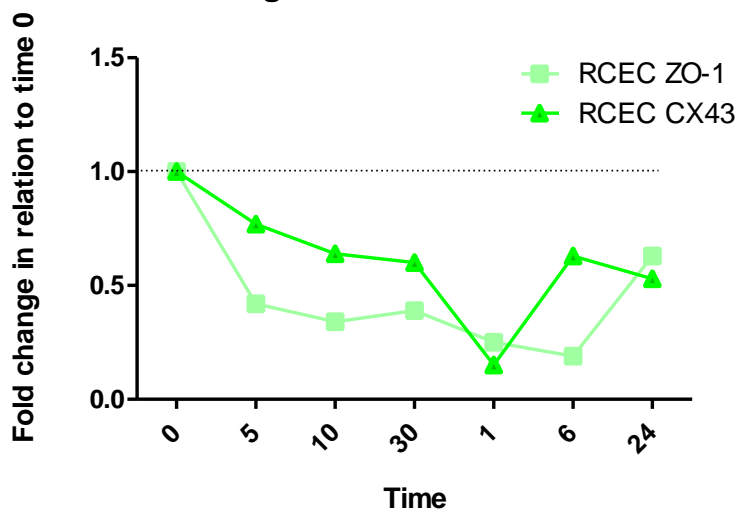
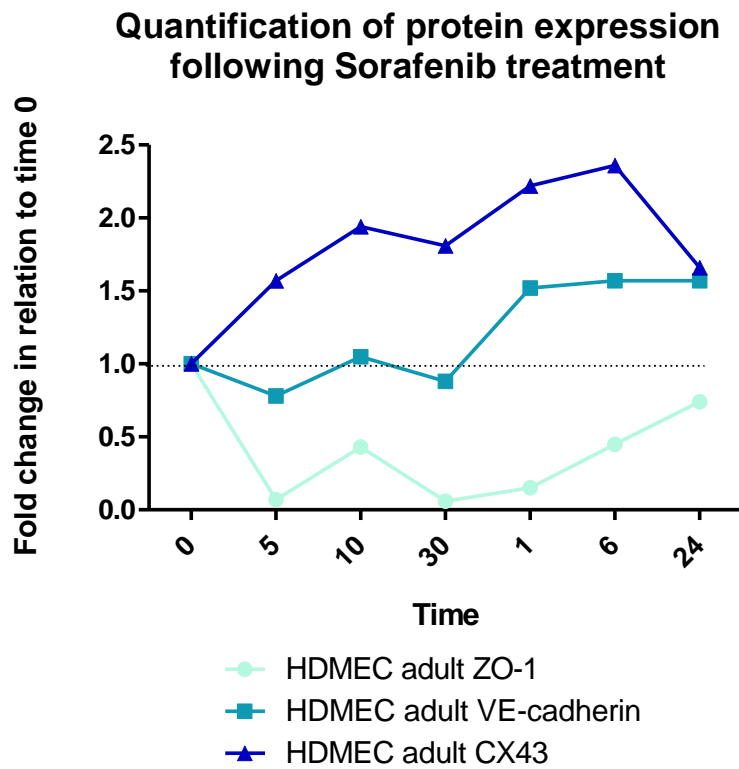
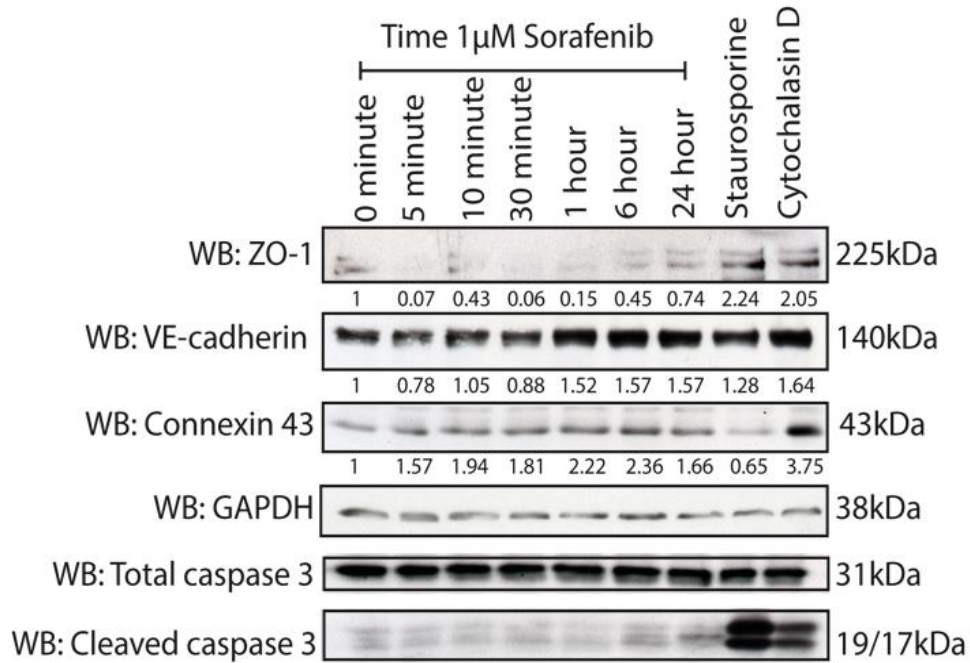
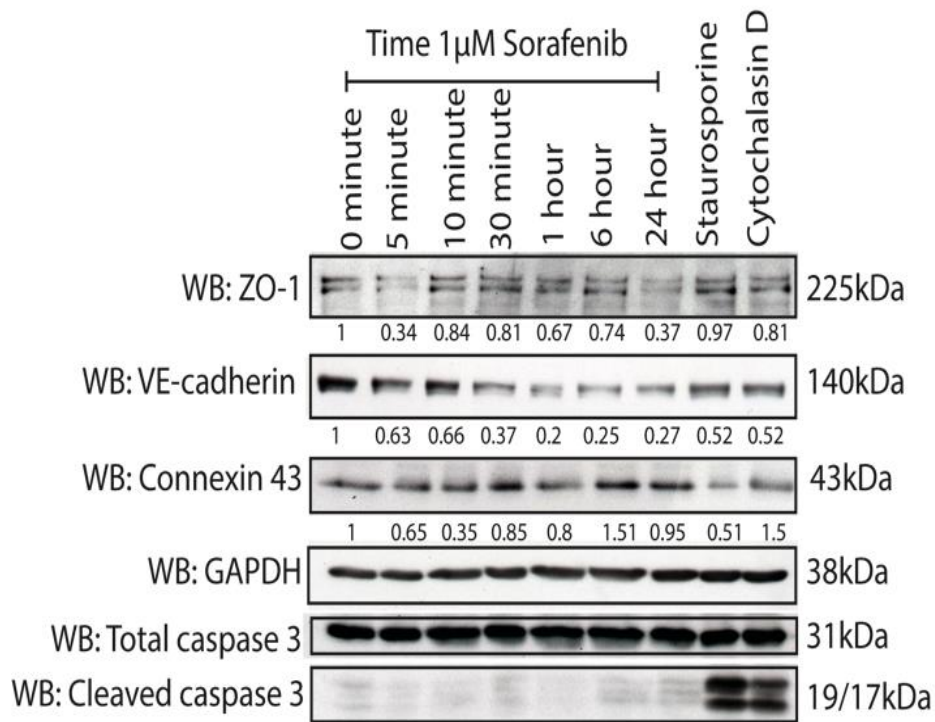


Figure 6.6. **Protein analysis of tight, adherens and gap junctions following doxorubicin treatment.** (A) HDMEC adult, (B) HCMEC and (C) RCEC were treated with doxorubicin 0.1  $\mu$ M over a time course ranging from 0 minutes – 24 hours. Blots were probed for: ZO-1, VE-cadherin, connexin 43, caspase 3, GAPDH was used as a loading control. Quantification was done using image J with band intensity represented as fold change relative to time 0, which was arbitrary expressed as 1.00, quantification was plotted in GraphPad Prism.

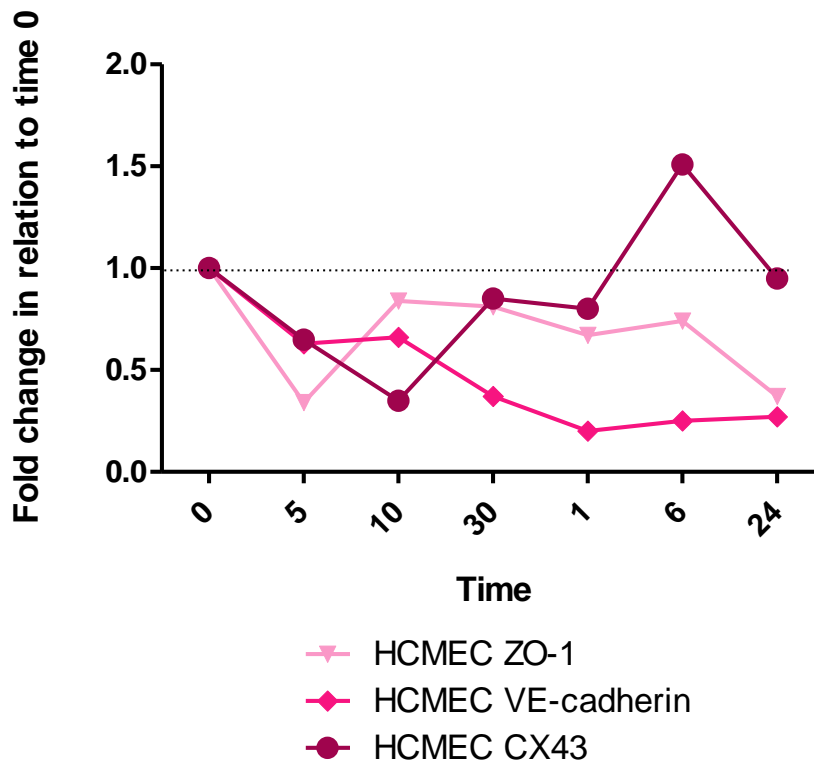
HDMEC adult



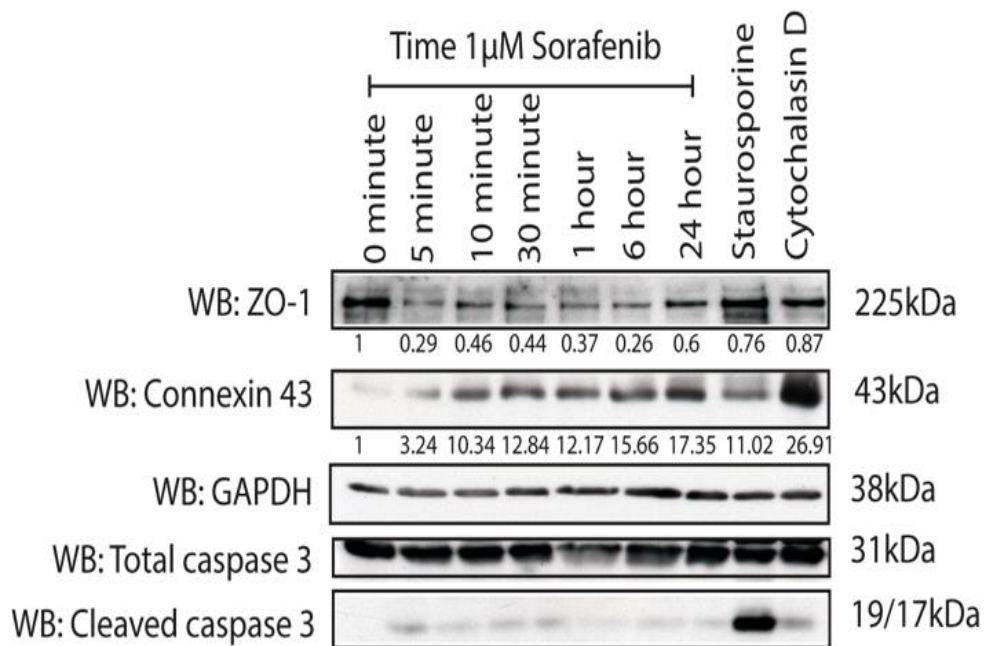
HCMEC



### Quantification of protein expression following Sorafenib treatment



RCEC



### Quantification of protein expression following Sorafenib treatment

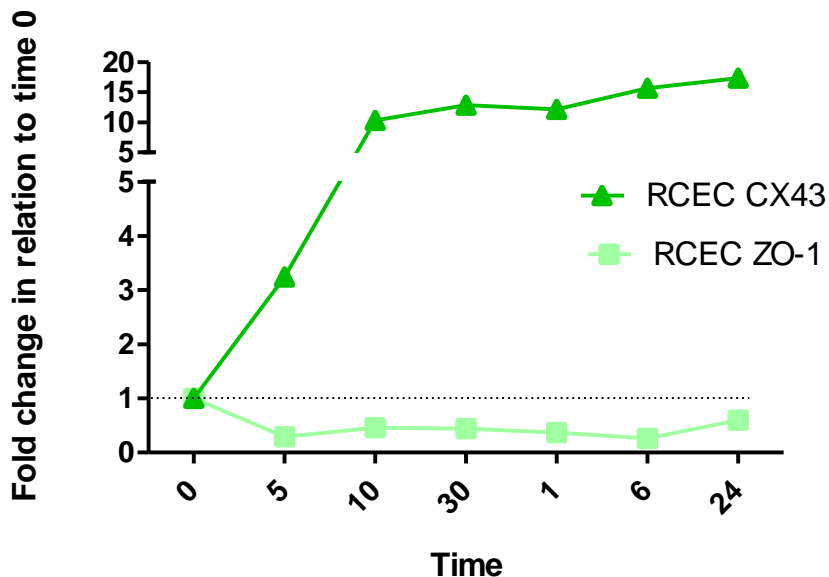
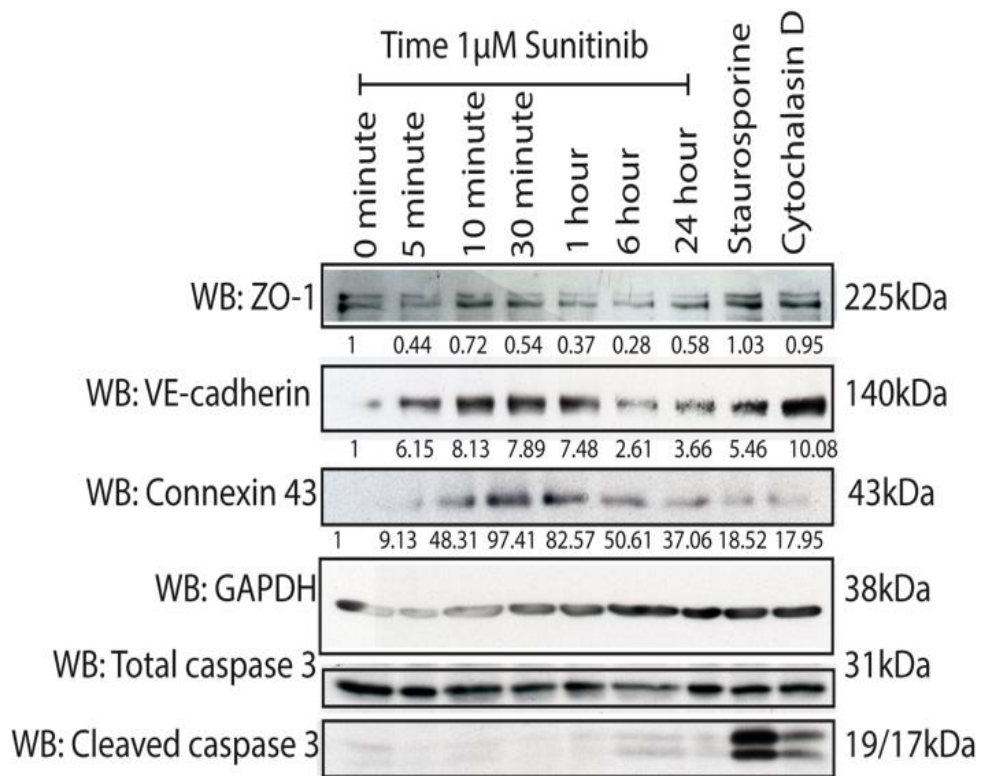
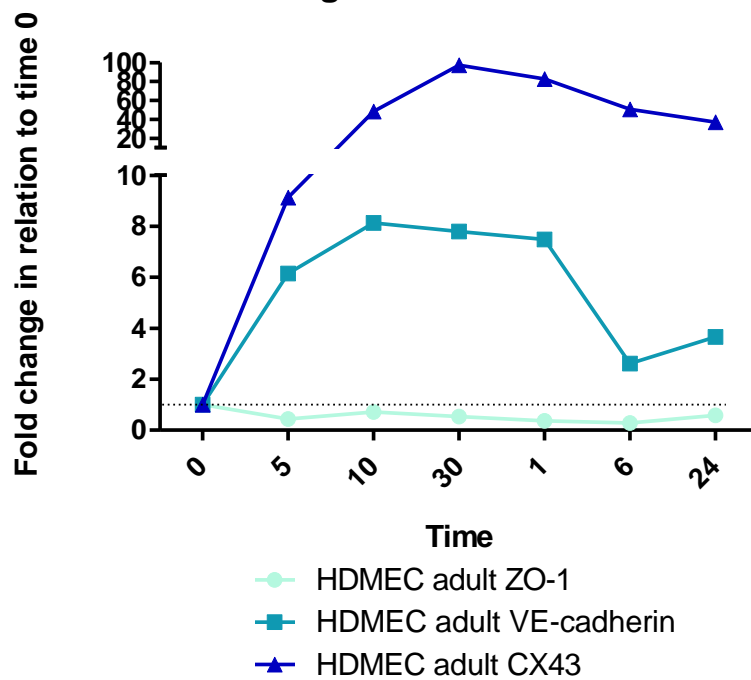


Figure 6.7. **Protein analysis of tight, adherens and gap junctions following sorafenib treatment.** (A) HDMEC adult, (B) HCMEC and (C) RCEC were treated with sorafenib 1  $\mu$ M over a time course ranging from 0 minutes – 24 hours. Blots were probed for: ZO-1, VE-cadherin, connexin 43, caspase 3, GAPDH was used as a loading control. Quantification was done using image J with band intensity represented as fold change relative to time 0, which was arbitrary expressed as 1.00, quantification was plotted in GraphPad Prism.

HDMEC adult

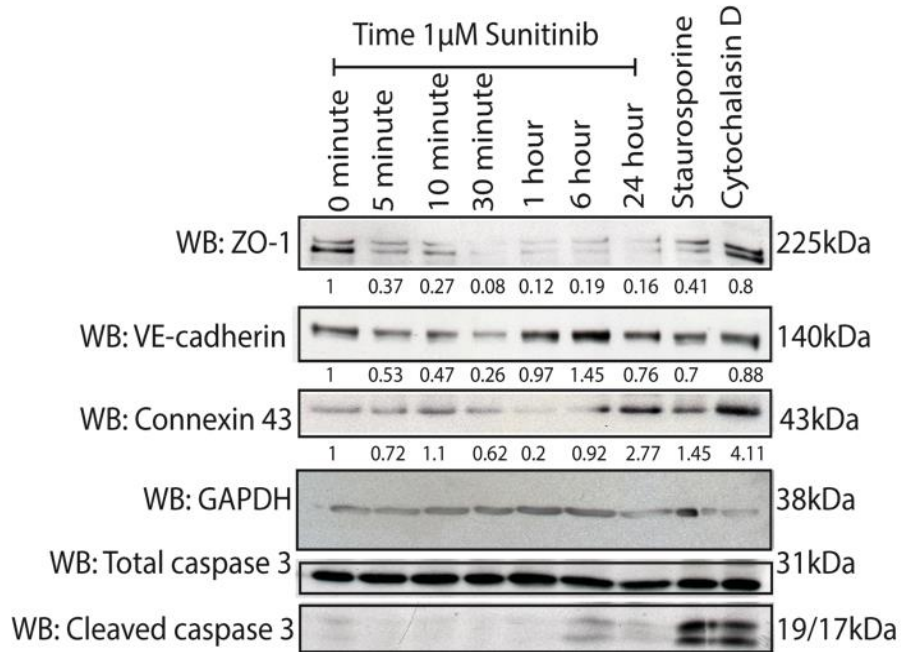


Quantification of protein expression following Sunitinib treatment

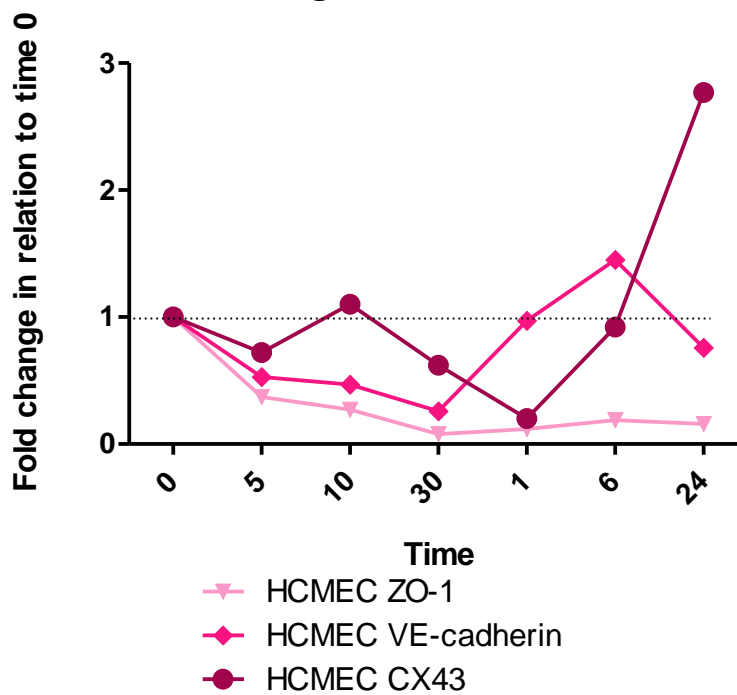




HCMEC



Quantification of protein expression following Sunitinib treatment



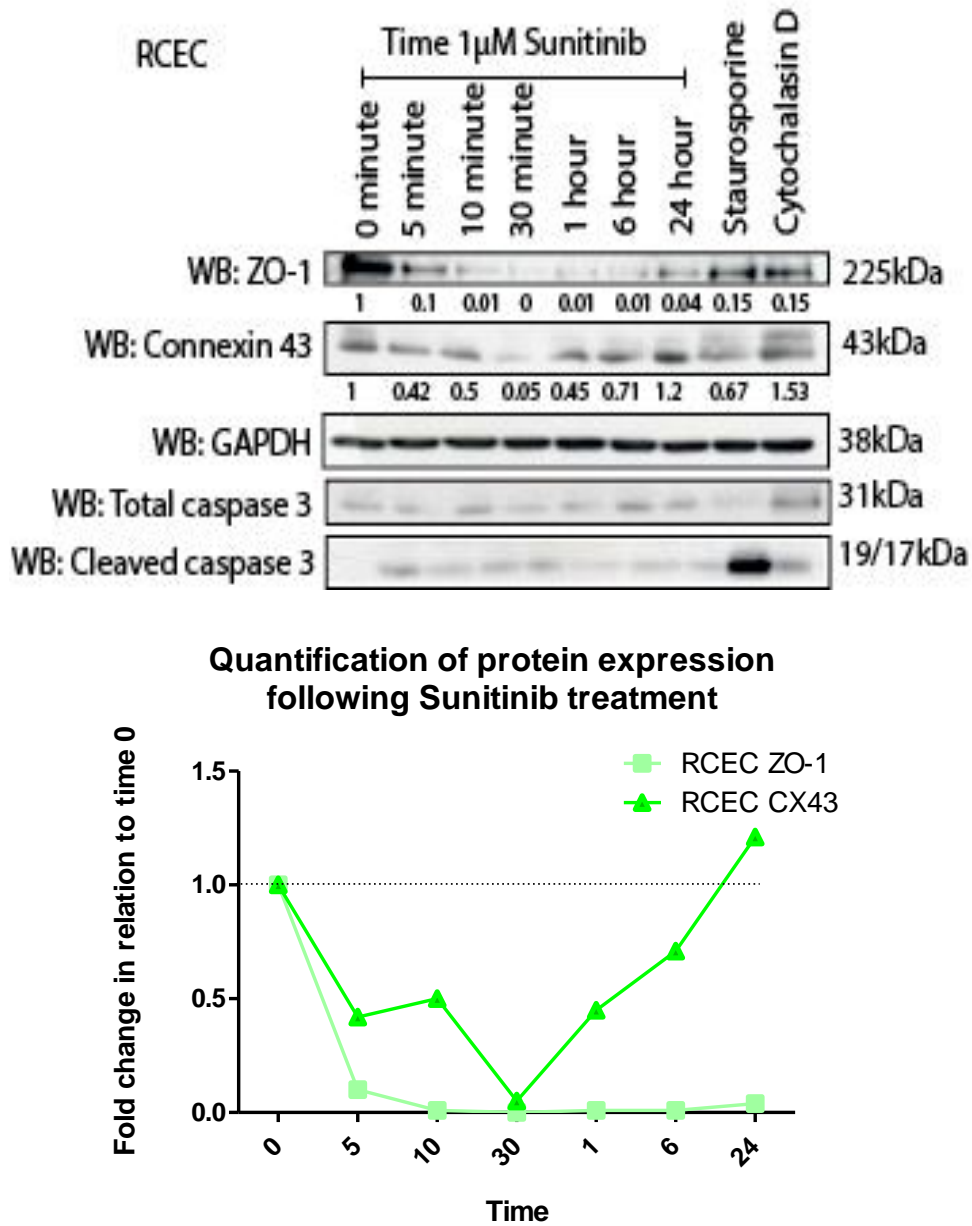


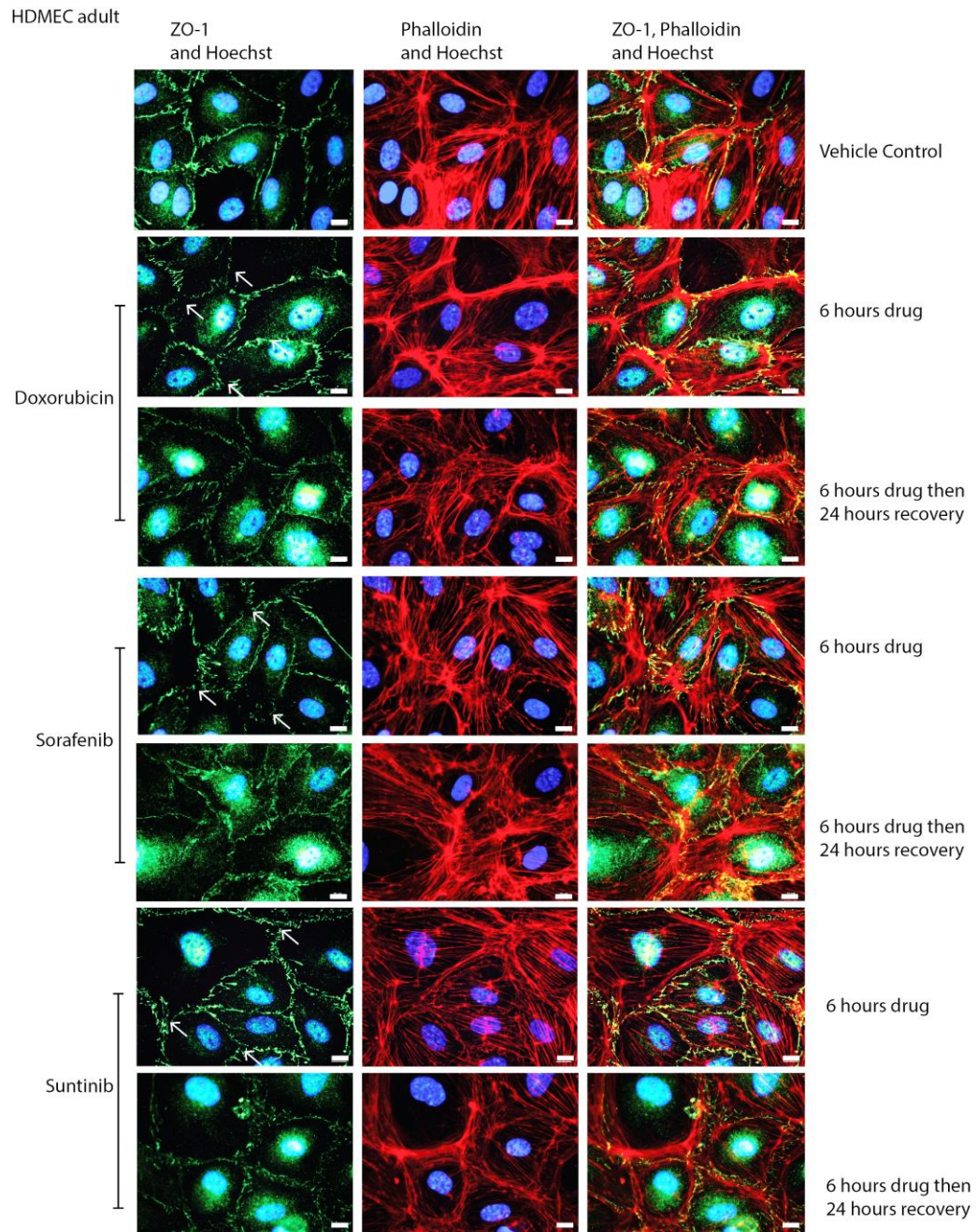
Figure 6.8. **Protein analysis of tight, adherens and gap junctions following sunitinib treatment.** (A) HDMEC adult, (B) HCMEC and (C) RCEC were treated with sunitinib 1  $\mu$ M over a time course ranging from 0 minutes – 24 hours. Blots were probed for: ZO-1, VE-cadherin, connexin 43, caspase 3, GAPDH was used as a loading control. Quantification was done using image J with band intensity represented as fold change relative to time 0, which was arbitrary expressed as 1.00, quantification was plotted in GraphPad Prism.

Tight junction protein ZO-1 decreased at the protein level following drug treatment with doxorubicin, sorafenib and sunitinib in HDMEC adult, HCMEC and RCEC, matching previous immunofluorescence data. By contrast, adherens junction protein VE-cadherin and gap junction protein CX43 both decreased only following sorafenib and sunitinib treatment in HCMEC. Overall these results indicate that disruption to the endothelial cell barrier was not specific to tight junctions but occurred across the range of junctions expressed by the endothelial cells.

Following treatment with doxorubicin, sorafenib and sunitinib, it was observed that there was low if any activation of cleaved caspase 3. Caspase 3 becomes cleaved following induction of apoptosis, and can be used as a marker to determine if cells are undergoing apoptosis (Grethe et al., 2006). This provided evidence that doxorubicin, sorafenib and sunitinib are not inducing apoptosis, suggesting barrier perturbment is not a consequence of apoptosis (Fig. 6.6 – 6.8).

### 6.2.3 Barrier recovery following anti-cancer drug treatment

Doxorubicin, sorafenib and sunitinib led to endothelial barrier perturbment. The next step investigated if the effect was reversible. This was studied by adding anti-cancer drugs to cells for 6 hours before washing and addition of endothelial MV2 FGM for 24 hours. Figure 6.9 provides evidence that the perturbment was reversible and that there was remodelling of the actin cytoskeleton upon barrier recovery.





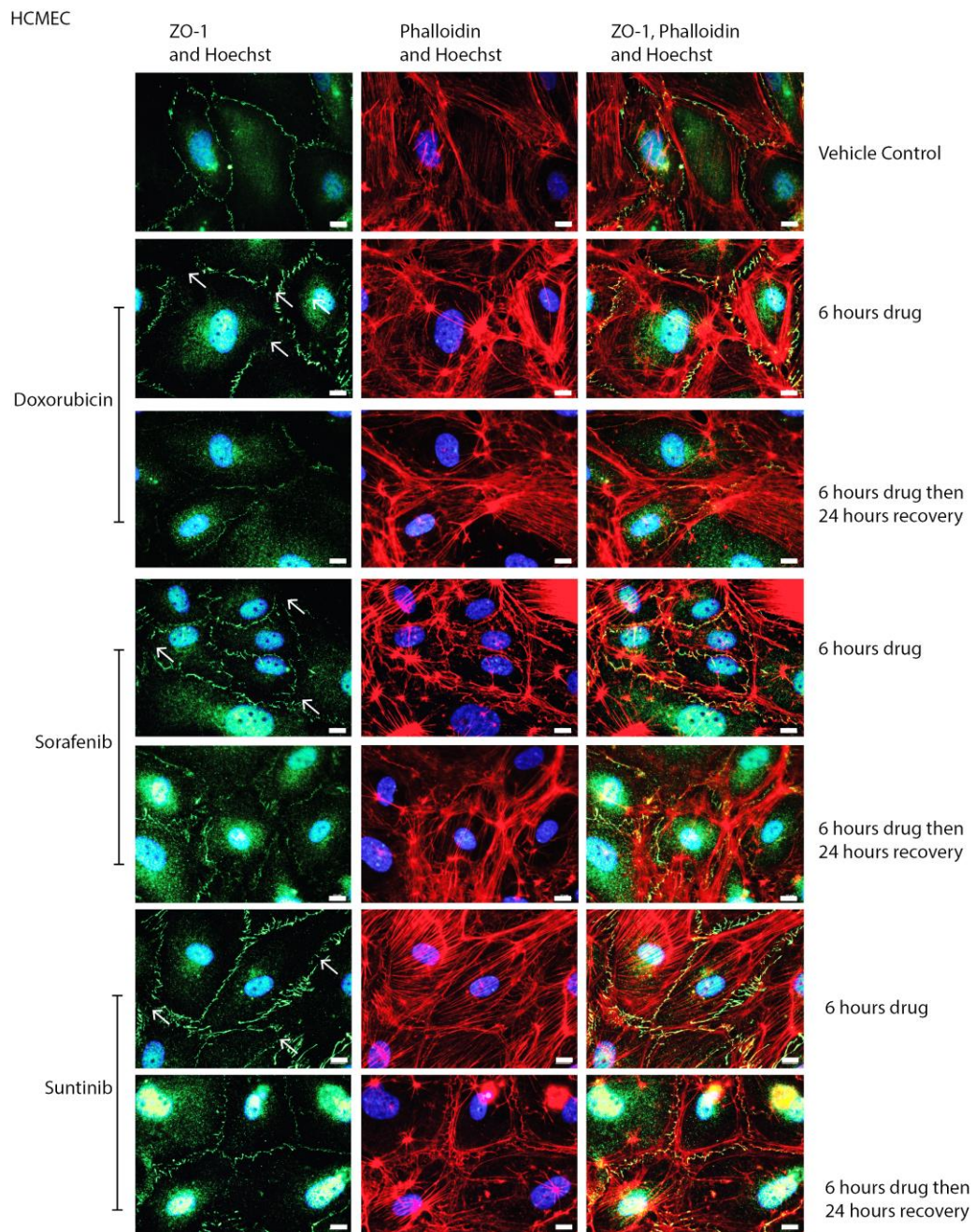


Figure 6.9. **Immunofluorescence analysis of the potential for barrier recovery.** (A) HDMEC adult and (B) HCMEC were treated with doxorubicin 0.1  $\mu\text{M}$ , sorafenib 1  $\mu\text{M}$  or sunitinib 1  $\mu\text{M}$  for 6 hours. Following this one set of cells was fixed and the other set were washed and had endothelial MV2 FGM added for a further 24 hours. Cells were stained with ZO-1 (tight junctions, green), phalloidin (actin fibers, red) and Hoechst (nuclei, blue). Arrows indicate barrier disruption, scale bar represents 10  $\mu\text{m}$ .

6.2.5 Simvastatin protects against drug-induced barrier perturbment in endothelial cells

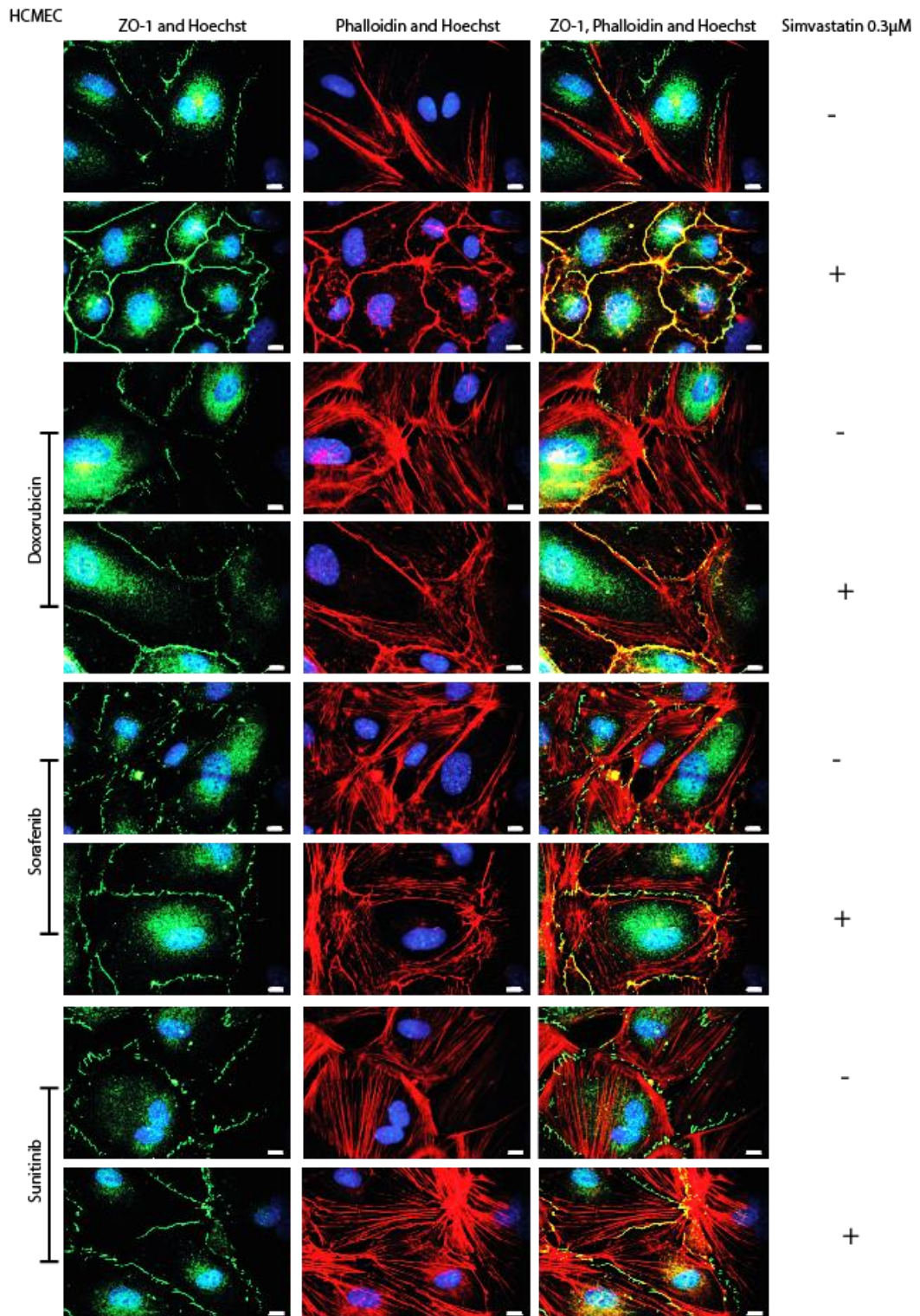
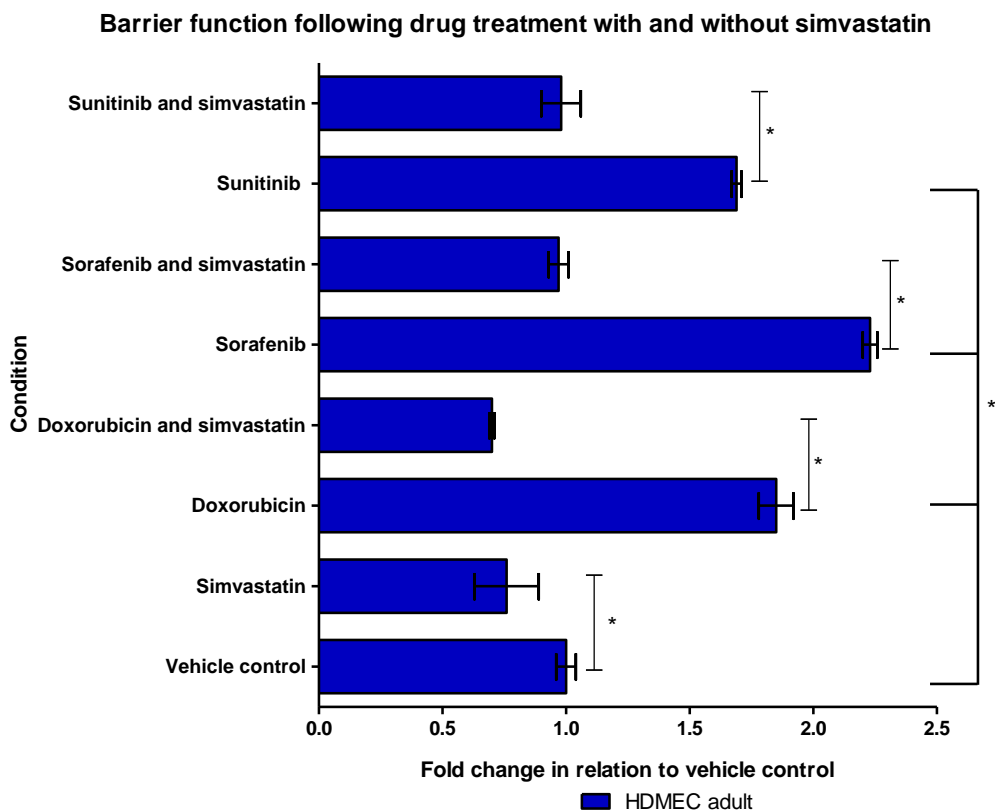


Figure 6.10. **Barrier protection with simvastatin pre-treatment.** HCMEC were pretreated with simvastatin at 0.3 μM for 6 hours prior to



addition of doxorubicin 0.1  $\mu\text{M}$ , sorafenib 1  $\mu\text{M}$  or sunitinib 1  $\mu\text{M}$  for a further 6 hours. Cells were stained with ZO-1 (tight junctions, green), phalloidin (actin fibers, red) and Hoechst (nuclei, blue). Scale bar represents 10  $\mu\text{m}$ .

From figure 6.10 it was evident that simvastatin protected against doxorubicin, sorafenib and sunitinib barrier perturbment. This result was further investigated by utilising the FITC-dextran based assay to measure barrier function. The results provided additional evidence that simvastatin pre-treatment significantly reduced dextran permeability (Fig. 6.11). Immunofluorescence analysis also revealed that simvastatin treatment led to ERK5 localisation at the cell membrane (Fig. 6.12).



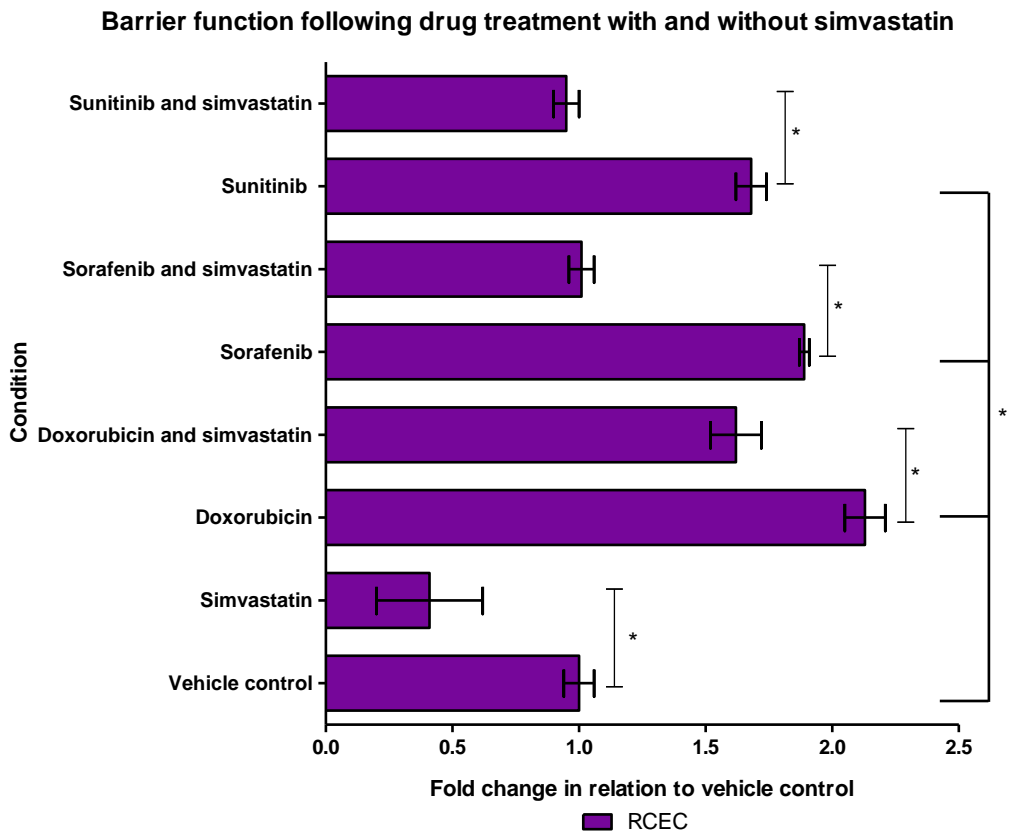
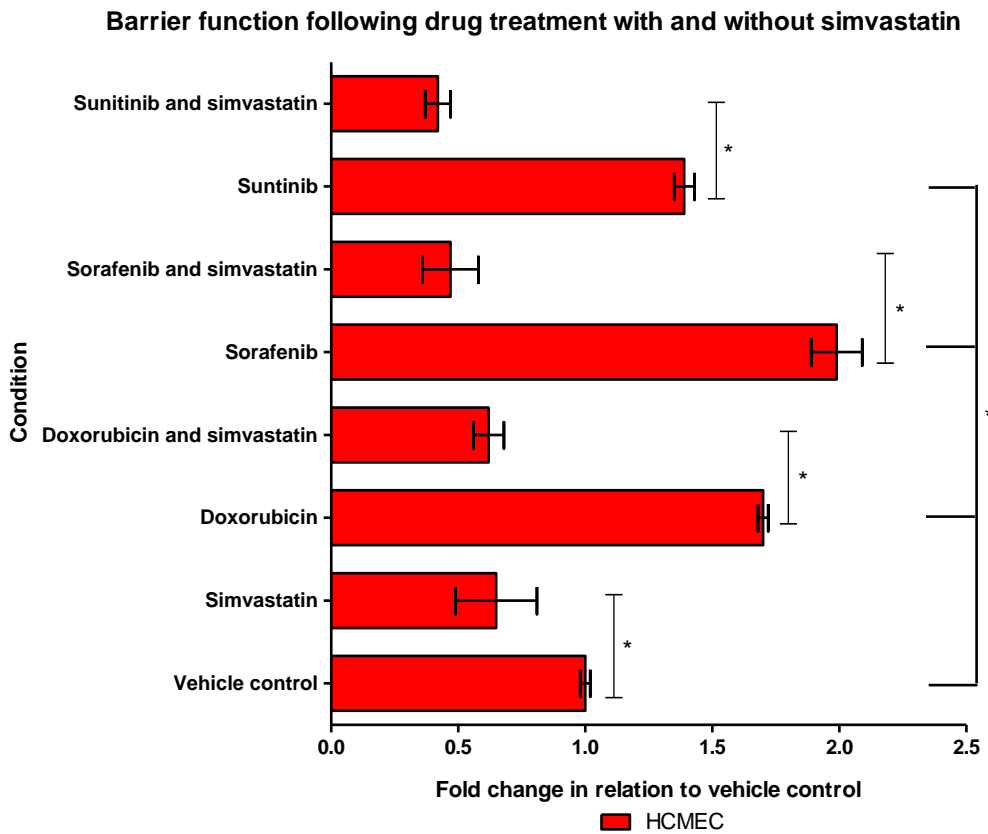


Figure 6.11. **Barrier function of sorafenib and sunitinib with and without pre-treatment with simvastatin.** (A) HDMEC adult, (B) HCMEC and (C) RCEC were pretreated with simvastatin 0.3  $\mu\text{M}$  for 6 hours prior to treatment with sorafenib 1  $\mu\text{M}$  or sunitinib 1  $\mu\text{M}$  for 6 hours before addition of 4 kDa FITC dextran to the ThinCert and the flow through measured. N=4 inserts. Data plotted as mean  $\pm$  SD, \* =  $P \leq 0.05$  with connections indicate comparisons, one-way ANOVA, SPSS, data plotted in GraphPad Prism.

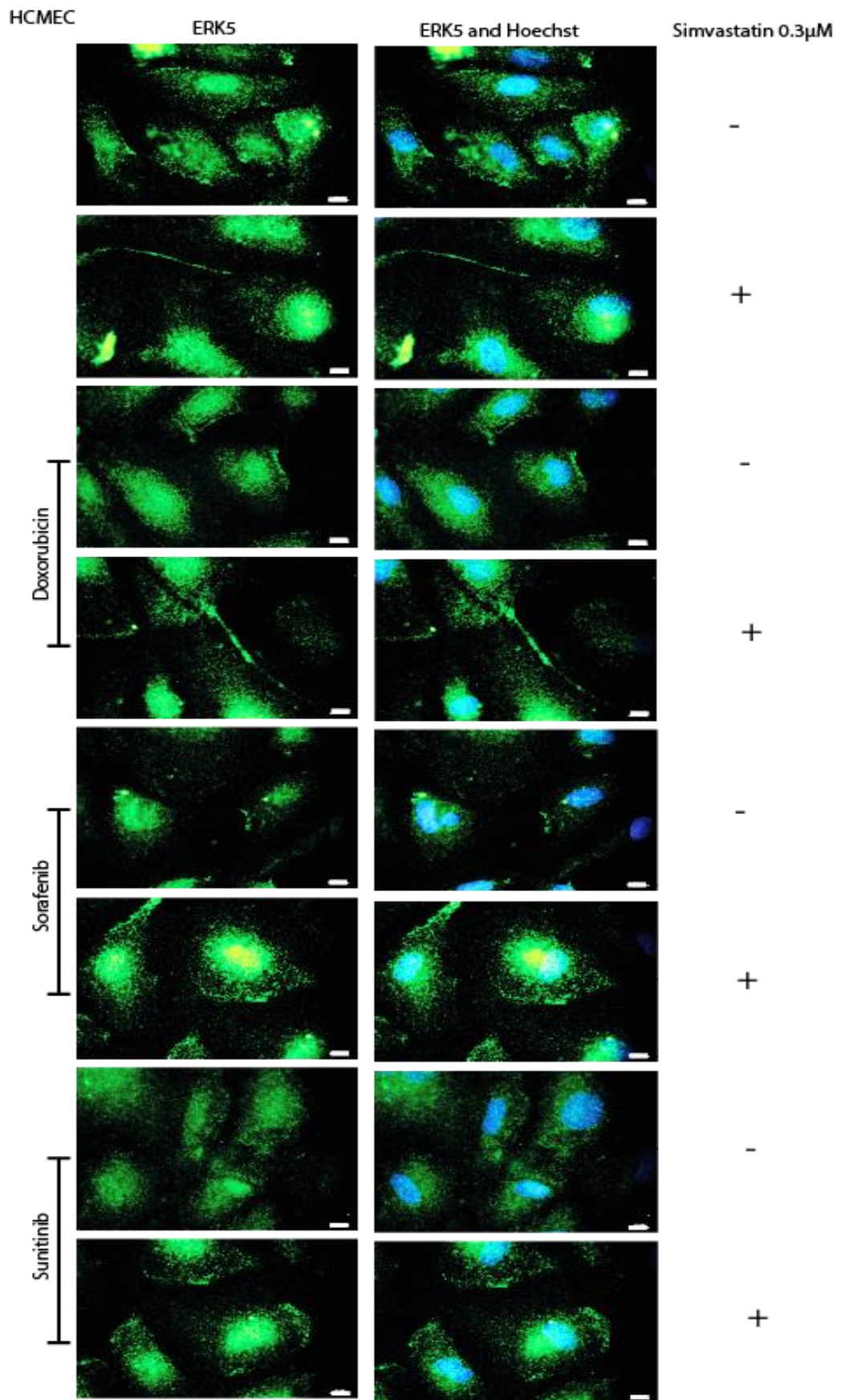
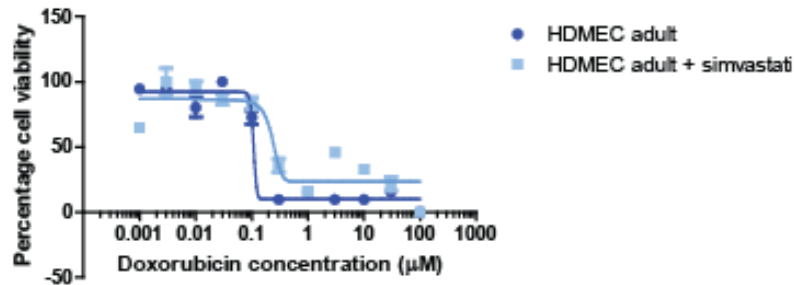


Figure 6.12. ***ERK5 localisation following sorafenib and sunitinib treatment with and without pre-incubation of simvastatin.*** HCMEC were pretreated with simvastatin 0.3  $\mu\text{M}$  for 6 hours then sorafenib 1  $\mu\text{M}$  or sunitinib 1  $\mu\text{M}$  for a further 6 hours. Cells were stained with ERK5 (green) and Hoechst (blue). Scale bar represents 10  $\mu\text{m}$ .

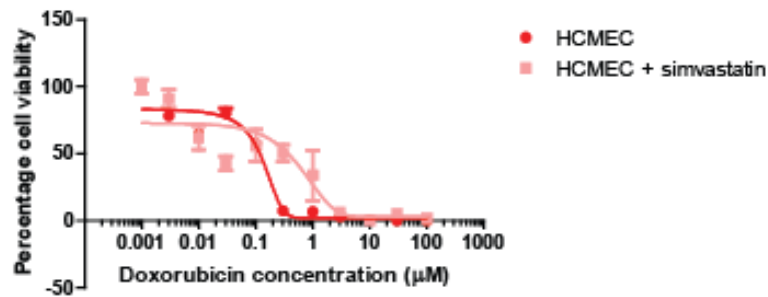
### ***6.2.5 Simvastatin alters cell viability***

Following reports that statins protect endothelial cells from anti-cancer treatment and increases susceptibility of ovarian cancer cells (HeLa) to treatments (Riad et al., 2009; Bardeleben et al., 2002; Chen et al., 2013; Sadeghi-Aliabadi et al., 2010; Henninger et al., 2015; Fritz et al., 2003), I aimed to analyse the effect of simvastatin on doxorubicin cell viability (Fig. 6.13). It can be observed that simvastatin has a protective effect on human endothelial cells (Fig. 6.13 A-C) as well as increasing the susceptibility of A2780 ovarian cancer cells to treatment both wild type (WT) and doxorubicin resistant cells (Fig. 6.13 D). A2780 are an ovarian cancer cell line for which a doxorubicin drug resistant clone is available. Ovarian cancers are known to be treated with doxorubicin, which is why an ovarian cancer cell line was used for viability testing.

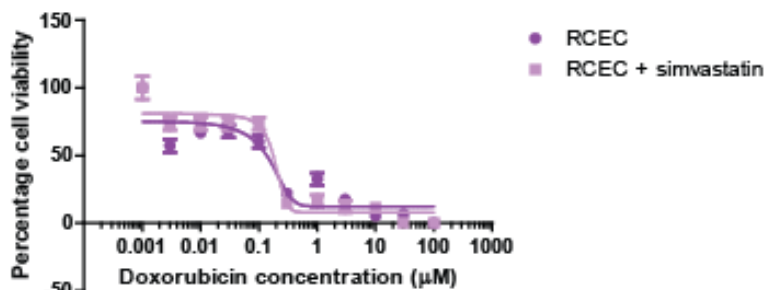
**A**  
Doxorubicin dose-response curve with and without simvastatin



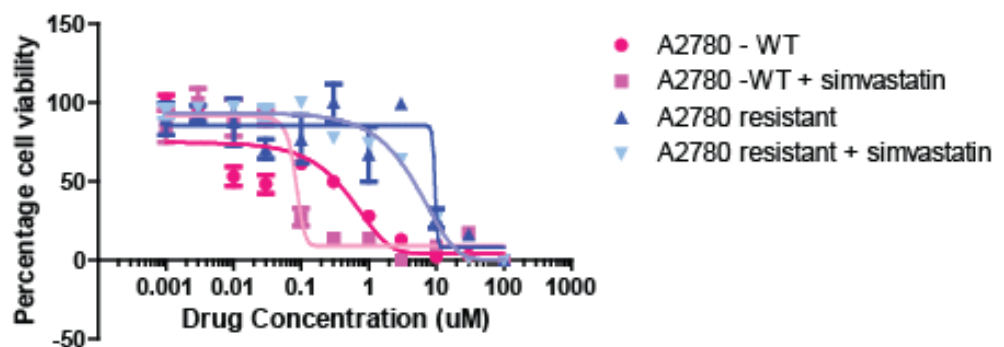
**B**  
Doxorubicin dose-response curve with and without simvastatin



**C**  
Doxorubicin dose-response curve with and without simvastatin



**D**  
Doxorubicin dose-response curve with and without simvastatin





E

	Doxorubicin IC50 (μM)	Doxorubicin IC50 (μM) + simvastatin
HDMEC adult	0.11 ± 0.13	0.23 ± 0.12
HCMEC	0.11 ± 0.06	0.31 ± 0.07
RCEC	0.12 ± 0.07	0.19 ± 0.12
A2780 – WT	0.34 ± 0.15	0.07 ± 0.06
A2780 – resistant (ADR resistant)	9.59 ± 0.03	3.85 ± 0.09

Figure 6.13. **Doxorubicin cell viability with and without simvastatin.** (A) HDMEC adult, (B) HCMEC, (C) RCEC and (D) A2780 were pretreated with simvastatin 0.3 μM for 30 minutes prior to treatment with doxorubicin at concentrations ranging from 100μM to 0.01μM. Viability analysis was measured with Cell Titer Glo®. (E) The IC50 was calculated using graphpad prism, N=4.

## 6.3 Discussion

### 6.3.1 Drug Screen

The anthracycline antibiotics doxorubicin and epirubicin and the protein kinase inhibitors (PKIs) sorafenib, sunitinib, imatinib, nilotinib and lapatinib are known to lead to drug-induced cardiovascular toxicity (Cheng and Force, 2010; Duran et al., 2014; Mego et al., 2007; Schmidinger et al., 2008; Will et al., 2008; Gandhi et al., 2013; Heger et al., 2013; Lupertz et al., 2010; Zhang et al., 2012). It has been previously observed that doxorubicin led to endothelial dysfunction (Wolf and Baynes, 2006). This observation stated that there is increased permeability but does not state whether it is the paracellular or transcellular barrier that is disrupted following doxorubicin treatment. The data in Chapter 4 outlines that doxorubicin is able to induce tight junction barrier perturbment leading to a significant decrease in barrier function.

In this Chapter a more detailed analysis of a wider range of drugs was conducted, which led to the observation that doxorubicin, sorafenib and sunitinib led to a more pronounced barrier perturbment than epirubicin, imatinib, nilotinib and lapatinib. These three anti-cancer treatments are carried forward for further analysis to determine a mechanism for the barrier perturbment. These drugs have already been focused on within the literature for their effect on endothelial and other non-cardiomyocyte cells. It was determined that this barrier perturbment resulted from decreased barrier function measured by dextran flow across endothelial cells, which coincides with data previously published on doxorubicin treatment (Wolf and Baynes, 2006).

### 6.3.2 Protein expression changes in junctions following drug treatment

Endothelial cells express adherens and gap junctions as well as tight junctions. To determine if the barrier perturbment is specific to the tight junctions, which are the primary regulators of barrier function, the protein levels of ZO-1 for tight junctions, VE-cadherin for adherens junctions and connexin 43 for gap junctions were assessed following drug treatment over time. The conclusion of this analysis is that tight junction protein decreases following drug treatment with doxorubicin, sorafenib and sunitinib in HDMEC adult, HCMEC and RCEC. The other junctions undergo disruption, but there are exceptions where the protein level increases following drug treatment for example: in HDMEC adult connexin 43 increased following sorafenib and sunitinib treatment and VE-cadherin increased following sunitinib treatment, while in RCEC connexin 43 increased following sorafenib treatment.

This work provided a more detailed analysis of how doxorubicin, sorafenib and sunitinib induced endothelial cell dysfunction (Wolf and Baynes, 2006; Greineder et al., 2011). Previous work with doxorubicin

had shown that endothelial barrier function decreased following treatment (Wolf and Baynes, 2006). My results show that the barrier function decreased as a result of alterations in the junctions between adjacent endothelial cells and that it could be overcome with simvastatin pre-treatment (Figs. 6.10 and 6.11). This observation has the potential to be clinically relevant by reducing the level of drug able to permeate to underlying cardiomyocytes. This leads to the hypothesis that this will reduce cardiovascular toxicity, as many of the current theories for the mechanism of cardiovascular toxicity onset involve the cardiomyocytes, if the drug is unable to reach them then the toxicity is reduced or eliminated.

### 6.3.3 Barrier recovery following anti-cancer drug treatment

Anti-cancer drug treatment has been demonstrated to induce endothelial tight junction barrier perturbment leading to decreased barrier function observed in this Chapter (doxorubicin, sorafenib and sunitinib) as well as Chapters 4 (Herceptin® and doxorubicin). The barrier perturbment resulting from anti-cancer treatment has been demonstrated to be reversible. Upon removal of drug and addition of endothelial MV2 FGM the actin cytoskeleton remodels and the barrier recovers to the normal physiological state. As the disruption is not permanent there is potential to prevent this event following drug treatment. Prevention of barrier disruption would reduce the concentration of drug able to gain access to underlying cells, which could potentially lead to reduced cardiovascular toxicity observed clinically. As it is known that cardiovascular toxicity is only observed after chronic treatment, barrier perturbment could be used as a marker to detect toxicity onset (Lavery et al., 2011). Decreased barrier function will allow for increased concentration of drugs to reach the underlying myocytes in the heart which can induce cardiovascular toxicity.

Simvastatin pre-treatment protects against doxorubicin, sorafenib and sunitinib induced barrier perturbment. Statins are able to protect against cardiovascular toxicity (Henninger et al., 2015). Simvastatin stimulated the endothelial tight junction barrier as demonstrated in Chapter 5, this provided a potential explanation for the pleiotropic effects observed with statin treatment. Statins are not only able to stimulate the endothelial tight junction barrier, statins are also able to overcome barrier perturbment induced by multiple anti-cancer therapies. As it has previously been demonstrated that statins provide protection against drug-induced cardiovascular toxicity both *in vivo* in mice and rats (Henninger et al., 2015) and *in vitro* (Bardeleben et al., 2003; Nubel et al., 2005; Nubel et al., 2006; Henninger et al., 2012). These studies have demonstrated how statins are able to reduce the cardiovascular toxicity observed following anticancer drug treatment in mice and rats. Furthermore, this work has also demonstrated a protective effect against renal toxicity, showing multi organ benefits (Liao, 2005; Kostapanos et al., 2009; Puri and Tuzcu, 2012). The data documented in these publications outlined the potential clinical benefit of statins, however, no clear mechanism is outlined. It has been hypothesised that the pleiotropic events observed following statin treatment are a result of GGPP inhibition leading to unprenylation of small GTPases, rather than the conventional cholesterol reduction (Bardeleben et al., 2002). The results from this study could hypothesise how statins are able to reduce the cardiovascular toxicity, through stimulating the tight junction barrier reducing the amount of drug able to pass between endothelial cells and get to underlying cardiomyocytes, which are predicted to be involved in the cardiovascular toxicity.

#### 6.3.4 Statins alter cell viability

Statins have been demonstrated to reduce toxicity when in combination with doxorubicin (Bardeleben et al., 2002; Damrot et al., 2006; Henninger et al., 2012; Henninger et al., 2015; Huelsenbeck et al., 2011; Kim et al.,

2012; Riad et al., 2009; Riganti et al., 2008; Sadeghi-Aliabadi et al., 2010; Werner et al., 2013; Werner et al., 2004). The pleiotropic effects of statins in reducing cell death within the heart following doxorubicin treatment, were predicted to be a contributing factor to the ability of statins to reduce drug-induced cardiovascular toxicity (Werner et al., 2013; Riad et al., 2009; Damrot et al., 2006; Huelsenbeck et al., 2011; Henninger et al., 2015). This Chapter demonstrated how the IC<sub>50</sub> of doxorubicin is increased indicating endothelial cell protection in the presence of simvastatin. It has also been demonstrated that statins sensitise cancer cells to doxorubicin (Fritz et al., 2003). This has further been demonstrated in figure 6.13 showing that A2780 ovarian cancer cells have a lower IC<sub>50</sub> for doxorubicin in the presence of simvastatin. Doxorubicin resistant A2780 cells are also more sensitive to doxorubicin in the presence of simvastatin.

This *in vitro* finding suggests that statins could be used clinically in combination therapy with doxorubicin to reduce drug-induced cardiovascular toxicity and increase efficacy of chemotherapeutic agents. This will ultimately provide better patient outcomes.



# **Chapter 7**

## General Discussion





## 7.1 Cardiovascular toxicity

### *7.1 Current approaches*

Drug-induced cardiovascular toxicity is problematic in multiple stages of the drug development process (Lavery et al., 2011). Cardiovascular toxicity and hepatotoxicity are the leading causes of drug attrition. The field of cardiovascular toxicity has developed to study both functional and structural toxicity. Within industry there are pre-clinical screening methods in place to detect symptoms of cardiovascular toxicity, such as, changes in electrophysiology (arrhythmias), changes in heart rate and blood pressure, oedema and thrombosis. However, these can only be detected following cardiovascular toxicity onset, at which point there is already potentially irreversible damage. This leaves this field open to investigate structural toxicity in order to determine cellular changes that can potentially predict drug-induced cardiovascular toxicity.

Structural cardiovascular toxicology research has primarily focused on effects on cardiomyocytes (Cheng and Force, 2010). The focus has recently shifted to investigating the role other cell types, within the heart, play in cardiovascular toxicity (Wolf and Baynes, 2006). An emerging area of research is investigating the role endothelial cells play in cardiovascular toxicity (Wolf and Baynes, 2006; Chiusa et al., 2012; Greineder et al., 2011). Endothelial cells form a monocellular layer on the luminal surface of the vasculature, and consequently are the first cardiac cell type to encounter the cardiovascular toxic drugs (Dejana et al., 1995; Vandenbroucke et al., 2008; Wang and Alexander, 2011). Understanding how these cells respond following exposure to anti-cancer drugs could begin to provide an understanding of the mechanism of cardiovascular toxicity. If the drug is unable to permeate to surrounding cells then drug-induced toxicity on that particular cell is irrelevant. Endothelial cells are known to form a protective barrier comprised of junctions and transporters

(Le Guelte and Gavard, 2011). This barrier functions to limit movement of unnecessary ions and free fatty acids from the circulation to underlying tissue. The endothelium in different tissues has been demonstrated to express different levels of transporters depending on the specific tissues requirements, for instance the liver is responsible for xenobiotic metabolism so the vasculature is highly permeable allowing passage of many ions, free fatty acids as well as drugs and toxins to the hepatocytes to undergo metabolism (Gonzalez-Mariscal et al., 2005). This is physiologically important to allow chemical modifications of toxins to ensure effective renal clearance to prevent buildup. In contrast to the liver, brain endothelial cells express a highly impermeable barrier, which functions to prevent entry of drugs and toxins to the brain (Garg et al., 2015). This data shows how endothelial cells from different anatomical locations can be physiologically different, for this reason this thesis has investigated the physiology of endothelial cells from the dermis and cardiac microvasculature to begin to understand the role of endothelial cells in cardiovascular toxicity.

### *7.2.1 Rat cardiac endothelial cells respond differently to human cardiac endothelial cells following growth factor stimulation*

Endothelial cells are known to respond to growth factors such as VEGF-A (Cudmore et al., 2012; Bruns et al., 2010; E et al., 2012; Chiusa et al., 2012). There have been reports that HGF also plays an important role in endothelial cells (Sulpice et al., 2009). This suggests the presence of functional VEGFR-2 and HGFR on endothelial cells, which are able to regulate intracellular signalling cascades controlling endothelial physiology. In order to determine if all endothelial cells express the same growth factor receptors a screen was conducted in Chapter 3 to analyse intracellular signalling in response to growth factors. The intracellular signalling kinases investigated include AKT and ERK1/2 as these kinases are involved in several endothelial responses, including: migration, proliferation and survival (Holmes et al., 2007; Roberts et al., 2010).

Chapter 3 investigated whether rat and human cardiac endothelial cells respond in the same way to growth factors. This is important to understand as many *in vivo* studies are conducted on rats to investigate drug-induced cardiovascular toxicity (Adamcova et al., 2007). It is widely known that there are species differences that can account for certain toxicities being overlooked in development, this has been apparent since the teratogenic deformities following thalidomide treatment in the 1960's (Fabro and Smith, 1966; Hay, 1964). Thalidomide was tested in rabbits and was originally marketed for respiratory infections, it was subsequently found to have an effective antiemetic effect so was further marketed for treatment of morning sickness (Fabro and Smith, 1966). At this time it was unknown that drugs were able to cross between the placenta and fetus, so no toxicity tests were conducted to determine safety. Subsequently, research outlined that toxicity studies were conducted on rabbits for thalidomide, which upon further evaluation showed no teratogenic deformities following thalidomide treatment to pregnant animals, showing a species difference and highlights how toxicities can be overlooked due to species differences, outlining the importance of testing drugs in multiple species that are known to be closely related to humans (Hay, 1964). The rationale behind investigating endothelial physiology in rats and humans will allow identification of cellular responses and allow species comparison, this will give an indication if rats are a valid cell model for studying drug-induced cardiovascular toxicity in endothelial cells.

A further comparison that will also provide useful information regarding endothelial cell physiology is comparing this to human dermal microvascular endothelial cells (HDMEC). Classical vasculature studies use HUVEC and HDMEC as these cells are readily available (Cale and Bird, 2006). However, the relevance of these cell lines to the vascular bed of interest has not evaluated, for this reason this thesis has compared HDMEC to HCMEC to determine if endothelial cells from different

anatomical locations respond differently to drugs and to provide evidence as to whether specific vasculature is required for toxicity testing.

Chapter 3 demonstrated that HDMEC adult, HCMEC and RCEC responded to VEGF-A and HGF. However, only HCMEC responded to EGF and TGF- $\alpha$ . This indicates the presence of EGFR on cardiac endothelial cells. As this response was not observed in rat cardiac endothelial cells, this shows a potential species difference. As EGFR is a target for several anti-cancer drugs that have been reported to induce cardiovascular toxicity, this could be of potential importance (Amin et al., 2006; Yewale et al., 2013). Data comparison indicates that RCECs respond in a similar way to HDMECs, this data suggests that potential endothelial cell responses to the anti-cancer drugs targeting EGFR could be missed in RCEC or HDMEC adult. This denotes the importance of using HCMEC to study drug-induced cardiovascular toxicity.

### *7.2.2 Herceptin only induces barrier perturbation in human cardiac endothelial cells*

Endothelial cells regulate the movement of drugs and their metabolites from the circulation to underlying tissues through paracellular and transcellular transport mechanisms (Vandenbroucke et al., 2008). Endothelial cells express transporters on the cell membrane at both apical, to control movement from circulation into the cell, and basolateral, to regulate movement from the endothelial cell to underlying tissue. Drugs are able to utilise these transporters to gain access to the cells and underlying tissues.

Endothelial cells provide a barrier to circulating anti-cancer drugs and their metabolites. Endothelial cells at different anatomical locations are known to have different permeability levels to these drugs so allowing different concentrations of drug to permeate to the surrounding tissues. For instance, the blood brain barrier is considered highly impermeable in

comparison to the liver, kidneys or aorta (Li and Poznansky, 1990). Tumour vasculature is considered highly permeable allowing drugs to permeate to underlying cells and the interstitium, leading to a higher than normal interstitial pressure (Chen et al., 2013). Interstitial pressure is regulated by the permeability of fluid from the vasculature to the interstitium. VEGF-A is known to induce vascular permeability therefore increased levels of VEGF-A in the tumours lead to increased vascular permeability and an increase in interstitial pressure. As tumour vasculature is considered highly leaky, it is hypothesised that the drugs are not required to alter the barrier in order to get access to the underlying tumour. The consequence of the drugs perturbing the endothelial barrier is that this allows them access to non-target cells, such as cardiomyocytes, resulting in cardiovascular toxicity. This thesis has discussed how anti-cancer drugs are able to perturb the endothelial barrier at the level of the tight junctions, leading to a space between the cells that the drugs are able to pass through which will allow them access to cardiomyocytes and hypothesises how the drugs induce toxicity. The defining mechanism to cardiovascular toxicity ultimately lies in the cardiomyocytes as they are non-regenerative cells. This thesis has discussed how the anti-cancer drugs affect the endothelial barrier and additionally how to overcome this barrier perturbation leading to the potential for reduced cardiovascular toxicity.

Although in cancer therapy it has been reported that barrier perturbation is not essential for drug delivery to target cells (Chen et al., 2013), there are certain conditions where vascular permeability provides particular problems for drug delivery, for example, when drugs are targeting the brain and drugs are required to permeate the blood brain barrier (BBB) (Zhang et al., 2014; Sardi et al., 2013; Liu et al., 2014). It has been demonstrated in Chapter 4 that doxorubicin and Herceptin® are able to induce barrier perturbation in HCMEC, but not HBMEC, suggesting that the barrier between the two endothelial cells is different, with the HBMEC having greater resistance to doxorubicin. A potential explanation for

barrier perturbation with Herceptin® is that only HCMEC express EGFR2. Herceptin® is known to target EGFR2, preventing heterodimerisation with EGFR4 (Valabrega et al., 2007; Jones and Buzdar, 2009). This leads to receptor internalisation or recruitment of immune cells that are able to induce cell death. It has been predicted that as there is no known ligand for EGFR2, this receptor can only be active as a heterodimer, primarily dimerising with EGFR4, which is activated by NRG-1.

As Chapter 4 demonstrates, Herceptin® treatment leads to barrier perturbation in HCMEC. In order to determine if this is a specific effect of EGFR2 inhibition, an additional EGFR2 inhibitor could be utilised. Pertuzumab is also a humanised monoclonal antibody that targets EGFR2, it has been demonstrated to target EGFR2 differently to Herceptin®. Pertuzumab targets the dimerisation domain preventing homodimerisation as well as heterodimerisation leading to inhibition of EGFR2 mediated intracellular signalling (Walshe et al., 2006). Herceptin® treatment leads to: receptor down modulation, prevents receptor extracellular domain cleavage at the juxtamembrane domain and induces recruitment of immune cells (Walshe et al., 2006). Antibody interactions with the immune system lead to antibody directed cell cytotoxicity (ADCC) (Kute et al., 2009). As Herceptin® and pertuzumab have differential binding sites on EGFR2, the observed effects are considered as a direct target of EGFR2 inhibition as oppose to non-specific anti-body effects (Hubalek et al., 2012). If pertuzumab induces barrier perturbation in HCMEC in a similar way to Herceptin® this will suggest that the EGFR2 is playing a role in barrier regulation in HCMEC. There are reports linking EGFRs to barrier regulation (Cameron et al., 2003; Samak et al., 2011; Liu et al., 2014). These reports have linked stimulated EGFRs to junction regulation, so the mechanism for Herceptin® induced EGFR2 barrier perturbation in HCMEC remains unexplained as EGFR2 is thought to be inactive on HCMEC. To explore this further and determine if EGFR2 is active on HCMEC, fluorescently labeled Herceptin® could be administered to the cells and through live



cell imaging the binding of Herceptin® to EGFR2 and localisation can be observed. This will allow visualisation of EGFR2 localisation following Herceptin® treatment to analyse receptor internalisation.

There have been recent advancements in humanised monoclonal antibody treatment with the development of antibody-drug conjugates (ADCs) these are antibodies coupled to cytotoxic chemotherapeutic agents (Guerin et al., 2015; Kim et al., 2014). Currently developed ADCs include: Adcetris that was approved in 2011 for treatment of Hodgkins lymphoma and Kadcylla (Ado-Trastuzumab Emtansine) approved in 2013 for EGFR2 overexpressing breast cancers (Kim et al., 2014). These ADCs are becoming increasingly popular as a second generation of monoclonal antibodies as it has been demonstrated that they have potential to reduce tumour mass in resistant tumours. Kadcylla consists of Herceptin® antibody coupled to the microtubule inhibitor emtansine and is effective against Herceptin® resistant tumours as well as having high clinically efficacy for EGFR2 overexpressing breast tumours since its recent approval in 2013 (Jackson et al., 2014). As these ADCs directly target tumours overexpressing EGFRs and delivery the cytotoxic chemotherapeutic agent to the tumours they are predicted to be less toxic. However, as has been demonstrated in Chapters 3 and 4 HCMEC express EGFR1 and 2 so these drugs have potential to be able to target HCMEC and exert cytotoxic effects inducing cell death. The data presented in this thesis would suggest that patients taking kadcylla may be at risk of cardiac microvascular injury and subsequently cardiovascular toxicity.

### *7.2.3 ERK5 regulates the endothelial tight junction barrier*

ERK5 is known to be important in embryogenesis. ERK5 knockout studies produce an embryonic lethal phenotype at E9.11-11.5. ERK5 knockout mice demonstrate collapsed and irregular capillaries with

fenestrations allowing for leakage out of the capillaries (Hayashi et al., 2004). It can also be noted that the surrounding pericytes and myocytes appear to show a relatively normal phenotype (Hayashi et al., 2004). Observation of ZO-1 knockout mice show a similar phenotype with embryonic lethality at E10.5 (Katsuno et al., 2008). This suggests that there could be a link between ERK5 and ZO-1 as gene ablation in mice results in a similar phenotype with embryonic lethality at similar stages in development.

Permeability is known to be dependent on many factors including plasma protein binding and metabolism of the drug, as well as the presence of efflux transporters (Garg et al., 2015). Transporters along with junctions play a key role in drug delivery to target cells. A drug's ability to permeate the endothelial barrier is important in drug development, with compounds being selected on their physical-chemical properties. Drugs to target the brain should possess lipophilic properties in order to passively diffuse across the cell membrane (Garg et al., 2015).

In order to increase a drug's ability to reach target cells at therapeutic concentrations, a method involving localised regulation of the endothelial barrier could be investigated. As has been demonstrated in this thesis (Chapter 5), ERK5 activation is able to stimulate the endothelial barrier; whereas inhibition of ERK5 leads to barrier perturbation. This response could be investigated clinically to determine if ERK5 inhibition could be localised to the blood brain barrier, allowing for drugs to gain access to the brain in conditions such as multiple sclerosis.

#### *7.2.3.1 ERK5 inhibition induces endothelial barrier perturbation*

Inhibition of ERK5 has been demonstrated to induce barrier perturbation, affecting tight, adherens and gap junctions. Previous investigations have linked ERK5 to connexin 43 (CX43) regulation (Cameron et al., 2003).

CX43 is one of the 3 main connexins expressed in cardiac endothelial cells; others include connexin 40 and 37 (Dejana et al., 1995). Cameron *et al.* reported a direct link between CX43 and ERK5. Specifically, they showed that application of the inhibitor PD98059, originally marketed as a MEK1/2 inhibitor but subsequently demonstrated to also inhibit MEK5, led to regulation of CX43. To further identify which MEK was primarily involved Cameron *et al.* transiently transfected HEK293 with plasmids to activate ERK1/2 and ERK5. This experiment provided evidence that ERK5 activation leads to CX43 regulation. There is further evidence to suggest that there is a link between CX43 and ZO-1 (Rhee et al., 2009), and that CX43 interacts with the PDZ2 domain on ZO-1 (Bazzoni and Dejana, 2004). These publications demonstrated that ERK5 regulates CX43 which in turn regulates ZO-1, providing an explanation for the data observed within this thesis, predicted pathway outlined in figure 7.1.

This novel finding has also lead to the discovery that barrier perturbation following ERK5 inhibition is more prominent in HCMEC and RCEC than HDMEC adult, suggesting a potential difference between cardiac and dermal endothelial cells. This vascular bed difference will require further analysis using cells isolated from different patients to confirm the difference is vascular bed specific and not a result of individual differences.

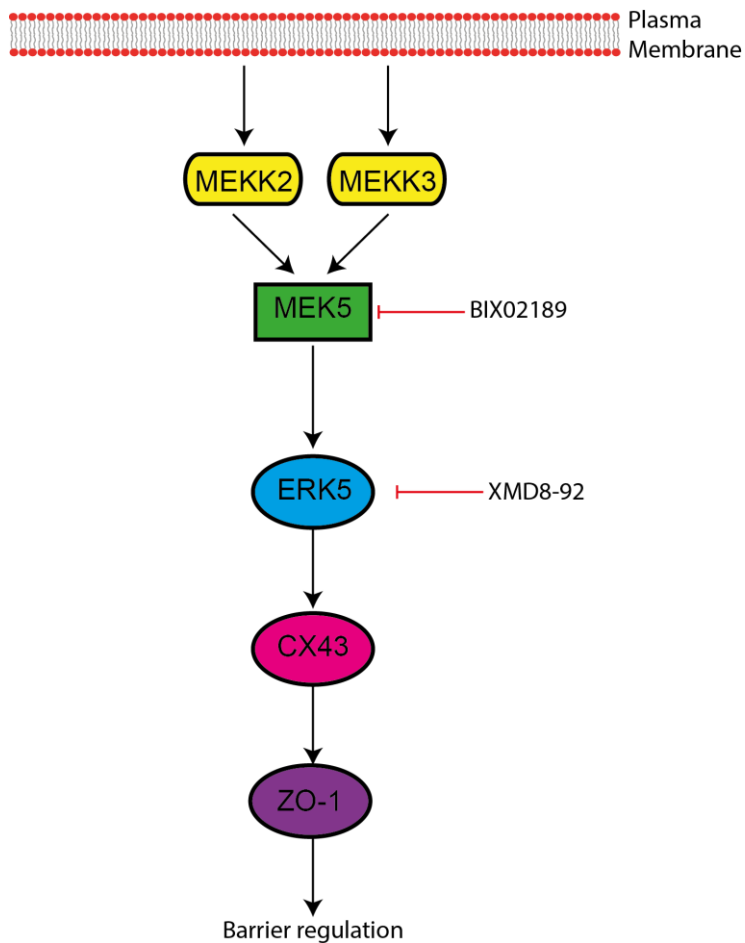


Figure 7.1. **Predicted ERK5 regulation of the tight junction barrier.** ERK5 signalling is known to be regulated through the MAPKs MEKK2/MEKK3 phosphorylating MEK5 which phosphorylates the T218/Y220 residues on ERK5. ERK5 has been demonstrated to regulate CX43, which in turn regulates ZO-1.

A possible explanation for this difference in vascular beds is the CX43 expression. CX43 is known to be expressed and important in cardiac endothelial gap junctions (Dejana et al., 1995; Inai and Shibata, 2009; Tien et al., 2013; Lo and Wessels, 1998). It has been demonstrated that expression and functionality of CX43 differs between vessels (Inai and Shibata, 2009). This can be investigated in follow up work to determine the number of CX43 per endothelial cell and compare HCMEC and HDMEC adult to determine if this provides an insight into the different responses to ERK5 inhibition in the endothelial cells.

#### *7.2.4 Pleiotropic effects of statins and regulation of ERK5 in endothelial cells*

In order to establish if the barrier perturbation could be prevented ERK5 activators were utilised. Research has shown that statins are able to induce ERK5 phosphorylation in vascular endothelial cells such as human aortic endothelial cells (HAECs) (Le et al., 2014; Ohnesorge et al., 2010; Wu et al., 2013). Analysis of various concentrations of statins showed that ERK5 phosphorylation coincided with barrier stimulation (Chapter 5), additionally statin treatment leads to ERK5 localisation at the plasma membrane and within the nucleus.

Statins were developed in the late 80's, with the primary effect to lower plasma LDL-cholesterol levels. Circumstantial evidence has shown pleiotropic effects that cannot be accounted for by cholesterol biosynthesis inhibition and subsequent lowering of plasma LDL-cholesterol levels (Stancu and Sima, 2001; Futterman and Lemberg, 2004). Statins have been demonstrated to activate ERK5 and to also induce cardio-protective effects, these two events have not yet been linked. This project has investigated the role of ERK5 in endothelial barrier regulation and how statins are able to stimulate the barrier which could explain the cardio-protective pleiotropic effects observed with statins.

As has been demonstrated in Chapter 5 through addback experiments, addition of GGPP prevents statin induced ERK5 phosphorylation. Clarification of the involvement of GGPP in ERK5 phosphorylation and barrier regulation was also analysed in Chapter 5, with the use of the GGPP inhibitor GGTI-298. GGTI-298 treatment of HCMEC induced ERK5 phosphorylation and barrier stimulation providing evidence that GGPP is involved in statin induced ERK5 phosphorylation and barrier stimulation. This indicated that statin induced barrier protection is due to the inhibition of GGPP, a molecule formed in cholesterol biosynthesis but is not directly involved in cholesterol production. GGPP has been shown

to have a potential role in many of statins pleiotropic effects (Ito et al., 2006; Futterman and Lemberg, 2004; Puri and Tuzcu, 2012; Kostapanos et al., 2009; Liao, 2005).

GGPP is known to regulate the prenylation of small GTPases Rho, Rac and Cdc42. It has been demonstrated in the literature that Rho is able to regulate tight junctions in epithelial cells (Terry et al., 2010; Gopalakrishnan et al., 1998; Vandenbroucke et al., 2008) and Cdc42 is able to regulate the actin cytoskeleton (Liao, 2005). The data from these two papers linking Rho and Cdc42 to tight junctions along with data from this thesis provides the hypothetical pathway outlined in figure 7.2.



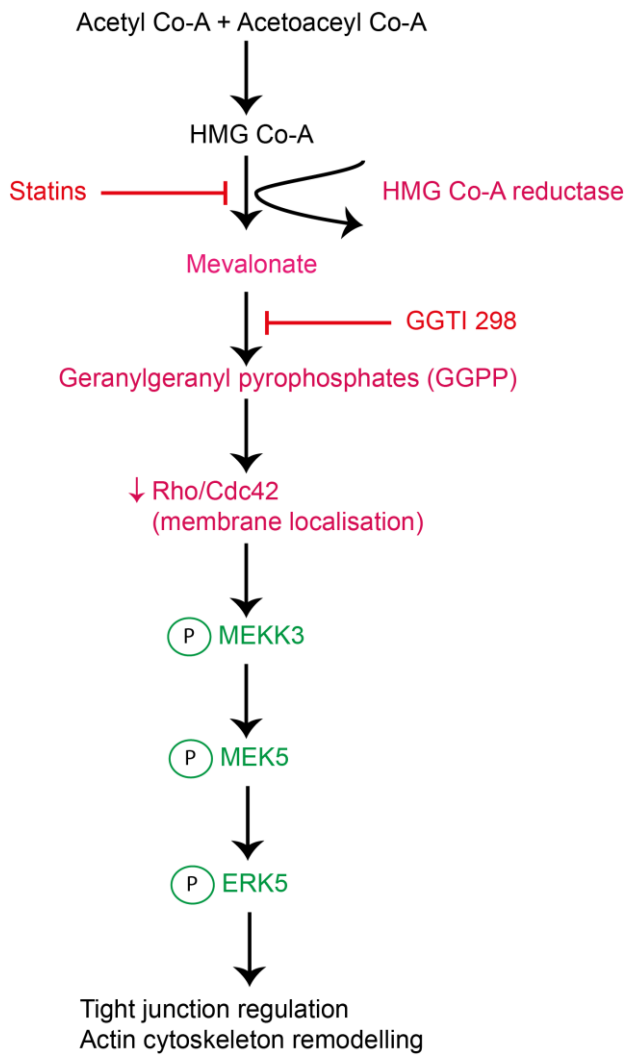


Figure 7.2. **Hypothesis for how statins induced barrier protection.** Statins inhibit the conversion of HMG Co-A to mevalonate preventing the formation of GGPP. This inhibits Rho/Cdc42 prenylation which leads to phosphorylation of ERK5 and regulation of the tight junction barrier as well as actin cytoskeleton remodelling. Precursors inhibited by statins are outlined in pink and phosphorylated kinases are outlined in green.

This hypothesis builds on the pathway outlined in figure 7.1 that demonstrates a potential link between ERK5 and ZO-1. The hypothesis in figure 7.2 takes reports from the literature to link statins to tight junction regulation. Statin treatment, through inhibition of HMG Co-A reductase, leads to the inhibition of GGPP which prevents prenylation of Rho and Cdc42 small GTPases (Molnar et al., 2001; Wilson et al., 1998). Rho inhibition is predicted to remove the inhibition on ERK5 phosphorylation, as small GTPases such as Rho are thought to negatively regulation ERK5

phosphorylation (Fukuhara et al., 2000). Data presented in this thesis has shown that ERK5 activation leads to tight junction formation. Reports in the literature link the small GTPase Rho to tight junction regulation, which provides further evidence for this potential hypothesis (Terry et al., 2010; Gopalakrishnan et al., 1998; Vandenbroucke et al., 2008; Fujita et al., 2000). There have been several reports linking small GTPases to actin remodeling and junction regulation (Birukova et al., 2012; Bazzoni and Dejana, 2004). Other small GTPases that have been linked to actin cytoskeleton remodeling include Cdc42 (Liao, 2005). There are reports linking inhibition of Cdc42 to ERK5 phosphorylation suggesting that this could also be a potential mechanism for how statins regulate the tight junction barrier and actin cytoskeleton (Zuo et al., 2015). The mechanism for how preventing Cdc42 or Rho prenylation, through statin treatment, leads to ERK5 phosphorylation has not been defined, however, the literature would suggest that the prenylation of small GTPases negatively regulates ERK5 phosphorylation (Fukuhara et al., 2000). The data in Chapter 5 has demonstrated that statins induce ERK5 phosphorylation through MEKK3. This suggests the link between the small GTPases and ERK5 is through MEKK3.

Small GTPases have been demonstrated to regulate various factors that play a role in cardiovascular disease progression. These factors include vasoconstriction, smooth muscle cell proliferation, thrombotic events and plaque instability regulated by Rho A; smooth muscle cell hypertrophy and endothelial dysfunction are regulated by Rac1 (Ito et al., 2006). This leaves the question: is ERK5 responsible for all the pleiotropic effects of statins? (Ito et al., 2006; Futterman and Lemberg, 2004; Puri and Tuzcu, 2012; Kostapanos et al., 2009; Liao, 2005). There are several reports in the literature demonstrating that ERK5 is able to regulate physiological events such as migration, angiogenesis, proliferation and survival in endothelial cells (Hayashi et al., 2004; Drew et al., 2012; Roberts et al., 2009). ERK5 has been demonstrated to regulate downstream signalling molecules that can regulate physiological events such as migration,

proliferation, angiogenesis and survival, these signalling molecules include AKT, KLF4, KLF2 and NRF2, reviewed by (Nithianandarajah-Jones et al., 2014).

Statins are able to stimulate the endothelial tight junction barrier sufficiently to overcome perturbation induced by anti-cancer drugs, doxorubicin, sorafenib and sunitinib. This provides a hypothesis to explain the cardio-protective effects of statins against anti-cancer drugs. If statins are able to stimulate the endothelial barrier, a lower concentration of chemotherapeutic drug will permeate to the underlying tissue, potentially leading to reduced toxicity. This hypothesis is further backed up by publications demonstrating that the cardiovascular toxicity observed is dose dependent (Vejjongsakul and Yeh, 2014; Zhang et al., 2012; Gandhi et al., 2013; Henninger et al., 2015).

#### *7.2.5 Barrier perturbation is not limited to one class of anti-cancer drugs*

From Chapters 4 and 6 it can be determined that anti-cancer drug induced barrier perturbation is not limited to a single class of anti-cancer drugs. These chapters have demonstrated that Herceptin®, a humanised monoclonal antibody (Baselga et al., 1998); doxorubicin, an anthracycline antibiotic (Perez-Arnaiz et al., 2014); sorafenib and sunitinib, protein kinase inhibitors (Schmidinger et al., 2008) are all able to induce endothelial tight junction barrier perturbation. Chapter 6 has demonstrated that not all members of these classes of drugs produce barrier perturbation to the same extent. This could be a time dependent factor, as it has been demonstrated in Chapter 6 with doxorubicin, sorafenib and sunitinib that barrier perturbation increases over time, so investigating all the drugs at 6 hours may not have provided sufficient time for them all to induce barrier perturbation. As cardiovascular toxicity is known to manifest after years of chemotherapy treatment this suggests that long-term treatments are key to determining a mechanism for toxicity.

Data from Chapter 6 shows how the barrier perturbation resulting from anti-cancer drug treatment can be overcome by statin treatment. This demonstrates that statin protection against drug-induced tight junction barrier perturbation is relevant to multiple classes of drugs. These effects would need to be tested with a greater range of drug classes to determine if statins can protect against endothelial tight junction perturbation in all classes of anti-cancer drugs. Animal studies can be conducted to confirm the hypothesis that statins prevent cardiovascular toxicity, this has already been demonstrated in mouse models using doxorubicin treatment, however, the mechanism for statin protection has not been confirmed (Henninger et al., 2015).

## 7.2 Study limitations and further directions

In order to further evaluate this hypothesis, linking ERK5 phosphorylation to junction stimulation, experiments would need to be conducted to confirm links between the proteins ERK5 and ZO-1. This could be achieved by inhibiting each stage of the hypothetical statin induced barrier stimulation pathway (Fig. 7.4). This thesis has demonstrated use of GGTI-298 to inhibit GGPP induces ERK5 phosphorylation and tight junction barrier stimulation. Further inhibitors to the small GTPases downstream of GGPP could be analysed these include: Rho inhibitor Y-27632 (Diao and Hong, 2015; Peh et al., 2015), Rac inhibitor C3 botulinum toxin (Didsbury et al., 1989) and Cdc42 inhibitors CID2950007 or CID44216842 (Surviladze et al., 2010; Hong et al., 2013), which, can be used not only to identify if inhibition of Rho/Rac/Cdc42 leads to barrier protection, but also to determine if Rho/Rac/Cdc42 regulate ERK5 activation. Determination of the small GTPase that is involved in ERK5 activation is the first step in confirming the link between statins and ERK5 activation.

Chapter 5 demonstrated that siRNA mediated gene silencing of MEKK3 and MEK5 prevented statin induced ERK5 activation, suggesting that it is through the MEKK3 – MEK5 – ERK5 signalling cascade that statins are able to induce activation of ERK5. This would suggest that the GTPase downstream of GGPP potentially regulate activation of MEKK3 resulting in downstream activation of ERK5. Western blotting analysis can determine if this is the mechanism for how Rho/Rac/Cdc42 regulate ERK5 activation.

An siRNA library can be used to knock down the small GTPases to determine which group are able to induce ERK5 phosphorylation and barrier stimulation. This can subsequently be conducted on specific GTPases in the group to determine the precise GTPases involved in ERK5 phosphorylation and barrier stimulation.

It has recently been demonstrated that a combination of GGTI-298 and FTI-277 (an FPP inhibitor) mimic the ERK5 activation induced by statins without exerting some of the toxic effects, such as muscle inflammation, seen with statin treatment (Chu et al., 2015). It has been demonstrated that FTI-277 and GGTI-298 exert endothelial protection (Chu et al., 2015). In order to determine if this is through ERK5 phosphorylation further analysis can be conducted on HCMEC to determine if the ERK5 phosphorylation and barrier stimulation observed with GGTI-298 is enhanced with the inhibitor combination.

Further work can also be conducted to determine how statins are able to overcome XMD8-92 inhibition of ERK5 but unable to overcome BIX02189 inhibition of ERK5 in stimulating tight junction formation. It has been demonstrated that MEKK3 and MEK5 siRNA knockdown prevent the ERK5 phosphorylation when cells are treated with simvastatin (Chapter 5), this suggests that both these signaling kinases are important for statin induced ERK5 phosphorylation. BIX02189 inhibits MEK5 (Tatake et al., 2008) and XMD8-92 inhibits ERK5 directly (Yang and Lee, 2011; Yang et

al., 2010), this leads to the hypothesis that MEK5 is critical for statin induced ERK5 activation through its ability to phosphorylate ERK5 on T218/Y220.

However, XMD8-92 has been demonstrated to inhibit phosphorylation of the C-terminal portion of ERK5 (unpublished data by Gopika Nithianandarajah-Jones and Michael Cross) a mechanism that can be independent of MEK5. This suggests that statin induced ERK5 phosphorylation occurs via T218/Y220, as simvastatin is able to overcome barrier perturbation induced by XMD8-92 but not BIX02189. This data suggests that inhibition of ERK5 phosphorylation at any site (T218/Y220 [MEK5 phosphorylation site], T732 or S763 [C-terminal phosphorylation sites]) can induce barrier perturbation. This theory will need to be investigated further with use mutant ERK5 such as ERK5-AEF adenovirus to determine if statins are still able to induce ERK5 phosphorylation.

Vascular permeability can be measured *in vivo*, this technique utilises the ability to inject rats with fluorescent dextran and following sacrifice, section the organs to visualise the spread of dextran within the tissue. This method can also be used with rats being treated with statins in order to determine if less drug is able to gain access to the heart proceeding statin treatment. Human ovarian tumour Xenograft studies in mice could be used to confirm that statins do not reduce clinical efficacy of drugs such as doxorubicin.

There is also scope to investigate the ability of statins to protect against other vascular injury. As Chapter 5 has demonstrated, the protective effects of statins are not limited to HCMEC they can also be observed in HDMEC so there is potential for protection of multiple vascular beds. Another emerging major cause for concern with cancer treatments, such as doxorubicin, is drug-induced kidney injury. There are reports also outlining that statins have potential pleiotropic effects on kidneys as well



as the heart (Henninger et al., 2012; Kostapanos et al., 2009). These effects could also be investigated using *in vivo* investigation where animals can be treated with doxorubicin, with or without statin pre-treatment, and compared to control animals for vascular permeability.

This work can further lead onto testing the hypothesis that localised inhibition of ERK5 at the BBB will lead to increased drug delivery to the brain. This work can include *in vitro* analysis to compare inhibition of MEKK3, MEK5 and ERK5 in HBMEC, HCMEC and HDMEC to determine if inhibition of any of the signaling molecules produce cell type specific difference in barrier perturbation. It has been demonstrated in Chapter 5 that ERK5 inhibition with small molecule inhibitors or siRNA mediated gene silencing leads to a more pronounced effect on barrier perturbation in HCMEC than HDMEC adult, suggesting vascular bed specific barrier perturbation in response to ERK5 inhibition. Allowing for localised barrier perturbation at the BBB has the potential to aid drug delivery to the brain. It is a current problem to direct drugs to the brain, if this hypothesis confirms that it is possible to inhibit ERK5 to increase vascular permeability, this will lead to many clinical possibilities to treat several diseases, such as brain tumours with increased chemotherapy drugs able to reach the tumour (Sardi et al., 2013). This also leads to possibilities in regulation of neurological disorders such as Alzheimers, multiple sclerosis, meningitis, encephalitis, ischemia or hypoxia, brain injury or amyloid angiopathy (Rosenberg, 2012). These conditions lead to barrier disruption through autoimmune targeting of macrophages or activation of astrocytes, infections either bacterial or viral, oedema or haemorrhage as well as pre-existing medical conditions such as hypertension, diabetes or hyperlipidemia (Rosenberg, 2012).

### 7.3 Overall conclusions

In overall conclusion, the data presented in this thesis provided initial evidence on differences in endothelial cells from different vascular beds, with specific focus on HCMEC and HDMEC adult, the data showed differences in the mRNA expression of *EGFRs*. Intracellular signalling kinases are activated in response to EGF and TGF- $\alpha$ , suggesting the receptors present on HCMEC are functional so could have a role in endothelial cell physiology. RCECs have been demonstrated to show low levels of *EGFR1*, indicating a potential species difference between human and rat. This data provided evidence to suggest that rats are potentially not a suitable model for cardiovascular toxicity studies as many current anti-cancer therapies known to induce toxicity target EGFRs, and difference in species receptor expression will lead to unreliable results that cannot be extrapolated to humans from animal models.

The data presented in this thesis demonstrated that ERK5 is able to regulate endothelial tight junctions, which have the potential to play a key role in regulating the vascular permeability of drugs known to cause cardiovascular toxicity. Activation of ERK5 using statins has potential to alleviate this toxicity, allowing for the drugs to have a safer clinical profile. The mechanism for statin induced ERK5 activation is thought to be via small GTPases which have been demonstrated to regulate the tight junctions and actin cytoskeleton.

It has been shown that endothelial cells from different vascular beds respond differently to the drugs, for example in Chapter 4, Herceptin® only induced barrier perturbation in HCMEC and not HDMEC or HBMEC. This provides evidence to suggest that vascular beds respond differently to specific drugs. This project has formed the base for future investigations that have the potential to provide advantageous clinical outcomes for drug delivery and toxicity.

## Chapter 8: References

- (1986) Therapeutic response to lovastatin (mevinolin) in nonfamilial hypercholesterolemia. A multicenter study. The Lovastatin Study Group II. *JAMA* 256: 2829-2834.
- Abe J, Kusuhara M, Ulevitch RJ, et al. (1996) Big mitogen-activated protein kinase 1 (BMK1) is a redox-sensitive kinase. *J Biol Chem* 271: 16586-16590.
- Adamcova M, Simunek T, Kaiserova H, et al. (2007) In vitro and in vivo examination of cardiac troponins as biochemical markers of drug-induced cardiotoxicity. *Toxicology* 237: 218-228.
- Adamcova M, Sterba M, Simunek T, et al. (2005) Troponin as a marker of myocardial damage in drug-induced cardiotoxicity. *Expert Opin Drug Saf* 4: 457-472.
- Ahmed LA and El-Maraghy SA. (2013) Nicorandil ameliorates mitochondrial dysfunction in doxorubicin-induced heart failure in rats: possible mechanism of cardioprotection. *Biochemical Pharmacology* 86: 1301-1310.
- Ahmed TA, Hayslip J and Leggas M. (2014) Simvastatin interacts synergistically with tipifarnib to induce apoptosis in leukemia cells through the disruption of RAS membrane localization and ERK pathway inhibition. *Leuk Res* 38: 1350-1357.
- Amin DN, Bielenberg DR, Lifshits E, et al. (2008) Targeting EGFR activity in blood vessels is sufficient to inhibit tumor growth and is accompanied by an increase in VEGFR-2 dependence in tumor endothelial cells. *Microvasc Res* 76: 15-22.
- Amin DN, Hida K, Bielenberg DR, et al. (2006) Tumor endothelial cells express epidermal growth factor receptor (EGFR) but not ErbB3 and are responsive to EGF and to EGFR kinase inhibitors. *Cancer Res* 66: 2173-2180.
- Antoine DJ, Srivastava A, Pirmohamed M, et al. (2010) Statins inhibit aminoglycoside accumulation and cytotoxicity to renal proximal tubule cells. *Biochemical Pharmacology* 79: 647-654.
- Arkhipov A, Shan Y, Kim ET, et al. (2013) Her2 activation mechanism reflects evolutionary preservation of asymmetric ectodomain dimers in the human EGFR family. *Elife* 2: e00708.
- Armstrong EJ and Bischoff J. (2004) Heart valve development: endothelial cell signaling and differentiation. *Circ Res* 95: 459-470.
- Armulik A, Genove G and Betsholtz C. (2011) Pericytes: developmental, physiological, and pathological perspectives, problems, and promises. *Dev Cell* 21: 193-215.
- Babij P, Askew GR, Nieuwenhuijsen B, et al. (1998) Inhibition of cardiac delayed rectifier K<sup>+</sup> current by overexpression of the long-QT syndrome HERG G628S mutation in transgenic mice. *Circ Res* 83: 668-678.

- Bardeleben R, Kaina B and Fritz G. (2003) Ultraviolet light-induced apoptotic death is impaired by the HMG-CoA reductase inhibitor lovastatin. *Biochem Biophys Res Commun* 307: 401-407.
- Bardeleben RV, Dunkern T, Kaina B, et al. (2002) The HMG-CoA reductase inhibitor lovastatin protects cells from the antineoplastic drugs doxorubicin and etoposide. *Int J Mol Med* 10: 473-479.
- Barkefors I, Le Jan S, Jakobsson L, et al. (2008) Endothelial cell migration in stable gradients of vascular endothelial growth factor A and fibroblast growth factor 2: effects on chemotaxis and chemokinesis. *J Biol Chem* 283: 13905-13912.
- Baselga J, Norton L, Albanell J, et al. (1998) Recombinant humanized anti-HER2 antibody (Herceptin) enhances the antitumor activity of paclitaxel and doxorubicin against HER2/neu overexpressing human breast cancer xenografts. *Cancer Res* 58: 2825-2831.
- Bazley LA and Gullick WJ. (2005) The epidermal growth factor receptor family. *Endocr Relat Cancer* 12 Suppl 1: S17-27.
- Bazzoni G and Dejana E. (2004) Endothelial cell-to-cell junctions: molecular organization and role in vascular homeostasis. *Physiol Rev* 84: 869-901.
- Besse S, Boucher F, Linguet G, et al. (2010) Intramyocardial protein therapy with vascular endothelial growth factor (VEGF-165) induces functional angiogenesis in rat senescent myocardium. *J Physiol Pharmacol* 61: 651-661.
- Birukova AA, Fu P, Wu T, et al. (2012) Afadin controls p120-catenin-ZO-1 interactions leading to endothelial barrier enhancement by oxidized phospholipids. *J Cell Physiol* 227: 1883-1890.
- Brown R, Clugston C, Burns P, et al. (1993) Increased accumulation of p53 protein in cisplatin-resistant ovarian cell lines. *Int J Cancer* 55: 678-684.
- Browne JA, Pearson AL, Zahr RA, et al. (2008) TGF-beta activates ERK5 in human renal epithelial cells. *Biochem Biophys Res Commun* 373: 440-444.
- Brunner HR, Nussberger J and Waeber B. (1993) Control of vascular tone by renin and angiotensin in cardiovascular disease. *Eur Heart J* 14 Suppl I: 149-153.
- Bruns AF, Herbert SP, Odell AF, et al. (2010) Ligand-stimulated VEGFR2 signaling is regulated by co-ordinated trafficking and proteolysis. *Traffic* 11: 161-174.
- Buchsbaum DJ, Bonner JA, Grizzle WE, et al. (2002) Treatment of pancreatic cancer xenografts with Erbitux (IMC-C225) anti-EGFR antibody, gemcitabine, and radiation. *Int J Radiat Oncol Biol Phys* 54: 1180-1193.
- Calcagno AM, Fostel JM, To KK, et al. (2008) Single-step doxorubicin-selected cancer cells overexpress the ABCG2 drug transporter through epigenetic changes. *Br J Cancer* 98: 1515-1524.
- Cale JM and Bird IM. (2006) Inhibition of MEK/ERK1/2 signalling alters endothelial nitric oxide synthase activity in an agonist-dependent manner. *Biochem J* 398: 279-288.

- Cameron SJ, Malik S, Akaike M, et al. (2003) Regulation of epidermal growth factor-induced connexin 43 gap junction communication by big mitogen-activated protein kinase1/ERK5 but not ERK1/2 kinase activation. *J Biol Chem* 278: 18682-18688.
- Carvajal-Vergara X, Tabera S, Montero JC, et al. (2005) Multifunctional role of Erk5 in multiple myeloma. *Blood* 105: 4492-4499.
- Chen PY, Sun JS, Tsuang YH, et al. (2010) Simvastatin promotes osteoblast viability and differentiation via Ras/Smad/Erk/BMP-2 signaling pathway. *Nutr Res* 30: 191-199.
- Chen Y, Zhang S, Peng G, et al. (2013) Endothelial NO synthase and reactive oxygen species mediated effect of simvastatin on vessel structure and function: pleiotropic and dose-dependent effect on tumor vascular stabilization. *Int J Oncol* 42: 1325-1336.
- Cheng C, Xue W, Diao H, et al. (2010) Antitumor activity and toxicological properties of doxorubicin conjugated to [alpha],[beta]-poly[(2-hydroxyethyl)-L-aspartamide] administered intraperitoneally in mice. *Anticancer Drugs* 21: 362-371.
- Cheng H and Force T. (2010) Why do kinase inhibitors cause cardiotoxicity and what can be done about it? *Prog Cardiovasc Dis* 53: 114-120.
- Chiba R, Nakagawa N, Kurasawa K, et al. (1999) Ligation of CD31 (PECAM-1) on endothelial cells increases adhesive function of alphavbeta3 integrin and enhances beta1 integrin-mediated adhesion of eosinophils to endothelial cells. *Blood* 94: 1319-1329.
- Chintalgattu V, Rees ML, Culver JC, et al. (2013) Coronary microvascular pericytes are the cellular target of sunitinib malate-induced cardiotoxicity. *Sci Transl Med* 5: 187ra169.
- Chiusa M, Hool SL, Truetsch P, et al. (2012) Cancer therapy modulates VEGF signaling and viability in adult rat cardiac microvascular endothelial cells and cardiomyocytes. *J Mol Cell Cardiol* 52: 1164-1175.
- Choi J, Yip-Schneider M, Albertin F, et al. (2008) The effect of doxorubicin on MEK-ERK signaling predicts its efficacy in HCC. *J Surg Res* 150: 219-226.
- Chouabe C, Drici MD, Romey G, et al. (1998) HERG and KvLQT1/IsK, the cardiac K<sup>+</sup> channels involved in long QT syndromes, are targets for calcium channel blockers. *Mol Pharmacol* 54: 695-703.
- Chu UB, Duellman T, Weaver SJ, et al. (2015) Endothelial protective genes induced by statin are mimicked by ERK5 activation as triggered by a drug combination of FTI-277 and GGTI-298. *Biochim Biophys Acta* 1850: 1415-1425.
- Clancy CE and Rudy Y. (2001) Cellular consequences of HERG mutations in the long QT syndrome: precursors to sudden cardiac death. *Cardiovasc Res* 50: 301-313.
- Collins DM, O'Donovan N, McGowan PM, et al. (2012) Trastuzumab induces antibody-dependent cell-mediated cytotoxicity (ADCC) in

- HER-2-non-amplified breast cancer cell lines. *Ann Oncol* 23: 1788-1795.
- Cudmore MJ, Hewett PW, Ahmad S, et al. (2012) The role of heterodimerization between VEGFR-1 and VEGFR-2 in the regulation of endothelial cell homeostasis. *Nat Commun* 3: 972.
- Curran ME, Splawski I, Timothy KW, et al. (1995) A molecular basis for cardiac arrhythmia: HERG mutations cause long QT syndrome. *Cell* 80: 795-803.
- Damrot J, Nubel T, Epe B, et al. (2006) Lovastatin protects human endothelial cells from the genotoxic and cytotoxic effects of the anticancer drugs doxorubicin and etoposide. *Br J Pharmacol* 149: 988-997.
- Dejana E, Corada M and Lampugnani MG. (1995) Endothelial cell-to-cell junctions. *FASEB J* 9: 910-918.
- Deweese JE and Osheroff N. (2009) The DNA cleavage reaction of topoisomerase II: wolf in sheep's clothing. *Nucleic Acids Res* 37: 738-748.
- Diao YM and Hong J. (2015) Rho-associated protein kinase inhibitor, Y-27632, significantly enhances cell adhesion and induces a delay in G1 to S phase transition in rabbit corneal endothelial cells. *Mol Med Rep* 12: 1951-1956.
- Didsbury J, Weber RF, Bokoch GM, et al. (1989) rac, a novel ras-related family of proteins that are botulinum toxin substrates. *J Biol Chem* 264: 16378-16382.
- Ding S, Merkulova-Rainon T, Han ZC, et al. (2003) HGF receptor up-regulation contributes to the angiogenic phenotype of human endothelial cells and promotes angiogenesis in vitro. *Blood* 101: 4816-4822.
- Drew BA, Burow ME and Beckman BS. (2012) MEK5/ERK5 pathway: the first fifteen years. *Biochim Biophys Acta* 1825: 37-48.
- Duijvestijn AM, van Goor H, Klatter F, et al. (1992) Antibodies defining rat endothelial cells: RECA-1, a pan-endothelial cell-specific monoclonal antibody. *Lab Invest* 66: 459-466.
- Duran JM, Makarewich CA, Trapanese D, et al. (2014) Sorafenib cardiotoxicity increases mortality after myocardial infarction. *Circ Res* 114: 1700-1712.
- Dyer LA and Patterson C. (2010) Development of the endothelium: an emphasis on heterogeneity. *Semin Thromb Hemost* 36: 227-235.
- E G, Cao Y, Bhattacharya S, et al. (2012) Endogenous vascular endothelial growth factor-A (VEGF-A) maintains endothelial cell homeostasis by regulating VEGF receptor-2 transcription. *J Biol Chem* 287: 3029-3041.
- East C, Grundy SM and Bilheimer DW. (1986) Normal cholesterol levels with lovastatin (mevinolin) therapy in a child with homozygous familial hypercholesterolemia following liver transplantation. *JAMA* 256: 2843-2848.
- English JM, Pearson G, Hockenberry T, et al. (1999) Contribution of the ERK5/MEK5 pathway to Ras/Raf signaling and growth control. *J Biol Chem* 274: 31588-31592.



- Fabro S and Smith RL. (1966) The teratogenic activity of thalidomide in the rabbit. *J Pathol Bacteriol* 91: 511-519.
- Fang Z, Tang Y, Fang J, et al. (2013) Simvastatin inhibits renal cancer cell growth and metastasis via AKT/mTOR, ERK and JAK2/STAT3 pathway. *PLoS One* 8: e62823.
- Faust PL and Kovacs WJ. (2014) Cholesterol biosynthesis and ER stress in peroxisome deficiency. *Biochimie* 98: 75-85.
- Fazakas C, Wilhelm I, Nagyoszi P, et al. (2011) Transmigration of melanoma cells through the blood-brain barrier: role of endothelial tight junctions and melanoma-released serine proteases. *PLoS One* 6: e20758.
- Feng C, Sun G, Wang Z, et al. (2014) Transport mechanism of doxorubicin loaded chitosan based nanogels across intestinal epithelium. *Eur J Pharm Biopharm* 87: 197-207.
- Force T, Krause DS and Van Etten RA. (2007) Molecular mechanisms of cardiotoxicity of tyrosine kinase inhibition. *Nat Rev Cancer* 7: 332-344.
- Fritz G, Brachetti C and Kaina B. (2003) Lovastatin causes sensitization of HeLa cells to ionizing radiation-induced apoptosis by the abrogation of G2 blockage. *Int J Radiat Biol* 79: 601-610.
- Fujita H, Katoh H, Hasegawa H, et al. (2000) Molecular decipherment of Rho effector pathways regulating tight-junction permeability. *Biochem J* 346 Pt 3: 617-622.
- Fukuhara S, Marinissen MJ, Chiariello M, et al. (2000) Signaling from G protein-coupled receptors to ERK5/Big MAPK 1 involves Galpha q and Galpha 12/13 families of heterotrimeric G proteins. Evidence for the existence of a novel Ras AND Rho-independent pathway. *J Biol Chem* 275: 21730-21736.
- Furuya M, Nishiyama M, Kasuya Y, et al. (2005) Pathophysiology of tumor neovascularization. *Vasc Health Risk Manag* 1: 277-290.
- Futterman LG and Lemberg L. (2004) Statin pleiotropy: fact or fiction? *Am J Crit Care* 13: 244-249.
- Gandhi H, Patel VB, Mistry N, et al. (2013) Doxorubicin mediated cardiotoxicity in rats: protective role of felodipine on cardiac indices. *Environ Toxicol Pharmacol* 36: 787-795.
- Garcia AN, Vogel SM, Komarova YA, et al. (2011) Permeability of endothelial barrier: cell culture and in vivo models. *Methods Mol Biol* 763: 333-354.
- Garg P, Dhakne R and Belekar V. (2015) Role of breast cancer resistance protein (BCRP) as active efflux transporter on blood-brain barrier (BBB) permeability. *Mol Divers* 19: 163-172.
- Garrington TP, Ishizuka T, Papst PJ, et al. (2000) MEKK2 gene disruption causes loss of cytokine production in response to IgE and c-Kit ligand stimulation of ES cell-derived mast cells. *EMBO J* 19: 5387-5395.
- Gonzalez-Mariscal L, Nava P and Hernandez S. (2005) Critical role of tight junctions in drug delivery across epithelial and endothelial cell layers. *J Membr Biol* 207: 55-68.

- Gopalakrishnan S, Raman N, Atkinson SJ, et al. (1998) Rho GTPase signaling regulates tight junction assembly and protects tight junctions during ATP depletion. *Am J Physiol* 275: C798-809.
- Greineder CF, Kohnstamm S and Ky B. (2011) Heart failure associated with sunitinib: lessons learned from animal models. *Curr Hypertens Rep* 13: 436-441.
- Grethe S, Coltella N, Di Renzo MF, et al. (2006) p38 MAPK downregulates phosphorylation of Bad in doxorubicin-induced endothelial apoptosis. *Biochem Biophys Res Commun* 347: 781-790.
- Guerin M, Sabatier R and Goncalves A. (2015) [Trastuzumab emtansine (Kadcyla((R))) approval in HER2-positive metastatic breast cancers]. *Bull Cancer* 102: 390-397.
- Gunzel D and Yu AS. (2013) Claudins and the modulation of tight junction permeability. *Physiol Rev* 93: 525-569.
- Guo Z, Clydesdale G, Cheng J, et al. (2002) Disruption of Mekk2 in mice reveals an unexpected role for MEKK2 in modulating T-cell receptor signal transduction. *Mol Cell Biol* 22: 5761-5768.
- Hanahan D and Weinberg RA. (2011) Hallmarks of cancer: the next generation. *Cell* 144: 646-674.
- Harhaj NS, Felinski EA, Wolpert EB, et al. (2006) VEGF activation of protein kinase C stimulates occludin phosphorylation and contributes to endothelial permeability. *Invest Ophthalmol Vis Sci* 47: 5106-5115.
- Hay MF. (1964) Effects of Thalidomide on Pregnancy in the Rabbit. *J Reprod Fertil* 8: 59-76.
- Hayashi M, Fearn C, Eliceiri B, et al. (2005) Big mitogen-activated protein kinase 1/extracellular signal-regulated kinase 5 signaling pathway is essential for tumor-associated angiogenesis. *Cancer Res* 65: 7699-7706.
- Hayashi M, Kim SW, Imanaka-Yoshida K, et al. (2004) Targeted deletion of BMK1/ERK5 in adult mice perturbs vascular integrity and leads to endothelial failure. *J Clin Invest* 113: 1138-1148.
- He YP, Zhao LY, Zheng QS, et al. (2008) Involvement of ERK and AKT signaling in the growth effect of arginine vasopressin on adult rat cardiac fibroblast and the modulation by simvastatin. *Mol Cell Biochem* 317: 33-41.
- Heger Z, Cernei N, Kudr J, et al. (2013) A novel insight into the cardiotoxicity of antineoplastic drug doxorubicin. *Int J Mol Sci* 14: 21629-21646.
- Henninger C, Huelsenbeck J, Huelsenbeck S, et al. (2012) The lipid lowering drug lovastatin protects against doxorubicin-induced hepatotoxicity. *Toxicol Appl Pharmacol* 261: 66-73.
- Henninger C, Huelsenbeck S, Wenzel P, et al. (2015) Chronic heart damage following doxorubicin treatment is alleviated by lovastatin. *Pharmacol Res* 91: 47-56.
- Holmes K, Roberts OL, Thomas AM, et al. (2007) Vascular endothelial growth factor receptor-2: structure, function, intracellular signalling and therapeutic inhibition. *Cell Signal* 19: 2003-2012.

- Hong L, Kenney SR, Phillips GK, et al. (2013) Characterization of a Cdc42 protein inhibitor and its use as a molecular probe. *J Biol Chem* 288: 8531-8543.
- Hoppe UC, Marban E and Johns DC. (2001) Distinct gene-specific mechanisms of arrhythmia revealed by cardiac gene transfer of two long QT disease genes, HERG and KCNE1. *Proc Natl Acad Sci U S A* 98: 5335-5340.
- Hor SY, Lee SC, Wong CI, et al. (2008) PXR, CAR and HNF4alpha genotypes and their association with pharmacokinetics and pharmacodynamics of docetaxel and doxorubicin in Asian patients. *Pharmacogenomics J* 8: 139-146.
- Huang C, Liu Z, Wang Z, et al. (2010) Simvastatin prevents ERK activation in myocardial hypertrophy of spontaneously hypertensive rats. *Scand Cardiovasc J* 44: 346-351.
- Hubalek M, Brantner C and Marth C. (2012) Role of pertuzumab in the treatment of HER2-positive breast cancer. *Breast Cancer (Dove Med Press)* 4: 65-73.
- Huelsenbeck J, Henninger C, Schad A, et al. (2011) Inhibition of Rac1 signaling by lovastatin protects against anthracycline-induced cardiac toxicity. *Cell Death Dis* 2: e190.
- Inai T and Shibata Y. (2009) Heterogeneous expression of endothelial connexin (Cx) 37, Cx40, and Cx43 in rat large veins. *Anat Sci Int* 84: 237-245.
- Ishiguro N, Nozawa T, Tsujihata A, et al. (2004) Influx and efflux transport of H1-antagonist epinastine across the blood-brain barrier. *Drug Metab Dispos* 32: 519-524.
- Ito MK, Talbert RL and Tsimikas S. (2006) Statin-associated pleiotropy: possible beneficial effects beyond cholesterol reduction. *Pharmacotherapy* 26: 85S-97S; discussion 98S-101S; quiz 106S-108S.
- Izawa Y, Yoshizumi M, Ishizawa K, et al. (2007) Big mitogen-activated protein kinase 1 (BMK1)/extracellular signal regulated kinase 5 (ERK5) is involved in platelet-derived growth factor (PDGF)-induced vascular smooth muscle cell migration. *Hypertens Res* 30: 1107-1117.
- Jackson D, Atkinson J, Guevara CI, et al. (2014) In vitro and in vivo evaluation of cysteine and site specific conjugated herceptin antibody-drug conjugates. *PLoS One* 9: e83865.
- Jia H, Bagherzadeh A, Bicknell R, et al. (2004) Vascular endothelial growth factor (VEGF)-D and VEGF-A differentially regulate KDR-mediated signaling and biological function in vascular endothelial cells. *J Biol Chem* 279: 36148-36157.
- Jones KL and Buzdar AU. (2009) Evolving novel anti-HER2 strategies. *Lancet Oncol* 10: 1179-1187.
- Kamakura S, Moriguchi T and Nishida E. (1999) Activation of the protein kinase ERK5/BMK1 by receptor tyrosine kinases. Identification and characterization of a signaling pathway to the nucleus. *J Biol Chem* 274: 26563-26571.

- Kasler HG, Victoria J, Duramad O, et al. (2000) ERK5 is a novel type of mitogen-activated protein kinase containing a transcriptional activation domain. *Mol Cell Biol* 20: 8382-8389.
- Kato Y, Kravchenko VV, Tapping RI, et al. (1997) BMK1/ERK5 regulates serum-induced early gene expression through transcription factor MEF2C. *EMBO J* 16: 7054-7066.
- Katsuno T, Umeda K, Matsui T, et al. (2008) Deficiency of zonula occludens-1 causes embryonic lethal phenotype associated with defected yolk sac angiogenesis and apoptosis of embryonic cells. *Mol Biol Cell* 19: 2465-2475.
- Kawaguchi Y, Kono K, Mizukami Y, et al. (2009) Mechanisms of escape from trastuzumab-mediated ADCC in esophageal squamous cell carcinoma: relation to susceptibility to perforin-granzyme. *Anticancer Res* 29: 2137-2146.
- Kesavan K, Lobel-Rice K, Sun W, et al. (2004) MEKK2 regulates the coordinate activation of ERK5 and JNK in response to FGF-2 in fibroblasts. *J Cell Physiol* 199: 140-148.
- Kevil CG, Okayama N, Trocha SD, et al. (1998) Expression of zonula occludens and adherens junctional proteins in human venous and arterial endothelial cells: role of occludin in endothelial solute barriers. *Microcirculation* 5: 197-210.
- Kik K, Studzian K, Wasowska-Lukawska M, et al. (2009) Cytotoxicity and inhibitory properties against topoisomerase II of doxorubicin and its formamidine derivatives. *Acta Biochim Pol* 56: 135-142.
- Kim MT, Chen Y, Marhoul J, et al. (2014) Statistical modeling of the drug load distribution on trastuzumab emtansine (Kadcyla), a lysine-linked antibody drug conjugate. *Bioconjug Chem* 25: 1223-1232.
- Kim YH, Park SM, Kim M, et al. (2012) Cardioprotective effects of rosuvastatin and carvedilol on delayed cardiotoxicity of doxorubicin in rats. *Toxicol Mech Methods* 22: 488-498.
- Kirby ML. (2002) Molecular embryogenesis of the heart. *Pediatr Dev Pathol* 5: 516-543.
- Kostapanos MS, Liberopoulos EN and Elisaf MS. (2009) Statin pleiotropy against renal injury. *J Cardiometab Syndr* 4: E4-9.
- Kute T, Stehle Jr JR, Ornelles D, et al. (2012) Understanding key assay parameters that affect measurements of trastuzumab-mediated ADCC against Her2 positive breast cancer cells. *Oncoimmunology* 1: 810-821.
- Kute TE, Savage L, Stehle JR, Jr., et al. (2009) Breast tumor cells isolated from in vitro resistance to trastuzumab remain sensitive to trastuzumab anti-tumor effects in vivo and to ADCC killing. *Cancer Immunol Immunother* 58: 1887-1896.
- Laflamme MA and Murry CE. (2011) Heart regeneration. *Nature* 473: 326-335.
- Lamallice L, Le Boeuf F and Huot J. (2007) Endothelial cell migration during angiogenesis. *Circ Res* 100: 782-794.

- Laugwitz KL, Moretti A, Caron L, et al. (2008) Islet1 cardiovascular progenitors: a single source for heart lineages? *Development* 135: 193-205.
- Laverty H, Benson C, Cartwright E, et al. (2011) How can we improve our understanding of cardiovascular safety liabilities to develop safer medicines? *Br J Pharmacol* 163: 675-693.
- Lazarowski A, Ramos AJ, García-Rivello H, et al. (2004) Neuronal and glial expression of the multidrug resistance gene product in an experimental epilepsy model. *Cell Mol Neurobiol* 24: 77-85.
- Le Guelte A and Gavard J. (2011) Role of endothelial cell-cell junctions in endothelial permeability. *Methods Mol Biol* 763: 265-279.
- Le NT, Takei Y, Izawa-Ishizawa Y, et al. (2014) Identification of activators of ERK5 transcriptional activity by high-throughput screening and the role of endothelial ERK5 in vasoprotective effects induced by statins and antimalarial agents. *J Immunol* 193: 3803-3815.
- Lee DK, Park EJ, Kim EK, et al. (2012) Atorvastatin and simvastatin, but not pravastatin, up-regulate LPS-induced MMP-9 expression in macrophages by regulating phosphorylation of ERK and CREB. *Cell Physiol Biochem* 30: 499-511.
- Lee JD, Ulevitch RJ and Han J. (1995) Primary structure of BMK1: a new mammalian map kinase. *Biochem Biophys Res Commun* 213: 715-724.
- Li CX and Poznansky MJ. (1990) Characterization of the ZO-1 protein in endothelial and other cell lines. *J Cell Sci* 97 ( Pt 2): 231-237.
- Liao JK. (2005) Clinical implications for statin pleiotropy. *Curr Opin Lipidol* 16: 624-629.
- Liu W, Wang P, Shang C, et al. (2014) Endophilin-1 regulates blood-brain barrier permeability by controlling ZO-1 and occludin expression via the EGFR-ERK1/2 pathway. *Brain Res* 1573: 17-26.
- Livak KJ and Schmittgen TD. (2001) Analysis of relative gene expression data using real-time quantitative PCR and the 2(-Delta Delta C(T)) Method. *Methods* 25: 402-408.
- Lo CW and Wessels A. (1998) Cx43 gap junctions in cardiac development. *Trends Cardiovasc Med* 8: 264-269.
- Lu WL, Qi XR, Zhang Q, et al. (2004) A pegylated liposomal platform: pharmacokinetics, pharmacodynamics, and toxicity in mice using doxorubicin as a model drug. *J Pharmacol Sci* 95: 381-389.
- Lupertz R, Watjen W, Kahl R, et al. (2010) Dose- and time-dependent effects of doxorubicin on cytotoxicity, cell cycle and apoptotic cell death in human colon cancer cells. *Toxicology* 271: 115-121.
- Mao WF, Shao MH, Gao PT, et al. (2012) The important roles of RET, VEGFR2 and the RAF/MEK/ERK pathway in cancer treatment with sorafenib. *Acta Pharmacol Sin* 33: 1311-1318.
- Matthews W, Jordan CT, Gavin M, et al. (1991) A receptor tyrosine kinase cDNA isolated from a population of enriched primitive hematopoietic cells and exhibiting close genetic linkage to c-kit. *Proc Natl Acad Sci U S A* 88: 9026-9030.



- Mego M, Reckova M, Obertova J, et al. (2007) Increased cardiotoxicity of sorafenib in sunitinib-pretreated patients with metastatic renal cell carcinoma. *Ann Oncol* 18: 1906-1907.
- Mellor HR, Bell AR, Valentin JP, et al. (2011) Cardiotoxicity associated with targeting kinase pathways in cancer. *Toxicol Sci* 120: 14-32.
- Millauer B, Wizigmann-Voos S, Schnurch H, et al. (1993) High affinity VEGF binding and developmental expression suggest Flk-1 as a major regulator of vasculogenesis and angiogenesis. *Cell* 72: 835-846.
- Miura S, Matsuo Y and Saku K. (2004) Simvastatin suppresses coronary artery endothelial tube formation by disrupting Ras/Raf/ERK signaling. *Atherosclerosis* 175: 235-243.
- Mizutani H, Tada-Oikawa S, Hiraku Y, et al. (2005) Mechanism of apoptosis induced by doxorubicin through the generation of hydrogen peroxide. *Life Sci* 76: 1439-1453.
- Molnar G, Dagher MC, Geiszt M, et al. (2001) Role of prenylation in the interaction of Rho-family small GTPases with GTPase activating proteins. *Biochemistry* 40: 10542-10549.
- Mori K, Tani M, Kamata K, et al. (2000) Mitogen-activated protein kinase, ERK1/2, is essential for the induction of vascular endothelial growth factor by ionizing radiation mediated by activator protein-1 in human glioblastoma cells. *Free Radic Res* 33: 157-166.
- Niessen CM. (2007) Tight junctions/adherens junctions: basic structure and function. *J Invest Dermatol* 127: 2525-2532.
- Nithianandarajah-Jones GN, Wilm B, Goldring CE, et al. (2012) ERK5: structure, regulation and function. *Cell Signal* 24: 2187-2196.
- Nithianandarajah-Jones GN, Wilm B, Goldring CE, et al. (2014) The role of ERK5 in endothelial cell function. *Biochem Soc Trans* 42: 1584-1589.
- Nitiss JL. (2009a) DNA topoisomerase II and its growing repertoire of biological functions. *Nat Rev Cancer* 9: 327-337.
- Nitiss JL. (2009b) Targeting DNA topoisomerase II in cancer chemotherapy. *Nat Rev Cancer* 9: 338-350.
- Nubel T, Damrot J, Roos WP, et al. (2006) Lovastatin protects human endothelial cells from killing by ionizing radiation without impairing induction and repair of DNA double-strand breaks. *Clin Cancer Res* 12: 933-939.
- Nubel T, Dippold W, Kaina B, et al. (2004a) Ionizing radiation-induced E-selectin gene expression and tumor cell adhesion is inhibited by lovastatin and all-trans retinoic acid. *Carcinogenesis* 25: 1335-1344.
- Nubel T, Dippold W, Kleinert H, et al. (2004b) Lovastatin inhibits Rho-regulated expression of E-selectin by TNFalpha and attenuates tumor cell adhesion. *FASEB J* 18: 140-142.
- Nubel T, Schmitt S, Kaina B, et al. (2005) Lovastatin stimulates p75 TNF receptor (TNFR2) expression in primary human endothelial cells. *Int J Mol Med* 16: 1139-1145.



- Ohnesorge N, Viemann D, Schmidt N, et al. (2010) Erk5 activation elicits a vasoprotective endothelial phenotype via induction of Kruppel-like factor 4 (KLF4). *J Biol Chem* 285: 26199-26210.
- Okabe M, Unno M, Harigae H, et al. (2005) Characterization of the organic cation transporter SLC22A16: a doxorubicin importer. *Biochem Biophys Res Commun* 333: 754-762.
- Olsson AK, Dimberg A, Kreuger J, et al. (2006) VEGF receptor signalling - in control of vascular function. *Nat Rev Mol Cell Biol* 7: 359-371.
- Ostrau C, Hulsbeck J, Herzog M, et al. (2009) Lovastatin attenuates ionizing radiation-induced normal tissue damage in vivo. *Radiother Oncol* 92: 492-499.
- Peh GS, Adnan K, George BL, et al. (2015) The effects of Rho-associated kinase inhibitor Y-27632 on primary human corneal endothelial cells propagated using a dual media approach. *Sci Rep* 5: 9167.
- Pentassuglia L and Sawyer DB. (2009) The role of Neuregulin-1beta/ErbB signaling in the heart. *Exp Cell Res* 315: 627-637.
- Perez-Arnaiz C, Busto N, Leal JM, et al. (2014) New insights into the mechanism of the DNA/doxorubicin interaction. *J Phys Chem B* 118: 1288-1295.
- Peters KG, De Vries C and Williams LT. (1993) Vascular endothelial growth factor receptor expression during embryogenesis and tissue repair suggests a role in endothelial differentiation and blood vessel growth. *Proc Natl Acad Sci U S A* 90: 8915-8919.
- Pommier Y, Leo E, Zhang H, et al. (2010) DNA topoisomerases and their poisoning by anticancer and antibacterial drugs. *Chem Biol* 17: 421-433.
- Puri R and Tuzcu EM. (2012) Statin pleiotropy in acute myocardial infarction--is it about timing? *Catheter Cardiovasc Interv* 80: 766-767.
- Regan CP, Li W, Boucher DM, et al. (2002) Erk5 null mice display multiple extraembryonic vascular and embryonic cardiovascular defects. *Proc Natl Acad Sci U S A* 99: 9248-9253.
- Ren S, Li C, Dai Y, et al. (2014) Comparison of pharmacokinetics, tissue distribution and pharmacodynamics of liposomal and free doxorubicin in tumour-bearing mice following intratumoral injection. *J Pharm Pharmacol* 66: 1231-1239.
- Rhee DY, Zhao XQ, Francis RJ, et al. (2009) Connexin 43 regulates epicardial cell polarity and migration in coronary vascular development. *Development* 136: 3185-3193.
- Riad A, Bien S, Westermann D, et al. (2009) Pretreatment with statin attenuates the cardiotoxicity of Doxorubicin in mice. *Cancer Res* 69: 695-699.
- Riganti C, Doublier S, Costamagna C, et al. (2008) Activation of nuclear factor-kappa B pathway by simvastatin and RhoA silencing increases doxorubicin cytotoxicity in human colon cancer HT29 cells. *Mol Pharmacol* 74: 476-484.

- Roberts OL, Holmes K, Muller J, et al. (2009) ERK5 and the regulation of endothelial cell function. *Biochem Soc Trans* 37: 1254-1259.
- Roberts OL, Holmes K, Muller J, et al. (2010) ERK5 is required for VEGF-mediated survival and tubular morphogenesis of primary human microvascular endothelial cells. *J Cell Sci* 123: 3189-3200.
- Rosenberg GA. (2012) Neurological diseases in relation to the blood-brain barrier. *J Cereb Blood Flow Metab* 32: 1139-1151.
- Roskoski R, Jr. (2012) ERK1/2 MAP kinases: structure, function, and regulation. *Pharmacol Res* 66: 105-143.
- Rossant J and Howard L. (2002) Signaling pathways in vascular development. *Annu Rev Cell Dev Biol* 18: 541-573.
- Sadeghi-Aliabadi H, Minaiyan M and Dabestan A. (2010) Cytotoxic evaluation of doxorubicin in combination with simvastatin against human cancer cells. *Res Pharm Sci* 5: 127-133.
- Samak G, Aggarwal S and Rao RK. (2011) ERK is involved in EGF-mediated protection of tight junctions, but not adherens junctions, in acetaldehyde-treated Caco-2 cell monolayers. *Am J Physiol Gastrointest Liver Physiol* 301: G50-59.
- Sardi I, la Marca G, Cardellicchio S, et al. (2013) Pharmacological modulation of blood-brain barrier increases permeability of doxorubicin into the rat brain. *Am J Cancer Res* 3: 424-432.
- Sartiano GP, Lynch WE and Bullington WD. (1979) Mechanism of action of the anthracycline anti-tumor antibiotics, doxorubicin, daunomycin and rubidazole: preferential inhibition of DNA polymerase alpha. *J Antibiot (Tokyo)* 32: 1038-1045.
- Schmidinger M, Zielinski CC, Vogl UM, et al. (2008) Cardiac toxicity of sunitinib and sorafenib in patients with metastatic renal cell carcinoma. *J Clin Oncol* 26: 5204-5212.
- Seghezzi G, Patel S, Ren CJ, et al. (1998) Fibroblast growth factor-2 (FGF-2) induces vascular endothelial growth factor (VEGF) expression in the endothelial cells of forming capillaries: an autocrine mechanism contributing to angiogenesis. *J Cell Biol* 141: 1659-1673.
- Shalaby F, Rossant J, Yamaguchi TP, et al. (1995) Failure of blood-island formation and vasculogenesis in Flk-1-deficient mice. *Nature* 376: 62-66.
- Sharma P, Templin T and Grabham P. (2012) Short term effects of gamma radiation on endothelial barrier function: Uncoupling of PECAM-1. *Microvasc Res*.
- Sharma P, Templin T and Grabham P. (2013) Short term effects of gamma radiation on endothelial barrier function: uncoupling of PECAM-1. *Microvasc Res* 86: 11-20.
- Sohn SJ, Sarvis BK, Cado D, et al. (2002) ERK5 MAPK regulates embryonic angiogenesis and acts as a hypoxia-sensitive repressor of vascular endothelial growth factor expression. *J Biol Chem* 277: 43344-43351.
- Souders CA, Bowers SL and Baudino TA. (2009) Cardiac fibroblast: the renaissance cell. *Circ Res* 105: 1164-1176.

- Spallarossa P, Altieri P, Barisione C, et al. (2010) p38 MAPK and JNK antagonistically control senescence and cytoplasmic p16INK4A expression in doxorubicin-treated endothelial progenitor cells. *PLoS One* 5: e15583.
- Spudich A, Kilic E, Xing H, et al. (2006) Inhibition of multidrug resistance transporter-1 facilitates neuroprotective therapies after focal cerebral ischemia. *Nat Neurosci* 9: 487-488.
- Stancu C and Sima A. (2001) Statins: mechanism of action and effects. *J Cell Mol Med* 5: 378-387.
- Sugiyama T, Sadzuka Y, Tanaka K, et al. (2001) Inhibition of glutamate transporter by theanine enhances the therapeutic efficacy of doxorubicin. *Toxicol Lett* 121: 89-96.
- Sulpice E, Ding S, Muscatelli-Groux B, et al. (2009) Cross-talk between the VEGF-A and HGF signalling pathways in endothelial cells. *Biol Cell* 101: 525-539.
- Sundararaj KP, Samuvel DJ, Li Y, et al. (2008) Simvastatin suppresses LPS-induced MMP-1 expression in U937 mononuclear cells by inhibiting protein isoprenylation-mediated ERK activation. *J Leukoc Biol* 84: 1120-1129.
- Surviladze Z, Waller A, Strouse JJ, et al. (2010) A Potent and Selective Inhibitor of Cdc42 GTPase. *Probe Reports from the NIH Molecular Libraries Program*. Bethesda (MD).
- Sviridov DD, Safonova IG, Pavlov MY, et al. (1990) Inhibition of cholesterol synthesis by lovastatin tested on six human cell types in vitro. *Lipids* 25: 177-179.
- Takahashi H and Shibuya M. (2005) The vascular endothelial growth factor (VEGF)/VEGF receptor system and its role under physiological and pathological conditions. *Clin Sci (Lond)* 109: 227-241.
- Takayama N, Kai H, Kudo H, et al. (2011) Simvastatin prevents large blood pressure variability induced aggravation of cardiac hypertrophy in hypertensive rats by inhibiting RhoA/Ras-ERK pathways. *Hypertens Res* 34: 341-347.
- Tatake RJ, O'Neill MM, Kennedy CA, et al. (2008) Identification of pharmacological inhibitors of the MEK5/ERK5 pathway. *Biochem Biophys Res Commun* 377: 120-125.
- Terry S, Nie M, Matter K, et al. (2010) Rho signaling and tight junction functions. *Physiology (Bethesda)* 25: 16-26.
- Tien T, Barrette KF, Chronopoulos A, et al. (2013) Effects of high glucose-induced Cx43 downregulation on occludin and ZO-1 expression and tight junction barrier function in retinal endothelial cells. *Invest Ophthalmol Vis Sci* 54: 6518-6525.
- Tirziu D, Giordano FJ and Simons M. (2010) Cell communications in the heart. *Circulation* 122: 928-937.
- Ulger H, Karabulut AK and Pratten MK. (2002) Labelling of rat endothelial cells with antibodies to vWF, RECA-1, PECAM-1, ICAM-1, OX-43 and ZO-1. *Anat Histol Embryol* 31: 31-35.

- Valabrega G, Montemurro F and Aglietta M. (2007) Trastuzumab: mechanism of action, resistance and future perspectives in HER2-overexpressing breast cancer. *Ann Oncol* 18: 977-984.
- Van Vliet P, Wu SM, Zaffran S, et al. (2012) Early cardiac development: a view from stem cells to embryos. *Cardiovasc Res* 96: 352-362.
- Vandenbroucke E, Mehta D, Minshall R, et al. (2008) Regulation of endothelial junctional permeability. *Ann N Y Acad Sci* 1123: 134-145.
- Vejpongsa P and Yeh ET. (2014) Topoisomerase 2beta: a promising molecular target for primary prevention of anthracycline-induced cardiotoxicity. *Clin Pharmacol Ther* 95: 45-52.
- Villa-Moruzzi E. (2011) Tyrosine phosphatases in the HER2-directed motility of ovarian cancer cells: Involvement of PTPN12, ERK5 and FAK. *Anal Cell Pathol (Amst)* 34: 101-112.
- Walker CA and Spinale FG. (1999) The structure and function of the cardiac myocyte: a review of fundamental concepts. *J Thorac Cardiovasc Surg* 118: 375-382.
- Walshe JM, Denduluri N, Berman AW, et al. (2006) A phase II trial with trastuzumab and pertuzumab in patients with HER2-overexpressed locally advanced and metastatic breast cancer. *Clin Breast Cancer* 6: 535-539.
- Wang X, Merritt AJ, Seyfried J, et al. (2005) Targeted deletion of mek5 causes early embryonic death and defects in the extracellular signal-regulated kinase 5/myocyte enhancer factor 2 cell survival pathway. *Mol Cell Biol* 25: 336-345.
- Wang Y and Alexander JS. (2011) Analysis of endothelial barrier function in vitro. *Methods Mol Biol* 763: 253-264.
- Werner M, Atil B, Sieczkowski E, et al. (2013) Simvastatin-induced compartmentalisation of doxorubicin sharpens up nuclear topoisomerase II inhibition in human rhabdomyosarcoma cells. *Naunyn Schmiedebergs Arch Pharmacol* 386: 605-617.
- Werner M, Sacher J and Hohenegger M. (2004) Mutual amplification of apoptosis by statin-induced mitochondrial stress and doxorubicin toxicity in human rhabdomyosarcoma cells. *Br J Pharmacol* 143: 715-724.
- Will Y, Dykens JA, Nadanaciva S, et al. (2008) Effect of the multitargeted tyrosine kinase inhibitors imatinib, dasatinib, sunitinib, and sorafenib on mitochondrial function in isolated rat heart mitochondria and H9c2 cells. *Toxicol Sci* 106: 153-161.
- Wilson AL, Erdman RA, Castellano F, et al. (1998) Prenylation of Rab8 GTPase by type I and type II geranylgeranyl transferases. *Biochem J* 333 ( Pt 3): 497-504.
- Wojcik T, Buczek E, Majzner K, et al. (2014) Comparative endothelial profiling of doxorubicin and daunorubicin in cultured endothelial cells. *Toxicol In Vitro*.
- Wolf MB and Baynes JW. (2006) The anti-cancer drug, doxorubicin, causes oxidant stress-induced endothelial dysfunction. *Biochim Biophys Acta* 1760: 267-271.

- Woo CH, Le NT, Shishido T, et al. (2010) Novel role of C terminus of Hsc70-interacting protein (CHIP) ubiquitin ligase on inhibiting cardiac apoptosis and dysfunction via regulating ERK5-mediated degradation of inducible cAMP early repressor. *FASEB J* 24: 4917-4928.
- Wu K, Tian S, Zhou H, et al. (2013) Statins protect human endothelial cells from TNF-induced inflammation via ERK5 activation. *Biochemical Pharmacology* 85: 1753-1760.
- Wu TY, Jen MH, Bottle A, et al. (2010) Ten-year trends in hospital admissions for adverse drug reactions in England 1999-2009. *J R Soc Med* 103: 239-250.
- Yamaguchi TP, Dumont DJ, Conlon RA, et al. (1993) flk-1, an flt-related receptor tyrosine kinase is an early marker for endothelial cell precursors. *Development* 118: 489-498.
- Yan L, Carr J, Ashby PR, et al. (2003) Knockout of ERK5 causes multiple defects in placental and embryonic development. *BMC Dev Biol* 3: 11.
- Yang F, Chen H, Liu Y, et al. (2013) Doxorubicin caused apoptosis of mesenchymal stem cells via p38, JNK and p53 pathway. *Cell Physiol Biochem* 32: 1072-1082.
- Yang J, Boerm M, McCarty M, et al. (2000) Mekk3 is essential for early embryonic cardiovascular development. *Nat Genet* 24: 309-313.
- Yang Q, Deng X, Lu B, et al. (2010) Pharmacological inhibition of BMK1 suppresses tumor growth through promyelocytic leukemia protein. *Cancer Cell* 18: 258-267.
- Yang Q and Lee JD. (2011) Targeting the BMK1 MAP kinase pathway in cancer therapy. *Clin Cancer Res* 17: 3527-3532.
- Yewale C, Baradia D, Vhora I, et al. (2013) Epidermal growth factor receptor targeting in cancer: a review of trends and strategies. *Biomaterials* 34: 8690-8707.
- Yoshida R, Tazawa H, Hashimoto Y, et al. (2012) Mechanism of resistance to trastuzumab and molecular sensitization via ADCC activation by exogenous expression of HER2-extracellular domain in human cancer cells. *Cancer Immunol Immunother* 61: 1905-1916.
- Zhang J, Sun T, Liang L, et al. (2014) Drug promiscuity of P-glycoprotein and its mechanism of interaction with paclitaxel and doxorubicin. *Soft Matter* 10: 438-445.
- Zhang S, Liu X, Bawa-Khalfe T, et al. (2012) Identification of the molecular basis of doxorubicin-induced cardiotoxicity. *Nat Med* 18: 1639-1642.
- Zhou G, Bao ZQ and Dixon JE. (1995) Components of a new human protein kinase signal transduction pathway. *J Biol Chem* 270: 12665-12669.
- Zuo Y, Wu Y, Wehrli B, et al. (2015) Modulation of ERK5 is a novel mechanism by which Cdc42 regulates migration of breast cancer cells. *J Cell Biochem* 116: 124-132.